ISSN 1007-9327 (print)
ISSN 2219-2840 (online)

World Journal of *Gastroenterology*

World J Gastroenterol 2020 April 7; 26(13): 1382-1545

Published by Baishideng Publishing Group Inc

World Journal of Gastroenterology

Contents

Weekly Volume 26 Number 13 April 7, 2020

Contents

World Journal of Gastroenterology

Volume 26 Number 13 April 7, 2020

NAME OF JOURNAL
World Journal of Gastroenterology

ISSN
ISSN 1007-9327 (print) ISSN 2219-2840 (online)

LAUNCH DATE
October 1, 1995

FREQUENCY
Weekly

EDITORS-IN-CHIEF
Subrata Ghosh, Andrzej S Tarnawski

EDITORIAL BOARD MEMBERS
http://www.wjgnet.com/1007-9327/editorialboard.htm

EDITORIAL OFFICE
Ze-Mao Gong, Director

PUBLICATION DATE
April 7, 2020

INSTRUCTIONS TO AUTHORS
https://www.wjgnet.com/bpg/gerinfo/204

GUIDELINES FOR ETHICS DOCUMENTS
https://www.wjgnet.com/bpg/GerInfo/287

GUIDELINES FOR NON-NATIVE SPEAKERS OF ENGLISH
https://www.wjgnet.com/bpg/gerinfo/240

PUBLICATION MISCONDUCT
https://www.wjgnet.com/bpg/gerinfo/208

ARTICLE PROCESSING CHARGE
https://www.wjgnet.com/bpg/gerinfo/242

STEPS FOR SUBMITTING MANUSCRIPTS
https://www.wjgnet.com/bpg/GerInfo/239

ONLINE SUBMISSION
https://www.f6publishing.com

World Journal of Gastroenterology

Submit a Manuscript: https://www.f6publishing.com

World J Gastroenterol 2020 April 7; 26(13): 1382-1393

DOI: 10.3748/wjg.v26.i13.1382

ISSN 1007-9327 (print) ISSN 2219-2840 (online)

OPINION REVIEW

Hereditary gastric cancer: Three rules to reduce missed diagnoses

Paula Assumpção, Taíssa Araújo, André Khayat, Geraldo Ishak, Sidney Santos, Williams Barra, João Felipe Acioli, Benedito Rossi, Paulo Assumpção

ORCID number: Paula Assumpção (0000-0003-2625-8037); Taíssa Araújo (0000-0002-1716-4445); André Khayat (0000-0002-3451-6369); Geraldo Ishak (0000-0002-0837-4803); Sidney Santos (0000-0002-9417-8622); Williams Barra (0000-0001-8954-4212); João Felipe Acioli (0000-0003-4344-7921); Benedito Rossi (0000-0003-2614-4910); Paulo Assumpção (0000-0003-3846-8445).

Author contributions: All authors equally contributed to this paper in terms of the conception and design of the study, literature review and analysis, drafting and critical revision and editing, and approval of the final version.

Conflict-of-interest statement: No potential conflicts of interest. No financial support.

Manuscript source: Unsolicited Manuscript

Received: December 10, 2019
Peer-review started: December 10,

Paula Assumpção, Programa de Pós-Graduação em Genética e Biologia Molecular, Universidade Federal do Pará, Belém 66075-110, Brazil

Taíssa Araújo, André Khayat, Sidney Santos, Williams Barra, Paulo Assumpção, Núcleo de Pesquisas em Oncologia, Universidade Federal do Pará, Belém 66073-000, Brazil

Geraldo Ishak, João Felipe Acioli, Hospital Universitário João de Barros Barreto, Universidade Federal do Pará, Belém 66073-000, Brazil

Benedito Rossi, Centro de Oncologia e Aconselhamento Genético, Hospital Sírio Libanês, São Paulo 01308-050, Brazil

Corresponding author: Paulo Assumpção, MD, PhD, Academic Research, Adjunct Professor, Surgical Oncologist, Núcleo de Pesquisas em Oncologia, Universidade Federal do Pará, Rua dos Mundurucus 4487, Belém 66073-000, Brazil. assumpcaopp@gmail.com

Abstract

Gastric cancer remains one of the most lethal cancers. The incidence and mortality rates are quite similar. The main reason for the high mortality is diagnosis at advanced stages of disease, when treatment options are poor. One of the supposed strategies to overcome late-stage diagnosis is identifying people at high risk with the aim of establishing rigorous clinical control, including routine endoscopy and biopsies. Hereditary gastric cancer (HGC) syndromes, though representing a sizeable group to monitor for prevention or, at least, for early diagnosis, are apparently extremely rare. The low rate of HGC diagnosis might be related to the low rates of suspicion, insufficient familiarity about clinical diagnosis criteria, and the supposed conditional necessity of a molecular diagnosis. In this review, we will discuss simple measures to increase HGC diagnosis by applying three rules that might provide an opportunity for precision care to benefit the families affected by this disease.

Key words: Hereditary gastric cancer; Rules; Diagnosis

Core tip: Although familial gastric cancer cases represent a potential source for the discovery of early-stage gastric cancer (and others) among patients' relatives, this possibility has been little explored due to the low rate of suspicion of hereditary gastric cancer syndromes, which could be improved by applying simple rules for hereditary gastric cancer screening that are accessible for unskilled healthcare professionals.

2019
First decision: February 14, 2020
Revised: February 17, 2020
Accepted: March 9, 2020
Article in press: March 9, 2020
Published online: April 7, 2020

P-Reviewer: Eleftheriadis N, Tanabe S
S-Editor: Gong ZM
L-Editor: A
E-Editor: Zhang YL

Citation: Assumpção P, Araújo T, Khayat A, Ishak G, Santos S, Barra W, Acioli JF, Rossi B, Assumpção P. Hereditary gastric cancer: Three rules to reduce missed diagnoses. *World J Gastroenterol* 2020; 26(13): 1382-1393
URL: https://www.wjgnet.com/1007-9327/full/v26/i13/1382.htm
DOI: https://dx.doi.org/10.3748/wjg.v26.i13.1382

GASTRIC ADENOCARCINOMA CAUSES AND PREVENTION

The main recognized causes of gastric adenocarcinoma are environmental, hereditary, and replicative DNA errors[1-4]. Measures to avoid environmental exposition are widely discussed, mainly *Helicobacter pylori* (*H. pylori*) prevention and treatment and changes in alimentary habits[5]. For replicative causes, there are no currently available alternatives for risk reduction[6,7].

Hereditary cancers, although representing a potential group for prevention and early diagnosis, seem to be disregarded, or even neglected, since their incidence is very uncommon, causing preventive measures to have low impact on gastric cancer burden and mortality.

THE HEREDITARY GASTRIC CANCER SYNDROMES

The incidence of hereditary gastric cancer (HGC) is approximately 1%, and a degree of genetic influence seems to be present in over 10% of sporadic gastric cancer (GC) cases[8].

The discrepancy in HGC incidence might be explained by two different concepts: Molecular diagnosis; and diagnosis based on meeting clinical statements for hereditary cancers without a molecular diagnosis; patients diagnosed via the former also represent HGC cases[9,10].

Since molecular diagnosis is tricky and not widely available, a focus on the clinical criteria for hereditary gastric cancer cases should increase the number of recognized cases and allow an intensive search for early diagnosis, as well as select a larger number of cases for practicing molecular investigations in reference centers.

There are three robustly identified HGC syndromes: Hereditary diffuse gastric cancer (HDGC); gastric adenocarcinoma and proximal polyposis of stomach (GAPPS); and familial intestinal gastric cancer (FIGC). Additionally, GC may arise from other hereditary cancer syndromes, such as Lynch syndrome, Li-Fraumeni syndrome, Peutz-Jeghers syndrome, and ovarian and breast syndromes, among others[10-12].

The clinical criteria for each of these syndromes are not widely known, and as a consequence, the low rate of suspicion results in rare investigations and diagnoses of such syndromes.

Estimating the number of missed clinically diagnosable cases of HGC is extremely difficult. Nevertheless, missed diagnoses might represent a significant number of families that could benefit from such active searching and subsequent adoption of measures to allow for early diagnosis and efficient treatments.

SIMPLE MEASURES TO INCREASE HEREDITARY GC DIAGNOSIS

Available initiatives to avoid sporadic GC are usually hard to implement since they include convincing the population to change alimentary habits, improving sanitary conditions in developing nations, and using large-scale antibiotics to treat *H. pylori*[6,7].

For HGC diagnosis, simple measures should be attempted as a first step to increase health professional suspicion and favor clinical diagnosis.

Three simple rules, accessible to every health-care professional, could improve the clinical diagnosis of HGC and allow referencing of such cases to specialized centers, either for patients to receive support at local units or, eventually, for patients to be transferred to those centers to benefit from complex measures.

Observation of the three rules might greatly increase the number of diagnosed cases of HGC, providing an opportunity for precision care to benefit these families.

The suggested rules are the age and number rule, the multiple tumor rule, and the polyposis rule.

THE AGE AND NUMBER RULE

This is the number one rule and allows capture of the great majority of HGC cases (probably more than 95% of cases). Since age of occurrence and number of affected relatives are part of the clinical criteria for almost every hereditary GC syndrome, a simple check of the patient's age and the occurrence of other cases among first- or second-degree relatives is sufficient to screen patients for a possible diagnosis of hereditary cancer[10,13,14] (Figure 1).

Patient age under 50, or the occurrence of at least one case of GC in relatives are enough to require further screening for hereditary GC syndromes and to implement protocols for family investigation and surveillance[15].

These can be done primarily at the site of the first consultation, but specialized remote support can be beneficial either for conducting the necessary investigation and procedures using local resources or for referring the case to a dedicated unit for ideal management.

THE MULTIPLE TUMOR RULE

The occurrence of additional cancers, both multiple GCs or cancers at other sites, such as breast, colon and others, might represent a potential for hereditary cancers[10,11] (Figure 2).

As discussed above, local and reference center investigations and management, according to available resources, are formally recommended.

THE POLYPOSIS RULE

Although it is very rare, GC-associated polyposis is another sign of hereditary cancers even if they are not caught by the two previous rules. Both HGC syndromes and other hereditary cancer syndromes may cause GC and stomach polyposis[10,11,13] (Figure 3).

Again, according to the availability of resources, those cases might be managed locally or referred to another center.

THE IMPACT OF THE THREE RULES IN CLINICAL PRACTICE

There are several criteria defining both HGC syndromes and other hereditary syndromes that might imply GC occurrence.

Considering only the three well-established HGC syndromes, at least 16 rules are currently published. Additionally, many of these rules are frequently updated, leading to a very complex net of possibilities to diagnose an HGC that, even for a specialist, let alone a generalist health worker, are very hard to remember[8,10,11,14].

An attempt to simplify these many criteria resulted in a three-rule method for the triage of patients for possible HGC formal diagnosis. None of the official criteria for diagnosis were questioned or modified. The aim of this simple method is to help clinicians and other health-care members remain alert for these possible diagnoses.

To demonstrate the simplicity and potential benefits of increasing HGC identification by applying the three rules strategy, some practical possibilities will be discussed.

All the criteria defined in recent meetings and conferences[8,13] are covered by the three rules, which can be used by any health-care professional, including nonspecialized ones, contributing to the avoidance of missed diagnoses (Figure 4).

THE POTENTIAL OF THE AGE AND NUMBER RULE IN CLINICAL PRACTICE

Just by applying this rule, a great number of cases can be selected for a possible diagnosis of HGC. The following examples present the minimal requirements that can favor the discovery of new HGC cases and imply important investigational and therapeutic procedures that might change the outlooks for patients and their relatives.

The 1 + 1 law

A case of diffuse-type GC in a patient under 50 years old and a case of GC among first- or second-degree relatives, regardless of the type of adenocarcinoma, are enough

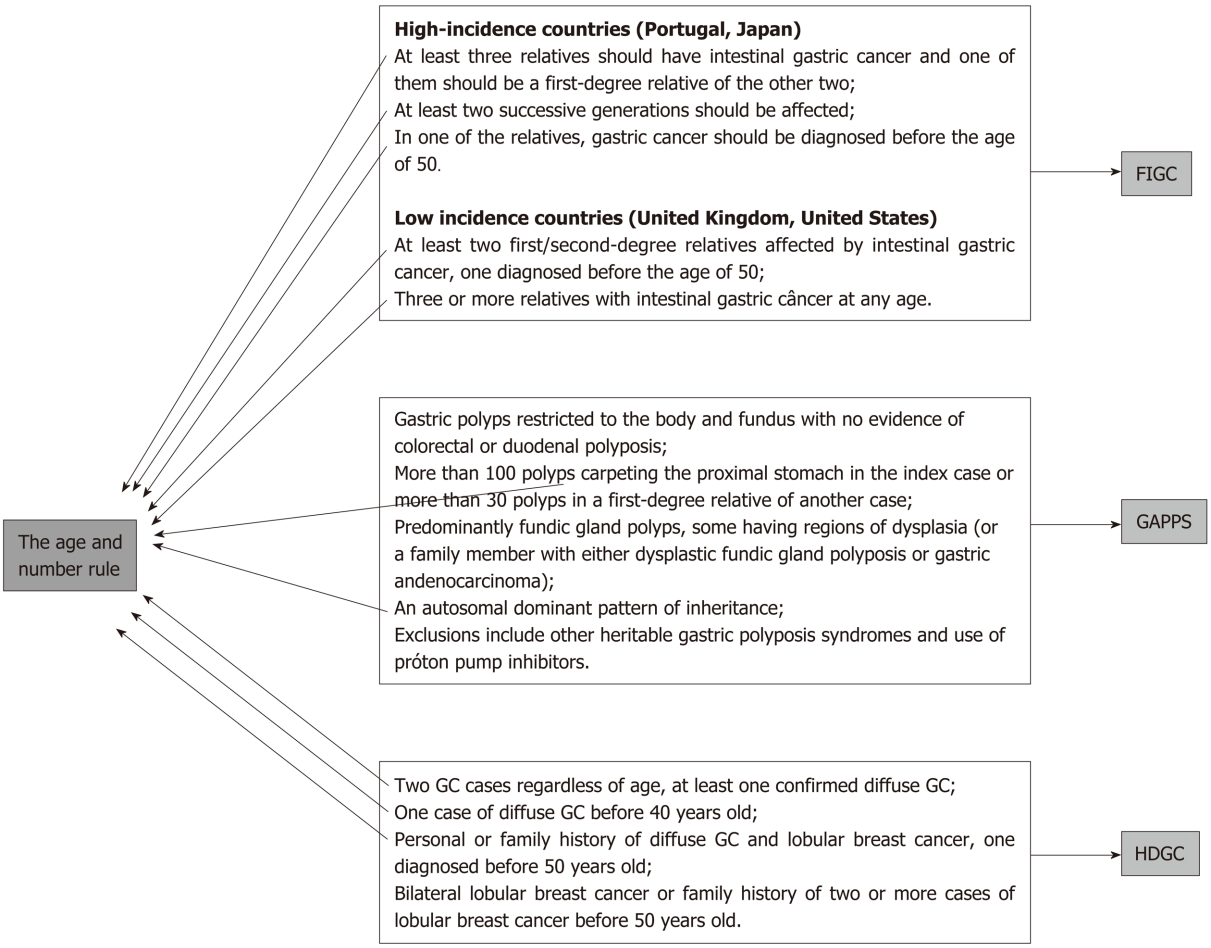

Figure 1 Diagnosis criteria for hereditary gastric cancer caught by rule number 1. GC: Gastric cancer; FIGC: Familial intestinal gastric cancer; GAPPS: Gastric adenocarcinoma and proximal polyposis of stomach; HDGC: Hereditary diffuse gastric cancer.

to establish a formal diagnosis of HGC, and this is very important, since it implies the potential for a molecular test (*CDH1* mutation).

If positive, prophylactic total gastrectomy for the affected relatives might be necessary. Even with a negative genetic test, every first- and second-degree relative will need a dedicated endoscopy every year beginning at 20 years old. The standard number of first- and second-degree relatives older than 19 is over 20 individuals, and these are the people at high risk; in these individuals, rigorous surveillance may result in avoidance of late GC diagnosis and might change outcomes.

The 1 + 0 law

This not so alarming situation indeed also represents a formal diagnosis of HGC in the case of patients under 40 years old with diffuse GC. The same procedures described above are needed, including molecular investigation, possibility of prophylactic total gastrectomy, and engagement of the relatives in a rigorous program of follow-up beginning at 20 years old.

The 0 + 2 law

Regardless of the age of occurrence, if a patient has diffuse GC, independently of the relative gastric adenocarcinoma type, a formal diagnosis of HGC is again reached, with the same needs and consequences described above.

This situation also results in a formal diagnosis of HGC in cases of the intestinal type according to the familial intestinal gastric cancer syndrome criteria for low-risk areas. For this syndrome, there is no molecular test, and the recommendation includes annual endoscopies for first- and second-degree relatives beginning at 40 years old[9,11,16].

The 0 + 3 law

Regardless of age or histological type of gastric adenocarcinoma, three or more cases of GC among first- or second-degree relatives always signify an HGC syndrome

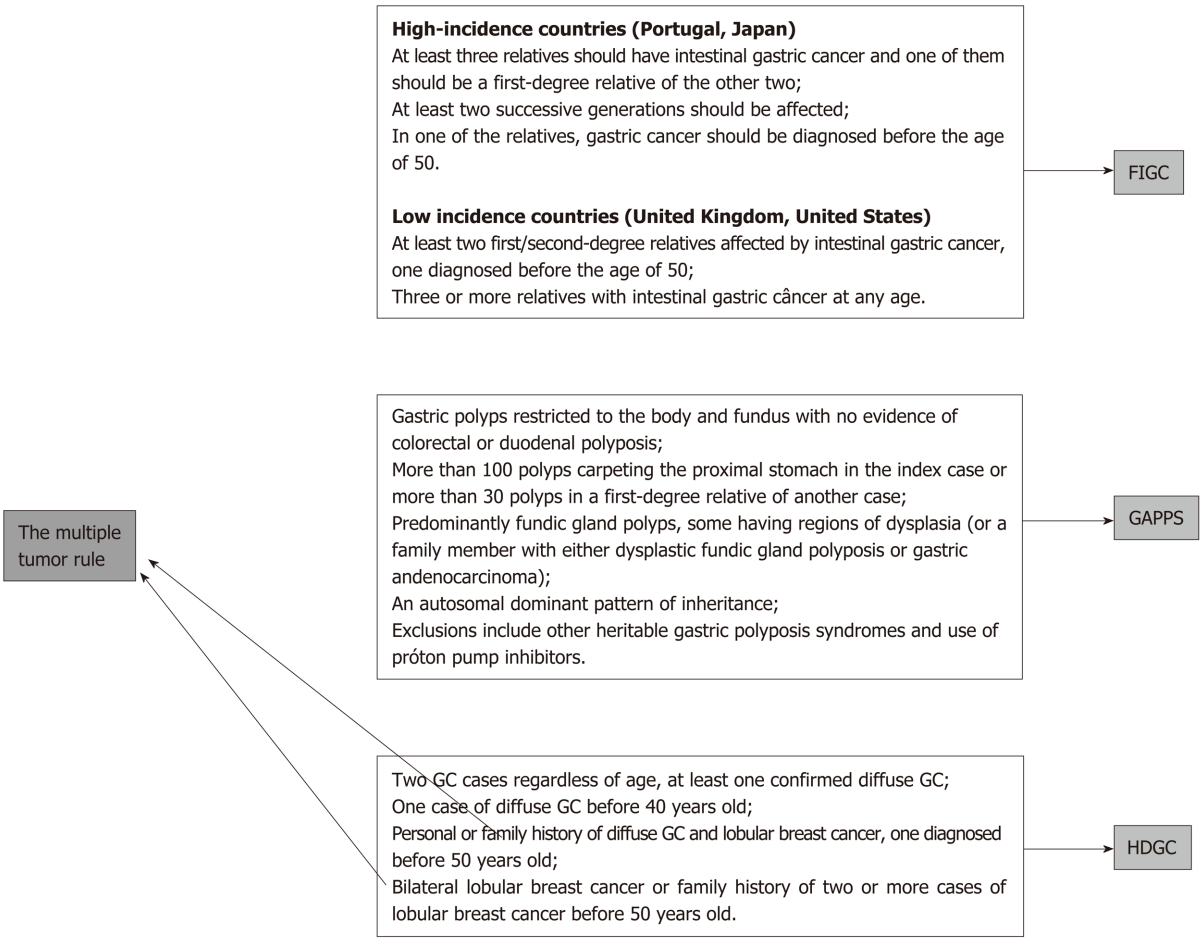

Figure 2 Diagnosis criteria for hereditary gastric cancer caught by rule number 2. GC: Gastric cancer; FIGC: Familial intestinal gastric cancer; GAPPS: Gastric adenocarcinoma and proximal polyposis of stomach; HDGC: Hereditary diffuse gastric cancer.

diagnosis, even in high-incidence areas. If every case is of the intestinal type, FIGC syndrome guidelines require annual endoscopies beginning at 40 years old for first- and second-degree relatives[9,11].

When at least one diffuse GC case is present, a molecular test is necessary, and according to this result, total prophylactic gastrectomy or dedicated annual endoscopies starting at 20 years old will be necessary[9,11,16].

Figure 5 presents some of the possibilities for identifying hereditary diffuse tumors via the application of rule number 1.

The management of hereditary diffuse gastric cancer syndrome is presented in Figure 6. With a clinical diagnosis of HDGC, there is a formal indication for genetic investigation by sequencing of the *CDH1* gene. If a functional mutation is discovered, every first- and second-degree relative will be investigated for that specific mutation by a much simpler and cheaper test, with no need for complete *CDH1* gene sequencing[11,17].

Everyone who carries the functional mutation needs to be evaluated by a multiprofessional team including a cancer geneticist and accordingly may undergo a prophylactic total gastrectomy. In the case of a negative genetic test, or if the carrier of the mutation does not agree to undergo total gastrectomy, annual dedicated endoscopies are indicated, including multiple insufflation and deflation schemes and both random and directed biopsies carried out by a senior endoscopist[16,17].

Regarding intestinal-type gastric cancers, rule number 1 will not result in a genetic test, but the patient's relatives identified by this rule will be included in a formal program of annual endoscopies beginning at 40 years old (Figure 7)[9,11,16].

POSSIBLE CONSEQUENCES OF THE POLYPOSIS RULE

Although extremely rare, the association of gastric polyposis and GC is a sign of HGC. GAPPS is very rare, with few affected families described. The main difference

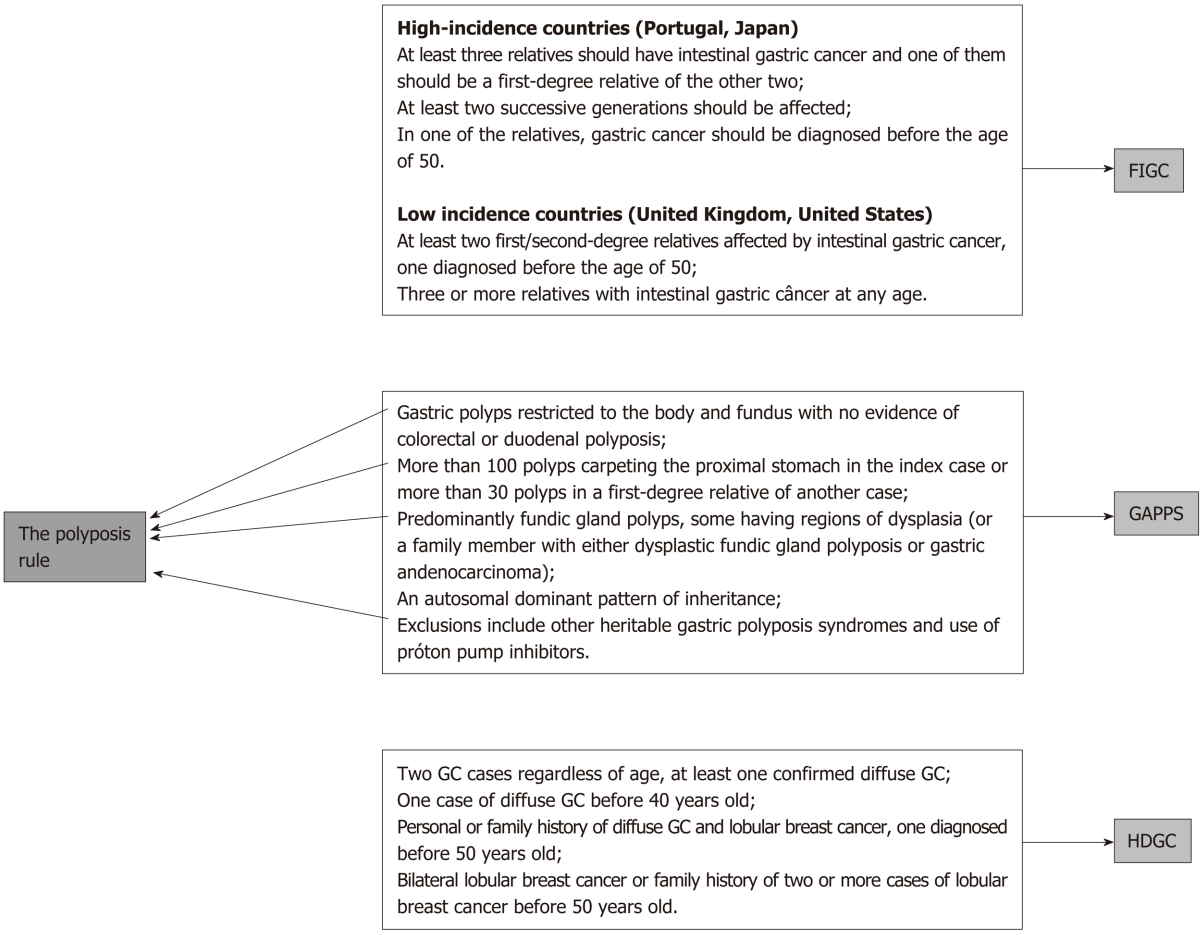

Figure 3 Diagnosis criteria for hereditary gastric cancer caught by rule number 3. GC: Gastric cancer; FIGC: Familial intestinal gastric cancer; GAPPS: Gastric adenocarcinoma and proximal polyposis of stomach; HDGC: Hereditary diffuse gastric cancer.

from other polyposis syndromes is the exclusive gastric involvement and the restricted localization of the polyps to the corpus and fundus. This syndrome is attributed to a mutation in the promoter region of the *APC* gene, the gene classically related to familial adenomatosis polyposis, which is characterized by colon polyposis and also carries a risk for associated GC[18-20].

In addition to FAP, juvenile polyposis and Peutz-Jeghers syndrome can also cause stomach polyposis and GC[11,21].

In the case of GC and polyposis, a specialized investigation is necessary, and the management will depend on the type of hereditary syndrome, potentially including investigational ant therapeutic procedures in other organs, such as the colon and rectum[11,21].

POSSIBILITIES OF THE MULTIPLE TUMOR RULE

The presence of multiple tumors, both those restricted to the stomach and other primary tumors affecting distant sites, should alert suspicion for HGC. Although second primary cancers can occur regardless of a hereditary cause, this rule should always be applied to allow rare hereditary cancer discovery[11,22].

GASTRIC + GASTRIC

A patient with two or more synchronic GC tumors may be affected by HGC. Multiple diffuse GCs are frequently found in diffuse hereditary gastric cancer syndrome. Even if not caught by rule number 1, a patient with diffuse tumors of signet ring cells, although not fulfilling the formal clinical criteria for this syndrome, must undergo a *CDH1* molecular investigation[11,22,23]. The recommendations for management according to the molecular diagnosis must be followed as described above.

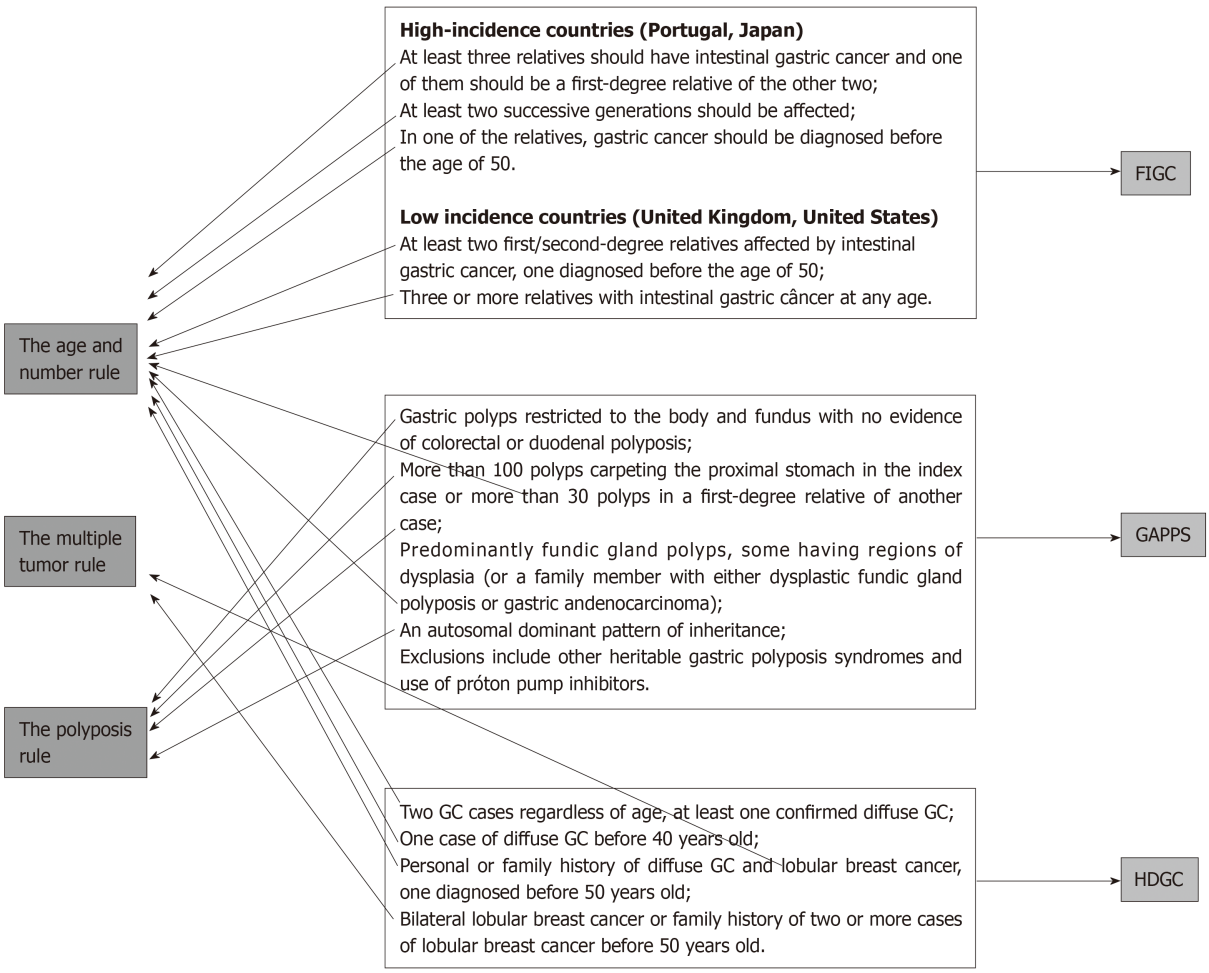

Figure 4 The three-rules strategy, comprising every current clinical criterion. GC: Gastric cancer; FIGC: Familial intestinal gastric cancer; GAPPS: Gastric adenocarcinoma and proximal polyposis of stomach; HDGC: Hereditary diffuse gastric cancer.

Gastric stump cancers following gastrectomy due to GC are usually related to environmental causes, such as Epstein-Barr virus infection and alkaline reflux[24,25]. Additionally, the cancer field effect plays a role in this situation, since previous exposure to carcinogenic insults might have caused previous driver mutations in the remaining mucosa, which favor posterior development of a second primary tumor. Nevertheless, diffuse histology enhances suspiciousness for HGC[26-28].

GASTRIC + BREAST

The association of diffuse gastric cancer and lobular breast cancer is enough to secure an HDGC clinical diagnosis and requires molecular *CDH1* investigation and additional investigational and therapeutic measures, as discussed. In addition to the already cited procedures, possible prophylactic bilateral mastectomy, according to genetic counsel, and mandatory annual breast MRIs are also recommended[17,27,29].

Typical breast cancer syndromes, in addition to bringing a high risk for breast and ovarian cancer, also carry GC risk, and those associations require specialized management[17,30].

GASTRIC + COLON

Many studies have suggested that HDGC may be associated with colorectal carcinoma (CRC) because this type of cancer has been observed in some HDGC families[31-36]. However, despite studies demonstrating the correlation between CRC and the *CDH1* mutation, there is insufficient evidence to propose that the risk of CRC in *CDH1* mutation carriers is significantly elevated, and there are no

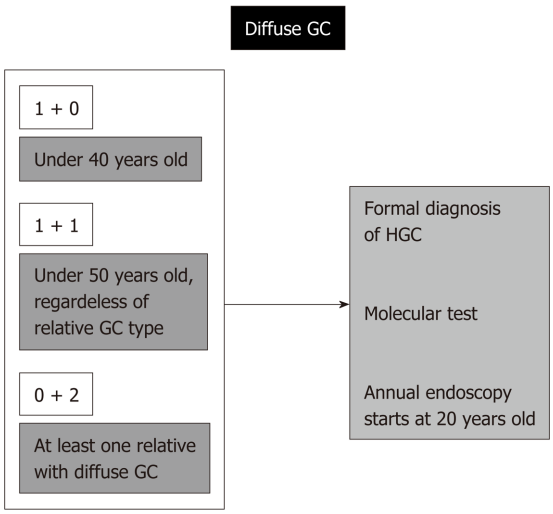

Figure 5 How to diagnose and manage hereditary diffuse gastric cancer by applying rule number 1. The first numbers in white squares refer to early-onset (under 50 years old) cases, and the second numbers refer to the quantity of affected relatives. GC: Gastric cancer; HGC: Hereditary gastric cancer.

recommendations in current clinical practice for CRC screening in *CDH1* mutation carriers[8,37].

RARE TUMORS

Although patients with rare tumors do not frequently harbor concomitant HGC, this suspicion should be maintained. Rare tumors usually result from hereditary cancer syndromes; thus, specialized care might be required.

ADDITIONAL BENEFITS OF THE AGE AND NUMBER RULE BEYOND HGC

Application of rule number 1 may bring additional benefits, favoring the early diagnosis of nonhereditary GCs.

Regarding environmentally caused GC, the environmental cancer-related factors that usually cause sporadic GC are also present in some of the patients' relatives, such as *H. pylori* and alimentary habits[2,6,7]. Since the majority of people exposed to such carcinogens will never develop GC, the affected minority might have a peculiar genetic background, such as specific gene polymorphisms. These polymorphisms are not enough to cause cancer, but in cases of exposure to environmental carcinogens, they favor cancer development[38,39]. The genetic background necessary for the occurrence of sporadic environmental GC includes germline traits shared by most of the patient's relatives. Therefore, investigating the relatives of GC patients caught by rule number 1, even if they do not reach a formal diagnosis of HGC, might result in finding additional sporadic cases or in subsequent fulfillment of the criteria for HGC.

The replicative cause of GC is due to random errors during the replication of stem cell DNA. Since these replicative errors might be more common in cases with an accumulation of DNA polymorphisms in replicative genes, as well as in DNA repair genes, these DNA polymorphisms might result in a major chance for "random" DNA replication errors to affect driver mutations in stem cells[40].

Accordingly, relatives sharing these genetic backgrounds might be identified by rule number 1.

To provide wide access to the benefits of the three rules, a mobile app is under development and will be available shortly free of charge.

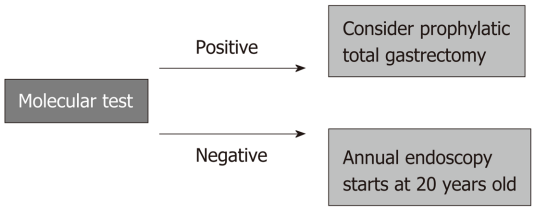

Figure 6 Clinical management of hereditary diffuse gastric cancer syndrome.

CONCLUSION

Although there is potential for discovering GC at early stages among relatives of patients affected by HGC, this possibility is mostly underexplored due to the low suspicion of HGC syndromes. A significant increase in HGC diagnosis may be achieved by applying simple rules for HGC diagnosis triage that are accessible to nonspecialized health-care professionals both in nations with high and low incidence of gastric cancer.

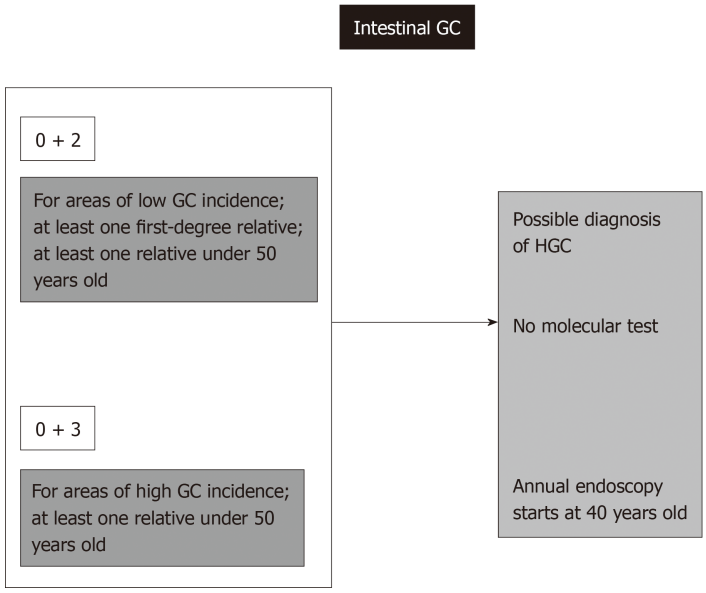

Figure 7 How to diagnose and manage familial intestinal gastric cancer by applying rule number 1. GC: Gastric cancer; HGC: Hereditary gastric cancer.

ACKNOWLEDGEMENTS

We acknowledge Universidade Federal do Pará (PROPESP and Fadesp) for technical support and Conselho Nacional de Desenvolvimento Científico e Tecnológico (CNPq) for fellowship support.

REFERENCES

1 **Tomasetti C**, Li L, Vogelstein B. Stem cell divisions, somatic mutations, cancer etiology, and cancer prevention. *Science* 2017; **355**: 1330-1334 [PMID: 28336671 DOI: 10.1126/science.aaf9011]
2 **Yusefi AR**, Bagheri Lankarani K, Bastani P, Radinmanesh M, Kavosi Z. Risk Factors for Gastric Cancer: A Systematic Review. *Asian Pac J Cancer Prev* 2018; **19**: 591-603 [PMID: 29579788 DOI: 10.22034/APJCP.2018.19.3.591]
3 **Petrovchich I**, Ford JM. Genetic predisposition to gastric cancer. *Semin Oncol* 2016; **43**: 554-559 [PMID: 27899187 DOI: 10.1053/j.seminoncol.2016.08.006]
4 **Shi J**, Qu YP, Hou P. Pathogenetic mechanisms in gastric cancer. *World J Gastroenterol* 2014; **20**: 13804-13819 [PMID: 25320518 DOI: 10.3748/wjg.v20.i38.13804]
5 **de Assumpção PP**, Araújo TMT, de Assumpção PB, Barra WF, Khayat AS, Assumpção CB, Ishak G, Nunes DN, Dias-Neto E, Coelho LGV. Suicide journey of H. pylori through gastric carcinogenesis: the role of non-H. pylori microbiome and potential consequences for clinical practice. *Eur J Clin Microbiol Infect Dis* 2019; **38**: 1591-1597 [PMID: 31114971 DOI: 10.1007/s10096-019-03564-5]
6 **Sitarz R**, Skierucha M, Mielko J, Offerhaus GJA, Maciejewski R, Polkowski WP. Gastric cancer: epidemiology, prevention, classification, and treatment. *Cancer Manag Res* 2018; **10**: 239-248 [PMID: 29445300 DOI: 10.2147/CMAR.S149619]
7 **Tsukamoto T**, Nakagawa M, Kiriyama Y, Toyoda T, Cao X. Prevention of Gastric Cancer: Eradication of Helicobacter Pylori and Beyond. *Int J Mol Sci* 2017; **18**: pii: E1699 [PMID: 28771198 DOI: 10.3390/ijms18081699]
8 **van der Post RS**, Oliveira C, Guilford P, Carneiro F. Hereditary gastric cancer: what's new? Update 2013-2018. *Fam Cancer* 2019; **18**: 363-367 [PMID: 30989426 DOI: 10.1007/s10689-019-00127-7]
9 **Boland CR**, Yurgelun MB. Historical Perspective on Familial Gastric Cancer. *Cell Mol Gastroenterol Hepatol* 2017; **3**: 192-200 [PMID: 28275686 DOI: 10.1016/j.jcmgh.2016.12.003]
10 **Syngal S**, Brand RE, Church JM, Giardiello FM, Hampel HL, Burt RW; American College of Gastroenterology. ACG clinical guideline: Genetic testing and management of hereditary gastrointestinal cancer syndromes. *Am J Gastroenterol* 2015; **110**: 223-62; quiz 263 [PMID: 25645574 DOI: 10.1038/ajg.2014.435]
11 **Setia N**, Clark JW, Duda DG, Hong TS, Kwak EL, Mullen JT, Lauwers GY. Familial Gastric Cancers. *Oncologist* 2015; **20**: 1365-1377 [PMID: 26424758 DOI: 10.1634/theoncologist.2015-0205]
12 **Chun N**, Ford JM. Genetic testing by cancer site: stomach. *Cancer J* 2012; **18**: 355-363 [PMID: 22846738 DOI: 10.1097/PPO.0b013e31826246dc]
13 **Vangala DB**, Cauchin E, Balmaña J, Wyrwicz L, van Cutsem E, Güller U, Castells A, Carneiro F, Hammel P, Ducreux M, van Laethem JL, Matysiak-Budnik T, Schmiegel W. Screening and surveillance in hereditary gastrointestinal cancers: Recommendations from the European Society of Digestive Oncology (ESDO) expert discussion at the 20th European Society for Medical Oncology (ESMO)/World Congress on Gastrointestinal Cancer, Barcelona, June 2018. *Eur J Cancer* 2018; **104**: 91-103 [PMID: 30342310 DOI: 10.1016/j.ejca.2018.09.004]
14 **Polom K**, Marrelli D, D'Ignazio A, Roviello F. Hereditary diffuse gastric cancer: how to look for and how to manage it. *Updates Surg* 2018; **70**: 161-166 [PMID: 29869323 DOI: 10.1007/s13304-018-0545-1]

15 **Kluijt I**, Sijmons RH, Hoogerbrugge N, Plukker JT, de Jong D, van Krieken JH, van Hillegersberg R, Ligtenberg M, Bleiker E, Cats A; Dutch Working Group on Hereditary Gastric Cancer. Familial gastric cancer: guidelines for diagnosis, treatment and periodic surveillance. *Fam Cancer* 2012; **11**: 363-369 [PMID: 22388873 DOI: 10.1007/s10689-012-9521-y]

16 **Oliveira C**, Pinheiro H, Figueiredo J, Seruca R, Carneiro F. Familial gastric cancer: genetic susceptibility, pathology, and implications for management. *Lancet Oncol* 2015; **16**: e60-e70 [PMID: 25638682 DOI: 10.1016/S1470-2045(14)71016-2]

17 **Kaurah P**, Huntsman DG. In: Adam MP, Ardinger HH, Pagon RA, Wallace SE, Bean LJH, Stephens K, Amemiya A, editors. Hereditary Diffuse Gastric Cancer. Seattle (WA): University of Washington, Seattle; 1993-2019 [PMID: 20301318]

18 **Rudloff U**. Gastric adenocarcinoma and proximal polyposis of the stomach: diagnosis and clinical perspectives. *Clin Exp Gastroenterol* 2018; **11**: 447-459 [PMID: 30584346 DOI: 10.2147/CEG.S163227]

19 **Mitsui Y**, Yokoyama R, Fujimoto S, Kagemoto K, Kitamura S, Okamoto K, Muguruma N, Bando Y, Eguchi H, Okazaki Y, Ishida H, Takayama T. First report of an Asian family with gastric adenocarcinoma and proximal polyposis of the stomach (GAPPS) revealed with the germline mutation of the APC exon 1B promoter region. *Gastric Cancer* 2018; **21**: 1058-1063 [PMID: 29968043 DOI: 10.1007/s10120-018-0855-5]

20 **Beer A**, Streubel B, Asari R, Dejaco C, Oberhuber G. Gastric adenocarcinoma and proximal polyposis of the stomach (GAPPS) - a rare recently described gastric polyposis syndrome - report of a case. *Z Gastroenterol* 2017; **55**: 1131-1134 [PMID: 29141268 DOI: 10.1055/s-0043-117182]

21 **Islam RS**, Patel NC, Lam-Himlin D, Nguyen CC. Gastric polyps: a review of clinical, endoscopic, and histopathologic features and management decisions. *Gastroenterol Hepatol (NY)* 2013; **9**: 640-651 [PMID: 24764778]

22 **Cybulski C**, Nazarali S, Narod SA. Multiple primary cancers as a guide to heritability. *Int J Cancer* 2014; **135**: 1756-1763 [PMID: 24945890 DOI: 10.1002/ijc.28988]

23 **Luo W**, Fedda F, Lynch P, Tan D. CDH1 Gene and Hereditary Diffuse Gastric Cancer Syndrome: Molecular and Histological Alterations and Implications for Diagnosis And Treatment. *Front Pharmacol* 2018; **9**: 1421 [PMID: 30568591 DOI: 10.3389/fphar.2018.01421]

24 **Rawla P**, Barsouk A. Epidemiology of gastric cancer: global trends, risk factors and prevention. *Prz Gastroenterol* 2019; **14**: 26-38 [PMID: 30944675 DOI: 10.5114/pg.2018.80001]

25 **Diogo Filho A**, Botelho LF, Nishiyama A, Zumpano LE, Monte RC, Rosa SC. Gastric stump cancer after gastrectomy by gastroduodenal peptic ulcer. *Arq Bras Cir Dig* 2016; **29**: 65 [PMID: 27120745 DOI: 10.1590/0102-6720201600010017]

26 **Assumpção MB**, Moreira FC, Hamoy IG, Magalhães L, Vidal A, Pereira A, Burbano R, Khayat A, Silva A, Santos S, Demachki S, Ribeiro-Dos-Santos Â, Assumpção P. High-Throughput miRNA Sequencing Reveals a Field Effect in Gastric Cancer and Suggests an Epigenetic Network Mechanism. *Bioinform Biol Insights* 2015; **9**: 111-117 [PMID: 26244015 DOI: 10.4137/BBI.S24066]

27 **Tan RY**, Ngeow J. Hereditary diffuse gastric cancer: What the clinician should know. *World J Gastrointest Oncol* 2015; **7**: 153-160 [PMID: 26380059 DOI: 10.4251/wjgo.v7.i9.153]

28 **Dotto GP**. Multifocal epithelial tumors and field cancerization: stroma as a primary determinant. *J Clin Invest* 2014; **124**: 1446-1453 [PMID: 24691479 DOI: 10.1172/JCI72589]

29 **Ford JM**. Hereditary Gastric Cancer: An Update at 15 Years. *JAMA Oncol* 2015; **1**: 16-18 [PMID: 26182297 DOI: 10.1001/jamaoncol.2014.187]

30 **Njoroge SW**, Burgess KR, Cobleigh MA, Alnajar HH, Gattuso P, Usha L. Hereditary diffuse gastric cancer and lynch syndromes in a BRCA1/2 negative breast cancer patient. *Breast Cancer Res Treat* 2017; **166**: 315-319 [PMID: 28702897 DOI: 10.1007/s10549-017-4393-3]

31 **Lo W**, Zhu B, Sabesan A, Wu HH, Powers A, Sorber RA, Ravichandran S, Chen I, McDuffie LA, Quadri HS, Beane JD, Calzone K, Miettinen MM, Hewitt SM, Koh C, Heller T, Wacholder S, Rudloff U. Associations of CDH1 germline variant location and cancer phenotype in families with hereditary diffuse gastric cancer (HDGC). *J Med Genet* 2019; **56**: 370-379 [PMID: 30745422 DOI: 10.1136/jmedgenet-2018-105361]

32 **Hamilton LE**, Jones K, Church N, Medlicott S. Synchronous appendiceal and intramucosal gastric signet ring cell carcinomas in an individual with CDH1-associated hereditary diffuse gastric carcinoma: a case report of a novel association and review of the literature. *BMC Gastroenterol* 2013; **13**: 114 [PMID: 23849133 DOI: 10.1186/1471-230X-13-114]

33 **Brooks-Wilson AR**, Kaurah P, Suriano G, Leach S, Senz J, Grehan N, Butterfield YS, Jeyes J, Schinas J, Bacani J, Kelsey M, Ferreira P, MacGillivray B, MacLeod P, Micek M, Ford J, Foulkes W, Australie K, Greenberg C, LaPointe M, Gilpin C, Nikkel S, Gilchrist D, Hughes R, Jackson CE, Monaghan KG, Oliveira MJ, Seruca R, Gallinger S, Caldas C, Huntsman D. Germline E-cadherin mutations in hereditary diffuse gastric cancer: assessment of 42 new families and review of genetic screening criteria. *J Med Genet* 2004; **41**: 508-517 [PMID: 15235021 DOI: 10.1136/jmg.2004.018275]

34 **Oliveira C**, Bordin MC, Grehan N, Huntsman D, Suriano G, Machado JC, Kiviluoto T, Aaltonen L, Jackson CE, Seruca R, Caldas C. Screening E-cadherin in gastric cancer families reveals germline mutations only in hereditary diffuse gastric cancer kindred. *Hum Mutat* 2002; **19**: 510-517 [PMID: 11968083 DOI: 10.1002/humu.10068]

35 **Pharoah PD**, Guilford P, Caldas C; International Gastric Cancer Linkage Consortium. Incidence of gastric cancer and breast cancer in CDH1 (E-cadherin) mutation carriers from hereditary diffuse gastric cancer families. *Gastroenterology* 2001; **121**: 1348-1353 [PMID: 11729114 DOI: 10.1053/gast.2001.29611]

36 **Salahshor S**, Hou H, Diep CB, Loukola A, Zhang H, Liu T, Chen J, Iselius L, Rubio C, Lothe RA, Aaltonen L, Sun XF, Lindmark G, Lindblom A. A germline E-cadherin mutation in a family with gastric and colon cancer. *Int J Mol Med* 2001; **8**: 439-443 [PMID: 11562785 DOI: 10.3892/ijmm.8.4.439]

37 **Figueiredo J**, Melo S, Carneiro P, Moreira AM, Fernandes MS, Ribeiro AS, Guilford P, Paredes J, Seruca R. Clinical spectrum and pleiotropic nature of *CDH1* germline mutations. *J Med Genet* 2019; **56**: 199-208 [PMID: 30661051 DOI: 10.1136/jmedgenet-2018-105807]

38 **Cai M**, Dai S, Chen W, Xia C, Lu L, Dai S, Qi J, Wang M, Wang M, Zhou L, Lei F, Zuo T, Zeng H, Zhao X. Environmental factors, seven GWAS-identified susceptibility loci, and risk of gastric cancer and its precursors in a Chinese population. *Cancer Med* 2017; **6**: 708-720 [PMID: 28220687 DOI: 10.1002/cam4.1038]

39 **Peng Q**, Chen Z, Lu Y, Lao X, Mo C, Li R, Qin X, Li S. Current evidences on XPC polymorphisms and gastric cancer susceptibility: a meta-analysis. *Diagn Pathol* 2014; **9**: 96 [PMID: 24886180 DOI: 10.1186/1746-1596-9-96]

40 **Tomasetti C**, Vogelstein B. Cancer etiology. Variation in cancer risk among tissues can be explained by the number of stem cell divisions. *Science* 2015; **347**: 78-81 [PMID: 25554788 DOI: 10.1126/science.1260825]

World Journal of Gastroenterology

Submit a Manuscript: https://www.f6publishing.com

World J Gastroenterol 2020 April 7; 26(13): 1394-1426

DOI: 10.3748/wjg.v26.i13.1394

ISSN 1007-9327 (print) ISSN 2219-2840 (online)

REVIEW

Mouse models of colorectal cancer: Past, present and future perspectives

Florian Bürtin, Christina S Mullins, Michael Linnebacher

ORCID number: Florian Bürtin (0000-0001-9927-1852); Christina S Mullins (0000-0003-2296-2027); Michael Linnebacher (0000-0001-8054-1402).

Author contributions: Linnebacher M was the main author involved in conception of the review including topics and angles addressed; Bürtin F performed the extensive PubMed search and drafted a first version; Mullins CS was the main author involved in manuscript editing including language editing; all authors participated in drafting the article and revising it critically for important intellectual content; and all authors gave their final approval of the submitted and revised version.

Supported by the State Mecklenburg-Vorpommern, No. TBI-V-1-241-VBW-084.

Conflict-of-interest statement: Dr. Linnebacher reports grants from Ministerium für Wirtschaft, Arbeit und Gesundheit Mecklenburg-Vorpommern during the conduct of the study.

Florian Bürtin, Department of General, Visceral, Vascular and Transplantation Surgery, University Medical Center Rostock, University of Rostock, Rostock 18057, Germany

Christina S Mullins, Department of Thoracic Surgery, University Medical Center Rostock, University of Rostock, Rostock 18057, Germany

Michael Linnebacher, Molecular Oncology and Immunotherapy, Department of General, Visceral, Vascular and Transplantation Surgery, University Medical Center Rostock, Rostock 18057, Germany

Corresponding author: Michael Linnebacher, PhD, Academic Fellow, Research Fellow, Research Scientist, Senior Researcher, Senior Scientist, Molecular Oncology and Immunotherapy, Department of General, Visceral, Vascular and Transplantation Surgery, University Medical Center Rostock, Schillingallee 69, Rostock 18057, Germany. michael.linnebacher@med.uni-rostock.de

Abstract

Colorectal cancer (CRC) is the third most common diagnosed malignancy among both sexes in the United States as well as in the European Union. While the incidence and mortality rates in western, high developed countries are declining, reflecting the success of screening programs and improved treatment regimen, a rise of the overall global CRC burden can be observed due to lifestyle changes paralleling an increasing human development index. Despite a growing insight into the biology of CRC and many therapeutic improvements in the recent decades, preclinical *in vivo* models are still indispensable for the development of new treatment approaches. Since the development of carcinogen-induced rodent models for CRC more than 80 years ago, a plethora of animal models has been established to study colon cancer biology. Despite tenuous invasiveness and metastatic behavior, these models are useful for chemoprevention studies and to evaluate colitis-related carcinogenesis. Genetically engineered mouse models (GEMM) mirror the pathogenesis of sporadic as well as inherited CRC depending on the specific molecular pathways activated or inhibited. Although the vast majority of CRC GEMM lack invasiveness, metastasis and tumor heterogeneity, they still have proven useful for examination of the tumor microenvironment as well as systemic immune responses; thus, supporting development of new therapeutic avenues. Induction of metastatic disease by orthotopic injection of CRC cell lines is possible, but the so generated models lack genetic diversity and the number of suited cell lines is very limited. Patient-derived xenografts, in contrast, maintain the pathological and molecular characteristics of the individual patient's CRC after subcutaneous implantation into immunodeficient mice and

Manuscript source: Invited manuscript

Received: December 18, 2019
Peer-review started: December 18, 2019
First decision: February 18, 2020
Revised: March 5, 2020
Accepted: March 10, 2020
Article in press: March 10, 2020
Published online: April 7, 2020

P-Reviewer: Li Y, Lin JM, Huang ZH
S-Editor: Dou Y
L-Editor: A
E-Editor: Ma YJ

are therefore most reliable for preclinical drug development – even in comparison to GEMM or cell line-based analyses. However, subcutaneous patient-derived xenograft models are less suitable for studying most aspects of the tumor microenvironment and anti-tumoral immune responses. The authors review the distinct mouse models of CRC with an emphasis on their clinical relevance and shed light on the latest developments in the field of preclinical CRC models.

Key words: Colorectal cancer; Mouse models; Patient-derived xenografts; Carcinogen-induced models; Genetically engineered mouse models; Preclinical drug development

Core tip: This review highlights the different approaches to model colorectal cancer in the mouse. Carcinogen-induced rodent models, genetically engineered mouse models, heterotopic and orthotopic models as well as patient-derived xenografts are discussed with an emphasis on their specific advantages and disadvantages. Moreover, the historical background of animal models for cancer research and the future perspectives of colorectal cancer research are reviewed as well.

Citation: Bürtin F, Mullins CS, Linnebacher M. Mouse models of colorectal cancer: Past, present and future perspectives. *World J Gastroenterol* 2020; 26(13): 1394-1426
URL: https://www.wjgnet.com/1007-9327/full/v26/i13/1394.htm
DOI: https://dx.doi.org/10.3748/wjg.v26.i13.1394

INTRODUCTION

Colorectal cancer (CRC) is the third most common diagnosed malignancy among both sexes in the United States as well as in the European Union[1,2]. A decrease in the incidence and overall mortality of CRC in countries with a very high development index over the last decades can be attributed to an interplay of screening programs with detection of precancerous lesions or early stage cancers on the one hand[3,4], and improved therapeutic concepts leading to an increased stage adjusted survival for all stages of CRC on the other hand[5]. This development is in sharp contrast to countries with a rapidly growing high development index. Together with an increased CRC incidence and mortality this reflects an adoption of the so-called "western lifestyle" including the risk factors for CRC. While obesity, smoking and red meat consumption are significantly associated with an elevated CRC risk[6], physical activity, high vegetable, fruit and fiber intake as well as metronomic aspirin therapy, have shown to decrease CRC risk[7,8]. Besides these modifiable risk factors, a variety of genetic factors influences CRC risk. About 5% of CRC cases are caused by hereditary, highly penetrant cancer syndromes, like familial adenomatous polyposis (FAP) and Lynch syndrome (LS); whereas up to 20%-30% of cases are considered as "familial" due to different germline mutations of varying penetrance[9]. Since the discovery of the link between APC germline mutations and FAP[10], followed by the genetic pathology of LS in the early 1990s[11,12], a myriad of mutations contributing to CRC genesis has been identified, constantly reshaping the genomic landscape of the disease[13]. The ideal model of CRC should recapitulate the progress from a precancerous adenoma to an invasive carcinoma with metastatic potential and at the same time it has to reflect the inter-individual molecular diversity of the disease. Consequently, a single (mouse) model of CRC simply cannot match all of these requirements. In this review, we discuss the different mouse models of CRC with their distinct advantages and disadvantages with a focus on their translational and clinical relevance.

CARCINOGEN-INDUCED MODELS

Carcinogen-induced models (CIM) in rodents look back on a long tradition but maintained their usefulness for certain applications to the present day. They provide a platform for dietary studies and give insights into the pathways of food-borne carcinogens and colitis-associated carcinogenesis. Administration of the chemical

compounds is possible *via* ad libitum feeding, oral gavage, intraperitoneal/subcutaneous (s.c.) or intramuscular injection, or enema.

In 1915, Yamagiwa *et al*[14] proofed the carcinogenic properties of coal tar by its repetitive application on the ears of rabbits. At about the same time, first researchers worked on colon carcinogenesis by applying chemical or radioactive substances[15-17]. In the 1960s, cycasin and its metabolite, methylazoxymethanol, have shown to induce cancers in rodents[18-20]. In the following years, the more chemically stable substances, azoxymethane (AOM) and its precursor molecule, 1,2-dimethylhydrazine as well as methylazoxymethyl acetate, were extensively used to induce colon carcinogenesis in mice and rats. All three compounds are metabolized to methylazoxyformaldehyde, which is able to alkylate the DNA bases guanine and thymine[21]. After being processed by Phase-II-reaction, it is secreted to the bile and exceeds its carcinogenic effect to the intestinal mucosa[22]. Interestingly, these compounds show different carcinogenic potential depending on the mouse strain, housing conditions and the way of administration[23-25]. Although most authors claim a certain organotropism for AOM and dimethylhydrazine, tumor formation happens mostly in the small intestine and relevant amounts of alkylated DNA adducts can be observed in the liver and the kidneys[26]. Moreover, intestinal carcinogenesis can be achieved by the oral or rectal application of the direct alkylating topic agents N-methyl-N-nitrosourea (MNU), 3,2′-dimethyl-4-aminobiphenyl and N-Methyl-N′-nitro-N-nitrosoguanidine of which the latter two are traditionally used in rats[27-29].

Other carcinogens gained attention in connection with the association between meat consumption and increased CRC risk[30]. Heterocyclic aromatic amines (HAA) form from the reaction between free amino acids, sugars and creatine at high temperatures during the cooking process of meat and fish[31], whereby 2-amino-1-methyl-6-phenylimidazo[4,5-b]pyridine (PhIP) and 2-Amino-9H-pyrido[2,3-b]indole are the most abundant HAA in various foods[32]. PhIP is metabolized by the liver enzyme CYP1A2 to N2-Hydroxy-PhIP, which then, after sulfation or acetylation, forms activated esters capable of DNA adduct formation[33]. Detoxification of PhIP and its metabolites is driven by glutathione conjugation and glucuronidation[34,35]. Glucuronide conjugates are excreted through urine and bile[36]. In case of the latter, hydrolyzation by bacterial beta-glucuronidases in the intestines liberate reactive PhIP metabolites, which not only affect the intestinal mucosa, but undergo enterohepatic circulation[37]. Important to consider is, that the metabolism of PhIP in rodents results in less reactive metabolites than in humans, and its carcinogenic potential measured in animal studies might be even higher in humans[38]. Nakagama *et al*[39], by combining a high fat diet with PhIP intake, showed the tumor enhancing properties of this food borne agent simulating the carcinogenic effects of the s.c. "western diet". Moreover, PhIP led to the formation of high-grade dysplasia and adenocarcinomas in a mouse model of chemical induced colitis[40]. Although other common foodborne HAAs have shown to induce dysplasia and carcinomas in rodents[41], they are rarely used for modelling colon carcinogenesis. Polycyclic aromatic hydrocarbons, as benzo[a]pyrene, may be used for chemoprevention studies but are insignificant for CRC modeling in general[42,43]. Dextran sodium sulfate (DSS) must also be mentioned when discussing chemical-induced CRC mouse models. Since the first report of an DSS-induced colitis model nearly 30 years ago[44], countless studies used DSS to simulate chronic inflammatory bowel diseases and we would recommend the reader to refer to excellent reviews discussing inflammatory bowel diseases and DSS[45]. As a sulfated polysaccharide, DSS directly damages the colonic epithelium resulting in an impairment of the mucosal barrier with consecutive entry of luminal bacteria and associated antigens into the mucosa, triggering inflammation[46]. Depending on the animal strain, DSS dosage and administration regimen, mice can develop acute and chronic colitis or even colitis-induced dysplastic lesions[47-50]. DSS in combination with carcinogenic compounds, primarily AOM, has been proven useful for the research of colitis-induced cancer[51]. By use of mice with germline *Apc* mutation (APC^{Min} mice) for DSS treatment, the rate of dysplasia and carcinoma formation was further enhanced[52]. Cooper *et al*[53] reported an increased CRC incidence of 40% in APC^{Min} mice after two cycles of 4% DSS treatment compared to untreated control animals and identified the loss of heterozygosity (LOH) of *Apc* as underlying cause.

Chemical-induced mouse models are not homogenous and possess specific advantages and disadvantages. They are by far the oldest method inducing CRC in animals and a multitude of studies has been traditionally carried out in rats and other rodents diminishing the comparability of older data with more recent results. Most models reflect very well the progression from aberrant crypt foci to adenomas to carcinomas of the human adenoma-carcinoma sequence[54]. Therefore, they are still useful to evaluate the influence of diet[55], dietary supplements[56,57], chemopreventive interventions[58,59] and the gut microbiome[60]. Especially the combination of DSS with carcinogenic agents provided many insights in the link between CRC and

inflammation[61]. However, chemical-induced carcinomas rarely show invasive properties and local or distant metastases are usually absent. Albeit Yang *et al*[62] reported lymph node metastases in an intrarectal MNU-model, the use of shrews (phylogenetic unrelated to rodents) as test animals interdicts the comparison to rodent animal models. A further exception is the work of Derry *et al*[63], who could observe a relevant number of lung metastases in an AOM-induced mouse model, which is to our knowledge the only report of metastatic spread in a chemical-induced mouse model. Besides the lack of invasiveness, a lot of CIM show a high latency from the first application to tumor development. Depending on the carcinogen, dosing protocol and mouse strain, latencies from 24 to 50 wk were reported[64-66]. By combining the carcinogen with DSS, the time to tumor development can be notably shortened to 10-18 wk[23,67]. Although the minority of sporadic CRC patients show synchronous adenomas[68,69], nearly all CIM show a "carpeting" of the colonic mucosa with polyps[70]. Tumor formation is not restricted to the colon, but can be commonly observed in the whole gastrointestinal tract[71,72]. Moreover, MNU additionally induces leukemia and lung adenomas[73] and PhIP leads to formation of mammary and prostate neoplasia[74]. Another complexing aspect of CIM concerns the genetic aberrations associated with the adenoma-carcinoma sequence, *i.e.*, the accumulation of mutations, predominantly affecting *APC, KRAS* and *P53*[75]. While the AOM model shows frequent *Kras* and *β-catenin* mutations, *Apc* and *P53* are rarely affected[76-79]. In contrast PhIP, IQ and MNU lead to *Apc* mutations, but show no *P53* or *Kras* mutations[21]. In general, the vast quantity of different dosing protocols, application forms and animal strains, makes direct comparisons and the selection of the right CIM difficult[54]. Another aspect, not to be neglected, is the agenda of animal welfare. Quite a few protocols lead to significant weight loss and diarrhea, which is, in combination with often long study durations, detrimental for the animal wellbeing[80].

GENETICALLY ENGINEERED MOUSE MODELS OF COLORECTAL CANCER

With the knowledge explosion concerning the genetic pathways altered in CRC at the end of the 20th century, the scientific community demanded specific genetic mouse models to focus on certain molecular mechanisms of colorectal carcinogenesis.

In the 1980s, the first genetically engineered mouse models (GEMM) of brain tumors, lymphoma, pancreatic cancer, breast cancer and osteosarcoma emerged[81-87]. Based on the groundbreaking work of Evans, Smithies and Capecchi[88] on gene targeting, the first tumor suppressor knock-out mouse models emerged in the early 1990s[89,90]. To circumvent the obstacle of frequent embryonic lethality caused by germline knock-outs of tumor suppressors, *Cre-loxP* mediated mouse models were designed to allow the tissue specific and conditional knock-out of tumor suppressor genes or activation of oncogenes, respectively[91-93]. Interestingly, the very first GEMM of CRC, the APC^{Min} mouse, was created without sophisticated methods. Moser *et al*[94] showed, that the application of N-ethyl-N-nitrosourea leads to nonsense mutations in codon 380 of the *Apc* gene and subsequent breeding of these animals established the first model for multiple intestinal neoplasia. APC^{Min} mice develop a large number of adenomas in the small intestine after 120-140 d due to LOH and show a high mortality with increasing age as a result of intestinal obstruction and anemia without progression to invasive carcinoma[95]. While these models contributed to the understanding of the early stages of FAP, they do not reflect the majority of spontaneous CRC[96]. Since a homozygous *Apc* mutation is lethal during embryonic development, breeding of homozygous APC^{Min} mice is impossible[97]. However, additional treatment of APC^{Min} mice with AOM or other carcinogenic compounds increases malignancy of the resulting tumors and simultaneously shortens the time to tumor development[98-100]. Till the present day, these models are in use for chemoprevention studies[101,102] and have enormously contributed to the understanding of the early tumor initiating events[103]. Interestingly, a change from C57BL/6 to a hybrid genetic background can extend the lifespan of APC^{Min} mice beyond one year, resulting in a high proportion of invasive adenocarcinoma[104]. Sødring *et al*[105] changed the APC^{Min} genetic background from C57BL/6 to A/J mice resulting in increased tumor formation in the colon, with a reasonable number of tumors progressing to carcinomas. Transgenic mice with alternative *Apc* mutations, like the APC$^{+/1638}$ mouse[106,107], the APC$^{\Delta 716}$ mouse[108] and the *APC*$^{\Delta 242/+}$ mouse[109] vary in tumor count and histopathology. Tumor formation predominantly in the small intestine instead of the colon is the major flaw of most *Apc*-based mouse models. Colnot *et al*[110] designed the APC$^{\Delta 14/+}$ mouse, which shows a more severe phenotype with invasion of the muscularis, an increased lethality and a higher colonic tumor

burden compared to APC^{Min} mice but unfavorably still shows relevant tumor development in the small intestine. Early attempts of combining *Apc* mutations with homozygous *P53* knockouts yielded conflicting results, with either no increase[111,112], or a small increase of gastrointestinal malignancy[113]. The most likely explanation is that in human cancers *P53* missense mutations frequently act in a dominant negative fashion, overruling the tumor-suppressive function of the wildtype allele[114,115]. In contrast, targeting *Kras* without tissue specific promoters leads either to embryogenic lethality[116] or few viable animals succumbing to rapidly developing lung tumors[117]. To avoid abundant distribution of mutations in the whole organism, transgene expression controlled by a tissue specific gene promotor, most commonly by application of the *Cre-loxP*-system[91], has proven to be extraordinarily useful. Many workgroups used *Villin-Cre* transgenes to restrict recombination of *floxP*-flanked genes to the epithelial cells of the small and large intestines either with a constitutive expression (Vil-Cre) or with a tamoxifen-inducible expression (Vil-Cre-ER^{T2})[118]. Another option of site-specific *Cre* expression is the fatty acid binding protein liver Cre transgene (*Fabpl Cre*), which can be combined with a tetracycline-inducible tet-on system[119]. Yet, both transgenes' expression is not limited to the large intestine: While *Villin-Cre* is expressed in the epithelial cells of the whole intestines, *Fabpl-Cre* expression can be detected in the distal small intestine, cecum and colon[119,120]. Also, the AhCre strain, carrying Cre under control of the Cyp1A promotor, is commonly used for colon cancer models[121,122]. Here, *Cre*-expression is induced by β-naphthoflavone in the liver and intestines, but constitutive recombination can be observed in other tissues like the renal epithelium[123]. To achieve a more colon specific expression of *Cre*-recombinase, Hinoi *et al*[124] constructed a transgene of *Cre* and the promotor region of the *CDX2* homeobox gene. By inserting a guanine repeat tract to this transgene (*CDX2P9.5-G22Cre*), stochastic activation of *Cre*-expression by means of spontaneous frameshift mutations leads to a mosaic-like recombination in the mucosa of the terminal ileum, cecum, and colon[125]. At last, carbonic anhydrase 1 promoter/enhancer-Cre recombinase transgene (*CAC*) facilitates recombination strictly limited to the large intestine[126]. Paralleling *Cre*-transgene implementation, others achieved spatiotemporal oncogene expression in the large intestine by delivering Cre by viral transfection *via* transanal injection, surgery or colonoscopy[127-129] leading to exquisite models of CRC with metastatic spread[130]. Supplied with this comprehensive genetic toolbox, a plethora of CRC mouse models were generated and used to evaluate the role of different mutations and their interplay. Among the non-hypermutated tumors, the most frequently mutated genes are *APC*, *P53*, *KRAS*, *PIK3CA*, *FBXW7*, *SMAD4*, and *TCF7L2*[13]. The role of *Apc* LOH as a driver mutation is highlighted in several mouse models. While generalized deletion of both *Apc* alleles (*Apc*$^{flox/flox}$) leads to rapid death by disorder of cell differentiation[131], mice with a mosaic–like deletion of both *Apc* genes die rapidly from florid polyposis[125]. Depending on the type and modality of *Apc* mutation, heterozygotes develop adenomas or invasive adenocarcinomas[120,132,133]. Whilst mutated *Kras* alone is insufficient to induce colorectal tumorigenesis, it increases the susceptibility of the intestinal mucosa to chemical carcinogenesis[134] and leads to accelerated tumor formation in combination with *Apc* loss[122,135]. *Nras* mutation, in contrast, does not alter the effect of *Apc* loss[136]. In humans, *P53* mutations are often associated with vascular and lymphatic invasion and advanced cancer stages[137,138]. In fact, the combination of *Apc* mutation with a dominant-negative *P53* mutation leads to increased invasiveness of intestinal tumors with signs of epithelial to mesenchymal transition[139,140]. Also, loss of *P53* in a constitutively active Notch signaling background leads to intestinal tumor formation and metastasis[141], whereas Notch signaling does not cooperate with the Wnt-pathway[142]. Nevertheless, *Apc* deficiency seems to represent a key prerequisite of cancer progression, since *Apc* restoration leads to spontaneous tumor regression of *Kras*-mutated, *P53*-deficient adenocarcinomas[143]. *FBXW7* codes for the F-box/WD repeat-containing protein 7, the substrate receptor of a ubiquitin ligase, which degrades several proto-oncogenes like *MYC, CCNE1, NOTCH1* and *JUN* and acts synergistically with *P53* as haploinsufficient tumor suppressor[144-146]. Intestinal *Fbxw7* deletion enhances tumor development in an *Apc*$^{Min/+}$background[147] and a combined deletion of *Fbxw7* and *P53* results in highly aggressive intestinal cancers with metastatic spread to the lymph nodes and liver[148]. The PI3K/AKT- pathway is well known for its pro-oncogenic and anti-apoptotic signaling and *PI3K* mutations are common in CRC and many other human cancers[149]. As demonstrated by Leystra *et al*[150], the intestinal expression of a constitutively active *Pi3k* (PIK3ca) is a sufficient driver mutation to induce rapid tumorigenesis with invasion of adjacent organs and addition of PIK3ca to a homozygous loss of *Apc*, drives adenoma-to-carcinoma progression with metastatic spread[129]. Although loss of *Pten*, the counterpart of *Pik3*, does not affect intestinal cell proliferation; in the context of *Apc* deficiency or other mutations, it promotes cancer progression[151-153]. *SMAD4* is

considered as a tumor suppressor, similar to other constitutes of the TGFβ-pathway[154,155]. Since the genes *Apc*, *Smad2* and *Smad4* are all located on chromosome 18 in the mouse, they are suited to generate distinct cis- and trans compound heterozygotes by meiotic recombination. Compared to their single mutation littermates, mice with combined *Apc* and *Smad4* mutations, show accelerated tumor development[156] and increased malignancy[157,158]. In contrast, compound heterozygotes of *Apc* and *Smad2* mutations show no increased tumor development compared to littermates with a single *Apc* mutation[159]. Notably, homozygous *Smad3* mutation leads to aggressive CRC with lymphatic spread and, upon *Apc* deficiency, drastically reduced life span[160,161]; but *SMAD3* is rarely mutated in human CRC[162]. Findings from several CRC-GEMM highlight the role of TGFβ-signaling as a strong tumor suppressor, since *Tgfβ*[163-165], as well as *Tgfβ*-receptor 2[140,166,167] knockout, induce local invasion and metastatic spread. Regarding the role of *TCF7L2* mutations in CRC, so far, no GEMM of CRC addressing this topic have been published. Besides the conventional adenoma-carcinoma sequence, the serrated pathway represents an alternative route of CRC development with distinct molecular and clinical features. The underlying *BRAFV600E* mutation occurs in 15%-20% of sporadic CRC, causes a constitutive activation of the MAPK/ERK pathway and is strongly associated with the CpG Island methylator phenotype and microsatellite instability (MSI) due to *MLH-1* methylation[168-170]. *BrafV600E* causes crypt hyperplasia and combined with *Apc* or *P53* mutations, as well as mutations affecting *Ink4A/Arf*, gives rise to invasive carcinomas[171-174]. Although not common in human CRC, mutation of the GSK3-β phosphorylation site causes degradation-resistant β-catenin[175,176], and has been remodeled in the mouse. GSK3β-resistant β-catenin increases proliferation of the intestinal epithelium and causes adenoma formation, but does not mediate malignant progression[177-179]. Paralleling the research on canonical cancer pathways, there has been reasonable effort to reproduce MSI, a hypermutable phenotype caused by malfunction of DNA mismatch repair (MMR) enzymes[180,181]. MSI-CRC can occur in the context of hereditary MMR gene mutations (LS) or can be detected in up to 15% of spontaneous CRC, caused by hypermethylation of MMR genes (spMSI)[182,183]. The constitutes of the MMR machinery have been extensively studied by somatic knockout models. Since the knockout of the MMR genes *MLH1*[184], *MSH2*[185,186], *MSH6*[187] and *PMS2*[188] predominantly cause hematopoietic malignancies with consecutive reduced lifespan in the mouse and consequently only a minor fraction of homozygotes develop intestinal neoplasia[189,190], these knockouts were frequently put in an APC deficient setting, to increase intestinal carcinogenesis[184,191,192]. Kucherlapati *et al*[193,194] demonstrated, that mutations of *Fen1* and/ or *Exo1*, both cooperation partners of MMR enzymes, lead to similar patterns of MSI tumor development. However, MSI-high tumors rarely show activation of the Wnt-pathway and are typically chromosomal stable, whereas *APC* mutations are typically associated with a chromosomal instable phenotype[195,196]. Therefore, these models do not adequately recapitulate Lynch-type or spMSI tumors. To overcome the aforementioned obstacles, a floxed *Msh2* allele was combined with either a LS related missense mutation ($Msh2^{G674D}$) or an $Msh2^{\Delta 7}$ null mutation in mice carrying a *Villin-Cre* transgene, leading to intestinal carcinogenesis and chemoresistance typical for MSI-high tumors[197]. An overview of the above addressed mutations can be found in Figure 1 and are summarized in Table 1.

In summary, GEMM have contributed enormously to the understanding of the molecular processes of CRC initiation, progression and crosstalk of common cancer-associated pathways. Besides the models for spontaneous CRC and common cancer syndromes, like Familiar Adenomatius Polyposis and LS, several models recapitulate metastatic disease, either as "classic" GEMM[141,148,166,198] or upon viral *Cre* delivery[129,130]. Yet, these models have several limitations. First of all, cancer development is a stepwise process with an initial driver mutation and subsequent acquisition of further mutations[199], and thus can only be partly reflected in tumor mouse models by the combination of a constitutively active with an inducible mutation[172]. Roper *et al*[128] recently demonstrated *in vivo* genome editing of *Apc* and *P53* by viral delivery of the correspondent sgRNA in mice expressing CRISPR-Cas9 under the control of a *Villin-Cre* transgene. Second, the number of combined mutations is limited in the mouse, since the resulting phenotype shows often a drastically reduced lifespan[152]. Triple mutant ($Car1^{CreER/+}$; $Apc^{fl/fl}$; $Kras^{LSL\text{-}G12D/+}$) and quadruple mutant mice ($Car1^{CreER/+}$; $Apc^{fl/fl}$; $Kras^{LSL\text{-}G12D/+}$; *P53*KO; $Smad4^{fl/fl}$) showed a reduced lifespan of merely one month. Moreover, GEMM are time consuming and expensive, since breeding of the transgenic mice often takes multiple generations and requires careful interbreeding to yield the desired alterations. In terms of animal welfare, it should be noted that the breeding process yields many "reject" mice, which are neither used for further breeding nor for research. Also, the construct of the transgene, or the viral vector, respectively, is complicated. While GEMM represent a valuable tool for basic

Table 1 Overview of genetically engineered mouse models

Link to Figure 1	Ref.	Methods	Results
1	[127]	*loxP* flanked *Apc exon* 14 (*Apc580S*) Colorectal tumor induction by rectal infection with *Cre*-delivering Adenovirus (*AxSRaCre*)	Adenoma formation in the distal rectum in most of the Apc^{580S} homozygotes. 50% of animals show invasive adenocarcinoma after 1 yr without lymphatic or distant metastases
2	[109]	$Apc^{\Delta 242/+}$	Adenomas: Higher in numbers but smaller in size and no differences in histology compared to $Apc^{Min/+}$ mice
3	[110]	$Apc^{\Delta 14/+}$	Shift of tumor distribution, more severe phenotype, invasion of muscularis propria, 50% dead after 12 mo
4	[120]	*Fabpl-Cre*; $Apc^{15lox/+}$	Increased survival due to lower number of tumors, but larger tumors predominantly in the colon, 91% at least low-grade adenoma, 50% carcinoma; invasiveness and metastases not reported
5	[108]	$Apc^{+/D716}$ (C57BL/6J background)	Intestinal polyposis with emphasis on the small intestine
6	[126]	*Cac*; $Apc^{580S/+}$	Transgene expression limited to the large intestine. Adenoma formation without malignancy
7	[125]	*CDX2P9.5-G22Cre* $Apc^{flox/flox}$	Frameshifted Cre-recombinase with a long guanine nucleotide tract under control of the homeobox promotor CDX2P9.5 leads to limited activation of Cre by spontaneous somatic mutations in the large intestine: $Apc^{flox/flox}$ homozygotes dye rapidly from florid polyposis of proximal colon and cecum
8	[374]	$Apc^{+/\Delta 716}$ $Cdx2^{+/-}$	Increased adenoma formation in the colon, reduced number of polyps in the small intestine
9	[132]	$Apc^{+/fle1-15}$; Villin-Cre mice (conditional) and $Apc^{\Delta e1-15}$ constitutive null allele	More severe polyposis compared to $Apc^{Min/+}$ mice
10	[375]	$BubR1^{+/-}$ $Apc^{Min/+}$	Increased tumor formation in the large intestine and higher malignancy through increased chromosomal instability (invasiveness and metastases not reported). Note, that *BUBR1* mutations are uncommon in CRC[376]
11	[377]	$\Delta^{cy}Ephb2;Apc^{Min/+}$ $Ephb3^{+/-};Apc^{Min/+}$ $Ephb3^{-/-};Apc^{Min/+}$	Reduced tumor formation in the small intestine, but large adenocarcinomas of the colorectum
12	[133]	$CDX2P\text{-}CreER^{T2}Apc^{flox/flox}$	Tamoxifen inducible *Apc*-knockout in the distal intestine
13	[378]	long living $Apc^{Min/+}$ mice	Some adenomas progress to adenocarcinomas
14	[104]	C57BL/6J $Apc^{Min/+}$ × SWR/J or C57BR/cdcJ	Hybrid $Apc^{Min/+}$ mice survive longer due to decreased adenoma frequency. After one-year high amount of invasive adenocarcinomas. 3% metastasis to lymph nodes
15	[105]	Change of the $Apc^{Min/+}$ genetic background from C57Bl6/J to A/J mice	Increased tumor formation in the intestine. 50% adenocarcinomas in the small intestine and 20% in the colon
16	[131]	$AhCre^{+}$; $Apc^{flox/flox}$	β-naphthoflavone-inducible Cyp1A promoter *Cre*-transgene (*AhCre*). Rapid death upon induction due to disruption of intestinal architecture
17	[98]	$Apc^{Min/+}$ + AOM	6-fold increase of colonic tumor formation compared to $Apc^{Min/+}$ mice
18	[379]	$Apc^{Min/+}$ + AOM	Increased incidence of colonic adenocarcinomas
19	[52]	$Apc^{Min/+}$ + DSS	High incidence of well differentiated colonic carcinomas
20	[380]	$Apc^{Min/+}$ + PhIP	2- to 3-fold increase of tumor formation compared to $Apc^{Min/+}$ mice

21	[99]	$Apc^{Min/+}$ + AOM + DSS	Mainly small intestinal tumor formation
22	[111]	$Apc^{Min/+}$ $P53^{-/-}$	No increased adenoma formation or malignancy compared to $Apc^{Min/+}$ $53^{-/+}$ - and $Apc^{Min/+}$ $P53^{+/+}$ -mice
23	[112]	$Apc^{Min/+}$ $P53^{-/-}$	No increased malignancy or adenoma formation compared to $Apc^{Min/+}$ mice
24	[381]	$Apc^{Min/+}$ $P53^{-/-}$	Slight, but not significant, increase in malignancy
25	[113]	$Apc^{Min/+}$ $Mom1^{R/R}$ $P53^{-/-}$ $Apc^{Min/+}$ $Mom1^{R/S}$ $P53^{-/-}$	P53 deficiency increases intestinal adenoma multiplicity and malignancy
26	[139]	$Apc^{\Delta 716}$ $Trp53^{+/LSL\cdot R270H}$ *Villin-CreER* $Apc^{\Delta 716}$ $Trp53^{LSL\cdot R270H/LSL\cdot R270H}$ *Villin-CreER*	Homozygotes die rapidly from lymphoma while heterozygous $P53^{R270H}$ leads to invasive adenocarcinomas with features of EMT
27	[128]	Deletion of *Apc and P53* by viral delivery of corresponding sgRNA into $Rosa26^{LSL\text{-}Cas9\text{-}eGFP/+}$; $Villin^{CreER}$	*In vivo* editing of *Apc* alone or in combination with P53 *via Cre* mediated Cas9-expression and provision of sgRNA by viral infection of the colonic epithelium leads to tumor formation without metastatic properties
28	[382]	*Fabpl:*$Cre^{+/o}$ $Tdg^{flox/-}$ $Apc^{Min/+}$	TDG knockout increases adenoma formation, no carcinomas
29	[122]	*AhCre*$^{+/T}$; $Kras^{+/LSLV12}$ *AhCre*$^{+/T}$; $Kras^{+/LSLV12}$, $Apc^{+/fl}$	Cytochrome p450 mediated Cre expression in the liver and intestine induced by β-naphthoflavone (*AhCre*). $Kras^{V12}$ mutation does not alter the intestinal epithelium, but combined with APC-loss, accelerates tumorigenesis in the intestine. 17% of the tumors are invasive adenocarcinomas
30	[383]	*CDX2P9.5-G22Cre;* $Apc^{flox/flox}$; $LSL\text{-}Kras^{G12D}$	Severe debilities in mice with reduced weight and lifespan and anal bulging. *Kras* mutation does not increase malignancy
31	[136]	*Fapbl-Cre;* $Apc^{2lox14/+}$; $Kras^{LSL\text{-}G12D/+}$ *Fapbl-Cre;* $Apc^{2lox14/+}$; $Nras^{LSL\text{-}G12D/+}$	$Kras^{G12D}$, but not $Nras^{G12D}$ drives colon cancer progression. *Nras* indistinct from $Apc^{Min/+}$ mice
32	[143]	*shApc/*$Kras^{G12D}$*/*$P53^{fl/fl}$*/Lgr5*	Mice with inducible and reversible *Apc* deletion *via* short hairpin RNA show duodenal and colonic tumor formation. Additional, conditional mutations drive cancer progression, but upon *Apc* restoration by withdrawal of doxycycline rapid tumor regression can be induced
33	[130,384]	Apc^{CKO}*/LSL-Kras*	Cre-mediated knockout of Apc and $Kras^{G12D}$ activation by surgical application of AdenoCre to the colonic epithelium leads to adenocarcinomas with 20% liver metastases after 20 weeks
34	[385]	$Apc^{+/580S}$, $Kras^{+/LSL}$, CAC^{+}	Only adenomas
35	[116]	*CMV-cre* × *LSL-* $Kras^{G12D}$ $LSL\text{-}Kras^{G12D}$*; Fabpl-Cre*	Germline embryonic expression of an endogenous $Kras^{G12D}$ allele is uniformly lethal. Diffuse colonic hyper- and dysplasia
36	[117]	$Kras^{+/V12}$ × *CMV-*$Cre^{+/T}$	High embryonic lethality; adult animals succumb to pulmonary neoplasia, no phenotypic changes in the intestine
37	[134]	$LSL\text{-}Kras^{G12D}$*/Villin-cre +AOM*	Increased number of microadenomas in the proximal colon
38	[198]	*Villin-Cre/K-*$ras^{G12Dint}$*/Ink4a/*$Arf^{-/-}$	Within 12 wk progression to invasive adenocarcinomas (79%) with 60% lung metastases
39	[165]	$Apc^{\Delta 716}$ $Tgfbr2^{flox/flox}$; *villin-CreER*	Disruption of TGFβ-signaling leads to locally invasive adenocarcinomas

40	[164]	AOM-treatment of *Fabpl*$^{4xat\text{-}132}$ *Cre; Tgfbr2*$^{flx/flx}$ mice	Higher incidence of colonic adenomas and adenocarcinomas
41	[167]	*Villin-Cre; Apc*$^{1638N/wt}$*; Tgfbr2*$^{flx/flx}$	Compared to *Apc*$^{1638N/wt}$ similar tumor incidence but increased progression to locally invasive adenocarcinoma
42	[163]	*Tgfb1*$^{-/-}$ *Rag2*$^{-/-}$	Rapid formation of adenomas and adenocarcinomas
43	[166]	*LSL-Kras*$^{G12D/wt}$*; Villin-Cre; Tgfbr2*$^{E2flx/E2flx}$	Wnt-independent induction of invasive carcinomas in the intestine with 15% distant metastases
44	[153]	*Villin-Cre; Pten*$^{flx/flx}$*; Tgfbr2*$^{flx/flx}$	Mice with inactivation of TGFβR2 combined with loss of PTEN show high number of mucinous adenocarcinomas throughout the intestine. 8% show distant metastases (not Wnt, but deregulation of CDK inhibitor expression). *Pten* loss without mutation has no effect
45	[152]	*Villin-CreER*^{T}*; Apc*$^{fl/+}$*; Pten*$^{fl/fl}$*; Kras*$^{LSL/+}$	*Villin-CreERT; Apcfl/+; Ptenfl/fl; KrasLSL/+* mice show rapid morbidity due to invasive small intestinal tumors
46	[151]	*AhCre; Pten*$^{f/f}$	PTEN is dispensable in the intestinal epithelium, but increases tumorigenesis in the context of APC deficiency
47	[386]	*Apc*$^{Min/+}$*Pld1*$^{-/-}$ *vs Apc*$^{Min/+}$*Pld1*$^{+/+}$ +AOM/DSS	*Pld1*-knockout/suppression leads to decreased tumor burden
48	[157]	*Dpc4*$^{+/-}$*: Apc*$^{+/\Delta 716}$	*Dpc4* and *Apc*$^{\Delta 716}$ cis-compound heterozygote mice show adenoma to carcinoma progression in the small intestine and colon with submucosal infiltration
49	[159]	*Smad2*$^{+/-}$*; Apc*$^{+/\Delta 716}$	Combination of *Apc* mutation and loss of *Smad2* leads to no changes in tumor size or properties compared to *Apc*$^{+/\Delta 716}$ mice
50	[161]	*Apc*$^{Min/+}$*; Smad3*$^{-/-}$	Reduced lifespan of 2 months due to rapid tumor development in the distal colon with mixed histology but no metastases
51	[156]	*Apc*$^{+/1638N}$/*Smad4*$^{+/E6sad}$ (cis and trans)	*Smad4* mutation leads to intestinal tumors without malignant properties. Both mutations lead to high tumor burden in the upper GI (cis>trans); some show invasion of the submucosa
52	[387]	*cis-Apc*$^{+/-}$/*Smad4*$^{+/-}$ *Mmp7*$^{-/-}$	*Mmp7* knockout reduces tumor size but does not affect invasiveness
53	[388]	*Smad2*$^{+/-}$*; Apc*$^{580D/+}$ *(cis)*	Larger tumors, higher incidence of malignant phenotype (compared to *Apc*$^{580D/+}$mice)
54	[160]	*Smad3*$^{-/-}$ (129/Sv genetic background)	Adenocarcinomas of the intestine with penetration of the whole intestinal wall and lymphatic spread. Lower tumor burden in C57/BL6 × 129/Sv *Smad3*$^{-/-}$ hybrids. Note, that *Smad3* mutations occur only in 2% of CRC (Fleming *et al*[162], 2013)
55	[179]	*Smad4*$^{f/f}$*;Catnb*$^{lox(ex3)/+}$*;Lgr5-Cre*^{ERT2}*-IRES-GFP*	Mosaic *Cre*-expression leads to adenoma formation
56	[178]	*Catnb*$^{+/lox(ex3)}$*: Krt1-19*$^{+/cre}$ *Catnb*$^{+/lox(ex3)}$*: Tg·Fabpl*^{cre}	Constitutional Cre-mediated excision of β-catenin phosphorylation site leads to a plethora of small intestine adenomas
57	[177]	*Villin-creER*^{T2}*/Catnb*$^{loxEx3/WT}$	Expression of GSK3β-resistant β-catenin leads to substitution of enterocytes by highly proliferative crypt stem cells (rapid death)
58	[142]	*Nicd/Apc*$^{+/1638N}$	NOTCH-signaling does not influence adenoma formation
59	[141]	*Nicd/P53*$^{-/-}$	*Villin-CreER*^{T2} tamoxifen-dependent *P53* deletion in constitutively active NOTCH-signaling background leads to intestinal tumor formation and metastasis
60	[158]	*Car1*$^{CreER/+}$*; Apc*$^{fl/fl}$*; Kras*$^{LSL\text{-}G12D/+}$*; P53*^{KO}*; Smad4*$^{fl/fl}$	Rapid tumor formation in cecum and proximal colon, but high mortality in triple and quadruple mutants
61	[192]	*Msh2*$^{\Delta 7N/\Delta 7N}$ */Apc*$^{+/1638N}$*. Msh2*$^{\Delta 7N/\Delta 7N}$ */Apc*$^{Min/+}$	Rapid tumor formation in the small intestine, early death (2-3 months), more tumors in *Msh2*$^{\Delta 7N/\Delta 7N}$ */Apc*$^{Min/+}$
62	[191]	*Apc*$^{Min/+}$*/Msh2*$^{+/+}$*; Apc*$^{Min/+}$*/Msh2*$^{+/-}$*; Apc*$^{Min/+}$*/Msh2*$^{-/-}$	Accelerated tumor formation in the small intestine in MSH2-deficient mice. Mice homozygous for Msh2$^{-/-}$ dye rapidly from lymphomas

63	[389]	$Kras^{V12}/Cre/Msh2^{-/-}$	β-naphthoflavone inducible Kras mutation ($AhCre^{+/T}$, $Kras^{+/LSLV12}$) combined with homozygous *Msh2*-knockout leads to increased number of intestinal adenomas. No carcinomas, relevant number of thymic lymphomas
64	[197]	$VCMsh2^{LoxP/LoxP}$ $VCMsh2^{LoxP/G674D}$ $VCMsh2^{LoxP/null}$	Villin-controlled *Cre*-expression leads to intestinal MMR-deficiency, similar to Lynch syndrome. 50% of tumors in the small intestine are malignant. A high proportion of *carcinomas* in $VCMsh2^{LoxP/null}$ mice are resistant to cisplatin and FOLFOX
65	[185,186]	$Msh2^{-/-}$	Death due to lymphoma
66	[194]	$Apc^{1638N/+}$ $Exo1^{+/-}$ $Fen1^{+/-}$	Increased tumor multiplicity and incidence, higher progression to malignancy, high incidence of hematopoietic cancers
67	[193]	$Fen1^{null}/Apc^{1638N}$	Increased malignancy of intestinal tumors compared to Apc^{1638N} mice through MSI
68	[184]	$Mlh1^{-/-}/Apc^{1638N}$	Increased tumor incidence and multiplicity, 30% adenocarcinomas, reduced lifespan of 3.3 mo. High amount of extraintestinal tumors
69	[187]	$Msh6^{-/+}$ $Msh6^{-/-}$	Reduced life span in hetero- and homozygotes due to lymphomas and gastrointestinal tumors. Tumors show no signs of MSI
70	[390]	$Msh3^{-/-}$; $Msh6^{-/-}$	Decreased life span, death due to intestinal adenocarcinomas or lymphomas
71	[190]	$Msh6^{TD/TD}$; $Msh6^{TD/+}$	B or T cell non-Hodgkin lymphomas, adenomas of the small intestine, basal cell carcinomas
72	[388]	$Pms2^{-/-}$; $Pms1^{-/-}$	*Pms2*-deficient mice develop lymphomas and sarcomas, but no intestinal tumors; Pms1 deficiency does not cause tumor development
73	[150]	Fc^{+}; $Pik3ca^{*+}$ (FVB/N-Tg(Fabp1-Cre)1Jig; $Gt(ROSA)26Sor^{tm7(Pik3ca*,EGFP)Rsky}$	Constitutively active PI3K causes mucinous adenocarcinomas of the proximal colon with infiltration of the whole intestinal wall
74	[129]	$Apc^{fl/fl}$ $Kras^{G12D/+}$ $Pik3ca^{p110*}$+ *Cre*-Adenovirus *via* coloscopic injection	Additional driver mutations do not increase tumor proliferation, but cause progression to adenocarcinoma and metastatic disease
75	[172]	$Apc^{CKO/CKO}$; $Braf^{CA/+}$, *AdenoCre* delivery *via* colonoscopy	*Cre*-mediated *Apc*-knockout combined with latent $Braf^{V600E}$ cause neoplasia of the distal colon (50% adenocarcinomas)
76	[174]	*Villin-Cre*;$Braf^{LSL-V637E/+}$ *Villin-Cre*;$Braf^{LSL-V637E/+}$;$P53^{LSL-R172H/+}$ *Villin-Cre*;$Braf^{LSL-V637E/+}$;$p16^{Ink4+}$	Some invasive adenocarcinomas (13%), dominant negative P53 mutation leads to 60% cancers with 2% metastases. Also, $p16^{ink4a}$ mutation causes carcinomas in a *Braf* mutational background
77	[171]	$Braf^{+/LSL-V600E}$; $AhCreER^{T+/o}$ *x* *Cdkn2a* (Ink4a/Arf$^{\Delta Ex2,3}$) = VE;Cdkn2a$^{\Delta Ex2,3/\Delta Ex2,3}$	*CypA1*-promotor-driven, tamoxifen-inducible *Cre*-recombinase facilitates $Braf^{V600E}$ expression in the small intestine with consecutive crypt hyperplasia. Repression of $p16^{Ink4A}$ leads to tumor formation in various tissues and decreased survival (6 wk)
78	[140]	$Apc^{\Delta 716}$ (A), $Kras^{+/LSL-G12D}$ (K), $Tgfbr2^{flox/flox}$ (T), $Trp53^{+/LSL-R270H}$ (P), $Fbxw7^{flox/flox}$ (F), and *Villin-CreER*	*Kras* mutation increases multiplicity of tumors, whilst P53 gain-of-function mutation and *Tgfβr*-knockout leads to invasiveness, no spontaneous metastases
79	[147]	$Apc^{Min/+}$; $Fbw7^{\Delta G}$	Reduced survival for *Fbw7* deficient mice, also in heterozygous setting
80	[148]	$Fbw7^{flox/flox}$; $P53^{flox/flox}$; *Villin-Cre*	Aggressive carcinomas with metastatic spread to lymph nodes and liver
81	[391]	$Mutyh^{-/-}$	Spontaneous adenoma and adenocarcinoma development in the intestine; predominantly in the upper small intestine. Tumorigenesis increased by oxidative stress ($KBrO_3$)

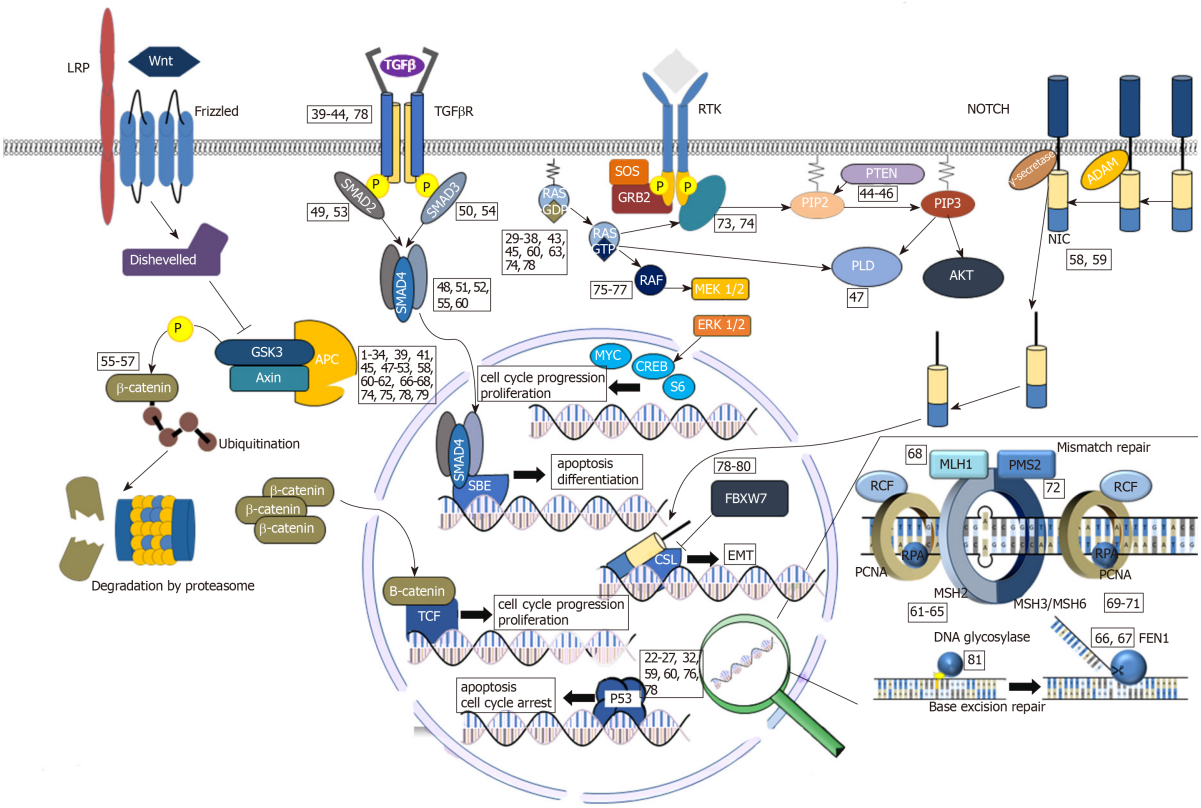

Figure 1 Overview of the frequently altered pathways in colorectal cancer. The numbers in square brackets label the corresponding model descriptions as given in Table 1.

research, their use for preclinical studies is limited due to a lack of genetic heterogeneity on the one hand, and discrepancies to the human tumor development on the other hand. On a final note, it should be added, that GEMM of CRC can be applied the other way round: Mice harboring mutagenic *SB* transposons were crossed to mice expressing SB transposase under control of a *Villin-Cre*-transgene, to generate mice, that develop intestinal lesions due to random insertional mutagenesis and can be screened for unknown CRC driver mutations[200]. Moreover, by combining this approach with well-known driver mutations, new pathway-associated mutations could be identified[201,202].

TRANSPLANT MODELS FOR COLORECTAL CANCER

Transplant mouse models can be classified in various ways: Syngeneic tumor transplantation is characterized by tumor tissue or cancer cell line engraftment within the same mouse strain; whereas xenogeneic grafts are derived from a different mouse strain or human donors. Additionally, it can be distinguished between heterotopic and orthotopic models. As cancer grafts, tumor cells, organoids and tumor tissue pieces can be employed. In 1876, Novinsky successfully transferred tumors (likely canine venereal sarcomas) from one dog to another in two independent trials[203]. Shortly thereafter, Hanau[204] and Morau (reviewed in[205]) reported independently the successful passaging of epithelial rodent tumors. Around the turn of the century, several transplantable rodent tumors, mostly of a sarcomatoid phenotype, were established[206]. Later, the discovery of the human leukocyte antigens and oncogenic viruses elucidated the results of the earlier transplantation studies[207,208]. Toolan pioneered in the xenograft field by attenuating graft rejection through X-radiation and cortisone treatment[209,210].

Animals for transplant models

A fundamental prerequisite for the successful engraftment of xenogeneic tissue in mice is the impairment of the host immune system. A detailed explanation of the development and sophistication of immunocompromised mice would fill several pages and is exquisitely reviewed elsewhere[211]. In short, with the discovery of "nude" mice (recessive mutation of FOXN1 leading to hairlessness and athymia)[212] and the

subsequent breeding of NMRI$^{nu/nu}$ mice, xenotransplantation was possible for the first time without additional immunoablative treatment[213]. A more immunodeficient animal strain, C:B:-17 scid, carrying a homozygous mutation of the *Prkdc* gene resulting in a lack of functional B and T lymphocytes, was established by Bosma *et al*[214] in 1983. To overcome NK cell function, SCID mice were crossed with non-obese diabetic mice (NOD)[215] by several workgroups generating NOD/LtSzscid[216], NOD/LtSz-scid β2m^{null}[217] and NOD/Shi-SCID mice[218]. However, the life span of NOD/SCID mice is limited by the development of thymic lymphomas[219] and they show relevant "immune leakiness" caused by spontaneous rearrangement of T and B cell receptors[220,221]. Lastly, to abolish NK cell activity completely, deficiency of the IL-2 receptor subunit gamma (IL2Rγ) and the Janus kinase 3 (Jak3) were introduced to NOD/SCID mice generating the commonly used strains NOG (NOD/SCID/IL2Rγ^{tm1Sug})[222], NSG (NOD/SCID/IL2Rγ^{tm1Wjl})[223] and NOJ (NOD/SCID/Jak3^{null})[224]. Since the DNA-dependent protein kinase catalytic subunit, encoded by the *Prkdc* gene, is also responsible for DNA repair, SCID mice are very sensitive for radiation and DNA-damaging agents. Therefore, Shultz *et al*[225] developed the more robust, but equal immunodeficient NOD/LtSz-Rag1^{null}Pfp^{null} strain. Since then, many more immunodeficient strains, with in part different genetic backgrounds, have been developed[211,226]. In general, it can be noted, that the more severe immunodeficient the host, the higher are the engraftment rates. Nevertheless the NMRI$^{nu/nu}$ strain is still of high relevance for xenografting: The strain is less prone to opportunistic infections[227], more tolerant for chemotherapeutic agents and shows reasonable engraftment rates for primary patient-derived xenografts (PDX) and good engraftment rates for subsequent mouse to mouse passaging[228,229]. An economical plus is that this mouse strain is the least expensive immunodeficient one. It is mandatory to house immunodeficient mice in a specific pathogen free environment, using sterile techniques and microisolator caging. For syngeneic mouse models, viz. transplantation of cell or organoids from mice, exact strain conformity of donor and recipient mouse must be guaranteed, since even closely related substrains can differ genetically[230].

Heterotopic tumor models

The advantages of s.c. tumor engraftments are glaring: They require nominal surgical skills, allow high throughput of samples due to time efficacy and tumor growth can be monitored by the naked eye. Early s.c. models of solid tumors were mostly carried out by injection of a tumor cell suspension into the mouse flank. Although some of these models correctly predicted clinical response for specific cancer entities and therapeutics[231] large drug screens revealed that these models are of rather modest value for the prediction of clinical response in humans[232-235]. Moreover, the resulting tumors from a homogenous cell suspension do not reflect the intratumor-heterogeneity and an adequate tumor microenvironment is also absent[236]. Especially established CRC cell lines show low genetic diversity due to high passage and selective pressure[237]. On a site note, one of the most cited CRC cell lines, HCT116, was established almost 40 years ago; enough time for mislabeling, cross-contaminations and high passage selection[238,239]. While tumor cell lines in general remain a cornerstone of cancer research[240,241], their heterotopic *in vivo* application creates no scientific added value. The creation of a s.c. tumor graft as intermediate step for subsequent orthotopic transplantation can be considered as an exception. Even though these cell-derived grafts are frequently referred to as PDX in the literature, we believe that this term should be avoided and "cell line-derived xenograft - CDX" is more reasonable. The implantation of tumor cells or tumor pieces under the renal capsule follows the rational that the high vascularized environment propagates better engraftment[242,243] and was historically used for the subrenal capsule assay[244]. While this model might be advantageous for some cancers[245], we see no advantage for CRC engraftment over the s.c. PDX model, a fortiori comparing practical effort, monitoring of tumor growth and animal welfare. Intravenous injection of cell suspension is often used to simulate hematogenous dissemination of tumor cells[246,247], but circumvents crucial steps of metastasis, namely degradation of the surrounding tissue and lymphatic and/or vascular invasion[248]. Thus, the same applies to the splenic injection of tumor cells to generate liver metastasis[249,250] or the intraperitoneal injection to simulate peritoneal carcinosis[251].

PDX models

PDX differ greatly from the aforementioned heterotopic tumor models. They are established by the s.c. implantation of a tumor piece from a surgical resection or biopsy into the flanks of immunocompromised mice; with lower tumor take rates for biopsy samples[237]. Tissue can either be implanted directly after resection or cryopreserved in fetal calf serum containing 10% DMSO for implantation at a later

time[229]. Incubation of the tissue in Matrigel® prior to tumor implantation, significantly increases engraftment rates[228]. In order to obtain sufficient tumor tissue for larger scale studies, the resulting tumor can be fragmented and re-grafted subsequently. In recent years, our workgroup focused on the build-up of a large CRC biobank consisting of more than 140 PDX-models (general procedure is presented in Figure 2). This PDX panel reflects adequately the clinical and molecular heterogeneity of the patient population undergoing surgical resection of primary or metastatic CRC[252]. It is well accepted that PDX closely recapitulate the histology of the original "donor" tumor over several passages[253-255] and are also genetically stable[256,257]. However, Ben-David *et al*[258] demonstrated recently that changes in copy number alterations occurred in early passages of PDX tumors compared with both the P0 PDX and the donor tumor. A common criticism in heterotopic mouse models is related to the absence of tumor-stroma interaction or the "tumor microenvironment"[259]. While this is true for immune cells, the stromal component remains intact in PDX[255]. Although the human stromal compounds (fibroblasts, blood vessels *etc*.) are quickly and steadily replaced by their murine counterparts, the overall architecture of the tumor remains unaffected in the majority of cases[260,261]. Moreover, these murine stroma cells adopt and maintain a human-like metabolic phenotype[262]. These features indicate that PDX are indeed good and valuable models for preclinical testing of conventional and novel anticancer agents in the era of personalized cancer therapy[263,264]. A proof of concept study with advanced refractory cancers demonstrated that drug responses measured in a PDX model, can be used for successful clinical decision making[265]. A PDX model of CRC metastases closely resembled the efficacy of cetuximab and identified druggable targets in resistant tumors[266]. Moreover, a PDX clinical trial approach (one animal per model per treatment) reflects well the heterogeneity of the patient population and allows testing of new drugs and combinatorial regimen[267]. A large study with over 1000 PDX models confirmed the consistency between clinical and PDX clinical trial drug response[268]. The ultimate goal of precision medicine would comprise of the profound genetic and functional characterization of a given tumor to identify relevant drug targets and subsequent validation of potential therapies with aid of a PDX bearing "avatar" mouse to provide the most efficient treatment for the individual patient[264,269]. Currently, several clinical trials following this approach for colorectal[270,271] and pancreatic cancer are recruiting[272]. Yet, a median duration of 12.2 mo until PDX model establishment[237] remains an unsolved issue for patients urgently in need for treatment. When it comes to drug testing, it should be considered, that immunotherapy approaches can only be restrictedly evaluated in immunodeficient host mice. A further disadvantage of PDX models is a potential selection for more aggressive tumors. The data concerning the association between successful PDX engraftment and clinical or molecular features is in part conflicting. While we and others could not find significant associations between tumor grading and PDX engraftment[237,252], a Korean study observed significant correlations with tumor staging and grading[273]. A smaller study with a high PDX establishment rate found a significant correlation of PDX success with positive nodal status and grading[274], while Julien *et al*[275] only found significances for the combination of a positive nodal status with an elevated carcinoembryonic antigen level. Moreover, we observed a significant correlation between PDX engraftment and molecular features like *KRAS* and *BRAF* mutations as well as MSI[252]. Apart from the tumor biology, choice of the host mouse strain, repeated attempts of engraftment, quantity and quality of the resected tissue as well as previous treatment of the patient are additional factors influencing the success of model establishment. Collins *et al*[276] recently reported PDX engraftment rates varying from 14 to 100% with a median PDX establishment rate of 68% reviewing 14 CRC-PDX studies. Compared to establishment rates for primary CRC cell lines of about 10%, the PDX is clearly superior[252,277]. A selection bias relating to cancer biology can be diminished by increasing the number of enrolled patients and molecular characterization of the individual PDX. In fact, a very recent PDX study found an underrepresentation of the consensus molecular subtype number 2, due to worse engraftment[278]. Another crucial pitfall of the PDX model is the development of EBV-associated lymphomas at the implantation site, which can mimic successful engraftment[279]. Depending on the mouse strain and cancer entity, between 2.3% (colorectal) and 75% (prostate cancer) of primary engrafted bona fide xenografts turn out to be human de-novo lymphomas[280-284]. Since this condition is more frequently reported in NSG and comparable strains, development of de-novo lymphoma in NMRI$^{nu/nu}$ mice might be hindered by high NK cell activity[285]. Thus, after successful engraftment of a PDX in NSG mice, we conduct the subsequent passaging in NMRI$^{nu/nu}$ mice and xenograft histology is frequently evaluated by an experienced pathologist. Interestingly, Butler *et al*[286] significantly reduced the frequency of lymphomas in an ovaria cancer PDX model by a unique dosage of rituximab during implantation. Additionally, PDX serve not only in the

field of therapy development; they are also a vital tool for the maintenance of a healthy biobank, allowing the establishment of secondary cell lines and supply sufficient tumor samples for the exchange with other work groups[252].

In summary, we consider the PDX model as keystone of cancer research, holding great potential in the developing field of precision medicine for CRC.

Orthotopic models

Orthotopic CRC models are implemented to overcome the drawbacks of heterotopic models, videlicet lack of an adequate tumor microenvironment and metastatic behavior.

At the beginning of the 1980s, the first orthotopic engraftments of CRC cell lines was reported by Snipes[287], demonstrating the feasibility of an intramural cell injection causing locally invasive cancer growth. A few years later, Bresalier *et al*[288] demonstrated that the orthotopic injection of human CRC cells causes metastases in the liver. In 1991, Fu *et al*[289] successfully engrafted 13 patient-derived tumors by removing the serosa and sewing the tumor pieces to the cecal wall. Beside the local tumor outgrowth, lymph node and liver metastases were reported for a few mice. Since the murine cecum is relatively large compared to its human counterpart and readily accessible by laparotomy, it rapidly became the favored site for orthotopical engraftment by different approaches. Many authors generated a s.c. cell graft in a donor mouse, of which a small piece was sewed to the cecum after damaging the serosa[290-292]. Several varieties of this technique can be found in the literature: While some authors removed the mucosa and sewed the tumor pieces onto the cecal wall[293,294], others formed a subserosal tunnel for tumor inoculation, which was afterwards closed by a suture[295] or surrounded the tumor piece with a "pouch" formed by a serosal duplicature[296]. Others reported the technically more challenging subserosal injection of a cell suspension into the cecal wall[297]. The cell injection method is often referred to as subserosal[298], while other work groups describe a submucosal injection[299]; both frequently with Matrigel® addition to the cell suspension to avoid cell spillage[300]. Considering the gauntness of the cecal wall, we will here refer to both techniques as "intracecal" injection. The possibility of a "preconditioning" *via* s.c. PDX has also been described for the cell injection approach[301]. Beside the cecum, other colonic sites like the descending colon can be accessed for cell injection[302,303]. Despite frequent metastases, some aspects of these techniques may be viewed critically. First, given the fact that CRC arise from the mucosa, these models cannot be considered as genuine orthotopic and also the injection approach might mimic an advanced CRC. Second, they allow the contact of cancerous tissue with the abdominal cavity, hence it cannot be ruled out that some of the metastases are the result of intraabdominal cell spillage. Moreover, these approaches require the opening of the abdomen and can cause inflammation and morbidity. Nevertheless, the cecal orthotopic model is frequently applied, especially for basic research to identify the underlying mechanisms of metastatic progression, since it can render metastatic, end stage disease within a few weeks[304]. The upregulation of genes associated with advanced CRC, could also be observed in liver metastasis from an orthotopic model[290,305]. The orthotopic approach allows to elucidate the role of certain molecular pathways by direct comparison of the metastatic properties of a given cell with their genetically engineered counterpart[306-310]. The additional transfection of these cells with a reporter, like GFP, DsRed or luciferase, allows monitoring of tumor progress by *in vivo* imaging[311-313]. The orthotopic approach can be used in transgenic mice to clarify the role of distinct molecules[314] or certain cell types[315]. To further stress the functionality of stromal components, a co-injection of tumor cells and stromal cells is feasible[316-318]. By using NSG mice, the efficiency of an immune cell-based therapy can be tested in the context of such an orthotopic model[319]. Furthermore, circulating tumor cells (CTC) can be isolated from murine blood[320]. In addition to the above discussed surgical approaches, there are less invasive concepts that do not require surgery and diminish the risk of intraabdominal cell spillage. Kashtan *et al*[321] demonstrated the successful engraftment of murine tumor cells by submucosal injection in the distal rectum in 1992 and this approach was adapted by several work groups[322-324]. To reach more proximal parts of the rectum or the descending colon, submucosal cell application can be performed *via* small endoscopic instruments[325,326]. Depending on the cell line, liver metastases have been observed[327]. Lastly, tumor cells can be inoculated in the colon mucosa by the acid enema approach described by Kishimoto *et al*[328]; a true orthotopic model with intramucosal tumor development and liver metastases. In brief, the mucosa is damaged by 4% acetic acid enema and after neutralization with PBS, a tumor cell suspension is instilled and the anus temporaryly sealed. Hite *et al*[329] subjected all three orthotopic models (intracecal injection, transanal submucosal injection and acid enema) to a direct comparison. They found the submucosal

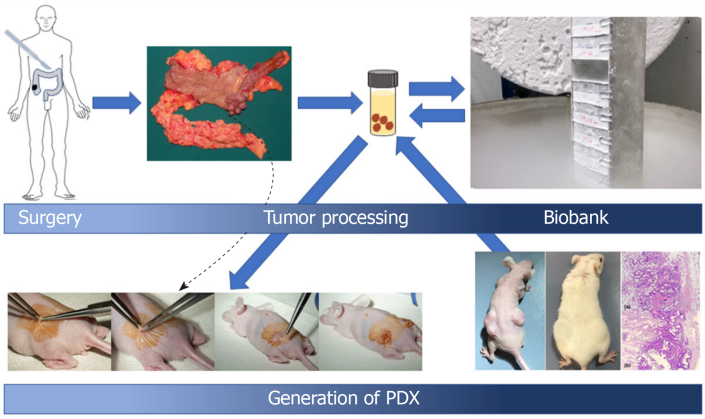

Figure 2 Establishment of PDX. After surgery, a small sample of the tumor, which is not needed for pathological diagnosis, is obtained and cut into pieces of 27 mm^3. These can be either implanted immediately in recipient mice or vitally cryopreserved in liquid nitrogen. The resulting patient-derived xenograft (b) closely reflects the histology of the donor tumor (a) (Previously published in[229]). Patient-derived xenograft can be further processed for subsequent implantation or cryopreservation.

injection to be the most efficient in tumor formation and metastatic behavior and at the same time well tolerated by the animals. In contrast, the acid enema approach showed the lowest tumor formation frequency but a considerable mortality of 15%. Enquist *et al*[312] pursued a different concept by sewing a tumor piece directly to the mucosa by creating an artificial rectal prolapse. They were able to engraft pieces from transgenic A*pcMin/+;KrasLSLG12D/+;Villin-Cre* adenomas in the colon of syngeneic animals and a small subset of these tumors progressed to carcinomas. More strikingly, they managed also to transfer s.c. human PDX to the colons of NSG mice reflecting stage-dependent biological behavior as lymph node metastases could be observed for stage III PDX[312].

Today, orthotopic models are copiously used for the *in vivo* validation of new therapeutic compounds and as a proof-of-principle approach[330-333]. However, their clinical relevance is limited by the common use of similar, poorly differentiated cell lines. The orthotopic PDX model is promising, but its tumor take rate is not higher as in the s.c. PDX model. A very recently published, "crossover" concept comprising the s.c. engraftment of a PDX, followed by enzymatic disintegration of the PDX to a cell suspension and subsequent orthotopic injection into the rectal submucosa yielded an engraftment rate of 70% for s.c. PDX and 46% for the orthotopic model. Moreover, a metastatic spread was observed for 60% of the tumors successfully engrafted orthotopically[334].

RECENT DEVELOPMENTS AND FUTURE PERSPECTIVES

The increasing field of precision medicine has a growing need for highly translational cancer models. Conversely, the increasingly negative public perception of animal studies constrains the scientific community to further stress the 3R-principle (replacement, reduction and refinement) in cancer research[335]. Aside from the improvement of *in vivo* models, this implies the refinement of *in vitro* methods as well.

Humanized mice are severely immunocompromised mice, which can be reconstituted with various types of human bone marrow-derived cells or $CD34^+$ hematopoietic stem cells[336,337]. Since human stem and progenitor cells can be attained from umbilical cord blood or from peripheral drawn blood samples after GM-CSF treatment and cultured *in vitro*[338], these cells can be transferred to sub-lethally irradiated NSG mice. Morton *et al*[339] observed that PDX of head and neck cancer engrafted into these, so called "Xact mice", are infiltrated with human B and T lymphocytes. Many transgenic mice further support engraftment with $CD34^+$ stem cells by overexpression of human interleukins and signaling molecules. Thus NBSGW[340], hIL2-NOG[341], NSG-SGM3[342] and SRG-15 mice[343] have been introduced recently and antitumor effects against PDX of different cancers could be observed[341,343]. These models hold great promise for the research of CRC immunotherapy, especially for highly immunogenic hypermutated CRC. Capasso *et al*[344] showed very recently that check point inhibition with nivolumab leads to growth inhibition of human MSI-H PDX thereby accurately reflecting the clinical response of this CRC subtype. In contrast, no sustainable growth inhibition was observed in MSS

tumors or MSI-H tumors in "standard" NSG mice[344,345].

Although patient-derived cell cultures are a valuable tool for high-throughput drug screenings, they exhibit considerable shortcomings[346]. First, the establishment rate of primary patient-derived CRC cells with conventional 2D culturing methods approximates some 10%[252,275], although higher success rates of 40% and more can be found in the literature[347,348]. Second, conventional 2D cultures change the biological properties of cells, possibly altering drug response *in vitro*[349]. Cell polarization, lack of stroma and abundance of growth factors, nutrients and oxygen are factors that might change the behavior of tumor cells[350]. In recent years, more complex cell culturing methods have emerged. CRC cells, cultured in an extracellular matrix form three dimensional spheres, so called spheroids, that differ in their biological properties from 2D cultured cells[351]. In contrast, organoids are three dimensional structures, derived from intact tumor pieces or tumor stem cells cultured in an extracellular matrix scaffold[352]. Patient-derived organoids (PDO), quite similar to PDX, recapitulate closely the histological and genetic properties of their parental tumors. Moreover, high rates of successful establishment have been reported[353] and reliable drug response prediction seems possible[354-356]. PDOs can be implanted s.c. or orthotopically into mice, resulting in PDO xenografts (PDOX)[264,354,357]. Furthermore, the Clevers group pioneered in the inauguration of non-malignant intestinal organoids exploiting the stem cell niche *in vitro*[358]. These organoids can be modified *in vitro* to exhibit malignant properties and used to enlighten the role of cancer-driving pathways by *in vivo* engraftment[359,360]. The available data strongly suggests, that PDOs reflect more faithfully the biological virtue and drug response of the parental tumor compared to conventional 2D cell cultures[352]. The circumstance, that organoids can be derived from CTC, could render them an excellent tool for the preclinical testing of patients with advanced stage cancer that do not undergo surgery[361]. Additionally, CTC reflect genetic changes associated with acquired drug resistance during chemotherapy[362]. Further steps to a reduction of animal experiments imply the faithful remodeling of the host organism *in vitro*. Several research groups created a "cancer on a chip" model that combines the advances of 3D cell culture connected with artificial organs that resemble the most common organs of metastatic spread[363]. Miller and Shuler introduced a "body on a chip model" with 14 artificial organs, which could be modified for cancer research[364]. At last, the widely acknowledged work of Guinney *et al*[365] regarding the consensus molecular subtypes of CRC draw great attention to the value of computed models in cancer science and the capabilities of bioinformatic research. Retrospective analysis of clinical trial samples partly demonstrated the association of drug response with molecular subtypes[366]. The constantly growing knowledge of cancer pathways and their crosstalk on the one hand, and the increased inter-individual complexity of tumors on the other hand, call for a method to integrate and interpret the overwhelming amount of data[367]. In silico methods, like data mining, pattern recognition, machine learning and network approaches, are able to predict the behavior of "virtual" HCT116 cells[368], can reveal genetic patterns associated with survival[369], can be used to detect new biomarkers[370], allow the identification of unknown driver mutations[371] and potential preclinical compounds[372]. Yet, in silico models often lack explanatory power and need careful interpretation by bioinformaticians. Their ability to correctly predict treatment response for an individual patient to a new compound is still a long way off[373].

ACKNOWLEDGEMENTS

We kindly thank Jenny Burmeister, graphical assistant, for the supply with excellent pictures.

REFERENCES

1 **Siegel RL**, Miller KD, Jemal A. Cancer statistics, 2019. *CA Cancer J Clin* 2019; **69**: 7-34 [PMID: 30620402 DOI: 10.3322/caac.21551]

2 **Ferlay J**, Colombet M, Soerjomataram I, Dyba T, Randi G, Bettio M, Gavin A, Visser O, Bray F. Cancer incidence and mortality patterns in Europe: Estimates for 40 countries and 25 major cancers in 2018. *Eur J Cancer* 2018; **103**: 356-387 [PMID: 30100160 DOI: 10.1016/j.ejca.2018.07.005]

3 **Mengual-Ballester M**, Pellicer-Franco E, Valero-Navarro G, Soria-Aledo V, García-Marín JA, Aguayo-Albasini JL. Increased survival and decreased recurrence in colorectal cancer patients diagnosed in a screening programme. *Cancer Epidemiol* 2016; **43**: 70-75 [PMID: 27399311 DOI: 10.1016/j.canep.2016.06.003]

4 **Hübner J**, Lewin P, Pritzkuleit R, Eisemann N, Maier W, Katalinic A. Colorectal cancer screening by colonoscopy and trends in disease-specific mortality: a population-based ecological study of 358 German districts. *Int J Colorectal Dis* 2019; **34**: 599-605 [PMID: 30627848 DOI: 10.1007/s00384-018-03226-6]

5 **Kawabata-Shoda E**, Charvat H, Ikeda A, Inoue M, Sawada N, Iwasaki M, Sasazuki S, Shimazu T, Yamaji T, Kimura H, Masuda S, Tsugane S. Trends in cancer prognosis in a population-based cohort survey: can recent advances in cancer therapy affect the prognosis? *Cancer Epidemiol* 2015; **39**: 97-103 [PMID: 25541411 DOI: 10.1016/j.canep.2014.11.008]

6 **Johnson CM**, Wei C, Ensor JE, Smolenski DJ, Amos CI, Levin B, Berry DA. Meta-analyses of colorectal cancer risk factors. *Cancer Causes Control* 2013; **24**: 1207-1222 [PMID: 23563998 DOI: 10.1007/s10552-013-0201-5]

7 **Waluga M**, Zorniak M, Fichna J, Kukla M, Hartleb M. Pharmacological and dietary factors in prevention of colorectal cancer. *J Physiol Pharmacol* 2018; **69** [PMID: 30149368 DOI: 10.26402/jpp.2018.3.02]

8 **Cole BF**, Logan RF, Halabi S, Benamouzig R, Sandler RS, Grainge MJ, Chaussade S, Baron JA. Aspirin for the chemoprevention of colorectal adenomas: meta-analysis of the randomized trials. *J Natl Cancer Inst* 2009; **101**: 256-266 [PMID: 19211452 DOI: 10.1093/jnci/djn485]

9 **Jasperson KW**, Tuohy TM, Neklason DW, Burt RW. Hereditary and familial colon cancer. *Gastroenterology* 2010; **138**: 2044-2058 [PMID: 20420945 DOI: 10.1053/j.gastro.2010.01.054]

10 **Bodmer WF**, Bailey CJ, Bodmer J, Bussey HJ, Ellis A, Gorman P, Lucibello FC, Murday VA, Rider SH, Scambler P. Localization of the gene for familial adenomatous polyposis on chromosome 5. *Nature* 1987; **328**: 614-616 [PMID: 3039373 DOI: 10.1038/328614a0]

11 **Peltomäki P**, Aaltonen LA, Sistonen P, Pylkkänen L, Mecklin JP, Järvinen H, Green JS, Jass JR, Weber JL, Leach FS. Genetic mapping of a locus predisposing to human colorectal cancer. *Science* 1993; **260**: 810-812 [PMID: 8484120 DOI: 10.1126/science.8484120]

12 **Lindblom A**, Tannergård P, Werelius B, Nordenskjöld M. Genetic mapping of a second locus predisposing to hereditary non-polyposis colon cancer. *Nat Genet* 1993; **5**: 279-282 [PMID: 7903889 DOI: 10.1038/ng1193-279]

13 **Cancer Genome Atlas Network**. Comprehensive molecular characterization of human colon and rectal cancer. *Nature* 2012; **487**: 330-337 [PMID: 22810696 DOI: 10.1038/nature11252]

14 **Yamagiwa K**, Ichikawa K. Experimental study of the pathogenesis of carcinoma. *CA Cancer J Clin* 1977; **27**: 174-181 [PMID: 406018 DOI: 10.3322/canjclin.27.3.174]

15 **Lorenz E**, Steward HL. Intestinal Carcinoma and Other Lesions in Mice Following Oral Administration of 1,2,5,6-Dibenzanthracene and 20-Methylcholanthrene. *J Natl Cancer Inst* 1940; **1**: 17-41 [DOI: 10.1093/jnci/1.1.17]

16 **Druckrey H**, Küpfmüller K. Quantitative Analyse der Krebsentstehung. *Zeitschrift für Naturforschung B* 1948; **3**: 254–266 [DOI: 10.1515/znb-1948-7-806]

17 **Lisco H**, Finkel MP, Brues AM. Carcinogenic properties of radioactive fission products and of plutonium. *Radiology* 1947; **49**: 361-363 [PMID: 20266010 DOI: 10.1148/49.3.361]

18 **Laqueur GL**. Carcinogenic Effects of Cycad Meal and Cycasin, Methylazoxymethanol Glycoside, in Rats and Effects of Cycasin in Germfree Rats. *Fed Proc* 1964; **23**: 1386-1388 [PMID: 14236160]

19 **Morgan RW**, Hoffmann GR. Cycasin and its mutagenic metabolites. *Mutat Res* 1983; **114**: 19-58 [PMID: 6338356 DOI: 10.1016/0165-1110(83)90018-0]

20 **Druckrey H**, Preussmann R, Ivanković S, Schmidt CH, So BT, Thomas C. [Carcinogenic effect of azoethane and azoxyethane on rats]. *Z Krebsforsch* 1965; **67**: 31-45 [PMID: 4221131]

21 **Rosenberg DW**, Giardina C, Tanaka T. Mouse models for the study of colon carcinogenesis. *Carcinogenesis* 2009; **30**: 183-196 [PMID: 19037092 DOI: 10.1093/carcin/bgn267]

22 **Fiala ES**, Stathopoulos C. Metabolism of methylazoxymethanol acetate in the F344 rat and strain-2 guinea pig and its inhibition by pyrazole and disulfiram. *J Cancer Res Clin Oncol* 1984; **108**: 129-134 [PMID: 6430908 DOI: 10.1007/bf00390984]

23 **Suzuki R**, Kohno H, Sugie S, Nakagama H, Tanaka T. Strain differences in the susceptibility to azoxymethane and dextran sodium sulfate-induced colon carcinogenesis in mice. *Carcinogenesis* 2006; **27**: 162-169 [PMID: 16081511 DOI: 10.1093/carcin/bgi205]

24 **Turusov VS**, Lanko NS, Krutovskikh VA, Parfenov YD. Strain differences in susceptibility of female mice to 1,2-dimethylhydrazine. *Carcinogenesis* 1982; **3**: 603-608 [PMID: 7116553 DOI: 10.1093/carcin/3.6.603]

25 **Izumi K**, Otsuka H, Furuya K, Akagi A. Carcinogenicity of 1,2-dimethylhydrazine dihydrochloride in BALB/c mice. Influence of the route of administration and dosage. *Virchows Arch A Pathol Anat Histol* 1979; **384**: 263-267 [PMID: 160118 DOI: 10.1007/bf00428228]

26 **Sohn OS**, Fiala ES, Requeijo SP, Weisburger JH, Gonzalez FJ. Differential effects of CYP2E1 status on the metabolic activation of the colon carcinogens azoxymethane and methylazoxymethanol. *Cancer Res* 2001; **61**: 8435-8440 [PMID: 11731424]

27 **Narisawa T**, Wong CQ, Maronpot RR, Weisburger JH. Large bowel carcinogenesis in mice and rats by several intrarectal doses of methylnitrosourea and negative effect of nitrite plus methylurea. *Cancer Res* 1976; **36**: 505-510 [PMID: 1260748]

28 **Reddy BS**, Ohmori T. Effect of intestinal microflora and dietary fat on 3,2'-dimethyl-4-aminobiphenyl-induced colon carcinogenesis in F344 rats. *Cancer Res* 1981; **41**: 1363-1367 [PMID: 7194137]

29 **Sugimura T**, Terada M. Experimental chemical carcinogenesis in the stomach and colon. *Jpn J Clin Oncol* 1998; **28**: 163-167 [PMID: 9614437 DOI: 10.1093/jjco/28.3.163]

30 **Bouvard V**, Loomis D, Guyton KZ, Grosse Y, Ghissassi FE, Benbrahim-Tallaa L, Guha N, Mattock H, Straif K; International Agency for Research on Cancer Monograph Working Group. Carcinogenicity of consumption of red and processed meat. *Lancet Oncol* 2015; **16**: 1599-1600 [PMID: 26514947 DOI: 10.1016/S1470-2045(15)00444-1]

31 **Jägerstad M**, Skog K. Genotoxicity of heat-processed foods. *Mutat Res* 2005; **574**: 156-172 [PMID: 15914214 DOI: 10.1016/j.mrfmmm.2005.01.030]

32 **Turesky RJ**. Formation and biochemistry of carcinogenic heterocyclic aromatic amines in cooked meats. *Toxicol Lett* 2007; **168**: 219-227 [PMID: 17174486 DOI: 10.1016/j.toxlet.2006.10.018]

33 **Cheung C**, Ma X, Krausz KW, Kimura S, Feigenbaum L, Dalton TP, Nebert DW, Idle JR, Gonzalez FJ. Differential metabolism of 2-amino-1-methyl-6-phenylimidazo[4,5-b]pyridine (PhIP) in mice humanized for CYP1A1 and CYP1A2. *Chem Res Toxicol* 2005; **18**: 1471-1478 [PMID: 16167840 DOI: 10.1021/tx050136g]

34 **Kaderlik KR**, Mulder GJ, Shaddock JG, Casciano DA, Teitel CH, Kadlubar FF. Effect of glutathione depletion and inhibition of glucuronidation and sulfation on 2-amino-1-methyl-6-phenylimidazo[4,5-b]pyridine (PhIP) metabolism, PhIP-DNA adduct formation and unscheduled DNA synthesis in primary rat hepatocytes. *Carcinogenesis* 1994; **15**: 1711-1716 [PMID: 8055653 DOI: 10.1093/carcin/15.8.1711]

35 **Alexander J**, Wallin H, Rossland OJ, Solberg KE, Holme JA, Becher G, Andersson R, Grivas S.

Formation of a glutathione conjugate and a semistable transportable glucuronide conjugate of N2-oxidized species of 2-amino-1-methyl-6-phenylimidazo[4,5-b]pyridine (PhIP) in rat liver. *Carcinogenesis* 1991; **12**: 2239-2245 [PMID: 1747923 DOI: 10.1093/carcin/12.12.2239]
36 **Malfatti MA**, Kulp KS, Knize MG, Davis C, Massengill JP, Williams S, Nowell S, MacLeod S, Dingley KH, Turteltaub KW, Lang NP, Felton JS. The identification of [2-(14)C]2-amino-1-methyl-6-phenylimidazo[4,5-b]pyridine metabolites in humans. *Carcinogenesis* 1999; **20**: 705-713 [PMID: 10223203 DOI: 10.1093/carcin/20.4.705]
37 **Zhang J**, Lacroix C, Wortmann E, Ruscheweyh HJ, Sunagawa S, Sturla SJ, Schwab C. Gut microbial beta-glucuronidase and glycerol/diol dehydratase activity contribute to dietary heterocyclic amine biotransformation. *BMC Microbiol* 2019; **19**: 99 [PMID: 31096909 DOI: 10.1186/s12866-019-1483-x]
38 **Frandsen H**. Biomonitoring of urinary metabolites of 2-amino-1-methyl-6-phenylimidazo[4,5-b]pyridine (PhIP) following human consumption of cooked chicken. *Food Chem Toxicol* 2008; **46**: 3200-3205 [PMID: 18692111 DOI: 10.1016/j.fct.2008.07.008]
39 **Nakagama H**, Ochiai M, Ubagai T, Tajima R, Fujiwara K, Sugimura T, Nagao M. A rat colon cancer model induced by 2-amino-1-methyl-6-phenylimidazo[4,5-b]pyridine, PhIP. *Mutat Res* 2002; **506-507**: 137-144 [PMID: 12351153 DOI: 10.1016/s0027-5107(02)00160-4]
40 **Chen JX**, Wang H, Liu A, Zhang L, Reuhl K, Yang CS. From the Cover: PhIP/DSS-Induced Colon Carcinogenesis in CYP1A-Humanized Mice and the Possible Role of Lgr5+ Stem Cells. *Toxicol Sci* 2017; **155**: 224-233 [PMID: 27664423 DOI: 10.1093/toxsci/kfw190]
41 **Sugimura T**, Wakabayashi K, Nakagama H, Nagao M. Heterocyclic amines: Mutagens/carcinogens produced during cooking of meat and fish. *Cancer Sci* 2004; **95**: 290-299 [PMID: 15072585 DOI: 10.1111/j.1349-7006.2004.tb03205.x]
42 **Huderson AC**, Myers JN, Niaz MS, Washington MK, Ramesh A. Chemoprevention of benzo(a)pyrene-induced colon polyps in ApcMin mice by resveratrol. *J Nutr Biochem* 2013; **24**: 713-724 [PMID: 22889612 DOI: 10.1016/j.jnutbio.2012.04.005]
43 **Diggs DL**, Harris KL, Rekhadevi PV, Ramesh A. Tumor microsomal metabolism of the food toxicant, benzo(a)pyrene, in ApcMin mouse model of colon cancer. *Tumour Biol* 2012; **33**: 1255-1260 [PMID: 22430258 DOI: 10.1007/s13277-012-0375-6]
44 **Okayasu I**, Hatakeyama S, Yamada M, Ohkusa T, Inagaki Y, Nakaya R. A novel method in the induction of reliable experimental acute and chronic ulcerative colitis in mice. *Gastroenterology* 1990; **98**: 694-702 [PMID: 1688816 DOI: 10.1016/0016-5085(90)90290-h]
45 **Kawada M**, Arihiro A, Mizoguchi E. Insights from advances in research of chemically induced experimental models of human inflammatory bowel disease. *World J Gastroenterol* 2007; **13**: 5581-5593 [PMID: 17948932 DOI: 10.3748/wjg.v13.i42.5581]
46 **Eichele DD**, Kharbanda KK. Dextran sodium sulfate colitis murine model: An indispensable tool for advancing our understanding of inflammatory bowel diseases pathogenesis. *World J Gastroenterol* 2017; **23**: 6016-6029 [PMID: 28970718 DOI: 10.3748/wjg.v23.i33.6016]
47 **Munyaka PM**, Rabbi MF, Khafipour E, Ghia JE. Acute dextran sulfate sodium (DSS)-induced colitis promotes gut microbial dysbiosis in mice. *J Basic Microbiol* 2016; **56**: 986-998 [PMID: 27112251 DOI: 10.1002/jobm.201500726]
48 **He X**, Wei Z, Wang J, Kou J, Liu W, Fu Y, Yang Z. Alpinetin attenuates inflammatory responses by suppressing TLR4 and NLRP3 signaling pathways in DSS-induced acute colitis. *Sci Rep* 2016; **6**: 28370 [PMID: 27321991 DOI: 10.1038/srep28370]
49 **Dieleman LA**, Palmen MJ, Akol H, Bloemena E, Peña AS, Meuwissen SG, Van Rees EP. Chronic experimental colitis induced by dextran sulphate sodium (DSS) is characterized by Th1 and Th2 cytokines. *Clin Exp Immunol* 1998; **114**: 385-391 [PMID: 9844047 DOI: 10.1046/j.1365-2249.1998.00728.x]
50 **Hoffmann M**, Schwertassek U, Seydel A, Weber K, Falk W, Hauschildt S, Lehmann J. A refined and translationally relevant model of chronic DSS colitis in BALB/c mice. *Lab Anim* 2018; **52**: 240-252 [PMID: 29192559 DOI: 10.1177/0023677217742681]
51 **Sussman DA**, Santaolalla R, Strobel S, Dheer R, Abreu MT. Cancer in inflammatory bowel disease: lessons from animal models. *Curr Opin Gastroenterol* 2012; **28**: 327-333 [PMID: 22614440 DOI: 10.1097/MOG.0b013e328354cc36]
52 **Tanaka T**, Kohno H, Suzuki R, Hata K, Sugie S, Niho N, Sakano K, Takahashi M, Wakabayashi K. Dextran sodium sulfate strongly promotes colorectal carcinogenesis in Apc(Min/+) mice: inflammatory stimuli by dextran sodium sulfate results in development of multiple colonic neoplasms. *Int J Cancer* 2006; **118**: 25-34 [PMID: 16049979 DOI: 10.1002/ijc.21282]
53 **Cooper HS**, Everley L, Chang WC, Pfeiffer G, Lee B, Murthy S, Clapper ML. The role of mutant Apc in the development of dysplasia and cancer in the mouse model of dextran sulfate sodium-induced colitis. *Gastroenterology* 2001; **121**: 1407-1416 [PMID: 11729120 DOI: 10.1053/gast.2001.29609]
54 **De Robertis M**, Massi E, Poeta ML, Carotti S, Morini S, Cecchetelli L, Signori E, Fazio VM. The AOM/DSS murine model for the study of colon carcinogenesis: From pathways to diagnosis and therapy studies. *J Carcinog* 2011; **10**: 9 [PMID: 21483655 DOI: 10.4103/1477-3163.78279]
55 **Velázquez KT**, Enos RT, Carson MS, Cranford TL, Bader JE, Chatzistamou I, Singh UP, Nagarkatti PS, Nagarkatti M, Davis JM, Carson JA, Murphy EA. Weight loss following diet-induced obesity does not alter colon tumorigenesis in the AOM mouse model. *Am J Physiol Gastrointest Liver Physiol* 2016; **311**: G699-G712 [PMID: 27609769 DOI: 10.1152/ajpgi.00207.2016]
56 **Cuellar-Nuñez ML**, Luzardo-Ocampo I, Campos-Vega R, Gallegos-Corona MA, González de Mejía E, Loarca-Piña G. Physicochemical and nutraceutical properties of moringa (Moringa oleifera) leaves and their effects in an in vivo AOM/DSS-induced colorectal carcinogenesis model. *Food Res Int* 2018; **105**: 159-168 [PMID: 29433203 DOI: 10.1016/j.foodres.2017.11.004]
57 **Canene-Adams K**, Sfanos KS, Liang CT, Yegnasubramanian S, Nelson WG, Brayton C, De Marzo AM. Dietary chemoprevention of PhIP induced carcinogenesis in male Fischer 344 rats with tomato and broccoli. *PLoS One* 2013; **8**: e79842 [PMID: 24312188 DOI: 10.1371/journal.pone.0079842]
58 **Chen JX**, Liu A, Lee MJ, Wang H, Yu S, Chi E, Reuhl K, Suh N, Yang CS. δ- and γ-tocopherols inhibit phIP/DSS-induced colon carcinogenesis by protection against early cellular and DNA damages. *Mol Carcinog* 2017; **56**: 172-183 [PMID: 27175800 DOI: 10.1002/mc.22481]
59 **Bi W**, Liu H, Shen J, Zhang LH, Li P, Peng B, Cao L, Zhang P, He C, Xiao P. Chemopreventive effects of Ku-jin tea against AOM-induced precancerous colorectal lesions in rats and metabolomic analysis. *Sci Rep* 2017; **7**: 15893 [PMID: 29162930 DOI: 10.1038/s41598-017-16237-0]
60 **Sun MC**, Zhang FC, Yin X, Cheng BJ, Zhao CH, Wang YL, Zhang ZZ, Hao HW, Zhang TH, Ye HQ. Lactobacillus reuteri F-9-35 Prevents DSS-Induced Colitis by Inhibiting Proinflammatory Gene

Expression and Restoring the Gut Microbiota in Mice. *J Food Sci* 2018; **83**: 2645-2652 [PMID: 30216448 DOI: 10.1111/1750-3841.14326]
61 **Snider AJ**, Bialkowska AB, Ghaleb AM, Yang VW, Obeid LM, Hannun YA. Murine Model for Colitis-Associated Cancer of the Colon. *Methods Mol Biol* 2016; **1438**: 245-254 [PMID: 27150094 DOI: 10.1007/978-1-4939-3661-8_14]
62 **Yang J**, Shikata N, Mizuoka H, Tsubura A. Colon carcinogenesis in shrews by intrarectal infusion of N-methyl-N-nitrosourea. *Cancer Lett* 1996; **110**: 105-112 [PMID: 9018088 DOI: 10.1016/s0304-3835(96)04468-0]
63 **Derry MM**, Raina K, Agarwal R, Agarwal C. Characterization of azoxymethane-induced colon tumor metastasis to lung in a mouse model relevant to human sporadic colorectal cancer and evaluation of grape seed extract efficacy. *Exp Toxicol Pathol* 2014; **66**: 235-242 [PMID: 24670932 DOI: 10.1016/j.etp.2014.02.003]
64 **Papanikolaou A**, Wang QS, Papanikolaou D, Whiteley HE, Rosenberg DW. Sequential and morphological analyses of aberrant crypt foci formation in mice of differing susceptibility to azoxymethane-induced colon carcinogenesis. *Carcinogenesis* 2000; **21**: 1567-1572 [PMID: 10910960]
65 **Nambiar PR**, Girnun G, Lillo NA, Guda K, Whiteley HE, Rosenberg DW. Preliminary analysis of azoxymethane induced colon tumors in inbred mice commonly used as transgenic/knockout progenitors. *Int J Oncol* 2003; **22**: 145-150 [PMID: 12469197 DOI: 10.3892/ijo.22.1.145]
66 **Clapp NK**, Henke MA, London JF, Shock TL. Enhancement of 1,2-dimethylhydrazine-induced large bowel tumorigenesis in Balb/c mice by corn, soybean, and wheat brans. *Nutr Cancer* 1984; **6**: 77-85 [PMID: 6100660 DOI: 10.1080/0163558850951381]
67 **Neufert C**, Becker C, Neurath MF. An inducible mouse model of colon carcinogenesis for the analysis of sporadic and inflammation-driven tumor progression. *Nat Protoc* 2007; **2**: 1998-2004 [PMID: 17703211 DOI: 10.1038/nprot.2007.279]
68 **Piñol V**, Andreu M, Castells A, Payá A, Bessa X, Jover R; Gastrointestinal Oncology Group of the Spanish Gastroenterological Association. Synchronous colorectal neoplasms in patients with colorectal cancer: predisposing individual and familial factors. *Dis Colon Rectum* 2004; **47**: 1192-1200 [PMID: 15164252 DOI: 10.1007/s10350-004-0562-7]
69 **Marqués-Lespier JM**, Soto-Salgado M, González-Pons M, Méndez V, Freyre K, Beltrán C, Pericchi LR, Cruz-Correa M. Prevalence of Synchronous Oligopolyposis in Incident Colorectal Cancer: A Population-Based Study. *P R Health Sci J* 2018; **37**: 39-45 [PMID: 29547683]
70 **Thaker AI**, Shaker A, Rao MS, Ciorba MA. Modeling colitis-associated cancer with azoxymethane (AOM) and dextran sulfate sodium (DSS). *J Vis Exp* 2012; (67) [PMID: 22990604 DOI: 10.3791/4100]
71 **Matsumoto K**, Iwase T, Hirono I, Nishida Y, Iwahori Y, Hori T, Asamoto M, Takasuka N, Kim DJ, Ushijima T, Nagao M, Tsuda H. Demonstration of ras and p53 gene mutations in carcinomas in the forestomach and intestine and soft tissue sarcomas induced by N-methyl-N-nitrosourea in the rat. *Jpn J Cancer Res* 1997; **88**: 129-136 [PMID: 9119740 DOI: 10.1111/j.1349-7006.1997.tb00357.x]
72 **Nordlinger B**, Panis Y, Puts JP, Herve JP, Delelo R, Ballet F. Experimental model of colon cancer: recurrences after surgery alone or associated with intraperitoneal 5-fluorouracil chemotherapy. *Dis Colon Rectum* 1991; **34**: 658-663 [PMID: 1855422 DOI: 10.1007/bf02050346]
73 **Narisawa T**, Weisburger JH. Colon cancer induction in mice by intrarectal instillation of N-methylnitosorurea (38498). *Proc Soc Exp Biol Med* 1975; **148**: 166-169 [PMID: 1129255 DOI: 10.3181/00379727-148-38498]
74 **Hasegawa R**, Sano M, Tamano S, Imaida K, Shirai T, Nagao M, Sugimura T, Ito N. Dose-dependence of 2-amino-1-methyl-6-phenylimidazo[4,5-b]-pyridine (PhIP) carcinogenicity in rats. *Carcinogenesis* 1993; **14**: 2553-2557 [PMID: 8269626 DOI: 10.1093/carcin/14.12.2553]
75 **Leslie A**, Carey FA, Pratt NR, Steele RJ. The colorectal adenoma-carcinoma sequence. *Br J Surg* 2002; **89**: 845-860 [PMID: 12081733 DOI: 10.1046/j.1365-2168.2002.02120.x]
76 **Jacoby RF**, Llor X, Teng BB, Davidson NO, Brasitus TA. Mutations in the K-ras oncogene induced by 1,2-dimethylhydrazine in preneoplastic and neoplastic rat colonic mucosa. *J Clin Invest* 1991; **87**: 624-630 [PMID: 1991846 DOI: 10.1172/JCI115039]
77 **De Filippo C**, Caderni G, Bazzicalupo M, Briani C, Giannini A, Fazi M, Dolara P. Mutations of the Apc gene in experimental colorectal carcinogenesis induced by azoxymethane in F344 rats. *Br J Cancer* 1998; **77**: 2148-2151 [PMID: 9649126 DOI: 10.1038/bjc.1998.359]
78 **Aaltonen LA**, Peltomäki P, Leach FS, Sistonen P, Pylkkänen L, Mecklin JP, Järvinen H, Powell SM, Jen J, Hamilton SR. Clues to the pathogenesis of familial colorectal cancer. *Science* 1993; **260**: 812-816 [PMID: 8484121 DOI: 10.1126/science.8484121]
79 **Pan Q**, Lou X, Zhang J, Zhu Y, Li F, Shan Q, Chen X, Xie Y, Su S, Wei H, Lin L, Wu L, Liu S. Genomic variants in mouse model induced by azoxymethane and dextran sodium sulfate improperly mimic human colorectal cancer. *Sci Rep* 2017; **7**: 25 [PMID: 28154415 DOI: 10.1038/s41598-017-00057-3]
80 **Cheung C**, Loy S, Li GX, Liu AB, Yang CS. Rapid induction of colon carcinogenesis in CYP1A-humanized mice by 2-amino-1-methyl-6-phenylimidazo[4,5-b]pyridine and dextran sodium sulfate. *Carcinogenesis* 2011; **32**: 233-239 [PMID: 21081470 DOI: 10.1093/carcin/bgq235]
81 **Brinster RL**, Chen HY, Messing A, van Dyke T, Levine AJ, Palmiter RD. Transgenic mice harboring SV40 T-antigen genes develop characteristic brain tumors. *Cell* 1984; **37**: 367-379 [PMID: 6327063 DOI: 10.1016/0092-8674(84)90367-2]
82 **Adams JM**, Harris AW, Pinkert CA, Corcoran LM, Alexander WS, Cory S, Palmiter RD, Brinster RL. The c-myc oncogene driven by immunoglobulin enhancers induces lymphoid malignancy in transgenic mice. *Nature* 1985; **318**: 533-538 [PMID: 3906410 DOI: 10.1038/318533a0]
83 **Ornitz DM**, Palmiter RD, Messing A, Hammer RE, Pinkert CA, Brinster RL. Elastase I promoter directs expression of human growth hormone and SV40 T antigen genes to pancreatic acinar cells in transgenic mice. *Cold Spring Harb Symp Quant Biol* 1985; **50**: 399-409 [PMID: 3006998 DOI: 10.1101/sqb.1985.050.01.050]
84 **Quaife CJ**, Pinkert CA, Ornitz DM, Palmiter RD, Brinster RL. Pancreatic neoplasia induced by ras expression in acinar cells of transgenic mice. *Cell* 1987; **48**: 1023-1034 [PMID: 3470144 DOI: 10.1016/0092-8674(87)90710-0]
85 **Stewart TA**, Pattengale PK, Leder P. Spontaneous mammary adenocarcinomas in transgenic mice that carry and express MTV/myc fusion genes. *Cell* 1984; **38**: 627-637 [PMID: 6488314 DOI: 10.1016/0092-8674(84)90257-5]
86 **Rüther U**, Garber C, Komitowski D, Müller R, Wagner EF. Deregulated c-fos expression interferes with normal bone development in transgenic mice. *Nature* 1987; **325**: 412-416 [PMID: 3027573 DOI:

10.1038/325412a0]
87 **Hanahan D**. Heritable formation of pancreatic beta-cell tumours in transgenic mice expressing recombinant insulin/simian virus 40 oncogenes. *Nature* 1985; **315**: 115-122 [PMID: 2986015 DOI: 10.1038/315115a0]
88 **Schäfer C**. Nobel Price for Medicine 2007. Knockout mice are revolutionizing genetics. *Ophthalmologe* 2007; **104**: 1080-1082 [PMID: 18074163 DOI: 10.1007/s00347-007-1663-1]
89 **Jacks T**, Fazeli A, Schmitt EM, Bronson RT, Goodell MA, Weinberg RA. Effects of an Rb mutation in the mouse. *Nature* 1992; **359**: 295-300 [PMID: 1406933 DOI: 10.1038/359295a0]
90 **Donehower LA**, Harvey M, Slagle BL, McArthur MJ, Montgomery CA, Butel JS, Bradley A. Mice deficient for p53 are developmentally normal but susceptible to spontaneous tumours. *Nature* 1992; **356**: 215-221 [PMID: 1552940 DOI: 10.1038/356215a0]
91 **Lakso M**, Sauer B, Mosinger B, Lee EJ, Manning RW, Yu SH, Mulder KL, Westphal H. Targeted oncogene activation by site-specific recombination in transgenic mice. *Proc Natl Acad Sci USA* 1992; **89**: 6232-6236 [PMID: 1631115 DOI: 10.1073/pnas.89.14.6232]
92 **Meuwissen R**, Linn SC, van der Valk M, Mooi WJ, Berns A. Mouse model for lung tumorigenesis through Cre/lox controlled sporadic activation of the K-Ras oncogene. *Oncogene* 2001; **20**: 6551-6558 [PMID: 11641780 DOI: 10.1038/sj.onc.1204837]
93 **Hingorani SR**, Petricoin EF, Maitra A, Rajapakse V, King C, Jacobetz MA, Ross S, Conrads TP, Veenstra TD, Hitt BA, Kawaguchi Y, Johann D, Liotta LA, Crawford HC, Putt ME, Jacks T, Wright CV, Hruban RH, Lowy AM, Tuveson DA. Preinvasive and invasive ductal pancreatic cancer and its early detection in the mouse. *Cancer Cell* 2003; **4**: 437-450 [PMID: 14706336 DOI: 10.1016/s1535-6108(03)00309-x]
94 **Moser AR**, Pitot HC, Dove WF. A dominant mutation that predisposes to multiple intestinal neoplasia in the mouse. *Science* 1990; **247**: 322-324 [PMID: 2296722 DOI: 10.1126/science.2296722]
95 **Shoemaker AR**, Gould KA, Luongo C, Moser AR, Dove WF. Studies of neoplasia in the Min mouse. *Biochim Biophys Acta* 1997; **1332**: F25-F48 [PMID: 9141462 DOI: 10.1016/s0304-419x(96)00041-8]
96 **Yamada Y**, Mori H. Multistep carcinogenesis of the colon in Apc(Min/+) mouse. *Cancer Sci* 2007; **98**: 6-10 [PMID: 17052257 DOI: 10.1111/j.1349-7006.2006.00348.x]
97 **Moser AR**, Shoemaker AR, Connelly CS, Clipson L, Gould KA, Luongo C, Dove WF, Siggers PH, Gardner RL. Homozygosity for the Min allele of Apc results in disruption of mouse development prior to gastrulation. *Dev Dyn* 1995; **203**: 422-433 [PMID: 7496034 DOI: 10.1002/aja.1002030405]
98 **Møllersen L**, Paulsen JE, Alexander J. Loss of heterozygosity and nonsense mutation in Apc in azoxymethane-induced colonic tumours in min mice. *Anticancer Res* 2004; **24**: 2595-2599 [PMID: 15517863]
99 **Ju J**, Nolan B, Cheh M, Bose M, Lin Y, Wagner GC, Yang CS. Voluntary exercise inhibits intestinal tumorigenesis in Apc(Min/+) mice and azoxymethane/dextran sulfate sodium-treated mice. *BMC Cancer* 2008; **8**: 316 [PMID: 18976499 DOI: 10.1186/1471-2407-8-316]
100 **Tanaka T**, Suzuki R, Kohno H, Sugie S, Takahashi M, Wakabayashi K. Colonic adenocarcinomas rapidly induced by the combined treatment with 2-amino-1-methyl-6-phenylimidazo[4,5-b]pyridine and dextran sodium sulfate in male ICR mice possess beta-catenin gene mutations and increases immunoreactivity for beta-catenin, cyclooxygenase-2 and inducible nitric oxide synthase. *Carcinogenesis* 2005; **26**: 229-238 [PMID: 15459021 DOI: 10.1093/carcin/bgh292]
101 **Jin D**, Liu T, Dong W, Zhang Y, Wang S, Xie R, Wang B, Cao H. Dietary feeding of freeze-dried whole cranberry inhibits intestinal tumor development in *Apc*$^{min/+}$ mice. *Oncotarget* 2017; **8**: 97787-97800 [PMID: 29228651 DOI: 10.18632/oncotarget.22081]
102 **Ni Y**, Wong VH, Tai WC, Li J, Wong WY, Lee MM, Fong FL, El-Nezami H, Panagiotou G. A metagenomic study of the preventive effect of Lactobacillus rhamnosus GG on intestinal polyp formation in Apc$^{Min/+}$ mice. *J Appl Microbiol* 2017; **122**: 770-784 [PMID: 28004480 DOI: 10.1111/jam.13386]
103 **Zhang L**, Shay JW. Multiple Roles of APC and its Therapeutic Implications in Colorectal Cancer. *J Natl Cancer Inst* 2017; **109** [PMID: 28423402 DOI: 10.1093/jnci/djw332]
104 **Halberg RB**, Waggoner J, Rasmussen K, White A, Clipson L, Prunuske AJ, Bacher JW, Sullivan R, Washington MK, Pitot HC, Petrini JH, Albertson DG, Dove WF. Long-lived Min mice develop advanced intestinal cancers through a genetically conservative pathway. *Cancer Res* 2009; **69**: 5768-5775 [PMID: 19584276 DOI: 10.1158/0008-5472.CAN-09-0446]
105 **Sødring M**, Gunnes G, Paulsen JE. Spontaneous initiation, promotion and progression of colorectal cancer in the novel A/J Min/+ mouse. *Int J Cancer* 2016; **138**: 1936-1946 [PMID: 26566853 DOI: 10.1002/ijc.29928]
106 **Fodde R**, Edelmann W, Yang K, van Leeuwen C, Carlson C, Renault B, Breukel C, Alt E, Lipkin M, Khan PM. A targeted chain-termination mutation in the mouse Apc gene results in multiple intestinal tumors. *Proc Natl Acad Sci USA* 1994; **91**: 8969-8973 [PMID: 8090754 DOI: 10.1073/pnas.91.19.8969]
107 **Smits R**, Kartheuser A, Jagmohan-Changur S, Leblanc V, Breukel C, de Vries A, van Kranen H, van Krieken JH, Williamson S, Edelmann W, Kucherlapati R, KhanPM, Fodde R. Loss of Apc and the entire chromosome 18 but absence of mutations at the Ras and Tp53 genes in intestinal tumors from Apc1638N, a mouse model for Apc-driven carcinogenesis. *Carcinogenesis* 1997; **18**: 321-327 [PMID: 9054624 DOI: 10.1093/carcin/18.2.321]
108 **Oshima M**, Oshima H, Kitagawa K, Kobayashi M, Itakura C, Taketo M. Loss of Apc heterozygosity and abnormal tissue building in nascent intestinal polyps in mice carrying a truncated Apc gene. *Proc Natl Acad Sci USA* 1995; **92**: 4482-4486 [PMID: 7753829 DOI: 10.1073/pnas.92.10.4482]
109 **Crist RC**, Roth JJ, Baran AA, McEntee BJ, Siracusa LD, Buchberg AM. The armadillo repeat domain of Apc suppresses intestinal tumorigenesis. *Mamm Genome* 2010; **21**: 450-457 [PMID: 20886217 DOI: 10.1007/s00335-010-9288-0]
110 **Colnot S**, Niwa-Kawakita M, Hamard G, Godard C, Le Plenier S, Houbron C, Romagnolo B, Berrebi D, Giovannini M, Perret C. Colorectal cancers in a new mouse model of familial adenomatous polyposis: influence of genetic and environmental modifiers. *Lab Invest* 2004; **84**: 1619-1630 [PMID: 15502862 DOI: 10.1038/labinvest.3700180]
111 **Fazeli A**, Steen RG, Dickinson SL, Bautista D, Dietrich WF, Bronson RT, Bresalier RS, Lander ES, Costa J, Weinberg RA. Effects of p53 mutations on apoptosis in mouse intestinal and human colonic adenomas. *Proc Natl Acad Sci USA* 1997; **94**: 10199-10204 [PMID: 9294187 DOI: 10.1073/pnas.94.19.10199]
112 **Clarke AR**, Cummings MC, Harrison DJ. Interaction between murine germline mutations in p53 and APC predisposes to pancreatic neoplasia but not to increased intestinal malignancy. *Oncogene* 1995; **11**: 1913-1920 [PMID: 7478622]
113 **Halberg RB**, Katzung DS, Hoff PD, Moser AR, Cole CE, Lubet RA, Donehower LA, Jacoby RF, Dove

WF. Tumorigenesis in the multiple intestinal neoplasia mouse: redundancy of negative regulators and specificity of modifiers. *Proc Natl Acad Sci USA* 2000; **97**: 3461-3466 [PMID: 10716720 DOI: 10.1073/pnas.050585597]

114 **Maslon MM**, Hupp TR. Drug discovery and mutant p53. *Trends Cell Biol* 2010; **20**: 542-555 [PMID: 20656489 DOI: 10.1016/j.tcb.2010.06.005]

115 **Billant O**, Léon A, Le Guellec S, Friocourt G, Blondel M, Voisset C. The dominant-negative interplay between p53, p63 and p73: A family affair. *Oncotarget* 2016; **7**: 69549-69564 [PMID: 27589690 DOI: 10.18632/oncotarget.11774]

116 **Tuveson DA**, Shaw AT, Willis NA, Silver DP, Jackson EL, Chang S, Mercer KL, Grochow R, Hock H, Crowley D, Hingorani SR, Zaks T, King C, Jacobetz MA, Wang L, Bronson RT, Orkin SH, DePinho RA, Jacks T. Endogenous oncogenic K-ras(G12D) stimulates proliferation and widespread neoplastic and developmental defects. *Cancer Cell* 2004; **5**: 375-387 [PMID: 15093544 DOI: 10.1016/s1535-6108(04)00085-6]

117 **Guerra C**, Mijimolle N, Dhawahir A, Dubus P, Barradas M, Serrano M, Campuzano V, Barbacid M. Tumor induction by an endogenous K-ras oncogene is highly dependent on cellular context. *Cancer Cell* 2003; **4**: 111-120 [PMID: 12957286 DOI: 10.1016/s1535-6108(03)00191-0]

118 **el Marjou F**, Janssen KP, Chang BH, Li M, Hindie V, Chan L, Louvard D, Chambon P, Metzger D, Robine S. Tissue-specific and inducible Cre-mediated recombination in the gut epithelium. *Genesis* 2004; **39**: 186-193 [PMID: 15282745 DOI: 10.1002/gene.20042]

119 **Saam JR**, Gordon JI. Inducible gene knockouts in the small intestinal and colonic epithelium. *J Biol Chem* 1999; **274**: 38071-38082 [PMID: 10608876 DOI: 10.1074/jbc.274.53.38071]

120 **Robanus-Maandag EC**, Koelink PJ, Breukel C, Salvatori DC, Jagmohan-Changur SC, Bosch CA, Verspaget HW, Devilee P, Fodde R, Smits R. A new conditional Apc-mutant mouse model for colorectal cancer. *Carcinogenesis* 2010; **31**: 946-952 [PMID: 20176656 DOI: 10.1093/carcin/bgq046]

121 **Ireland H**, Kemp R, Houghton C, Howard L, Clarke AR, Sansom OJ, Winton DJ. Inducible Cre-mediated control of gene expression in the murine gastrointestinal tract: effect of loss of beta-catenin. *Gastroenterology* 2004; **126**: 1236-1246 [PMID: 15131783 DOI: 10.1053/j.gastro.2004.03.020]

122 **Sansom OJ**, Meniel V, Wilkins JA, Cole AM, Oien KA, Marsh V, Jamieson TJ, Guerra C, Ashton GH, Barbacid M, Clarke AR. Loss of Apc allows phenotypic manifestation of the transforming properties of an endogenous K-ras oncogene in vivo. *Proc Natl Acad Sci USA* 2006; **103**: 14122-14127 [PMID: 16959882 DOI: 10.1073/pnas.0604130103]

123 **Sansom OJ**, Griffiths DF, Reed KR, Winton DJ, Clarke AR. Apc deficiency predisposes to renal carcinoma in the mouse. *Oncogene* 2005; **24**: 8205-8210 [PMID: 16116480 DOI: 10.1038/sj.onc.1208956]

124 **Hinoi T**, Akyol A, Theisen BK, Ferguson DO, Greenson JK, Williams BO, Cho KR, Fearon ER. Mouse model of colonic adenoma-carcinoma progression based on somatic Apc inactivation. *Cancer Res* 2007; **67**: 9721-9730 [PMID: 17942902 DOI: 10.1158/0008-5472.CAN-07-2735]

125 **Akyol A**, Hinoi T, Feng Y, Bommer GT, Glaser TM, Fearon ER. Generating somatic mosaicism with a Cre recombinase-microsatellite sequence transgene. *Nat Methods* 2008; **5**: 231-233 [PMID: 18264107 DOI: 10.1038/nmeth.1182]

126 **Xue Y**, Johnson R, Desmet M, Snyder PW, Fleet JC. Generation of a transgenic mouse for colorectal cancer research with intestinal cre expression limited to the large intestine. *Mol Cancer Res* 2010; **8**: 1095-1104 [PMID: 20663863 DOI: 10.1158/1541-7786.MCR-10-0195]

127 **Shibata H**, Toyama K, Shioya H, Ito M, Hirota M, Hasegawa S, Matsumoto H, Takano H, Akiyama T, Toyoshima K, Kanamaru R, Kanegae Y, Saito I, Nakamura Y, Shiba K, Noda T. Rapid colorectal adenoma formation initiated by conditional targeting of the Apc gene. *Science* 1997; **278**: 120-123 [PMID: 9311916 DOI: 10.1126/science.278.5335.120]

128 **Roper J**, Tammela T, Cetinbas NM, Akkad A, Roghanian A, Rickelt S, Almeqdadi M, Wu K, Oberli MA, Sánchez-Rivera FJ, Park YK, Liang X, Eng G, Taylor MS, Azimi R, Kedrin D, Neupane R, Beyaz S, Sicinska ET, Suarez Y, Yoo J, Chen L, Zukerberg L, Katajisto P, Deshpande V, Bass AJ, Tsichlis PN, Lees J, Langer R, Hynes RO, Chen J, Bhutkar A, Jacks T, Yilmaz ÖH. In vivo genome editing and organoid transplantation models of colorectal cancer and metastasis. *Nat Biotechnol* 2017; **35**: 569-576 [PMID: 28459449 DOI: 10.1038/nbt.3836]

129 **Hadac JN**, Leystra AA, Paul Olson TJ, Maher ME, Payne SN, Yueh AE, Schwartz AR, Albrecht DM, Clipson L, Pasch CA, Matkowskyj KA, Halberg RB, Deming DA. Colon Tumors with the Simultaneous Induction of Driver Mutations in APC, KRAS, and PIK3CA Still Progress through the Adenoma-to-carcinoma Sequence. *Cancer Prev Res (Phila)* 2015; **8**: 952-961 [PMID: 26276752 DOI: 10.1158/1940-6207.CAPR-15-0003]

130 **Hung KE**, Maricevich MA, Richard LG, Chen WY, Richardson MP, Kunin A, Bronson RT, Mahmood U, Kucherlapati R. Development of a mouse model for sporadic and metastatic colon tumors and its use in assessing drug treatment. *Proc Natl Acad Sci USA* 2010; **107**: 1565-1570 [PMID: 20080688 DOI: 10.1073/pnas.0908682107]

131 **Sansom OJ**, Reed KR, Hayes AJ, Ireland H, Brinkmann H, Newton IP, Batlle E, Simon-Assmann P, Clevers H, Nathke IS, Clarke AR, Winton DJ. Loss of Apc in vivo immediately perturbs Wnt signaling, differentiation, and migration. *Genes Dev* 2004; **18**: 1385-1390 [PMID: 15198980 DOI: 10.1101/gad.287404]

132 **Cheung AF**, Carter AM, Kostova KK, Woodruff JF, Crowley D, Bronson RT, Haigis KM, Jacks T. Complete deletion of Apc results in severe polyposis in mice. *Oncogene* 2010; **29**: 1857-1864 [PMID: 20010873 DOI: 10.1038/onc.2009.457]

133 **Feng Y**, Sentani K, Wiese A, Sands E, Green M, Bommer GT, Cho KR, Fearon ER. Sox9 induction, ectopic Paneth cells, and mitotic spindle axis defects in mouse colon adenomatous epithelium arising from conditional biallelic Apc inactivation. *Am J Pathol* 2013; **183**: 493-503 [PMID: 23769888 DOI: 10.1016/j.ajpath.2013.04.013]

134 **Calcagno SR**, Li S, Colon M, Kreinest PA, Thompson EA, Fields AP, Murray NR. Oncogenic K-ras promotes early carcinogenesis in the mouse proximal colon. *Int J Cancer* 2008; **122**: 2462-2470 [PMID: 18271008 DOI: 10.1002/ijc.23383]

135 **Luo F**, Brooks DG, Ye H, Hamoudi R, Poulogiannis G, Patek CE, Winton DJ, Arends MJ. Mutated K-ras(Asp12) promotes tumourigenesis in Apc(Min) mice more in the large than the small intestines, with synergistic effects between K-ras and Wnt pathways. *Int J Exp Pathol* 2009; **90**: 558-574 [PMID: 19765110 DOI: 10.1111/j.1365-2613.2009.00667.x]

136 **Haigis KM**, Kendall KR, Wang Y, Cheung A, Haigis MC, Glickman JN, Niwa-Kawakita M, Sweet-Cordero A, Sebolt-Leopold J, Shannon KM, Settleman J, Giovannini M, Jacks T. Differential effects of

oncogenic K-Ras and N-Ras on proliferation, differentiation and tumor progression in the colon. *Nat Genet* 2008; **40**: 600-608 [PMID: 18372904 DOI: 10.1038/ng.115]
137 **Russo A**, Bazan V, Iacopetta B, Kerr D, Soussi T, Gebbia N; TP53-CRC Collaborative Study Group. The TP53 colorectal cancer international collaborative study on the prognostic and predictive significance of p53 mutation: influence of tumor site, type of mutation, and adjuvant treatment. *J Clin Oncol* 2005; **23**: 7518-7528 [PMID: 16172461 DOI: 10.1200/JCO.2005.00.471]
138 **Iacopetta B**, Russo A, Bazan V, Dardanoni G, Gebbia N, Soussi T, Kerr D, Elsaleh H, Soong R, Kandioler D, Janschek E, Kappel S, Lung M, Leung CS, Ko JM, Yuen S, Ho J, Leung SY, Crapez E, Duffour J, Ychou M, Leahy DT, O'Donoghue DP, Agnese V, Cascio S, Di Fede G, Chieco-Bianchi L, Bertorelle R, Belluco C, Giaretti W, Castagnola P, Ricevuto E, Ficorella C, Bosari S, Arizzi CD, Miyaki M, Onda M, Kampman E, Diergaarde B, Royds J, Lothe RA, Diep CB, Meling GI, Ostrowski J, Trzeciak L, Guzinska-Ustymowicz K, Zalewski B, Capellá GM, Moreno V, Peinado MA, Lönnroth C, Lundholm K, Sun XF, Jansson A, Bouzourene H, Hsieh LL, Tang R, Smith DR, Allen-Mersh TG, Khan ZA, Shorthouse AJ, Silverman ML, Kato S, Ishioka C; TP53-CRC Collaborative Group. Functional categories of TP53 mutation in colorectal cancer: results of an International Collaborative Study. *Ann Oncol* 2006; **17**: 842-847 [PMID: 16524972 DOI: 10.1093/annonc/mdl035]
139 **Nakayama M**, Sakai E, Echizen K, Yamada Y, Oshima H, Han TS, Ohki R, Fujii S, Ochiai A, Robine S, Voon DC, Tanaka T, Taketo MM, Oshima M. Intestinal cancer progression by mutant p53 through the acquisition of invasiveness associated with complex glandular formation. *Oncogene* 2017; **36**: 5885-5896 [PMID: 28628120 DOI: 10.1038/onc.2017.194]
140 **Sakai E**, Nakayama M, Oshima H, Kouyama Y, Niida A, Fujii S, Ochiai A, Nakayama KI, Mimori K, Suzuki Y, Hong CP, Ock CY, Kim SJ, Oshima M. Combined Mutation of *Apc, Kras*, and *Tgfbr2* Effectively Drives Metastasis of Intestinal Cancer. *Cancer Res* 2018; **78**: 1334-1346 [PMID: 29282223 DOI: 10.1158/0008-5472.CAN-17-3303]
141 **Chanrion M**, Kuperstein I, Barrière C, El Marjou F, Cohen D, Vignjevic D, Stimmer L, Paul-Gilloteaux P, Bièche I, Tavares Sdos R, Boccia GF, Cacheux W, Meseure D, Fre S, Martignetti L, Legoix-Né P, Girard E, Fetler L, Barillot E, Louvard D, Zinovyev A, Robine S. Concomitant Notch activation and p53 deletion trigger epithelial-to-mesenchymal transition and metastasis in mouse gut. *Nat Commun* 2014; **5**: 5005 [PMID: 25295490 DOI: 10.1038/ncomms6005]
142 **Fre S**, Pallavi SK, Huyghe M, Laé M, Janssen KP, Robine S, Artavanis-Tsakonas S, Louvard D. Notch and Wnt signals cooperatively control cell proliferation and tumorigenesis in the intestine. *Proc Natl Acad Sci USA* 2009; **106**: 6309-6314 [PMID: 19251639 DOI: 10.1073/pnas.0900427106]
143 **Dow LE**, O'Rourke KP, Simon J, Tschaharganeh DF, van Es JH, Clevers H, Lowe SW. Apc Restoration Promotes Cellular Differentiation and Reestablishes Crypt Homeostasis in Colorectal Cancer. *Cell* 2015; **161**: 1539-1552 [PMID: 26091037 DOI: 10.1016/j.cell.2015.05.033]
144 **Mao JH**, Perez-Losada J, Wu D, Delrosario R, Tsunematsu R, Nakayama KI, Brown K, Bryson S, Balmain A. Fbxw7/Cdc4 is a p53-dependent, haploinsufficient tumour suppressor gene. *Nature* 2004; **432**: 775-779 [PMID: 15592418 DOI: 10.1038/nature03155]
145 **Welcker M**, Clurman BE. FBW7 ubiquitin ligase: a tumour suppressor at the crossroads of cell division, growth and differentiation. *Nat Rev Cancer* 2008; **8**: 83-93 [PMID: 18094723 DOI: 10.1038/nrc2290]
146 **Babaei-Jadidi R**, Li N, Saadeddin A, Spencer-Dene B, Jandke A, Muhammad B, Ibrahim EE, Muraleedharan R, Abuzinadah M, Davis H, Lewis A, Watson S, Behrens A, Tomlinson I, Nateri AS. FBXW7 influences murine intestinal homeostasis and cancer, targeting Notch, Jun, and DEK for degradation. *J Exp Med* 2011; **208**: 295-312 [PMID: 21282377 DOI: 10.1084/jem.20100830]
147 **Sancho R**, Jandke A, Davis H, Diefenbacher ME, Tomlinson I, Behrens A. F-box and WD repeat domain-containing 7 regulates intestinal cell lineage commitment and is a haploinsufficient tumor suppressor. *Gastroenterology* 2010; **139**: 929-941 [PMID: 20638938 DOI: 10.1053/j.gastro.2010.05.078]
148 **Grim JE**, Knoblaugh SE, Guthrie KA, Hagar A, Swanger J, Hespelt J, Delrow JJ, Small T, Grady WM, Nakayama KI, Clurman BE. Fbw7 and p53 cooperatively suppress advanced and chromosomally unstable intestinal cancer. *Mol Cell Biol* 2012; **32**: 2160-2167 [PMID: 22473991 DOI: 10.1128/MCB.00305-12]
149 **Faes S**, Dormond O. PI3K and AKT: Unfaithful Partners in Cancer. *Int J Mol Sci* 2015; **16**: 21138-21152 [PMID: 26404259 DOI: 10.3390/ijms160921138]
150 **Leystra AA**, Deming DA, Zahm CD, Farhoud M, Olson TJ, Hadac JN, Nettekoven LA, Albrecht DM, Clipson L, Sullivan R, Washington MK, Torrealba JR, Weichert JP, Halberg RB. Mice expressing activated PI3K rapidly develop advanced colon cancer. *Cancer Res* 2012; **72**: 2931-2936 [PMID: 22525701 DOI: 10.1158/0008-5472.CAN-11-4097]
151 **Marsh V**, Winton DJ, Williams GT, Dubois N, Trumpp A, Sansom OJ, Clarke AR. Epithelial Pten is dispensable for intestinal homeostasis but suppresses adenoma development and progression after Apc mutation. *Nat Genet* 2008; **40**: 1436-1444 [PMID: 19011632 DOI: 10.1038/ng.256]
152 **Davies EJ**, Marsh Durban V, Meniel V, Williams GT, Clarke AR. PTEN loss and KRAS activation leads to the formation of serrated adenomas and metastatic carcinoma in the mouse intestine. *J Pathol* 2014; **233**: 27-38 [PMID: 24293351 DOI: 10.1002/path.4312]
153 **Yu M**, Trobridge P, Wang Y, Kanngurn S, Morris SM, Knoblaugh S, Grady WM. Inactivation of TGF-β signaling and loss of PTEN cooperate to induce colon cancer in vivo. *Oncogene* 2014; **33**: 1538-1547 [PMID: 23604118 DOI: 10.1038/onc.2013.102]
154 **Syed V**. TGF-β Signaling in Cancer. *J Cell Biochem* 2016; **117**: 1279-1287 [PMID: 26774024 DOI: 10.1002/jcb.25496]
155 **Nagaraj NS**, Datta PK. Targeting the transforming growth factor-beta signaling pathway in human cancer. *Expert Opin Investig Drugs* 2010; **19**: 77-91 [PMID: 20001556 DOI: 10.1517/13543780903382609]
156 **Alberici P**, Jagmohan-Changur S, De Pater E, Van Der Valk M, Smits R, Hohenstein P, Fodde R. Smad4 haploinsufficiency in mouse models for intestinal cancer. *Oncogene* 2006; **25**: 1841-1851 [PMID: 16288217 DOI: 10.1038/sj.onc.1209226]
157 **Takaku K**, Oshima M, Miyoshi H, Matsui M, Seldin MF, Taketo MM. Intestinal tumorigenesis in compound mutant mice of both Dpc4 (Smad4) and Apc genes. *Cell* 1998; **92**: 645-656 [PMID: 9506519 DOI: 10.1016/s0092-8674(00)81132-0]
158 **Tetteh PW**, Kretzschmar K, Begthel H, van den Born M, Korving J, Morsink F, Farin H, van Es JH, Offerhaus GJ, Clevers H. Generation of an inducible colon-specific Cre enzyme mouse line for colon cancer research. *Proc Natl Acad Sci USA* 2016; **113**: 11859-11864 [PMID: 27708166 DOI: 10.1073/pnas.1614057113]
159 **Takaku K**, Wrana JL, Robertson EJ, Taketo MM. No effects of Smad2 (madh2) null mutation on malignant progression of intestinal polyps in Apc(delta716) knockout mice. *Cancer Res* 2002; **62**: 4558-

4561 [PMID: 12183405]
160 **Zhu Y**, Richardson JA, Parada LF, Graff JM. Smad3 mutant mice develop metastatic colorectal cancer. *Cell* 1998; **94**: 703-714 [PMID: 9753318 DOI: 10.1016/s0092-8674(00)81730-4]
161 **Sodir NM**, Chen X, Park R, Nickel AE, Conti PS, Moats R, Bading JR, Shibata D, Laird PW. Smad3 deficiency promotes tumorigenesis in the distal colon of ApcMin/+ mice. *Cancer Res* 2006; **66**: 8430-8438 [PMID: 16951153 DOI: 10.1158/0008-5472.CAN-06-1437]
162 **Fleming NI**, Jorissen RN, Mouradov D, Christie M, Sakthianandeswaren A, Palmieri M, Day F, Li S, Tsui C, Lipton L, Desai J, Jones IT, McLaughlin S, Ward RL, Hawkins NJ, Ruszkiewicz AR, Moore J, Zhu HJ, Mariadason JM, Burgess AW, Busam D, Zhao Q, Strausberg RL, Gibbs P, Sieber OM. SMAD2, SMAD3 and SMAD4 mutations in colorectal cancer. *Cancer Res* 2013; **73**: 725-735 [PMID: 23139211 DOI: 10.1158/0008-5472.CAN-12-2706]
163 **Engle SJ**, Hoying JB, Boivin GP, Ormsby I, Gartside PS, Doetschman T. Transforming growth factor beta1 suppresses nonmetastatic colon cancer at an early stage of tumorigenesis. *Cancer Res* 1999; **59**: 3379-3386 [PMID: 10416598]
164 **Biswas S**, Guix M, Rinehart C, Dugger TC, Chytil A, Moses HL, Freeman ML, Arteaga CL. Inhibition of TGF-beta with neutralizing antibodies prevents radiation-induced acceleration of metastatic cancer progression. *J Clin Invest* 2007; **117**: 1305-1313 [PMID: 17415413 DOI: 10.1172/JCI30740]
165 **Oshima H**, Nakayama M, Han TS, Naoi K, Ju X, Maeda Y, Robine S, Tsuchiya K, Sato T, Sato H, Taketo MM, Oshima M. Suppressing TGFβ signaling in regenerating epithelia in an inflammatory microenvironment is sufficient to cause invasive intestinal cancer. *Cancer Res* 2015; **75**: 766-776 [PMID: 25687406 DOI: 10.1158/0008-5472.CAN-14-2036]
166 **Trobridge P**, Knoblaugh S, Washington MK, Munoz NM, Tsuchiya KD, Rojas A, Song X, Ulrich CM, Sasazuki T, Shirasawa S, Grady WM. TGF-beta receptor inactivation and mutant Kras induce intestinal neoplasms in mice via a beta-catenin-independent pathway. *Gastroenterology* 2009; **136**: 1680-8.e7 [PMID: 19208363 DOI: 10.1053/j.gastro.2009.01.066]
167 **Muñoz NM**, Upton M, Rojas A, Washington MK, Lin L, Chytil A, Sozmen EG, Madison BB, Pozzi A, Moon RT, Moses HL, Grady WM. Transforming growth factor beta receptor type II inactivation induces the malignant transformation of intestinal neoplasms initiated by Apc mutation. *Cancer Res* 2006; **66**: 9837-9844 [PMID: 17047044 DOI: 10.1158/0008-5472.CAN-06-0890]
168 **Rajagopalan H**, Bardelli A, Lengauer C, Kinzler KW, Vogelstein B, Velculescu VE. Tumorigenesis: RAF/RAS oncogenes and mismatch-repair status. *Nature* 2002; **418**: 934 [PMID: 12198537 DOI: 10.1038/418934a]
169 **Hinoue T**, Weisenberger DJ, Lange CP, Shen H, Byun HM, Van Den Berg D, Malik S, Pan F, Noushmehr H, van Dijk CM, Tollenaar RA, Laird PW. Genome-scale analysis of aberrant DNA methylation in colorectal cancer. *Genome Res* 2012; **22**: 271-282 [PMID: 21659424 DOI: 10.1101/gr.117523.110]
170 **Bond CE**, Whitehall VLJ. How the *BRAF* V600E Mutation Defines a Distinct Subgroup of Colorectal Cancer: Molecular and Clinical Implications. *Gastroenterol Res Pract* 2018; **2018**: 9250757 [PMID: 30598662 DOI: 10.1155/2018/9250757]
171 **Carragher LA**, Snell KR, Giblett SM, Aldridge VS, Patel B, Cook SJ, Winton DJ, Marais R, Pritchard CA. V600EBraf induces gastrointestinal crypt senescence and promotes tumour progression through enhanced CpG methylation of p16INK4a. *EMBO Mol Med* 2010; **2**: 458-471 [PMID: 20941790 DOI: 10.1002/emmm.201000099]
172 **Coffee EM**, Faber AC, Roper J, Sinnamon MJ, Goel G, Keung L, Wang WV, Vecchione L, de Vriendt V, Weinstein BJ, Bronson RT, Tejpar S, Xavier RJ, Engelman JA, Martin ES, Hung KE. Concomitant BRAF and PI3K/mTOR blockade is required for effective treatment of BRAF(V600E) colorectal cancer. *Clin Cancer Res* 2013; **19**: 2688-2698 [PMID: 23549875 DOI: 10.1158/1078-0432.CCR-12-2556]
173 **Anderson RL**, Balasas T, Callaghan J, Coombes RC, Evans J, Hall JA, Kinrade S, Jones D, Jones PS, Jones R, Marshall JF, Panico MB, Shaw JA, Steeg PS, Sullivan M, Tong W, Westwell AD, Ritchie JWA; Cancer Research UK and Cancer Therapeutics CRC Australia Metastasis Working Group. A framework for the development of effective anti-metastatic agents. *Nat Rev Clin Oncol* 2019; **16**: 185-204 [PMID: 30514977 DOI: 10.1038/s41571-018-0134-8]
174 **Rad R**, Cadiñanos J, Rad L, Varela I, Strong A, Kriegl L, Constantino-Casas F, Eser S, Hieber M, Seidler B, Price S, Fraga MF, Calvanese V, Hoffman G, Ponstingl H, Schneider G, Yusa K, Grove C, Schmid RM, Wang W, Vassiliou G, Kirchner T, McDermott U, Liu P, Saur D, Bradley A. A genetic progression model of Braf(V600E)-induced intestinal tumorigenesis reveals targets for therapeutic intervention. *Cancer Cell* 2013; **24**: 15-29 [PMID: 23845441 DOI: 10.1016/j.ccr.2013.05.014]
175 **Anwar M**, Kochhar R, Singh R, Bhatia A, Vaiphei K, Mahmood A, Mahmood S. Frequent activation of the β-catenin gene in sporadic colorectal carcinomas: A mutational & expression analysis. *Mol Carcinog* 2016; **55**: 1627-1638 [PMID: 26373808 DOI: 10.1002/mc.22414]
176 **Abdelmaksoud-Damak R**, Miladi-Abdennadher I, Triki M, Khabir A, Charfi S, Ayadi L, Frikha M, Sellami-Boudawara T, Mokdad-Gargouri R. Expression and mutation pattern of β-catenin and adenomatous polyposis coli in colorectal cancer patients. *Arch Med Res* 2015; **46**: 54-62 [PMID: 25660336 DOI: 10.1016/j.arcmed.2015.01.001]
177 **Schwitalla S**, Fingerle AA, Cammareri P, Nebelsiek T, Göktuna SI, Ziegler PK, Canli O, Heijmans J, Huels DJ, Moreaux G, Rupec RA, Gerhard M, Schmid R, Barker N, Clevers H, Lang R, Neumann J, Kirchner T, Taketo MM, van den Brink GR, Sansom OJ, Arkan MC, Greten FR. Intestinal tumorigenesis initiated by dedifferentiation and acquisition of stem-cell-like properties. *Cell* 2013; **152**: 25-38 [PMID: 23273993 DOI: 10.1016/j.cell.2012.12.012]
178 **Harada N**, Tamai Y, Ishikawa T, Sauer B, Takaku K, Oshima M, Taketo MM. Intestinal polyposis in mice with a dominant stable mutation of the beta-catenin gene. *EMBO J* 1999; **18**: 5931-5942 [PMID: 10545105 DOI: 10.1093/emboj/18.21.5931]
179 **Perekatt AO**, Shah PP, Cheung S, Jariwala N, Wu A, Gandhi V, Kumar N, Feng Q, Patel N, Chen L, Joshi S, Zhou A, Taketo MM, Xing J, White E, Gao N, Gatza ML, Verzi MP. SMAD4 Suppresses WNT-Driven Dedifferentiation and Oncogenesis in the Differentiated Gut Epithelium. *Cancer Res* 2018; **78**: 4878-4890 [PMID: 29986996 DOI: 10.1158/0008-5472.CAN-18-0043]
180 **Ionov Y**, Peinado MA, Malkhosyan S, Shibata D, Perucho M. Ubiquitous somatic mutations in simple repeated sequences reveal a new mechanism for colonic carcinogenesis. *Nature* 1993; **363**: 558-561 [PMID: 8505985 DOI: 10.1038/363558a0]
181 **Thibodeau SN**, Bren G, Schaid D. Microsatellite instability in cancer of the proximal colon. *Science* 1993; **260**: 816-819 [PMID: 8484122 DOI: 10.1126/science.8484122]
182 **Peltomäki P**, Lothe RA, Aaltonen LA, Pylkkänen L, Nyström-Lahti M, Seruca R, David L, Holm R,

Ryberg D, Haugen A. Microsatellite instability is associated with tumors that characterize the hereditary non-polyposis colorectal carcinoma syndrome. *Cancer Res* 1993; **53**: 5853-5855 [PMID: 8261393]
183 **Yamamoto H**, Imai K. Microsatellite instability: an update. *Arch Toxicol* 2015; **89**: 899-921 [PMID: 25701956 DOI: 10.1007/s00204-015-1474-0]
184 **Edelmann W**, Yang K, Kuraguchi M, Heyer J, Lia M, Kneitz B, Fan K, Brown AM, Lipkin M, Kucherlapati R. Tumorigenesis in Mlh1 and Mlh1/Apc1638N mutant mice. *Cancer Res* 1999; **59**: 1301-1307 [PMID: 10096563]
185 **Reitmair AH**, Schmits R, Ewel A, Bapat B, Redston M, Mitri A, Waterhouse P, Mittrücker HW, Wakeham A, Liu B. MSH2 deficient mice are viable and susceptible to lymphoid tumours. *Nat Genet* 1995; **11**: 64-70 [PMID: 7550317 DOI: 10.1038/ng0995-64]
186 **de Wind N**, Dekker M, Berns A, Radman M, te Riele H. Inactivation of the mouse Msh2 gene results in mismatch repair deficiency, methylation tolerance, hyperrecombination, and predisposition to cancer. *Cell* 1995; **82**: 321-330 [PMID: 7628020 DOI: 10.1016/0092-8674(95)90319-4]
187 **Edelmann W**, Yang K, Umar A, Heyer J, Lau K, Fan K, Liedtke W, Cohen PE, Kane MF, Lipford JR, Yu N, Crouse GF, Pollard JW, Kunkel T, Lipkin M, Kolodner R, Kucherlapati R. Mutation in the mismatch repair gene Msh6 causes cancer susceptibility. *Cell* 1997; **91**: 467-477 [PMID: 9390556 DOI: 10.1016/s0092-8674(00)80433-x]
188 **Prolla TA**, Baker SM, Harris AC, Tsao JL, Yao X, Bronner CE, Zheng B, Gordon M, Reneker J, Arnheim N, Shibata D, Bradley A, Liskay RM. Tumour susceptibility and spontaneous mutation in mice deficient in Mlh1, Pms1 and Pms2 DNA mismatch repair. *Nat Genet* 1998; **18**: 276-279 [PMID: 9500552 DOI: 10.1038/ng0398-276]
189 **Baker SM**, Plug AW, Prolla TA, Bronner CE, Harris AC, Yao X, Christie DM, Monell C, Arnheim N, Bradley A, Ashley T, Liskay RM. Involvement of mouse Mlh1 in DNA mismatch repair and meiotic crossing over. *Nat Genet* 1996; **13**: 336-342 [PMID: 8673133 DOI: 10.1038/ng0796-336]
190 **Yang G**, Scherer SJ, Shell SS, Yang K, Kim M, Lipkin M, Kucherlapati R, Kolodner RD, Edelmann W. Dominant effects of an Msh6 missense mutation on DNA repair and cancer susceptibility. *Cancer Cell* 2004; **6**: 139-150 [PMID: 15324697 DOI: 10.1016/j.ccr.2004.06.024]
191 **Reitmair AH**, Cai JC, Bjerknes M, Redston M, Cheng H, Pind MT, Hay K, Mitri A, Bapat BV, Mak TW, Gallinger S. MSH2 deficiency contributes to accelerated APC-mediated intestinal tumorigenesis. *Cancer Res* 1996; **56**: 2922-2926 [PMID: 8674041]
192 **Smits R**, Hofland N, Edelmann W, Geugien M, Jagmohan-Changur S, Albuquerque C, Breukel C, Kucherlapati R, Kielman MF, Fodde R. Somatic Apc mutations are selected upon their capacity to inactivate the beta-catenin downregulating activity. *Genes Chromosomes Cancer* 2000; **29**: 229-239 [PMID: 10992298]
193 **Kucherlapati M**, Yang K, Kuraguchi M, Zhao J, Lia M, Heyer J, Kane MF, Fan K, Russell R, Brown AM, Kneitz B, Edelmann W, Kolodner RD, Lipkin M, Kucherlapati R. Haploinsufficiency of Flap endonuclease (Fen1) leads to rapid tumor progression. *Proc Natl Acad Sci USA* 2002; **99**: 9924-9929 [PMID: 12119409 DOI: 10.1073/pnas.152321699]
194 **Kucherlapati M**, Nguyen A, Kuraguchi M, Yang K, Fan K, Bronson R, Wei K, Lipkin M, Edelmann W, Kucherlapati R. Tumor progression in Apc(1638N) mice with Exo1 and Fen1 deficiencies. *Oncogene* 2007; **26**: 6297-6306 [PMID: 17452984 DOI: 10.1038/sj.onc.1210453]
195 **Panarelli NC**, Vaughn CP, Samowitz WS, Yantiss RK. Sporadic microsatellite instability-high colon cancers rarely display immunohistochemical evidence of Wnt signaling activation. *Am J Surg Pathol* 2015; **39**: 313-317 [PMID: 25602793 DOI: 10.1097/PAS.0000000000000380]
196 **Marisa L**, de Reyniès A, Duval A, Selves J, Gaub MP, Vescovo L, Etienne-Grimaldi MC, Schiappa R, Guenot D, Ayadi M, Kirzin S, Chazal M, Fléjou JF, Benchimol D, Berger A, Lagarde A, Pencreach E, Piard F, Elias D, Parc Y, Olschwang S, Milano G, Laurent-Puig P, Boige V. Gene expression classification of colon cancer into molecular subtypes: characterization, validation, and prognostic value. *PLoS Med* 2013; **10**: e1001453 [PMID: 23700391 DOI: 10.1371/journal.pmed.1001453]
197 **Kucherlapati MH**, Lee K, Nguyen AA, Clark AB, Hou H, Rosulek A, Li H, Yang K, Fan K, Lipkin M, Bronson RT, Jelicks L, Kunkel TA, Kucherlapati R, Edelmann W. An Msh2 conditional knockout mouse for studying intestinal cancer and testing anticancer agents. *Gastroenterology* 2010; **138**: 993-1002.e1 [PMID: 19931261 DOI: 10.1053/j.gastro.2009.11.009]
198 **Bennecke M**, Kriegl L, Bajbouj M, Retzlaff K, Robine S, Jung A, Arkan MC, Kirchner T, Greten FR. Ink4a/Arf and oncogene-induced senescence prevent tumor progression during alternative colorectal tumorigenesis. *Cancer Cell* 2010; **18**: 135-146 [PMID: 20708155 DOI: 10.1016/j.ccr.2010.06.013]
199 **Huang D**, Sun W, Zhou Y, Li P, Chen F, Chen H, Xia D, Xu E, Lai M, Wu Y, Zhang H. Mutations of key driver genes in colorectal cancer progression and metastasis. *Cancer Metastasis Rev* 2018; **37**: 173-187 [PMID: 29322354 DOI: 10.1007/s10555-017-9726-5]
200 **Starr TK**, Allaei R, Silverstein KA, Staggs RA, Sarver AL, Bergemann TL, Gupta M, O'Sullivan MG, Matise I, Dupuy AJ, Collier LS, Powers S, Oberg AL, Asmann YW, Thibodeau SN, Tessarollo L, Copeland NG, Jenkins NA, Cormier RT, Largaespada DA. A transposon-based genetic screen in mice identifies genes altered in colorectal cancer. *Science* 2009; **323**: 1747-1750 [PMID: 19251594 DOI: 10.1126/science.1163040]
201 **Takeda H**, Wei Z, Koso H, Rust AG, Yew CC, Mann MB, Ward JM, Adams DJ, Copeland NG, Jenkins NA. Transposon mutagenesis identifies genes and evolutionary forces driving gastrointestinal tract tumor progression. *Nat Genet* 2015; **47**: 142-150 [PMID: 25559195 DOI: 10.1038/ng.3175]
202 **Morris SM**, Davison J, Carter KT, O'Leary RM, Trobridge P, Knoblaugh SE, Myeroff LL, Markowitz SD, Brett BT, Scheetz TE, Dupuy AJ, Starr TK, Grady WM. Transposon mutagenesis identifies candidate genes that cooperate with loss of transforming growth factor-beta signaling in mouse intestinal neoplasms. *Int J Cancer* 2017; **140**: 853-863 [PMID: 27790711 DOI: 10.1002/ijc.30491]
203 **Shabad LM**. Mstislav Novinsky, pioneer of tumour transplantation. *Cancer Lett* 1976; **2**: 1-3 [PMID: 797444 DOI: 10.1016/s0304-3835(76)80002-x]
204 **Hanau A**. Erfolgreiche Übertragung von Carcinom. *Fortschr d Med* 1889; **7**: 321
205 **Triolo VA**. Nineteenth century foundations of cancer research. Origins of experimental research. *Cancer Res* 1964; **24**: 4-27 [PMID: 14106160]
206 **DeVita VT**, Chu E. A history of cancer chemotherapy. *Cancer Res* 2008; **68**: 8643-8653 [PMID: 18974103 DOI: 10.1158/0008-5472.CAN-07-6611]
207 **Thorsby E**. A short history of HLA. *Tissue Antigens* 2009; **74**: 101-116 [PMID: 19523022 DOI: 10.1111/j.1399-0039.2009.01291.x]
208 **Wyke JA**. Oncogenic viruses. *J Pathol* 1981; **135**: 39-85 [PMID: 6271940 DOI:

10.1002/path.1711350105]
209 **TOOLAN HW**. Successful subcutaneous growth and transplantation of human tumors in X-irradiated laboratory animals. *Proc Soc Exp Biol Med* 1951; **77**: 572-578 [PMID: 14864665 DOI: 10.3181/00379727-77-18854]
210 **TOOLAN HW**. Transplantable human neoplasms maintained in cortisone-treated laboratory animals: H.S. No. 1; H.Ep. No. 1; H.Ep. No. 2; H.Ep. No. 3; and H.Emb.Rh. No. 1. *Cancer Res* 1954; **14**: 660-666 [PMID: 13209540]
211 **Yong KSM**, Her Z, Chen Q. Humanized Mice as Unique Tools for Human-Specific Studies. *Arch Immunol Ther Exp (Warsz)* 2018; **66**: 245-266 [PMID: 29411049 DOI: 10.1007/s00005-018-0506-x]
212 **Flanagan SP**. 'Nude', a new hairless gene with pleiotropic effects in the mouse. *Genet Res* 1966; **8**: 295-309 [PMID: 5980117 DOI: 10.1017/s0016672300010168]
213 **Rygaard J**, Povlsen CO. Heterotransplantation of a human malignant tumour to "Nude" mice. *Acta Pathol Microbiol Scand* 1969; **77**: 758-760 [PMID: 5383844 DOI: 10.1111/j.1699-0463.1969.tb04520.x]
214 **Bosma GC**, Custer RP, Bosma MJ. A severe combined immunodeficiency mutation in the mouse. *Nature* 1983; **301**: 527-530 [PMID: 6823332 DOI: 10.1038/301527a0]
215 **Makino S**, Kunimoto K, Muraoka Y, Mizushima Y, Katagiri K, Tochino Y. Breeding of a non-obese, diabetic strain of mice. *Jikken Dobutsu* 1980; **29**: 1-13 [PMID: 6995140 DOI: 10.1538/expanim1978.29.1_1]
216 **Greiner DL**, Shultz LD, Yates J, Appel MC, Perdrizet G, Hesselton RM, Schweitzer I, Beamer WG, Shultz KL, Pelsue SC. Improved engraftment of human spleen cells in NOD/LtSz-scid/scid mice as compared with C.B-17-scid/scid mice. *Am J Pathol* 1995; **146**: 888-902 [PMID: 7717456]
217 **Christianson SW**, Greiner DL, Hesselton RA, Leif JH, Wagar EJ, Schweitzer IB, Rajan TV, Gott B, Roopenian DC, Shultz LD. Enhanced human CD4+ T cell engraftment in beta2-microglobulin-deficient NOD-scid mice. *J Immunol* 1997; **158**: 3578-3586 [PMID: 9103418]
218 **Ueda T**, Tsuji K, Yoshino H, Ebihara Y, Yagasaki H, Hisakawa H, Mitsui T, Manabe A, Tanaka R, Kobayashi K, Ito M, Yasukawa K, Nakahata T. Expansion of human NOD/SCID-repopulating cells by stem cell factor, Flk2/Flt3 ligand, thrombopoietin, IL-6, and soluble IL-6 receptor. *J Clin Invest* 2000; **105**: 1013-1021 [PMID: 10749580 DOI: 10.1172/JCI8583]
219 **Santagostino SF**, Arbona RJR, Nashat MA, White JR, Monette S. Pathology of Aging in NOD scid gamma Female Mice. *Vet Pathol* 2017; **54**: 855-869 [PMID: 28355107 DOI: 10.1177/0300985817698210]
220 **Nonoyama S**, Smith FO, Bernstein ID, Ochs HD. Strain-dependent leakiness of mice with severe combined immune deficiency. *J Immunol* 1993; **150**: 3817-3824 [PMID: 8473734]
221 **Shultz LD**, Ishikawa F, Greiner DL. Humanized mice in translational biomedical research. *Nat Rev Immunol* 2007; **7**: 118-130 [PMID: 17259968 DOI: 10.1038/nri2017]
222 **Ito M**, Hiramatsu H, Kobayashi K, Suzue K, Kawahata M, Hioki K, Ueyama Y, Koyanagi Y, Sugamura K, Tsuji K, Heike T, Nakahata T. NOD/SCID/gamma(c)(null) mouse: an excellent recipient mouse model for engraftment of human cells. *Blood* 2002; **100**: 3175-3182 [PMID: 12384415 DOI: 10.1182/blood-2001-12-0207]
223 **Shultz LD**, Lyons BL, Burzenski LM, Gott B, Chen X, Chaleff S, Kotb M, Gillies SD, King M, Mangada J, Greiner DL, Handgretinger R. Human lymphoid and myeloid cell development in NOD/LtSz-scid IL2R gamma null mice engrafted with mobilized human hemopoietic stem cells. *J Immunol* 2005; **174**: 6477-6489 [PMID: 15879151 DOI: 10.4049/jimmunol.174.10.6477]
224 **Suzuki K**, Nakajima H, Saito Y, Saito T, Leonard WJ, Iwamoto I. Janus kinase 3 (Jak3) is essential for common cytokine receptor gamma chain (gamma(c))-dependent signaling: comparative analysis of gamma(c), Jak3, and gamma(c) and Jak3 double-deficient mice. *Int Immunol* 2000; **12**: 123-132 [PMID: 10653847 DOI: 10.1093/intimm/12.2.123]
225 **Shultz LD**, Banuelos S, Lyons B, Samuels R, Burzenski L, Gott B, Lang P, Leif J, Appel M, Rossini A, Greiner DL. NOD/LtSz-Rag1nullPfpnull mice: a new model system with increased levels of human peripheral leukocyte and hematopoietic stem-cell engraftment. *Transplantation* 2003; **76**: 1036-1042 [PMID: 14557749 DOI: 10.1097/01.TP.0000083041.44829.2C]
226 **Pearson T**, Greiner DL, Shultz LD. Creation of "humanized" mice to study human immunity. *Curr Protoc Immunol* 2008; **Chapter** 15: Unit 15.21 [PMID: 18491294 DOI: 10.1002/0471142735.im1521s81]
227 **Foreman O**, Kavirayani AM, Griffey SM, Reader R, Shultz LD. Opportunistic bacterial infections in breeding colonies of the NSG mouse strain. *Vet Pathol* 2011; **48**: 495-499 [PMID: 20817888 DOI: 10.1177/0300985810378282]
228 **Gock M**, Kühn F, Mullins CS, Krohn M, Prall F, Klar E, Linnebacher M. Tumor Take Rate Optimization for Colorectal Carcinoma Patient-Derived Xenograft Models. *Biomed Res Int* 2016; **2016**: 1715053 [PMID: 27999790 DOI: 10.1155/2016/1715053]
229 **Linnebacher M**, Maletzki C, Ostwald C, Klier U, Krohn M, Klar E, Prall F. Cryopreservation of human colorectal carcinomas prior to xenografting. *BMC Cancer* 2010; **10**: 362 [PMID: 20615215 DOI: 10.1186/1471-2407-10-362]
230 **Simon MM**, Greenaway S, White JK, Fuchs H, Gailus-Durner V, Wells S, Sorg T, Wong K, Bedu E, Cartwright EJ, Dacquin R, Djebali S, Estabel J, Graw J, Ingham NJ, Jackson IJ, Lengeling A, Mandillo S, Marvel J, Meziane H, Preitner F, Puk O, Roux M, Adams DJ, Atkins S, Ayadi A, Becker L, Blake A, Brooker D, Cater H, Champy MF, Combe R, Danecek P, di Fenza A, Gates H, Gerdin AK, Golini E, Hancock JM, Hans W, Hölter SM, Hough T, Jurdic P, Keane TM, Morgan H, Müller W, Neff F, Nicholson G, Pasche B, Roberson LA, Rozman J, Sanderson M, Santos L, Selloum M, Shannon C, Southwell A, Tocchini-Valentini GP, Vancollie VE, Westerberg H, Wurst W, Zi M, Yalcin B, Ramirez-Solis R, Steel KP, Mallon AM, de Angelis MH, Herault Y, Brown SD. A comparative phenotypic and genomic analysis of C57BL/6J and C57BL/6N mouse strains. *Genome Biol* 2013; **14**: R82 [PMID: 23902802 DOI: 10.1186/gb-2013-14-7-r82]
231 **Houghton PJ**, Morton CL, Tucker C, Payne D, Favours E, Cole C, Gorlick R, Kolb EA, Zhang W, Lock R, Carol H, Tajbakhsh M, Reynolds CP, Maris JM, Courtright J, Keir ST, Friedman HS, Stopford C, Zeidner J, Wu J, Liu T, Billups CA, Khan J, Ansher S, Zhang J, Smith MA. The pediatric preclinical testing program: description of models and early testing results. *Pediatr Blood Cancer* 2007; **49**: 928-940 [PMID: 17066459 DOI: 10.1002/pbc.21078]
232 **Johnson JI**, Decker S, Zaharevitz D, Rubinstein LV, Venditti JM, Schepartz S, Kalyandrug S, Christian M, Arbuck S, Hollingshead M, Sausville EA. Relationships between drug activity in NCI preclinical in vitro and in vivo models and early clinical trials. *Br J Cancer* 2001; **84**: 1424-1431 [PMID: 11355958 DOI: 10.1054/bjoc.2001.1796]
233 **Talmadge JE**, Singh RK, Fidler IJ, Raz A. Murine models to evaluate novel and conventional therapeutic

strategies for cancer. *Am J Pathol* 2007; **170**: 793-804 [PMID: 17322365 DOI: 10.2353/ajpath.2007.060929]
234 **Boven E**, Winograd B, Berger DP, Dumont MP, Braakhuis BJ, Fodstad O, Langdon S, Fiebig HH. Phase II preclinical drug screening in human tumor xenografts: a first European multicenter collaborative study. *Cancer Res* 1992; **52**: 5940-5947 [PMID: 1394220]
235 **Voskoglou-Nomikos T**, Pater JL, Seymour L. Clinical predictive value of the in vitro cell line, human xenograft, and mouse allograft preclinical cancer models. *Clin Cancer Res* 2003; **9**: 4227-4239 [PMID: 14519650]
236 **Golovko D**, Kedrin D, Yilmaz ÖH, Roper J. Colorectal cancer models for novel drug discovery. *Expert Opin Drug Discov* 2015; **10**: 1217-1229 [PMID: 26295972 DOI: 10.1517/17460441.2015.1079618]
237 **Katsiampoura A**, Raghav K, Jiang ZQ, Menter DG, Varkaris A, Morelli MP, Manuel S, Wu J, Sorokin AV, Rizi BS, Bristow C, Tian F, Airhart S, Cheng M, Broom BM, Morris J, Overman MJ, Powis G, Kopetz S. Modeling of Patient-Derived Xenografts in Colorectal Cancer. *Mol Cancer Ther* 2017; **16**: 1435-1442 [PMID: 28468778 DOI: 10.1158/1535-7163.MCT-16-0721]
238 **Brattain MG**, Fine WD, Khaled FM, Thompson J, Brattain DE. Heterogeneity of malignant cells from a human colonic carcinoma. *Cancer Res* 1981; **41**: 1751-1756 [PMID: 7214343]
239 **Horbach SPJM**, Halffman W. The ghosts of HeLa: How cell line misidentification contaminates the scientific literature. *PLoS One* 2017; **12**: e0186281 [PMID: 29023500 DOI: 10.1371/journal.pone.0186281]
240 **Mouradov D**, Sloggett C, Jorissen RN, Love CG, Li S, Burgess AW, Arango D, Strausberg RL, Buchanan D, Wormald S, O'Connor L, Wilding JL, Bicknell D, Tomlinson IP, Bodmer WF, Mariadason JM, Sieber OM. Colorectal cancer cell lines are representative models of the main molecular subtypes of primary cancer. *Cancer Res* 2014; **74**: 3238-3247 [PMID: 24755471 DOI: 10.1158/0008-5472.CAN-14-0013]
241 **Wilding JL**, Bodmer WF. Cancer cell lines for drug discovery and development. *Cancer Res* 2014; **74**: 2377-2384 [PMID: 24717177 DOI: 10.1158/0008-5472.CAN-13-2971]
242 **Tanaka Y**, Wu AY, Ikekawa N, Iseki K, Kawai M, Kobayashi Y. Inhibition of HT-29 human colon cancer growth under the renal capsule of severe combined immunodeficient mice by an analogue of 1,25-dihydroxyvitamin D3, DD-003. *Cancer Res* 1994; **54**: 5148-5153 [PMID: 7923132]
243 **Lawrentschuk N**, Rigopoulos A, Lee FT, Davis ID, Scott AM, Bolton DM. Xenografting tumour beneath the renal capsule using modern surgical equipment. *Eur Surg Res* 2006; **38**: 340-346 [PMID: 16791005 DOI: 10.1159/000094093]
244 **Edelstein MB**. The subrenal capsule assay: a critical commentary. *Eur J Cancer Clin Oncol* 1986; **22**: 757-760 [PMID: 3533556 DOI: 10.1016/0277-5379(86)90359-7]
245 **Wang Y**, Wang JX, Xue H, Lin D, Dong X, Gout PW, Gao X, Pang J. Subrenal capsule grafting technology in human cancer modeling and translational cancer research. *Differentiation* 2016; **91**: 15-19 [PMID: 26547391 DOI: 10.1016/j.diff.2015.10.012]
246 **Li C**, Wang J, Kong J, Tang J, Wu Y, Xu E, Zhang H, Lai M. GDF15 promotes EMT and metastasis in colorectal cancer. *Oncotarget* 2016; **7**: 860-872 [PMID: 26497212 DOI: 10.18632/oncotarget.6205]
247 **Murdocca M**, Capuano R, Pucci S, Cicconi R, Polidoro C, Catini A, Martinelli E, Paolesse R, Orlandi A, Mango R, Novelli G, Di Natale C, Sangiuolo F. Targeting LOX-1 Inhibits Colorectal Cancer Metastasis in an Animal Model. *Front Oncol* 2019; **9**: 927 [PMID: 31608230 DOI: 10.3389/fonc.2019.00927]
248 **Hanahan D**, Weinberg RA. Hallmarks of cancer: the next generation. *Cell* 2011; **144**: 646-674 [PMID: 21376230 DOI: 10.1016/j.cell.2011.02.013]
249 **Brand MI**, Casillas S, Dietz DW, Milsom JW, Vladisavljevic A. Development of a reliable colorectal cancer liver metastasis model. *J Surg Res* 1996; **63**: 425-432 [PMID: 8661237 DOI: 10.1006/jsre.1996.0287]
250 **Fleten KG**, Bakke KM, Mælandsmo GM, Abildgaard A, Redalen KR, Flatmark K. Use of non-invasive imaging to monitor response to aflibercept treatment in murine models of colorectal cancer liver metastases. *Clin Exp Metastasis* 2017; **34**: 51-62 [PMID: 27812769 DOI: 10.1007/s10585-016-9829-3]
251 **Li Z**, Wang J, Zhou T, Ye X. Establishment of a colorectal cancer nude mouse visualization model of HIF-1α overexpression. *Oncol Lett* 2016; **11**: 2725-2732 [PMID: 27073543 DOI: 10.3892/ol.2016.4287]
252 **Mullins CS**, Micheel B, Matschos S, Leuchter M, Bürtin F, Krohn M, Hühns M, Klar E, Prall F, Linnebacher M. Integrated Biobanking and Tumor Model Establishment of Human Colorectal Carcinoma Provides Excellent Tools for Preclinical Research. *Cancers (Basel)* 2019; **11** [PMID: 31601052 DOI: 10.3390/cancers11101520]
253 **Prall F**, Maletzki C, Hühns M, Krohn M, Linnebacher M. Colorectal carcinoma tumour budding and podia formation in the xenograft microenvironment. *PLoS One* 2017; **12**: e0186271 [PMID: 29040282 DOI: 10.1371/journal.pone.0186271]
254 **Guenot D**, Guérin E, Aguillon-Romain S, Pencreach E, Schneider A, Neuville A, Chenard MP, Duluc I, Du Manoir S, Brigand C, Oudet P, Kedinger M, Gaub MP. Primary tumour genetic alterations and intra-tumoral heterogeneity are maintained in xenografts of human colon cancers showing chromosome instability. *J Pathol* 2006; **208**: 643-652 [PMID: 16450341 DOI: 10.1002/path.1936]
255 **Burgenske DM**, Monsma DJ, Dylewski D, Scott SB, Sayfie AD, Kim DG, Luchtefeld M, Martin KR, Stephenson P, Hostetter G, Dujovny N, MacKeigan JP. Establishment of genetically diverse patient-derived xenografts of colorectal cancer. *Am J Cancer Res* 2014; **4**: 824-837 [PMID: 25520871]
256 **Mattie M**, Christensen A, Chang MS, Yeh W, Said S, Shostak Y, Capo L, Verlinsky A, An Z, Joseph I, Zhang Y, Kumar-Ganesan S, Morrison K, Stover D, Challita-Eid P. Molecular characterization of patient-derived human pancreatic tumor xenograft models for preclinical and translational development of cancer therapeutics. *Neoplasia* 2013; **15**: 1138-1150 [PMID: 24204193 DOI: 10.1593/neo.13922]
257 **Cho YB**, Hong HK, Choi YL, Oh E, Joo KM, Jin J, Nam DH, Ko YH, Lee WY. Colorectal cancer patient-derived xenografted tumors maintain characteristic features of the original tumors. *J Surg Res* 2014; **187**: 502-509 [PMID: 24332554 DOI: 10.1016/j.jss.2013.11.010]
258 **Ben-David U**, Ha G, Tseng YY, Greenwald NF, Oh C, Shih J, McFarland JM, Wong B, Boehm JS, Beroukhim R, Golub TR. Patient-derived xenografts undergo mouse-specific tumor evolution. *Nat Genet* 2017; **49**: 1567-1575 [PMID: 28991255 DOI: 10.1038/ng.3967]
259 **Sebolt-Leopold JS**. Development of Preclinical Models to Understand and Treat Colorectal Cancer. *Clin Colon Rectal Surg* 2018; **31**: 199-204 [PMID: 29720906 DOI: 10.1055/s-0037-1602240]
260 **Moro M**, Bertolini G, Tortoreto M, Pastorino U, Sozzi G, Roz L. Patient-derived xenografts of non small cell lung cancer: resurgence of an old model for investigation of modern concepts of tailored therapy and cancer stem cells. *J Biomed Biotechnol* 2012; **2012**: 568567 [PMID: 22547927 DOI: 10.1155/2012/568567]

261 **Hylander BL**, Punt N, Tang H, Hillman J, Vaughan M, Bshara W, Pitoniak R, Repasky EA. Origin of the vasculature supporting growth of primary patient tumor xenografts. *J Transl Med* 2013; **11**: 110 [PMID: 23639003 DOI: 10.1186/1479-5876-11-110]

262 **Blomme A**, Van Simaeys G, Doumont G, Costanza B, Bellier J, Otaka Y, Sherer F, Lovinfosse P, Boutry S, Palacios AP, De Pauw E, Hirano T, Yokobori T, Hustinx R, Bellahcène A, Delvenne P, Detry O, Goldman S, Nishiyama M, Castronovo V, Turtoi A. Murine stroma adopts a human-like metabolic phenotype in the PDX model of colorectal cancer and liver metastases. *Oncogene* 2018; **37**: 1237-1250 [PMID: 29242606 DOI: 10.1038/s41388-017-0018-x]

263 **Lazzari L**, Corti G, Picco G, Isella C, Montone M, Arcella P, Durinikova E, Zanella ER, Novara L, Barbosa F, Cassingena A, Cancelliere C, Medico E, Sartore-Bianchi A, Siena S, Garnett MJ, Bertotti A, Trusolino L, Di Nicolantonio F, Linnebacher M, Bardelli A, Arena S. Patient-Derived Xenografts and Matched Cell Lines Identify Pharmacogenomic Vulnerabilities in Colorectal Cancer. *Clin Cancer Res* 2019; **25**: 6243-6259 [PMID: 31375513 DOI: 10.1158/1078-0432.CCR-18-3440]

264 **Pauli C**, Hopkins BD, Prandi D, Shaw R, Fedrizzi T, Sboner A, Sailer V, Augello M, Puca L, Rosati R, McNary TJ, Churakova Y, Cheung C, Triscott J, Pisapia D, Rao R, Mosquera JM, Robinson B, Faltas BM, Emerling BE, Gadi VK, Bernard B, Elemento O, Beltran H, Demichelis F, Kemp CJ, Grandori C, Cantley LC, Rubin MA. Personalized *In Vitro* and *In Vivo* Cancer Models to Guide Precision Medicine. *Cancer Discov* 2017; **7**: 462-477 [PMID: 28331002 DOI: 10.1158/2159-8290.CD-16-1154]

265 **Hidalgo M**, Bruckheimer E, Rajeshkumar NV, Garrido-Laguna I, De Oliveira E, Rubio-Viqueira B, Strawn S, Wick MJ, Martell J, Sidransky D. A pilot clinical study of treatment guided by personalized tumorgrafts in patients with advanced cancer. *Mol Cancer Ther* 2011; **10**: 1311-1316 [PMID: 21673092 DOI: 10.1158/1535-7163.MCT-11-0233]

266 **Bertotti A**, Migliardi G, Galimi F, Sassi F, Torti D, Isella C, Corà D, Di Nicolantonio F, Buscarino M, Petti C, Ribero D, Russolillo N, Muratore A, Massucco P, Pisacane A, Molinaro L, Valtorta E, Sartore-Bianchi A, Risio M, Capussotti L, Gambacorta M, Siena S, Medico E, Sapino A, Marsoni S, Comoglio PM, Bardelli A, Trusolino L. A molecularly annotated platform of patient-derived xenografts ("xenopatients") identifies HER2 as an effective therapeutic target in cetuximab-resistant colorectal cancer. *Cancer Discov* 2011; **1**: 508-523 [PMID: 22586653 DOI: 10.1158/2159-8290.CD-11-0109]

267 **Migliardi G**, Sassi F, Torti D, Galimi F, Zanella ER, Buscarino M, Ribero D, Muratore A, Massucco P, Pisacane A, Risio M, Capussotti L, Marsoni S, Di Nicolantonio F, Bardelli A, Comoglio PM, Trusolino L, Bertotti A. Inhibition of MEK and PI3K/mTOR suppresses tumor growth but does not cause tumor regression in patient-derived xenografts of RAS-mutant colorectal carcinomas. *Clin Cancer Res* 2012; **18**: 2515-2525 [PMID: 22392911 DOI: 10.1158/1078-0432.CCR-11-2683]

268 **Gao H**, Korn JM, Ferretti S, Monahan JE, Wang Y, Singh M, Zhang C, Schnell C, Yang G, Zhang Y, Balbin OA, Barbe S, Cai H, Casey F, Chatterjee S, Chiang DY, Chuai S, Cogan SM, Collins SD, Dammassa E, Ebel N, Embry M, Green J, Kauffmann A, Kowal C, Leary RJ, Lehar J, Liang Y, Loo A, Lorenzana E, Robert McDonald E, McLaughlin ME, Merkin J, Meyer R, Naylor TL, Patawaran M, Reddy A, Röelli C, Ruddy DA, Salangsang F, Santacroce F, Singh AP, Tang Y, Tinetto W, Tobler S, Velazquez R, Venkatesan K, Von Arx F, Wang HQ, Wang Z, Wiesmann M, Wyss D, Xu F, Bitter H, Atadja P, Lees E, Hofmann F, Li E, Keen N, Cozens R, Jensen MR, Pryer NK, Williams JA, Sellers WR. High-throughput screening using patient-derived tumor xenografts to predict clinical trial drug response. *Nat Med* 2015; **21**: 1318-1325 [PMID: 26479923 DOI: 10.1038/nm.3954]

269 **Witkiewicz AK**, Balaji U, Eslinger C, McMillan E, Conway W, Posner B, Mills GB, O'Reilly EM, Knudsen ES. Integrated Patient-Derived Models Delineate Individualized Therapeutic Vulnerabilities of Pancreatic Cancer. *Cell Rep* 2016; **16**: 2017-2031 [PMID: 27498862 DOI: 10.1016/j.celrep.2016.07.023]

270 **Cescon D**. Personalized Patient Derived Xenograft (pPDX) Modeling to Test Drug Response in Matching Host (REFLECT). [accessed 2019 Oct 25]. In: ClinicalTrials.gov [Internet]. Bethesda (MD): U.S. National Library of Medicine. Available from: https://clinicaltrials.gov/ct2/show/record/NCT02732860 ClinicalTrials.gov Identifier: NCT02732860

271 **Heinemann V**. Optimization of Individualized Therapy for CRCs With Secondary RESISTance Towards Anti-EGFR Targeted Therapy Using an Avatar Model. [accessed 2019 Oct 25]. In: ClinicalTrials.gov [Internet]. Bethesda (MD): U.S. National Library of Medicine. Available from: https://clinicaltrials.gov/ct2/show/NCT03263663 ClinicalTrials.gov Identifier: NCT03263663

272 **Perea S**, Sarno F. Personalised Therapy for Metastatic ADPC Determined by Genetic Testing and Avatar Model Generation (AVATAR). [accessed 2019 Oct 25]. In: ClinicalTrials.gov [Internet]. Bethesda (MD): U.S. National Library of Medicine. Available from: https://clinicaltrials.gov/ct2/show/NCT02795650 ClinicalTrials.gov Identifier: NCT02795650

273 **Oh BY**, Lee WY, Jung S, Hong HK, Nam DH, Park YA, Huh JW, Yun SH, Kim HC, Chun HK, Cho YB. Correlation between tumor engraftment in patient-derived xenograft models and clinical outcomes in colorectal cancer patients. *Oncotarget* 2015; **6**: 16059-16068 [PMID: 25965827 DOI: 10.18632/oncotarget.3863]

274 **Puig I**, Chicote I, Tenbaum SP, Arqués O, Herance JR, Gispert JD, Jimenez J, Landolfi S, Caci K, Allende H, Mendizabal L, Moreno D, Charco R, Espín E, Prat A, Elez ME, Argilés G, Vivancos A, Tabernero J, Rojas S, Palmer HG. A personalized preclinical model to evaluate the metastatic potential of patient-derived colon cancer initiating cells. *Clin Cancer Res* 2013; **19**: 6787-6801 [PMID: 24170545 DOI: 10.1158/1078-0432.CCR-12-1740]

275 **Julien S**, Merino-Trigo A, Lacroix L, Pocard M, Goéré D, Mariani P, Landron S, Bigot L, Nemati F, Dartigues P, Weiswald LB, Lantuas D, Morgand L, Pham E, Gonin P, Dangles-Marie V, Job B, Dessen P, Bruno A, Pierré A, De Thé H, Soliman H, Nunes M, Lardier G, Calvet L, Demers B, Prévost G, Vrignaud P, Roman-Roman S, Duchamp O, Berthet C. Characterization of a large panel of patient-derived tumor xenografts representing the clinical heterogeneity of human colorectal cancer. *Clin Cancer Res* 2012; **18**: 5314-5328 [PMID: 22825584 DOI: 10.1158/1078-0432.CCR-12-0372]

276 **Collins AT**, Lang SH. A systematic review of the validity of patient derived xenograft (PDX) models: the implications for translational research and personalised medicine. *PeerJ* 2018; **6**: e5981 [PMID: 30498642 DOI: 10.7717/peerj.5981]

277 **Dangles-Marie V**, Pocard M, Richon S, Weiswald LB, Assayag F, Saulnier P, Judde JG, Janneau JL, Auger N, Validire P, Dutrillaux B, Praz F, Bellet D, Poupon MF. Establishment of human colon cancer cell lines from fresh tumors versus xenografts: comparison of success rate and cell line features. *Cancer Res* 2007; **67**: 398-407 [PMID: 17210723 DOI: 10.1158/0008-5472.CAN-06-0594]

278 **Prasetyanti PR**, van Hooff SR, van Herwaarden T, de Vries N, Kalloe K, Rodermond H, van Leersum R, de Jong JH, Franitza M, Nürnberg P, Todaro M, Stassi G, Medema JP. Capturing colorectal cancer inter-

tumor heterogeneity in patient-derived xenograft (PDX) models. *Int J Cancer* 2019; **144**: 366-371 [PMID: 30151914 DOI: 10.1002/ijc.31767]

279 **Wetterauer C**, Vlajnic T, Schüler J, Gsponer JR, Thalmann GN, Cecchini M, Schneider J, Zellweger T, Pueschel H, Bachmann A, Ruiz C, Dirnhofer S, Bubendorf L, Rentsch CA. Early development of human lymphomas in a prostate cancer xenograft program using triple knock-out immunocompromised mice. *Prostate* 2015; **75**: 585-592 [PMID: 25585936 DOI: 10.1002/pros.22939]

280 **Zhang L**, Liu Y, Wang X, Tang Z, Li S, Hu Y, Zong X, Wu X, Bu Z, Wu A, Li Z, Li Z, Huang X, Jia L, Kang Q, Liu Y, Sutton D, Wang L, Luo L, Ji J. The extent of inflammatory infiltration in primary cancer tissues is associated with lymphomagenesis in immunodeficient mice. *Sci Rep* 2015; **5**: 9447 [PMID: 25819560 DOI: 10.1038/srep09447]

281 **Bondarenko G**, Ugolkov A, Rohan S, Kulesza P, Dubrovskyi O, Gursel D, Mathews J, O'Halloran TV, Wei JJ, Mazar AP. Patient-Derived Tumor Xenografts Are Susceptible to Formation of Human Lymphocytic Tumors. *Neoplasia* 2015; **17**: 735-741 [PMID: 26476081 DOI: 10.1016/j.neo.2015.09.004]

282 **Chen K**, Ahmed S, Adeyi O, Dick JE, Ghanekar A. Human solid tumor xenografts in immunodeficient mice are vulnerable to lymphomagenesis associated with Epstein-Barr virus. *PLoS One* 2012; **7**: e39294 [PMID: 22723990 DOI: 10.1371/journal.pone.0039294]

283 **Taurozzi AJ**, Beekharry R, Wantoch M, Labarthe MC, Walker HF, Seed RI, Simms M, Rodrigues G, Bradford J, van der Horst G, van der Pluijm G, Collins AT. Spontaneous development of Epstein-Barr Virus associated human lymphomas in a prostate cancer xenograft program. *PLoS One* 2017; **12**: e0188228 [PMID: 29145505 DOI: 10.1371/journal.pone.0188228]

284 **John T**, Yanagawa N, Kohler D, Craddock KJ, Bandarchi-Chamkhaleh B, Pintilie M, Sykes J, To C, Li M, Panchal D, Chen W, Shepherd FA, Tsao MS. Characterization of lymphomas developing in immunodeficient mice implanted with primary human non-small cell lung cancer. *J Thorac Oncol* 2012; **7**: 1101-1108 [PMID: 22617243 DOI: 10.1097/JTO.0b013e3182519d4d]

285 **McCormick KH**, Giovanella BC, Klein G, Nilsson K, Stehlin JS. Diploid human lymphoblastoid and Burkitt lymphoma cell lines: susceptibility to murine NK cells and heterotransplantation to nude mice. *Int J Cancer* 1981; **28**: 455-458 [PMID: 6273332 DOI: 10.1002/ijc.2910280410]

286 **Butler KA**, Hou X, Becker MA, Zanfagnin V, Enderica-Gonzalez S, Visscher D, Kalli KR, Tienchaianada P, Haluska P, Weroha SJ. Prevention of Human Lymphoproliferative Tumor Formation in Ovarian Cancer Patient-Derived Xenografts. *Neoplasia* 2017; **19**: 628-636 [PMID: 28658648 DOI: 10.1016/j.neo.2017.04.007]

287 **Snipes RL**. Anatomy of the cecum of the laboratory mouse and rat. *Anat Embryol (Berl)* 1981; **162**: 455-474 [PMID: 7347499 DOI: 10.1007/bf00301871]

288 **Bresalier RS**, Raper SE, Hujanen ES, Kim YS. A new animal model for human colon cancer metastasis. *Int J Cancer* 1987; **39**: 625-630 [PMID: 3032811 DOI: 10.1002/ijc.2910390514]

289 **Fu XY**, Besterman JM, Monosov A, Hoffman RM. Models of human metastatic colon cancer in nude mice orthotopically constructed by using histologically intact patient specimens. *Proc Natl Acad Sci USA* 1991; **88**: 9345-9349 [PMID: 1924398]

290 **Rajput A**, Agarwal E, Leiphrakpam P, Brattain MG, Chowdhury S. Establishment and Validation of an Orthotopic Metastatic Mouse Model of Colorectal Cancer. *ISRN Hepatol* 2013; **2013**: 206875 [PMID: 27340651 DOI: 10.1155/2013/206875]

291 **Chow AK**, Cheng NS, Lam CS, Ng L, Wong SK, Wan TM, Man JH, Cheung AH, Yau TC, Poon JT, Law WL, Pang RW. Preclinical analysis of the anti-tumor and anti-metastatic effects of Raf265 on colon cancer cells and CD26(+) cancer stem cells in colorectal carcinoma. *Mol Cancer* 2015; **14**: 80 [PMID: 25884645 DOI: 10.1186/s12943-015-0352-y]

292 **Abou-Elkacem L**, Arns S, Brix G, Gremse F, Zopf D, Kiessling F, Lederle W. Regorafenib inhibits growth, angiogenesis, and metastasis in a highly aggressive, orthotopic colon cancer model. *Mol Cancer Ther* 2013; **12**: 1322-1331 [PMID: 23619301 DOI: 10.1158/1535-7163.MCT-12-1162]

293 **Zhao L**, Liu L, Wang S, Zhang YF, Yu L, Ding YQ. Differential proteomic analysis of human colorectal carcinoma cell lines metastasis-associated proteins. *J Cancer Res Clin Oncol* 2007; **133**: 771-782 [PMID: 17503081 DOI: 10.1007/s00432-007-0222-0]

294 **Chunhua L**, Donglan L, Xiuqiong F, Lihua Z, Qin F, Yawei L, Liang Z, Ge W, Linlin J, Ping Z, Kun L, Xuegang S. Apigenin up-regulates transgelin and inhibits invasion and migration of colorectal cancer through decreased phosphorylation of AKT. *J Nutr Biochem* 2013; **24**: 1766-1775 [PMID: 23773626 DOI: 10.1016/j.jnutbio.2013.03.006]

295 **Wang J**, Rajput A, Kan JL, Rose R, Liu XQ, Kuropatwinski K, Hauser J, Beko A, Dominquez I, Sharratt EA, Brattain L, Levea C, Sun FL, Keane DM, Gibson NW, Brattain MG. Knockdown of Ron kinase inhibits mutant phosphatidylinositol 3-kinase and reduces metastasis in human colon carcinoma. *J Biol Chem* 2009; **284**: 10912-10922 [PMID: 19224914 DOI: 10.1074/jbc.M809551200]

296 **Lin W**, Zhuang Q, Zheng L, Cao Z, Shen A, Li Q, Fu C, Feng J, Peng J. Pien Tze Huang inhibits liver metastasis by targeting TGF-β signaling in an orthotopic model of colorectal cancer. *Oncol Rep* 2015; **33**: 1922-1928 [PMID: 25653118 DOI: 10.3892/or.2015.3784]

297 **Kochall S**, Thepkaysone ML, García SA, Betzler AM, Weitz J, Reissfelder C, Schölch S. Isolation of Circulating Tumor Cells in an Orthotopic Mouse Model of Colorectal Cancer. *J Vis Exp* 2017; (125) [PMID: 28745637 DOI: 10.3791/55357]

298 **Yang JL**, Seetoo DQ, Wang Y, Ranson M, Berney CR, Ham JM, Russell PJ, Crowe PJ. Urokinase-type plasminogen activator and its receptor in colorectal cancer: Independent prognostic factors of metastasis and cancer-specific survival and potential therapeutic targets. *Int J Cancer* 2000; **89**: 431–439 [DOI: 10.1002/1097-0215(20000920)89:53.0.CO;2-V]

299 **Céspedes MV**, Espina C, García-Cabezas MA, Trias M, Boluda A, Gómez del Pulgar MT, Sancho FJ, Nistal M, Lacal JC, Mangues R. Orthotopic microinjection of human colon cancer cells in nude mice induces tumor foci in all clinically relevant metastatic sites. *Am J Pathol* 2007; **170**: 1077-1085 [PMID: 17322390 DOI: 10.2353/ajpath.2007.060773]

300 **Klose J**, Eissele J, Volz C, Schmitt S, Ritter A, Ying S, Schmidt T, Heger U, Schneider M, Ulrich A. Salinomycin inhibits metastatic colorectal cancer growth and interferes with Wnt/β-catenin signaling in $CD133^{+}$ human colorectal cancer cells. *BMC Cancer* 2016; **16**: 896 [PMID: 27855654 DOI: 10.1186/s12885-016-2879-8]

301 **Alamo P**, Gallardo A, Pavón MA, Casanova I, Trias M, Mangues MA, Vázquez E, Villaverde A, Mangues R, Céspedes MV. Subcutaneous preconditioning increases invasion and metastatic dissemination in mouse colorectal cancer models. *Dis Model Mech* 2014; **7**: 387-396 [PMID: 24487410 DOI: 10.1242/dmm.013995]

302 **Schulz P**, Dierkes C, Wiedenmann B, Grötzinger C. Near-Infrared Confocal Laser Endomicroscopy Detects Colorectal Cancer via an Integrin αvβ3 Optical Probe. *Mol Imaging Bio* 2015; **17**: 450–460 [DOI: 10.1007/s11307-015-0825-9]

303 **Künzli BM**, Bernlochner MI, Rath S, Käser S, Csizmadia E, Enjyoji K, Cowan P, d'Apice A, Dwyer K, Rosenberg R, Perren A, Friess H, Maurer CA, Robson SC. Impact of CD39 and purinergic signalling on the growth and metastasis of colorectal cancer. *Purinergic Signal* 2011; **7**: 231-241 [PMID: 21484085 DOI: 10.1007/s11302-011-9228-9]

304 **Lee WY**, Hong HK, Ham SK, Kim CI, Cho YB. Comparison of colorectal cancer in differentially established liver metastasis models. *Anticancer Res* 2014; **34**: 3321-3328 [PMID: 24982336]

305 **Sasaki H**, Miura K, Horii A, Kaneko N, Fujibuchi W, Kiseleva L, Gu Z, Murata Y, Karasawa H, Mizoi T, Kobayashi T, Kinouchi M, Ohnuma S, Yazaki N, Unno M, Sasaki I. Orthotopic implantation mouse model and cDNA microarray analysis indicates several genes potentially involved in lymph node metastasis of colorectal cancer. *Cancer Sci* 2008; **99**: 711-719 [PMID: 18307535 DOI: 10.1111/j.1349-7006.2008.00725.x]

306 **Tang W**, Zhu Y, Gao J, Fu J, Liu C, Liu Y, Song C, Zhu S, Leng Y, Wang G, Chen W, Du P, Huang S, Zhou X, Kang J, Cui L. MicroRNA-29a promotes colorectal cancer metastasis by regulating matrix metalloproteinase 2 and E-cadherin via KLF4. *Br J Cancer* 2014; **110**: 450-458 [PMID: 24281002 DOI: 10.1038/bjc.2013.724]

307 **Alamo P**, Gallardo A, Di Nicolantonio F, Pavón MA, Casanova I, Trias M, Mangues MA, Lopez-Pousa A, Villaverde A, Vázquez E, Bardelli A, Céspedes MV, Mangues R. Higher metastatic efficiency of KRas G12V than KRas G13D in a colorectal cancer model. *FASEB J* 2015; **29**: 464-476 [PMID: 25359494 DOI: 10.1096/fj.14-262303]

308 **Chen HN**, Yuan K, Xie N, Wang K, Huang Z, Chen Y, Dou Q, Wu M, Nice EC, Zhou ZG, Huang C. PDLIM1 Stabilizes the E-Cadherin/β-Catenin Complex to Prevent Epithelial-Mesenchymal Transition and Metastatic Potential of Colorectal Cancer Cells. *Cancer Res* 2016; **76**: 1122-1134 [PMID: 26701804 DOI: 10.1158/0008-5472.CAN-15-1962]

309 **Meunier K**, Ferron M, Calmel C, Fléjou JF, Pocard M, Praz F. Impact of MLH1 expression on tumor evolution after curative surgical tumor resection in a murine orthotopic xenograft model for human MSI colon cancer. *Genes Chromosomes Cancer* 2017; **56**: 681-690 [PMID: 28512763 DOI: 10.1002/gcc.22472]

310 **Xu H**, Zhang Y, Peña MM, Pirisi L, Creek KE. Six1 promotes colorectal cancer growth and metastasis by stimulating angiogenesis and recruiting tumor-associated macrophages. *Carcinogenesis* 2017; **38**: 281-292 [PMID: 28199476 DOI: 10.1093/carcin/bgw121]

311 **Paulson B**, Kim IH, Namgoong JM, Kim YG, Lee S, Moon Y, Shin DM, Choo MS, Kim JK. Longitudinal micro-endoscopic monitoring of high-success intramucosal xenografts for mouse models of colorectal cancer. *Int J Med Sci* 2019; **16**: 1453-1460 [PMID: 31673236 DOI: 10.7150/ijms.35666]

312 **Enquist IB**, Good Z, Jubb AM, Fuh G, Wang X, Junttila MR, Jackson EL, Leong KG. Lymph node-independent liver metastasis in a model of metastatic colorectal cancer. *Nat Commun* 2014; **5**: 3530 [PMID: 24667486 DOI: 10.1038/ncomms4530]

313 **Rapic S**, Vangestel C, Verhaeghe J, Van den Wyngaert T, Hinz R, Verhoye M, Pauwels P, Staelens S, Stroobants S. Characterization of an Orthotopic Colorectal Cancer Mouse Model and Its Feasibility for Accurate Quantification in Positron Emission Tomography. *Mol Imaging Biol* 2017; **19**: 762-771 [PMID: 28194632 DOI: 10.1007/s11307-017-1051-4]

314 **Mira A**, Morello V, Céspedes MV, Perera T, Comoglio PM, Mangues R, Michieli P. Stroma-derived HGF drives metabolic adaptation of colorectal cancer to angiogenesis inhibitors. *Oncotarget* 2017; **8**: 38193-38213 [PMID: 28445144 DOI: 10.18632/oncotarget.16942]

315 **Afik R**, Zigmond E, Vugman M, Klepfish M, Shimshoni E, Pasmanik-Chor M, Shenoy A, Bassat E, Halpern Z, Geiger T, Sagi I, Varol C. Tumor macrophages are pivotal constructors of tumor collagenous matrix. *J Exp Med* 2016; **213**: 2315-2331 [PMID: 27697834 DOI: 10.1084/jem.20151193]

316 **Hu CT**, Guo LL, Feng N, Zhang L, Zhou N, Ma LL, Shen L, Tong GH, Yan QW, Zhu SJ, Bian XW, Lai MD, Deng YJ, Ding YQ. MIF, secreted by human hepatic sinusoidal endothelial cells, promotes chemotaxis and outgrowth of colorectal cancer in liver prometastasis. *Oncotarget* 2015; **6**: 22410-22423 [PMID: 26087187 DOI: 10.18632/oncotarget.4198]

317 **Basilico C**, Hultberg A, Blanchetot C, de Jonge N, Festjens E, Hanssens V, Osepa SI, De Boeck G, Mira A, Cazzanti M, Morello V, Dreier T, Saunders M, de Haard H, Michieli P. Four individually druggable MET hotspots mediate HGF-driven tumor progression. *J Clin Invest* 2014; **124**: 3172-3186 [PMID: 24865428 DOI: 10.1172/JCI72316]

318 **Margolin DA**, Myers T, Zhang X, Bertoni DM, Reuter BA, Obokhare I, Borgovan T, Grimes C, Green H, Driscoll T, Lee CG, Davis NK, Li L. The critical roles of tumor-initiating cells and the lymph node stromal microenvironment in human colorectal cancer extranodal metastasis using a unique humanized orthotopic mouse model. *FASEB J* 2015; **29**: 3571-3581 [PMID: 25962655 DOI: 10.1096/fj.14-268938]

319 **Devaud C**, Rousseau B, Netzer S, Pitard V, Paroissin C, Khairallah C, Costet P, Moreau JF, Couillaud F, Dechanet-Merville J, Capone M. Anti-metastatic potential of human Vδ1(+) γδ T cells in an orthotopic mouse xenograft model of colon carcinoma. *Cancer Immunol Immunother* 2013; **62**: 1199-1210 [PMID: 23619975 DOI: 10.1007/s00262-013-1402-1]

320 **Schölch S**, García SA, Iwata N, Niemietz T, Betzler AM, Nanduri LK, Bork U, Kahlert C, Thepkaysone ML, Swiersy A, Büchler MW, Reissfelder C, Weitz J, Rahbari NN. Circulating tumor cells exhibit stem cell characteristics in an orthotopic mouse model of colorectal cancer. *Oncotarget* 2016; **7**: 27232-27242 [PMID: 27029058 DOI: 10.18632/oncotarget.8373]

321 **Kashtan H**, Rabau M, Mullen JB, Wong AH, Roder JC, Shpitz B, Stern HS, Gallinger S. Intra-rectal injection of tumour cells: a novel animal model of rectal cancer. *Surg Oncol* 1992; **1**: 251-256 [PMID: 1341258 DOI: 10.1016/0960-7404(92)90072-s]

322 **Donigan M**, Norcross LS, Aversa J, Colon J, Smith J, Madero-Visbal R, Li S, McCollum N, Ferrara A, Gallagher JT, Baker CH. Novel murine model for colon cancer: non-operative trans-anal rectal injection. *J Surg Res* 2009; **154**: 299-303 [PMID: 19101690 DOI: 10.1016/j.jss.2008.05.028]

323 **Cohen G**, Lecht S, Arien-Zakay H, Ettinger K, Amsalem O, Oron-Herman M, Yavin E, Prus D, Benita S, Nissan A, Lazarovici P. Bio-imaging of colorectal cancer models using near infrared labeled epidermal growth factor. *PLoS One* 2012; **7**: e48803 [PMID: 23144978 DOI: 10.1371/journal.pone.0048803]

324 **Kim YI**, Jeong S, Jung KO, Song MG, Lee CH, Chung SJ, Park JY, Cha MG, Lee SG, Jun BH, Lee YS, Hwang DW, Youn H, Kang KW, Lee YS, Jeong DH, Lee DS. Simultaneous Detection of EGFR and VEGF in Colorectal Cancer using Fluorescence-Raman Endoscopy. *Sci Rep* 2017; **7**: 1035 [PMID:

28432289 DOI: 10.1038/s41598-017-01020-y]
325 **Zigmond E**, Halpern Z, Elinav E, Brazowski E, Jung S, Varol C. Utilization of murine colonoscopy for orthotopic implantation of colorectal cancer. *PLoS One* 2011; **6**: e28858 [PMID: 22174916 DOI: 10.1371/journal.pone.0028858]
326 **Zaytseva YY**, Elliott VA, Rychahou P, Mustain WC, Kim JT, Valentino J, Gao T, O'Connor KL, Neltner JM, Lee EY, Weiss HL, Evers BM. Cancer cell-associated fatty acid synthase activates endothelial cells and promotes angiogenesis in colorectal cancer. *Carcinogenesis* 2014; **35**: 1341-1351 [PMID: 24510238 DOI: 10.1093/carcin/bgu042]
327 **Bettenworth D**, Mücke MM, Schwegmann K, Faust A, Poremba C, Schäfers M, Domagk D, Lenz P. Endoscopy-guided orthotopic implantation of colorectal cancer cells results in metastatic colorectal cancer in mice. *Clin Exp Metastasis* 2016; **33**: 551-562 [PMID: 27146063 DOI: 10.1007/s10585-016-9797-7]
328 **Kishimoto H**, Momiyama M, Aki R, Kimura H, Suetsugu A, Bouvet M, Fujiwara T, Hoffman RM. Development of a clinically-precise mouse model of rectal cancer. *PLoS One* 2013; **8**: e79453 [PMID: 24265772 DOI: 10.1371/journal.pone.0079453]
329 **Hite N**, Klinger A, Hellmers L, Maresh GA, Miller PE, Zhang X, Li L, Margolin DA. An Optimal Orthotopic Mouse Model for Human Colorectal Cancer Primary Tumor Growth and Spontaneous Metastasis. *Dis Colon Rectum* 2018; **61**: 698-705 [PMID: 29722728 DOI: 10.1097/DCR.0000000000001096]
330 **Prasad S**, Yadav VR, Sung B, Reuter S, Kannappan R, Deorukhkar A, Diagaradjane P, Wei C, Baladandayuthapani V, Krishnan S, Guha S, Aggarwal BB. Ursolic acid inhibits growth and metastasis of human colorectal cancer in an orthotopic nude mouse model by targeting multiple cell signaling pathways: chemosensitization with capecitabine. *Clin Cancer Res* 2012; **18**: 4942-4953 [PMID: 22832932 DOI: 10.1158/1078-0432.CCR-11-2805]
331 **Wang J**, Chen C, Wang S, Zhang Y, Yin P, Gao Z, Xu J, Feng D, Zuo Q, Zhao R, Chen T. Bufalin Inhibits HCT116 Colon Cancer Cells and Its Orthotopic Xenograft Tumor in Mice Model through Genes Related to Apoptotic and PTEN/AKT Pathways. *Gastroenterol Res Pract* 2015; **2015**: 457193 [PMID: 26770191 DOI: 10.1155/2015/457193]
332 **Bhome R**, Goh RW, Bullock MD, Pillar N, Thirdborough SM, Mellone M, Mirnezami R, Galea D, Veselkov K, Gu Q, Underwood TJ, Primrose JN, De Wever O, Shomron N, Sayan AE, Mirnezami AH. Exosomal microRNAs derived from colorectal cancer-associated fibroblasts: role in driving cancer progression. *Aging (Albany NY)* 2017; **9**: 2666-2694 [PMID: 29283887 DOI: 10.18632/aging.101355]
333 **Tan X**, Zhang Z, Yao H, Shen L. Tim-4 promotes the growth of colorectal cancer by activating angiogenesis and recruiting tumor-associated macrophages via the PI3K/AKT/mTOR signaling pathway. *Cancer Lett* 2018; **436**: 119-128 [PMID: 30118845 DOI: 10.1016/j.canlet.2018.08.012]
334 **Mizukoshi K**, Okazawa Y, Haeno H, Koyama Y, Sulidan K, Komiyama H, Saeki H, Ohtsuji N, Ito Y, Kojima Y, Goto M, Habu S, Hino O, Sakamoto K, Orimo A. Metastatic seeding of human colon cancer cell clusters expressing the hybrid epithelial/mesenchymal state. *Int J Cancer* 2019 [PMID: 31506938 DOI: 10.1002/ijc.32672]
335 **Russell WMS**, Burch RL. The principles of humane experimental technique. London: Methuen&Co. Ltd., 1959
336 **Wege AK**, Ernst W, Eckl J, Frankenberger B, Vollmann-Zwerenz A, Männel DN, Ortmann O, Kroemer A, Brockhoff G. Humanized tumor mice--a new model to study and manipulate the immune response in advanced cancer therapy. *Int J Cancer* 2011; **129**: 2194-2206 [PMID: 21544806 DOI: 10.1002/ijc.26159]
337 **Choi Y**, Lee S, Kim K, Kim SH, Chung YJ, Lee C. Studying cancer immunotherapy using patient-derived xenografts (PDXs) in humanized mice. *Exp Mol Med* 2018; **50**: 99 [PMID: 30089794 DOI: 10.1038/s12276-018-0115-0]
338 **Bird GA**, Polsky A, Estes P, Hanlon T, Hamilton H, Morton JJ, Gutman J, Jimeno A, Turner BC, Refaeli Y. Expansion of human and murine hematopoietic stem and progenitor cells ex vivo without genetic modification using MYC and Bcl-2 fusion proteins. *PLoS One* 2014; **9**: e105525 [PMID: 25170611 DOI: 10.1371/journal.pone.0105525]
339 **Morton JJ**, Bird G, Keysar SB, Astling DP, Lyons TR, Anderson RT, Glogowska MJ, Estes P, Eagles JR, Le PN, Gan G, McGettigan B, Fernandez P, Padilla-Just N, Varella-Garcia M, Song JI, Bowles DW, Schedin P, Tan AC, Roop DR, Wang XJ, Refaeli Y, Jimeno A. XactMice: humanizing mouse bone marrow enables microenvironment reconstitution in a patient-derived xenograft model of head and neck cancer. *Oncogene* 2016; **35**: 290-300 [PMID: 25893296 DOI: 10.1038/onc.2015.94]
340 **McIntosh BE**, Brown ME, Duffin BM, Maufort JP, Vereide DT, Slukvin II, Thomson JA. Nonirradiated NOD,B6.SCID Il2rγ-/- Kit(W41/W41) (NBSGW) mice support multilineage engraftment of human hematopoietic cells. *Stem Cell Reports* 2015; **4**: 171-180 [PMID: 25601207 DOI: 10.1016/j.stemcr.2014.12.005]
341 **Jespersen H**, Lindberg MF, Donia M, Söderberg EMV, Andersen R, Keller U, Ny L, Svane IM, Nilsson LM, Nilsson JA. Clinical responses to adoptive T-cell transfer can be modeled in an autologous immune-humanized mouse model. *Nat Commun* 2017; **8**: 707 [PMID: 28955032 DOI: 10.1038/s41467-017-00786-z]
342 **Jangalwe S**, Shultz LD, Mathew A, Brehm MA. Improved B cell development in humanized NOD-*scid IL2Rγnull* mice transgenically expressing human stem cell factor, granulocyte-macrophage colony-stimulating factor and interleukin-3. *Immun Inflamm Dis* 2016; **4**: 427-440 [PMID: 27980777 DOI: 10.1002/iid3.124]
343 **Herndler-Brandstetter D**, Shan L, Yao Y, Stecher C, Plajer V, Lietzenmayer M, Strowig T, de Zoete MR, Palm NW, Chen J, Blish CA, Frleta D, Gurer C, Macdonald LE, Murphy AJ, Yancopoulos GD, Montgomery RR, Flavell RA. Humanized mouse model supports development, function, and tissue residency of human natural killer cells. *Proc Natl Acad Sci USA* 2017; **114**: E9626-E9634 [PMID: 29078283 DOI: 10.1073/pnas.1705301114]
344 **Capasso A**, Lang J, Pitts TM, Jordan KR, Lieu CH, Davis SL, Diamond JR, Kopetz S, Barbee J, Peterson J, Freed BM, Yacob BW, Bagby SM, Messersmith WA, Slansky JE, Pelanda R, Eckhardt SG. Characterization of immune responses to anti-PD-1 mono and combination immunotherapy in hematopoietic humanized mice implanted with tumor xenografts. *J Immunother Cancer* 2019; **7**: 37 [PMID: 30736857 DOI: 10.1186/s40425-019-0518-z]
345 **Overman MJ**, Lonardi S, Wong KYM, Lenz HJ, Gelsomino F, Aglietta M, Morse MA, Van Cutsem E, McDermott R, Hill A, Sawyer MB, Hendlisz A, Neyns B, Svrcek M, Moss RA, Ledeine JM, Cao ZA, Kamble S, Kopetz S, André T. Durable Clinical Benefit With Nivolumab Plus Ipilimumab in DNA Mismatch Repair-Deficient/Microsatellite Instability-High Metastatic Colorectal Cancer. *J Clin Oncol*

2018; **36**: 773-779 [PMID: 29355075 DOI: 10.1200/JCO.2017.76.9901]
346 **Barretina J**, Caponigro G, Stransky N, Venkatesan K, Margolin AA, Kim S, Wilson CJ, Lehár J, Kryukov GV, Sonkin D, Reddy A, Liu M, Murray L, Berger MF, Monahan JE, Morais P, Meltzer J, Korejwa A, Jané-Valbuena J, Mapa FA, Thibault J, Bric-Furlong E, Raman P, Shipway A, Engels IH, Cheng J, Yu GK, Yu J, Aspesi P, de Silva M, Jagtap K, Jones MD, Wang L, Hatton C, Palescandolo E, Gupta S, Mahan S, Sougnez C, Onofrio RC, Liefeld T, MacConaill L, Winckler W, Reich M, Li N, Mesirov JP, Gabriel SB, Getz G, Ardlie K, Chan V, Myer VE, Weber BL, Porter J, Warmuth M, Finan P, Harris JL, Meyerson M, Golub TR, Morrissey MP, Sellers WR, Schlegel R, Garraway LA. The Cancer Cell Line Encyclopedia enables predictive modelling of anticancer drug sensitivity. *Nature* 2012; **483**: 603-607 [PMID: 22460905 DOI: 10.1038/nature11003]
347 **Krbal L**, Soukup J, Stanislav J, Hanusova V. Derivation and basic characterization of colorectal carcinoma primary cell lines. *Biomed Pap Med Fac Univ Palacky Olomouc Czech Repub* 2017; **161**: 360-368 [PMID: 29042709 DOI: 10.5507/bp.2017.040]
348 **Bolck HA**, Pauli C, Göbel E, Mühlbauer K, Dettwiler S, Moch H, Schraml P. Cancer Sample Biobanking at the Next Level: Combining Tissue With Living Cell Repositories to Promote Precision Medicine. *Front Cell Dev Biol* 2019; **7**: 246 [PMID: 31696117 DOI: 10.3389/fcell.2019.00246]
349 **Kang Y**, Zhang R, Suzuki R, Li SQ, Roife D, Truty MJ, Chatterjee D, Thomas RM, Cardwell J, Wang Y, Wang H, Katz MH, Fleming JB. Two-dimensional culture of human pancreatic adenocarcinoma cells results in an irreversible transition from epithelial to mesenchymal phenotype. *Lab Invest* 2015; **95**: 207-222 [PMID: 25485535 DOI: 10.1038/labinvest.2014.143]
350 **Hickman JA**, Graeser R, de Hoogt R, Vidic S, Brito C, Gutekunst M, van der Kuip H; IMI PREDECT Consortium. Three-dimensional models of cancer for pharmacology and cancer cell biology: capturing tumor complexity in vitro/ex vivo. *Biotechnol J* 2014; **9**: 1115-1128 [PMID: 25174503 DOI: 10.1002/biot.201300492]
351 **Luca AC**, Mersch S, Deenen R, Schmidt S, Messner I, Schäfer KL, Baldus SE, Huckenbeck W, Piekorz RP, Knoefel WT, Krieg A, Stoecklein NH. Impact of the 3D microenvironment on phenotype, gene expression, and EGFR inhibition of colorectal cancer cell lines. *PLoS One* 2013; **8**: e59689 [PMID: 23555746 DOI: 10.1371/journal.pone.0059689]
352 **van Tienderen GS**, Groot Koerkamp B, IJzermans JNM, van der Laan LJW, Verstegen MMA. Recreating Tumour Complexity in a Dish: Organoid Models to Study Liver Cancer Cells and their Extracellular Environment. *Cancers (Basel)* 2019; **11** [PMID: 31683901 DOI: 10.3390/cancers11111706]
353 **van de Wetering M**, Francies HE, Francis JM, Bounova G, Iorio F, Pronk A, van Houdt W, van Gorp J, Taylor-Weiner A, Kester L, McLaren-Douglas A, Blokker J, Jaksani S, Bartfeld S, Volckman R, van Sluis P, Li VS, Seepo S, Sekhar Pedamallu C, Cibulskis K, Carter SL, McKenna A, Lawrence MS, Lichtenstein L, Stewart C, Koster J, Versteeg R, van Oudenaarden A, Saez-Rodriguez J, Vries RG, Getz G, Wessels L, Stratton MR, McDermott U, Meyerson M, Garnett MJ, Clevers H. Prospective derivation of a living organoid biobank of colorectal cancer patients. *Cell* 2015; **161**: 933-945 [PMID: 25957691 DOI: 10.1016/j.cell.2015.03.053]
354 **Vlachogiannis G**, Hedayat S, Vatsiou A, Jamin Y, Fernández-Mateos J, Khan K, Lampis A, Eason K, Huntingford I, Burke R, Rata M, Koh DM, Tunariu N, Collins D, Hulkki-Wilson S, Ragulan C, Spiteri I, Moorcraft SY, Chau I, Rao S, Watkins D, Fotiadis N, Bali M, Darvish-Damavandi M, Lote H, Eltahir Z, Smyth EC, Begum R, Clarke PA, Hahne JC, Dowsett M, de Bono J, Workman P, Sadanandam A, Fassan M, Sansom OJ, Eccles S, Starling N, Braconi C, Sottoriva A, Robinson SP, Cunningham D, Valeri N. Patient-derived organoids model treatment response of metastatic gastrointestinal cancers. *Science* 2018; **359**: 920-926 [PMID: 29472484 DOI: 10.1126/science.aao2774]
355 **Tiriac H**, Belleau P, Engle DD, Plenker D, Deschênes A, Somerville TDD, Froeling FEM, Burkhart RA, Denroche RE, Jang GH, Miyabayashi K, Young CM, Patel H, Ma M, LaComb JF, Palmaira RLD, Javed AA, Huynh JC, Johnson M, Arora K, Robine N, Shah M, Sanghvi R, Goetz AB, Lowder CY, Martello L, Driehuis E, LeComte N, Askan G, Iacobuzio-Donahue CA, Clevers H, Wood LD, Hruban RH, Thompson E, Aguirre AJ, Wolpin BM, Sasson A, Kim J, Wu M, Bucobo JC, Allen P, Sejpal DV, Nealon W, Sullivan JD, Winter JM, Gimotty PA, Grem JL, DiMaio DJ, Buscaglia JM, Grandgenett PM, Brody JR, Hollingsworth MA, O'Kane GM, Notta F, Kim E, Crawford JM, Devoe C, Ocean A, Wolfgang CL, Yu KH, Li E, Vakoc CR, Hubert B, Fischer SE, Wilson JM, Moffitt R, Knox J, Krasnitz A, Gallinger S, Tuveson DA. Organoid Profiling Identifies Common Responders to Chemotherapy in Pancreatic Cancer. *Cancer Discov* 2018; **8**: 1112-1129 [PMID: 29853643 DOI: 10.1158/2159-8290.CD-18-0349]
356 **Yan HHN**, Siu HC, Law S, Ho SL, Yue SSK, Tsui WY, Chan D, Chan AS, Ma S, Lam KO, Bartfeld S, Man AHY, Lee BCH, Chan ASY, Wong JWH, Cheng PSW, Chan AKW, Zhang J, Shi J, Fan X, Kwong DLW, Mak TW, Yuen ST, Clevers H, Leung SY. A Comprehensive Human Gastric Cancer Organoid Biobank Captures Tumor Subtype Heterogeneity and Enables Therapeutic Screening. *Cell Stem Cell* 2018; **23**: 882-897.e11 [PMID: 30344100 DOI: 10.1016/j.stem.2018.09.016]
357 **Lee SH**, Hong JH, Park HK, Park JS, Kim BK, Lee JY, Jeong JY, Yoon GS, Inoue M, Choi GS, Lee IK. Colorectal cancer-derived tumor spheroids retain the characteristics of original tumors. *Cancer Lett* 2015; **367**: 34-42 [PMID: 26185002 DOI: 10.1016/j.canlet.2015.06.024]
358 **Sato T**, Vries RG, Snippert HJ, van de Wetering M, Barker N, Stange DE, van Es JH, Abo A, Kujala P, Peters PJ, Clevers H. Single Lgr5 stem cells build crypt-villus structures in vitro without a mesenchymal niche. *Nature* 2009; **459**: 262-265 [PMID: 19329995 DOI: 10.1038/nature07935]
359 **Drost J**, van Jaarsveld RH, Ponsioen B, Zimberlin C, van Boxtel R, Buijs A, Sachs N, Overmeer RM, Offerhaus GJ, Begthel H, Korving J, van de Wetering M, Schwank G, Logtenberg M, Cuppen E, Snippert HJ, Medema JP, Kops GJ, Clevers H. Sequential cancer mutations in cultured human intestinal stem cells. *Nature* 2015; **521**: 43-47 [PMID: 25924068 DOI: 10.1038/nature14415]
360 **Fumagalli A**, Drost J, Suijkerbuijk SJ, van Boxtel R, de Ligt J, Offerhaus GJ, Begthel H, Beerling E, Tan EH, Sansom OJ, Cuppen E, Clevers H, van Rheenen J. Genetic dissection of colorectal cancer progression by orthotopic transplantation of engineered cancer organoids. *Proc Natl Acad Sci USA* 2017; **114**: E2357-E2364 [PMID: 28270604 DOI: 10.1073/pnas.1701219114]
361 **Gao D**, Vela I, Sboner A, Iaquinta PJ, Karthaus WR, Gopalan A, Dowling C, Wanjala JN, Undvall EA, Arora VK, Wongvipat J, Kossai M, Ramazanoglu S, Barboza LP, Di W, Cao Z, Zhang QF, Sirota I, Ran L, MacDonald TY, Beltran H, Mosquera JM, Touijer KA, Scardino PT, Laudone VP, Curtis KR, Rathkopf DE, Morris MJ, Danila DC, Slovin SF, Solomon SB, Eastham JA, Chi P, Carver B, Rubin MA, Scher HI, Clevers H, Sawyers CL, Chen Y. Organoid cultures derived from patients with advanced prostate cancer. *Cell* 2014; **159**: 176-187 [PMID: 25201530 DOI: 10.1016/j.cell.2014.08.016]
362 **Agnoletto C**, Corrà F, Minotti L, Baldassari F, Crudele F, Cook WJJ, Di Leva G, d'Adamo AP, Gasparini

P, Volinia S. Heterogeneity in Circulating Tumor Cells: The Relevance of the Stem-Cell Subset. *Cancers (Basel)* 2019; **11** [PMID: 30959764 DOI: 10.3390/cancers11040483]

363 **Aleman J**, Skardal A. A multi-site metastasis-on-a-chip microphysiological system for assessing metastatic preference of cancer cells. *Biotechnol Bioeng* 2019; **116**: 936-944 [PMID: 30450540 DOI: 10.1002/bit.26871]

364 **Miller PG**, Shuler ML. Design and demonstration of a pumpless 14 compartment microphysiological system. *Biotechnol Bioeng* 2016; **113**: 2213-2227 [PMID: 27070809 DOI: 10.1002/bit.25989]

365 **Guinney J**, Dienstmann R, Wang X, de Reyniès A, Schlicker A, Soneson C, Marisa L, Roepman P, Nyamundanda G, Angelino P, Bot BM, Morris JS, Simon IM, Gerster S, Fessler E, De Sousa E Melo F, Missiaglia E, Ramay H, Barras D, Homicsko K, Maru D, Manyam GC, Broom B, Boige V, Perez-Villamil B, Laderas T, Salazar R, Gray JW, Hanahan D, Tabernero J, Bernards R, Friend SH, Laurent-Puig P, Medema JP, Sadanandam A, Wessels L, Delorenzi M, Kopetz S, Vermeulen L, Tejpar S. The consensus molecular subtypes of colorectal cancer. *Nat Med* 2015; **21**: 1350-1356 [PMID: 26457759 DOI: 10.1038/nm.3967]

366 **Mooi JK**, Wirapati P, Asher R, Lee CK, Savas P, Price TJ, Townsend A, Hardingham J, Buchanan D, Williams D, Tejpar S, Mariadason JM, Tebbutt NC. The prognostic impact of consensus molecular subtypes (CMS) and its predictive effects for bevacizumab benefit in metastatic colorectal cancer: molecular analysis of the AGITG MAX clinical trial. *Ann Oncol* 2018; **29**: 2240-2246 [PMID: 30247524 DOI: 10.1093/annonc/mdy410]

367 **Jean-Quartier C**, Jeanquartier F, Jurisica I, Holzinger A. In silico cancer research towards 3R. *BMC Cancer* 2018; **18**: 408 [PMID: 29649981 DOI: 10.1186/s12885-018-4302-0]

368 **Christopher R**, Dhiman A, Fox J, Gendelman R, Haberitcher T, Kagle D, Spizz G, Khalil IG, Hill C. Data-driven computer simulation of human cancer cell. *Ann N Y Acad Sci* 2004; **1020**: 132-153 [PMID: 15208190 DOI: 10.1196/annals.1310.014]

369 **Uhlen M**, Zhang C, Lee S, Sjöstedt E, Fagerberg L, Bidkhori G, Benfeitas R, Arif M, Liu Z, Edfors F, Sanli K, von Feilitzen K, Oksvold P, Lundberg E, Hober S, Nilsson P, Mattsson J, Schwenk JM, Brunnström H, Glimelius B, Sjöblom T, Edqvist PH, Djureinovic D, Micke P, Lindskog C, Mardinoglu A, Ponten F. A pathology atlas of the human cancer transcriptome. *Science* 2017; **357** [PMID: 28818916 DOI: 10.1126/science.aan2507]

370 **Farshidfar F**, Weljie AM, Kopciuk KA, Hilsden R, McGregor SE, Buie WD, MacLean A, Vogel HJ, Bathe OF. A validated metabolomic signature for colorectal cancer: exploration of the clinical value of metabolomics. *Br J Cancer* 2016; **115**: 848-857 [PMID: 27560555 DOI: 10.1038/bjc.2016.243]

371 **Porta-Pardo E**, Garcia-Alonso L, Hrabe T, Dopazo J, Godzik A. A Pan-Cancer Catalogue of Cancer Driver Protein Interaction Interfaces. *PLoS Comput Biol* 2015; **11**: e1004518 [PMID: 26485003 DOI: 10.1371/journal.pcbi.1004518]

372 **Subramanian A**, Narayan R, Corsello SM, Peck DD, Natoli TE, Lu X, Gould J, Davis JF, Tubelli AA, Asiedu JK, Lahr DL, Hirschman JE, Liu Z, Donahue M, Julian B, Khan M, Wadden D, Smith IC, Lam D, Liberzon A, Toder C, Bagul M, Orzechowski M, Enache OM, Piccioni F, Johnson SA, Lyons NJ, Berger AH, Shamji AF, Brooks AN, Vrcic A, Flynn C, Rosains J, Takeda DY, Hu R, Davison D, Lamb J, Ardlie K, Hogstrom L, Greenside P, Gray NS, Clemons PA, Silver S, Wu X, Zhao WN, Read-Button W, Wu X, Haggarty SJ, Ronco LV, Boehm JS, Schreiber SL, Doench JG, Bittker JA, Root DE, Wong B, Golub TR. A Next Generation Connectivity Map: L1000 Platform and the First 1,000,000 Profiles. *Cell* 2017; **171**: 1437-1452.e17 [PMID: 29195078 DOI: 10.1016/j.cell.2017.10.049]

373 **Kim YA**, Cho DY, Przytycka TM. Understanding Genotype-Phenotype Effects in Cancer via Network Approaches. *PLoS Comput Biol* 2016; **12**: e1004747 [PMID: 26963104 DOI: 10.1371/journal.pcbi.1004747]

374 **Aoki K**, Tamai Y, Horiike S, Oshima M, Taketo MM. Colonic polyposis caused by mTOR-mediated chromosomal instability in Apc+/Delta716 Cdx2+/- compound mutant mice. *Nat Genet* 2003; **35**: 323-330 [PMID: 14625550 DOI: 10.1038/ng1265]

375 **Rao CV**, Yang YM, Swamy MV, Liu T, Fang Y, Mahmood R, Jhanwar-Uniyal M, Dai W. Colonic tumorigenesis in BubR1+/-ApcMin/+ compound mutant mice is linked to premature separation of sister chromatids and enhanced genomic instability. *Proc Natl Acad Sci USA* 2005; **102**: 4365-4370 [PMID: 15767571 DOI: 10.1073/pnas.0407822102]

376 **Hahn MM**, Vreede L, Bemelmans SA, van der Looij E, van Kessel AG, Schackert HK, Ligtenberg MJ, Hoogerbrugge N, Kuiper RP, de Voer RM. Prevalence of germline mutations in the spindle assembly checkpoint gene BUB1B in individuals with early-onset colorectal cancer. *Genes Chromosomes Cancer* 2016; **55**: 855-863 [PMID: 27239782 DOI: 10.1002/gcc.22385]

377 **Batlle E**, Bacani J, Begthel H, Jonkheer S, Gregorieff A, van de Born M, Malats N, Sancho E, Boon E, Pawson T, Gallinger S, Pals S, Clevers H. EphB receptor activity suppresses colorectal cancer progression. *Nature* 2005; **435**: 1126-1130 [PMID: 15973414 DOI: 10.1038/nature03626]

378 **Paul Olson TJ**, Hadac JN, Sievers CK, Leystra AA, Deming DA, Zahm CD, Albrecht DM, Nomura A, Nettekoven LA, Plesh LK, Clipson L, Sullivan R, Newton MA, Schelman WR, Halberg RB. Dynamic tumor growth patterns in a novel murine model of colorectal cancer. *Cancer Prev Res (Phila)* 2014; **7**: 105-113 [PMID: 24196829 DOI: 10.1158/1940-6207.CAPR-13-0163]

379 **Suzui M**, Okuno M, Tanaka T, Nakagama H, Moriwaki H. Enhanced colon carcinogenesis induced by azoxymethane in min mice occurs via a mechanism independent of beta-catenin mutation. *Cancer Lett* 2002; **183**: 31-41 [PMID: 12049812 DOI: 10.1016/S0304-3835(02)00114-3]

380 **Møllersen L**, Vikse R, Andreassen A, Steffensen IL, Mikalsen A, Paulsen JE, Alexander J. Adenomatous polyposis coli truncation mutations in 2-amino-1-methyl-6-phenylimidazo[4,5-b]pyridine (PhIP)-induced intestinal tumours of multiple intestinal neoplasia mice. *Mutat Res* 2004; **557**: 29-40 [PMID: 14706516 DOI: 10.1016/j.mrgentox.2003.09.008]

381 **Smits R**, van der Houven van Oordt W, Luz A, Zurcher C, Jagmohan-Changur S, Breukel C, Khan PM, Fodde R. Apc1638N: a mouse model for familial adenomatous polyposis-associated desmoid tumors and cutaneous cysts. *Gastroenterology* 1998; **114**: 275-283 [PMID: 9453487 DOI: 10.1016/s0016-5085(98)70478-0]

382 **Xu J**, Cortellino S, Tricarico R, Chang WC, Scher G, Devarajan K, Slifker M, Moore R, Bassi MR, Caretti E, Clapper M, Cooper H, Bellacosa A. *Thymine DNA Glycosylase (TDG)* is involved in the pathogenesis of intestinal tumors with reduced *APC* expression. *Oncotarget* 2017; **8**: 89988-89997 [PMID: 29163805 DOI: 10.18632/oncotarget.21219]

383 **Kawaguchi Y**, Hinoi T, Saito Y, Adachi T, Miguchi M, Niitsu H, Sasada T, Shimomura M, Egi H, Oka S, Tanaka S, Chayama K, Sentani K, Oue N, Yasui W, Ohdan H. Mouse model of proximal colon-specific

tumorigenesis driven by microsatellite instability-induced Cre-mediated inactivation of Apc and activation of Kras. *J Gastroenterol* 2016; **51**: 447-457 [PMID: 26361962 DOI: 10.1007/s00535-015-1121-9]

384 **Roper J**, Richardson MP, Wang WV, Richard LG, Chen W, Coffee EM, Sinnamon MJ, Lee L, Chen PC, Bronson RT, Martin ES, Hung KE. The dual PI3K/mTOR inhibitor NVP-BEZ235 induces tumor regression in a genetically engineered mouse model of PIK3CA wild-type colorectal cancer. *PLoS One* 2011; **6**: e25132 [PMID: 21966435 DOI: 10.1371/journal.pone.0025132]

385 **Byun AJ**, Hung KE, Fleet JC, Bronson RT, Mason JB, Garcia PE, Crott JW. Colon-specific tumorigenesis in mice driven by Cre-mediated inactivation of Apc and activation of mutant Kras. *Cancer Lett* 2014; **347**: 191-195 [PMID: 24632531 DOI: 10.1016/j.canlet.2014.03.004]

386 **Kang DW**, Lee SW, Hwang WC, Lee BH, Choi YS, Suh YA, Choi KY, Min DS. Phospholipase D1 Acts through Akt/TopBP1 and RB1 to Regulate the E2F1-Dependent Apoptotic Program in Cancer Cells. *Cancer Res* 2017; **77**: 142-152 [PMID: 27793841 DOI: 10.1158/0008-5472.CAN-15-3032]

387 **Kitamura T**, Biyajima K, Aoki M, Oshima M, Taketo MM. Matrix metalloproteinase 7 is required for tumor formation, but dispensable for invasion and fibrosis in SMAD4-deficient intestinal adenocarcinomas. *Lab Invest* 2009; **89**: 98-105 [PMID: 19002110 DOI: 10.1038/labinvest.2008.107]

388 **Hamamoto T**, Beppu H, Okada H, Kawabata M, Kitamura T, Miyazono K, Kato M. Compound disruption of smad2 accelerates malignant progression of intestinal tumors in apc knockout mice. *Cancer Res* 2002; **62**: 5955-5961 [PMID: 12384562]

389 **Luo F**, Brooks DG, Ye H, Hamoudi R, Poulogiannis G, Patek CE, Winton DJ, Arends MJ. Conditional expression of mutated K-ras accelerates intestinal tumorigenesis in Msh2-deficient mice. *Oncogene* 2007; **26**: 4415-4427 [PMID: 17297472 DOI: 10.1038/sj.onc.1210231]

390 **Edelmann W**, Umar A, Yang K, Heyer J, Kucherlapati M, Lia M, Kneitz B, Avdievich E, Fan K, Wong E, Crouse G, Kunkel T, Lipkin M, Kolodner RD, Kucherlapati R. The DNA mismatch repair genes Msh3 and Msh6 cooperate in intestinal tumor suppression. *Cancer Res* 2000; **60**: 803-807 [PMID: 10706084]

391 **Sakamoto K**, Tominaga Y, Yamauchi K, Nakatsu Y, Sakumi K, Yoshiyama K, Egashira A, Kura S, Yao T, Tsuneyoshi M, Maki H, Nakabeppu Y, Tsuzuki T. MUTYH-null mice are susceptible to spontaneous and oxidative stress induced intestinal tumorigenesis. *Cancer Res* 2007; **67**: 6599-6604 [PMID: 17638869 DOI: 10.1158/0008-5472.CAN-06-4802]

World Journal of Gastroenterology

Submit a Manuscript: https://www.f6publishing.com

World J Gastroenterol 2020 April 7; 26(13): 1427-1438

DOI: 10.3748/wjg.v26.i13.1427

ISSN 1007-9327 (print) ISSN 2219-2840 (online)

REVIEW

Possible role of intestinal stem cells in the pathophysiology of irritable bowel syndrome

Magdy El-Salhy

ORCID number: Magdy El-Salhy (0000-0003-3398-3288).

Author contributions: El-Salhy M wrote, conceived and edited this aricle.

Conflict-of-interest statement: Authors declare no conflict of interests for this article.

Manuscript source: Invited Manuscript

Received: December 3, 2019
Peer-review started: December 3, 2019
First decision: January 13, 2020
Revised: February 8, 2020
Accepted: March 14, 2020
Article in press: March 14, 2020
Published online: April 7, 2020

P-Reviewer: Finsterer J, Gregorio BM
S-Editor: Tang JZ
L-Editor: A
E-Editor: Ma YJ

Magdy El-Salhy, Section for Gastroenterology, Department of Medicine, Stord Hospital, Stord 54 09, Norway

Magdy El-Salhy, Department of Clinical Medicine, University of Bergen, Bergen 50 21, Norway

Corresponding author: Magdy El-Salhy, BSc, MA, MD, PhD, Chief Doctor, Professor, Consultant Gastroenterologist, Section for Gastroenterology, Department of Medicine, Stord Hospital, Box 4000, Stord 54 09, Norway. magdy.el-salhy@helse-fonna.no

Abstract

The pathophysiology of irritable bowel syndrome (IBS) is not completely understood. However, several factors are known to play a role in pathophysiology of IBS such as genetics, diet, gut microbiota, gut endocrine cells, stress and low-grade inflammation. Understanding the pathophysiology of IBS may open the way for new treatment approaches. Low density of intestinal stem cells and low differentiation toward enteroendocrine cells has been reported recently in patients with IBS. These abnormalities are believed to be the cause of the low density of enteroendocrine cells seen in patients with IBS. Enteroendocrine cells regulate gastrointestinal motility, secretion, absorption and visceral sensitivity. Gastrointestinal dysmotility, abnormal absorption/secretion and visceral hypersensitivity are all seen in patients with IBS and haven been attributed to the low density the intestinal enteroendocrine cells in these patients. The present review conducted a literature search in Medline (PubMed) covering the last ten years until November 2019, where articles in English were included. Articles about the intestinal stem cells and their possible role in the pathophysiology of IBS are discussed in the present review. The present review discusses the assumption that intestinal stem cells play a central role in the pathophysiology of IBS and that the other factors known to contribute to the pathophysiology of IBS such as genetics, diet gut microbiota, stress, and low-grade inflammation exert their effects through affecting the intestinal stem cells. It reports further the data that support this assumption on genetics, diet, gut microbiota, stress with depletion of glutamine, and inflammation.

Key words: Diet; Gut enteroendocrine cells; Gut microbiota; Low grade inflammation; Stress

Core tip: The pathophysiology of irritable bowel syndrome (IBS) is not completely understood. Understanding the pathophysiology of IBS may enable us to find an effective treatment for this disorder. The density of intestinal stem cells is low in patients with IBS. Moreover, the differentiation of stem cells into enteroendocrine cells is abnormal. It seems that these abnormalities in intestinal stem cells is the cause of the low density of enteroendocrine cells seen in patients with IBS. It is believed that the low density of enteroendocrine cells is behind the gastrointestinal dysmotility, abnormal secretion/absorption and hypersensitivity observed in patients with IBS. This review presents the observations that suggest that the factors known to contribute to the pathophysiology of IBS may exert their effects through affecting the intestinal stem cells.

Citation: El-Salhy M. Possible role of intestinal stem cells in the pathophysiology of irritable bowel syndrome. *World J Gastroenterol* 2020; 26(13): 1427-1438
URL: https://www.wjgnet.com/1007-9327/full/v26/i13/1427.htm
DOI: https://dx.doi.org/10.3748/wjg.v26.i13.1427

INTRODUCTION

Irritable bowel syndrome (IBS) is a wide spread condition affecting 12.1% of the world population[1,2]. The prevalence of IBS differs considerably between different parts of the world with the lowest prevalence in Asia and the highest in South America[1]. The cardinal symptom of IBS is intermittent abdominal pain accompanied by altered bowel habits and abdominal bloating/distention[3]. There is no biochemical, radiological or clinical test/examination for diagnosing IBS and the IBS diagnosis is based on symptoms assessment[4]. IBS reduces significantly the patients' quality of life in the same degree as major chronic diseases such heart failure, renal failure, diabetes, and inflammatory bowel disease[2,3]. It has been reported that 12%-14% of primary care patient visit, and 28% of referrals to gastroenterologists are IBS patients[5-7] and consequently IBS patients are more common in the healthcare than patients with diabetes, hypertension or asthma[8,9]. There is no effective treatment for IBS and the available treatment in clinic is directed to symptom relief[4].

Several factors are known to play pivot role in pathophysiology of IBS. These factors are genetics, diet, gut microbiota, gut endocrine cells, stress and low-grade inflammation[2,10]. Abnormalities in the intestinal stem cells has been reported recently[11-13]. The present review aimed at discussing the possibility that the factors known to contribute to the pathophysiology of IBS may exert their effects through affecting the intestinal stem cells. The present review conducted a literature search in MEDLINE (PubMed) covering the last ten years until November 2019, where articles in English were included. Articles about the intestinal stem cells and their possible role in the pathophysiology of IBS are discussed.

FCACORS INVOLVED IN THE PATHOPHYSIOLOGY OF IBS

Genetics

Studies of family history and family cluster as well as twin studies provided strong evidences that IBS is hereditary[14-21]. However, the possible mutant gene(s) responsible for IBS is/are not found yet[2].

Diet

Patients with IBS avoid certain food items as they believe they worsen/trigger their symptoms[22-26]. However, there is no difference in intake of calories, or the meal patterns between IBS patients and community controls[23,27,28].

The effect of diet on IBS symptoms cannot be explained by food allergy/intolerance[29]. However, it is generally accepted that poorly absorbed carbohydrates and fibers play an important role in development IBS symptoms[29,30]. The intake of low fermentable oligo-, di-, monosaccharides and polyols-diet and National Institute for Health and Care Excellence-modified diet improve both symptoms and quality of life in IBS patients[22,29,31,32]. However, a recent review and meta-analysis showed that there is very low quality evidence showing that low fermentable oligo-, di-,

monosaccharides and polyols diet reliefs IBS symptoms[33].

Based on a case report published in 1978, non-celiac gluten sensitivity was coined[34-36]. In this case, a patient without celiac disease, suffered from abdominal pain and diarrhea who experienced symptoms improved when she used gluten-free diet. Several studies showed that withdrawal of wheat products in patients with non-celiac IBS-like symptoms improve these symptoms[37-42]. However, a double-blind placebo-controlled study showed that it is fructan in the wheat rather than gluten that trigger IBS symptoms[43]. In a recently published meta-analysis concluded that there is insufficient evidence that gluten-free diet improves IBS symptoms[33].

Gut microbiota

The gastrointestinal microbiota comprises 12 different bacteria phyla, but most of the gut bacteria belongs to the Proteobacteria, Firmicutes, Actinobacteria and Bacteroidetes[44,45]. The anaerobic Firmicutes and Bacteroidetes phyla dominate the bacterial population in the intestinal of healthy adults, with a few members from of the Proteobacteria and Actinobacteria phyla[45,46]. A low microbial diversity in the gut (dysbiosis) has been reported to be associated with several diseases[47,48].

In healthy subjects, the intestinal microbiota composition is affected by the individual genetic composition and environmental factors one is exposed for[44,48]. The intestinal microbiota in IBS patients differs from that of healthy subjects[48-51], and have a lower diversity (dysbiosis)[48-51]. It is believed that this difference in the intestinal microbiota plays a pivot role in the pathophysiology of IBS[49].

Gastrointestinal endocrine cells

The gastrointestinal endocrine cells are scattered in-between the epithelial cells facing the gut lumen (Figure 1)[52-54].These cells are localized to the stomach, small-and large intestine[53]. Among the different segments of the gastrointestinal tract the density of the endocrine cells is highest in the duodenum (Figure 2)[25]. These cells secret over 10 different hormones that interact and integrate with the enteric, autonomic and central nervous system to regulate: Gastrointestinal motility, secretion of enzymes and bile acid, absorption of nutrients, visceral sensation, gastrointestinal cell proliferation, local immune defense and appetite[3,22,52,55-69]. These cells have sensory microvilli that project into the gastrointestinal lumen that sense gastrointestinal lumen contents and respond by releasing their hormones into the lamina propria[70-82]. These hormones can act locally on the nearby structures (paracrine mode of action) or reach the blood stream and act on far structure (endocrine mode of action)[70-82].

Several abnormalities in different endocrine cell types of the stomach, small- and large intestine have been described in IBS patients (Figure 3)[53,83-97]. Generally, IBS patients have a lower gut endocrine cell density than healthy subjects[52].

Stress

Stress is defined as an acute threat, real or perceived, to the homeostasis of an organism[10]. Stress is a known factor that trigger/worsen the IBS symptoms[98]. The exact mechanisms by which stress affects IBS are not exactly known. However, the negative effect of stress on IBS symptoms is believed to be caused by an interaction between the gut and the central nervous system (gut-brain axis)[10].

Low grade inflammation

Intestinal low-grade inflammation is believed to be a factor that contribute to the pathophysiology of IBS[86]. Lowgrade inflammation in the intestinal mucosa occurs only in a subset of IBS, *i.e.*, post-infectious IBS, but not in sporadic (non-specific) IBS[86,99-102].

THE ROLE OF INTESTINAL STEM CELLS IN THE PATHOPHYSIOLOGY OF IBS

Intestinal stem cells

Each intestinal crypt contains four to six pluripotent (stem) cells[103]. Stem cell perform 2 activities, namely self-renewal by dividing into identical stem cell (clonogeny) to maintain a constant number of stem cells and differentiation progeny[103]. In the differentiation progeny, the stem cells differentiate into all cell types of the villus epithelium through 2 cell lineages: The secretory lineage giving raise to goblet cells, endocrine cells and Paneth cells, and the absorptive lineage giving raise to absorptive enterocytes. This differentiation takes place through a series of precursors (progenitors) (Figure 4)[68,69,104-112].

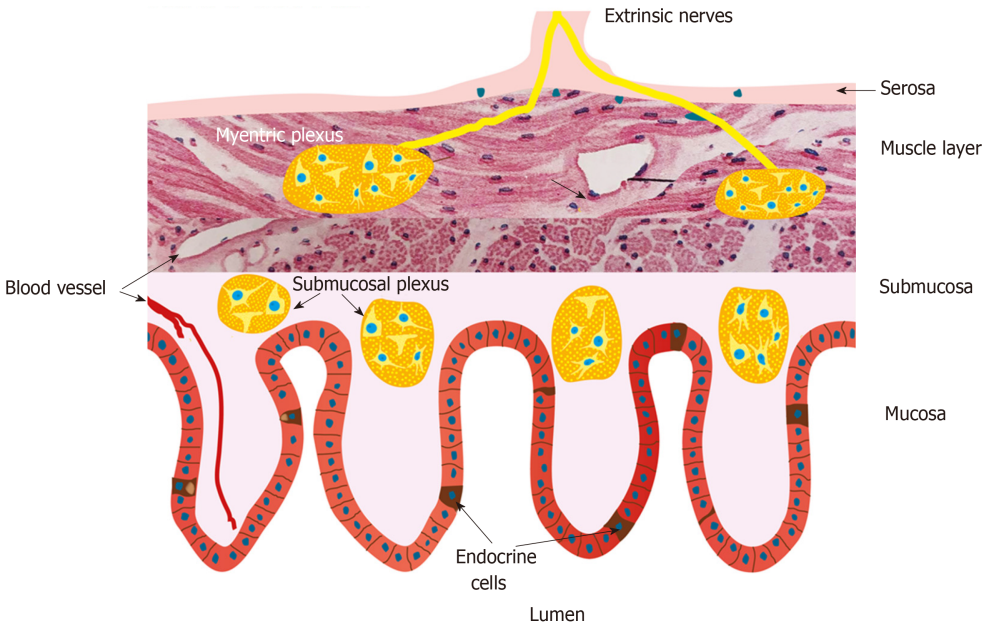

Figure 1 Schematic illustration of the enteroendocrine cells and their anatomic relation to the enteric nervous system. The enteroendocrine cells are scattered among the epithelial cells lining the intestinal lumen. They interact and intergrade with each other's and with enteric nervous system. Reproduced from El-Salhy *et al*[54] by permission of the authors and the publisher.

The relation between the abnormalities in intestinal stem cells and enteroendocrine cells

As mentioned previously, the densities of the gastrointestinal endocrine cells are lower than that of healthy subjects[53,83-97]. The cell density of Musashi 1, and neurogenin 3 immunoreactive cells in the small and large intestine of patients with IBS are lower than that of healthy subjects (Figures 5 and 6)[11-13]. Musashi 1 is marker for intestinal stem cells and their early progeny, and neurogenin 3 is expressed in early intestinal endocrine cell progenitors originated from stem cells[103,113-118]. The low densities of enteroendocrine cells in patients with IBS could be explained by the abnormalities in intestinal stem cells[119]. Thus, low densities of Msi-1 and NEUROG3 small and large intestine in IBS patients indicate that the intestinal stem cells in these patients exhibit reduced clonogenic activity and low differentiation progeny toward endocrine cells[119,120].

HYPOTHESIS

Based on the data presented above, one may hypothesized that IBS patients may have a gene mutation controlling the number of the stem cells and/or NEUROG3 gene mutation. Furthermore, environmental factors such as diet, inflammation, stress and gut microbiota may affect the stem cells and their progeny (Figure 7). This hypothesis gets support from the following facts: (1) Low density of intestinal endocrine cells has been described in patients with congenital malabsorptive diarrhoea, which is an autosomal recessive disorder[121]. The low density of intestinal endocrine cells in this disorder is caused by loss-of-function mutations in NEUROG3 gene[121]. Similarly, low density of intestinal endocrine cells has been observed in small-intestine allograft rejection, and in NEUROG3-knockout mice[117,120]. The low density of intestinal endocrine cells in these conditions was associated with a reduction in number of intestinal neurogenin 3 cells[117,120]; (2) Changing from the common Norwegian diet to a National Institute for Health and Care Excellence-modified diet, which improved symptoms and quality of life in IBS patients is associated with changes in the densities of gastrointestinal cells[91,122-127]; (3) Modulation of the intestinal microbiota by fecal microbiota transplantation improved both symptoms and the quality of life in patients with IBS[128]. This improvement was accompanied by a change in in the densities of enteroendocrine cells[128]; (4) Glutamine is the main energy source for intestinal enterocytes and plays a major role in intestinal homeostasis and other physiological functions[129-133]. Stress, infection or inflammation cause a depletion of

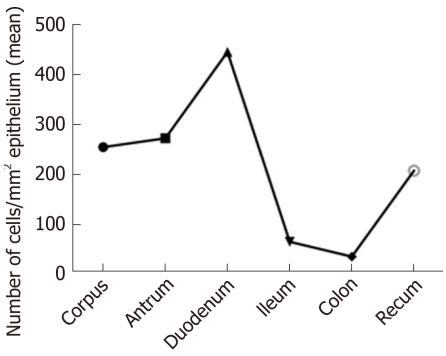

Figure 2 The density of gut endocrine cells as detected by chromogranin a immunoreactivity. Reproduced from El-Salhy *et al*[25] by permission of the authors and the publisher.

glutamine[129-133] In a randomized placebo-controlled study, dietary glutamine supplements improved symptoms in patients with post-infectious IBS[134]. Glutamine have a trophic effect on the intestinal stem cells and promotes stem cell differentiation[129,135,136]. One may speculate that stress results in the depletion of glutamine, which causes disturbance in the differentiation of the intestinal cells. This in turn would cause low density in enteroendocrine cells and the development of IBS symptoms; and (5) In animal models of human ulcerative colitis and Crohn's disease, the changes in enteroendocrine cells have been found to be strongly correlated with changes in the intestinal stem cells and their differentiation progeny toward intestinal endocrine cells[137,138].

CLINICAL IMPLICATIONS

Assuming that IBS is caused by abnormalities in stem cells, which in turn caused by genetic and environmental factors, intestinal stem cell transplantation might be an effective tool in the treatment of IBS.

CONCLUSION

The intestinal stem cells appear to play a central role in the pathophysiology of IBS. Factors that are known to be involved in the pathophysiology of IBS exert their effects probably through affecting the intestinal stem cells.

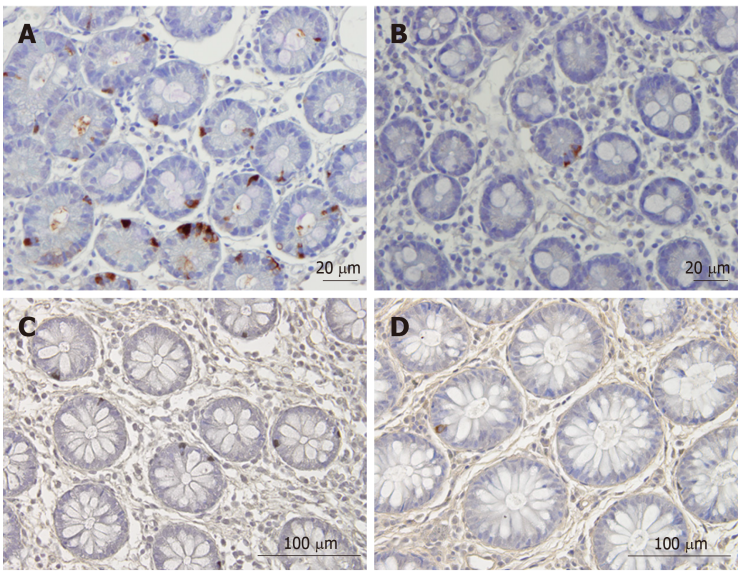

Figure 3 Chromogranin immunoreactive cells in the duodenum of a healthy subject and of a patient with irritable bowel syndrome. A: Chromogranin immunoreactive cells in the duodenum of a healthy subject; B: Chromogranin immunoreactive cells in the duodenum of a patient with irritable bowel syndrome (IBS); C: Chromogranin A cells in the colon of a healthy control; D: Chromogranin A cells in the colon of a patient with IBS. Chromogranin A is a common marker for enteroendocrine cells. The density of Chromogranin A in the duodenum and colon of patients with IBS is lower than that of healthy subjects.

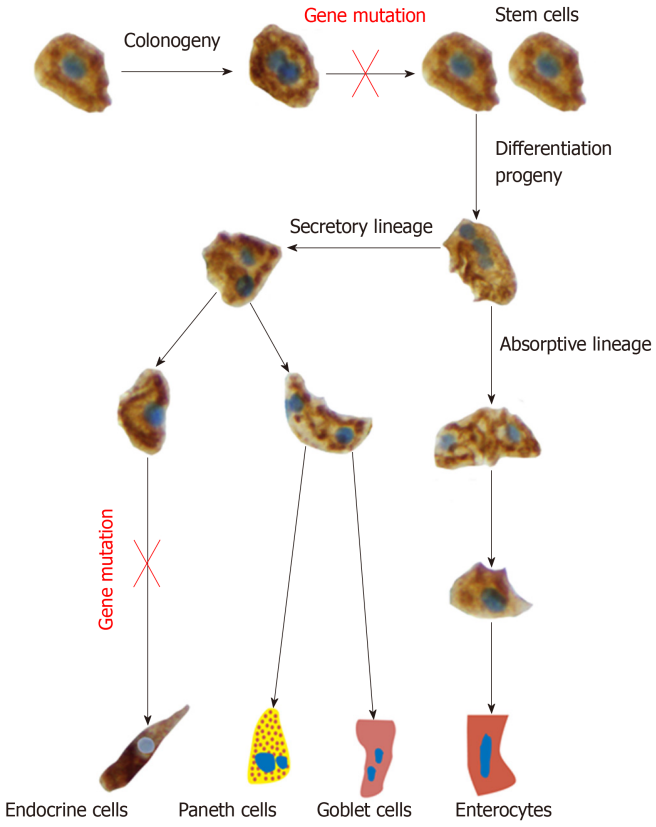

Figure 4 The intestinal stem cell divides into 2 identical cells (clonogeny). One of these cells remain inactive, while the other stem cell differentiates into all cell types of the villus epithelium through 2 cell lineages: The secretory lineage giving raise to goblet cells, endocrine cells and Paneth cells, and the absorptive lineage giving raise to absorptive enterocytes. This differentiation occurs through a series of progenitors. The observations that the density of stem cells and progenitors for enteroendocrine cells, led to the assumption of gene mutations affecting the stem cell and neurogenin 3 gene.

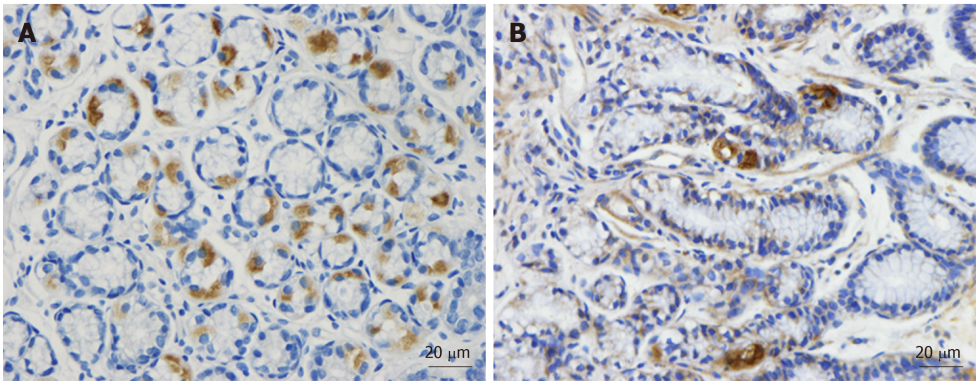

Figure 5 Musashi 1 immunoreactive cells in duodenum. A: A healthy subject; B: A patient with irritable bowel syndrome (IBS). Musashi 1 is a marker for intestinal stem cells and their early progeny. The density of Musashi 1 cells in healthy subjects is higher than that of the IBS patients. Furthermore, Musashi 1 cells in healthy subjects appear to have more proliferation activity than that of IBS patients.

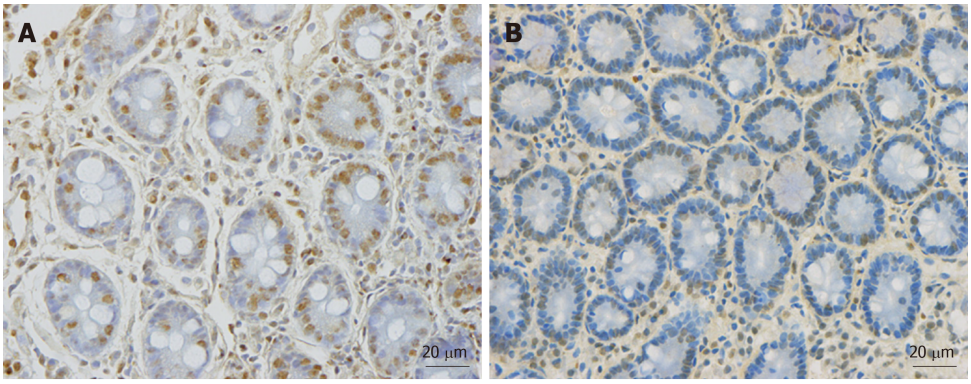

Figure 6 Neurogenin 3 immunoreactive cells in the duodenum. A: A healthy control; B: A patient with irritable bowel syndrome. Neurogenin 3 is expressed in the nuclei (brown) of early intestinal endocrine cell progenitors. The healthy subjects have higher density of neurogenin 3 than irritable bowel syndrome patients.

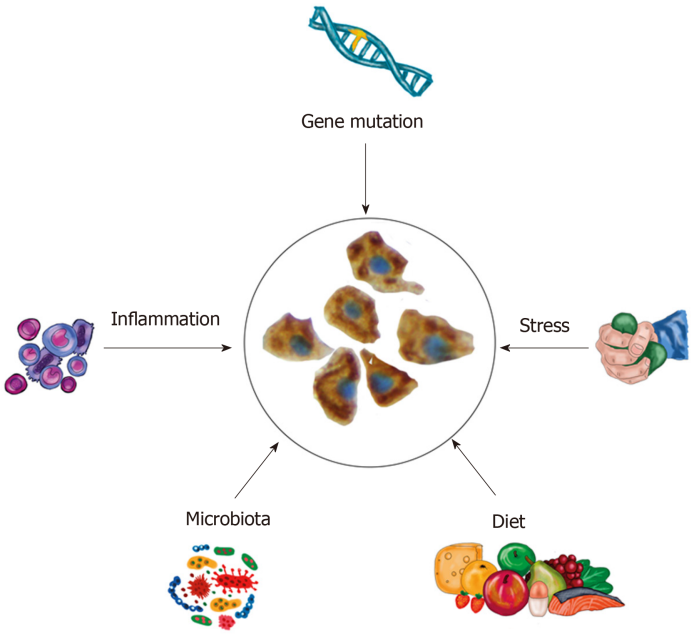

Figure 7 Schematic drawing to illustrate the hypothesis that intestinal stem cells play a central role in the pathophysiology of irritable bowel syndrome. The abnormalities in the intestinal stem cells can be caused by gene mutation or by environmental factors such as diet, intestinal microbiota, stress and low-grade inflammation.

REFERENCES

1 **Canavan C**, West J, Card T. The epidemiology of irritable bowel syndrome. *Clin Epidemiol* 2014; **6**: 71-80 [PMID: 24523597 DOI: 10.2147/CLEP.S40245]
2 **El-Salhy M**. Recent developments in the pathophysiology of irritable bowel syndrome. *World J Gastroenterol* 2015; **21**: 7621-7636 [PMID: 26167065 DOI: 10.3748/wjg.v21.i25.7621]
3 **El-Salhy M**. Irritable bowel syndrome: diagnosis and pathogenesis. *World J Gastroenterol* 2012; **18**: 5151-5163 [PMID: 23066308 DOI: 10.3748/wjg.v18.i37.5151]
4 **El-Salhy M**, Gilja OH, Hatlebakk JG. Overlapping of irritable bowel syndrome with erosive esophagitis and the performance of Rome criteria in diagnosing IBS in a clinical setting. *Mol Med Rep* 2019; **20**: 787-794 [PMID: 31180516 DOI: 10.3892/mmr.2019.10284]
5 **Talley NJ**, Gabriel SE, Harmsen WS, Zinsmeister AR, Evans RW. Medical costs in community subjects with irritable bowel syndrome. *Gastroenterology* 1995; **109**: 1736-1741 [PMID: 7498636 DOI: 10.1016/0016-5085(95)90738-6]
6 **Jones R**, Lydeard S. Irritable bowel syndrome in the general population. *BMJ* 1992; **304**: 87-90 [PMID: 1737146 DOI: 10.1136/bmj.304.6819.87]
7 **Hungin AP**, Whorwell PJ, Tack J, Mearin F. The prevalence, patterns and impact of irritable bowel syndrome: an international survey of 40,000 subjects. *Aliment Pharmacol Ther* 2003; **17**: 643-650 [PMID: 12641512 DOI: 10.1046/j.1365-2036.2003.01456.x]
8 **Schuster MM**. Defining and diagnosing irritable bowel syndrome. *Am J Manag Care* 2001; **7**: S246-S251 [PMID: 11474909]
9 **Mitchell CM**, Drossman DA. Survey of the AGA membership relating to patients with functional gastrointestinal disorders. *Gastroenterology* 1987; **92**: 1282-1284 [PMID: 3557021 DOI: 10.1016/s0016-5085(87)91099-7]
10 **Konturek PC**, Brzozowski T, Konturek SJ. Stress and the gut: pathophysiology, clinical consequences, diagnostic approach and treatment options. *J Physiol Pharmacol* 2011; **62**: 591-599 [PMID: 22314561]
11 **El-Salhy M**, Gilja OH. Abnormalities in ileal stem, neurogenin 3, and enteroendocrine cells in patients with irritable bowel syndrome. *BMC Gastroenterol* 2017; **17**: 90 [PMID: 28764761 DOI: 10.1186/s12876-017-0643-4]
12 **El-Salhy M**, Hatlebakk JG, Hausken T. Reduction in duodenal endocrine cells in irritable bowel syndrome is associated with stem cell abnormalities. *World J Gastroenterol* 2015; **21**: 9577-9587 [PMID: 26327765 DOI: 10.3748/wjg.v21.i32.9577]
13 **El-Salhy M**, Patcharatrakul T, Hatlebakk JG, Hausken T, Gilja OH, Gonlachanvit S. Enteroendocrine, Musashi 1 and neurogenin 3 cells in the large intestine of Thai and Norwegian patients with irritable bowel syndrome. *Scand J Gastroenterol* 2017; **52**: 1331-1339 [PMID: 28853300 DOI: 10.1080/00365521.2017.1371793]
14 **Locke GR**, Zinsmeister AR, Talley NJ, Fett SL, Melton LJ. Familial association in adults with functional gastrointestinal disorders. *Mayo Clin Proc* 2000; **75**: 907-912 [PMID: 10994826 DOI: 10.4065/75.9.907]
15 **Kalantar JS**, Locke GR, Zinsmeister AR, Beighley CM, Talley NJ. Familial aggregation of irritable bowel syndrome: a prospective study. *Gut* 2003; **52**: 1703-1707 [PMID: 14633946 DOI: 10.1136/gut.52.12.1703]
16 **Kanazawa M**, Endo Y, Whitehead WE, Kano M, Hongo M, Fukudo S. Patients and nonconsulters with irritable bowel syndrome reporting a parental history of bowel problems have more impaired psychological distress. *Dig Dis Sci* 2004; **49**: 1046-1053 [PMID: 15309899 DOI: 10.1023/b:ddas.0000034570.52305.10]
17 **Morris-Yates A**, Talley NJ, Boyce PM, Nandurkar S, Andrews G. Evidence of a genetic contribution to functional bowel disorder. *Am J Gastroenterol* 1998; **93**: 1311-1317 [PMID: 9707057 DOI: 10.1111/j.1572-0241.1998.440_j.x]
18 **Levy RL**, Jones KR, Whitehead WE, Feld SI, Talley NJ, Corey LA. Irritable bowel syndrome in twins: heredity and social learning both contribute to etiology. *Gastroenterology* 2001; **121**: 799-804 [PMID: 11606493 DOI: 10.1053/gast.2001.27995]
19 **Lembo A**, Zaman M, Jones M, Talley NJ. Influence of genetics on irritable bowel syndrome, gastro-oesophageal reflux and dyspepsia: a twin study. *Aliment Pharmacol Ther* 2007; **25**: 1343-1350 [PMID: 17509102 DOI: 10.1111/j.1365-2036.2007.03326.x]
20 **Wojczynski MK**, North KE, Pedersen NL, Sullivan PF. Irritable bowel syndrome: a co-twin control analysis. *Am J Gastroenterol* 2007; **102**: 2220-2229 [PMID: 17897337 DOI: 10.1111/j.1572-0241.2007.01479.x]
21 **Bengtson MB**, Rønning T, Vatn MH, Harris JR. Irritable bowel syndrome in twins: genes and environment. *Gut* 2006; **55**: 1754-1759 [PMID: 17008364 DOI: 10.1136/gut.2006.097287]
22 **El-Salhy M**, Ostgaard H, Gundersen D, Hatlebakk JG, Hausken T. The role of diet in the pathogenesis and management of irritable bowel syndrome (Review). *Int J Mol Med* 2012; **29**: 723-731 [PMID: 22366773 DOI: 10.3892/ijmm.2012.926]
23 **Ostgaard H**, Hausken T, Gundersen D, El-Salhy M. Diet and effects of diet management on quality of life and symptoms in patients with irritable bowel syndrome. *Mol Med Rep* 2012; **5**: 1382-1390 [PMID: 22446969 DOI: 10.3892/mmr.2012.843]
24 **El-Salhy M**, Gilja OH, Gundersen D, Hatlebakk JG, Hausken T. Interaction between ingested nutrients and gut endocrine cells in patients with irritable bowel syndrome (review). *Int J Mol Med* 2014; **34**: 363-371 [PMID: 24939595 DOI: 10.3892/ijmm.2014.1811]
25 **El-Salhy M**, Mazzawi T, Hausken T, Hatlebakk JG. Interaction between diet and gastrointestinal endocrine cells. *Biomed Rep* 2016; **4**: 651-656 [PMID: 27284402 DOI: 10.3892/br.2016.649]
26 **El-Salhy M**, Lilbo E, Reinemo A, Salmeøid L, Hausken T. Effects of a health program comprising reassurance, diet management, probiotic administration and regular exercise on symptoms and quality of life in patients with irritable bowel syndrome. *Gastroenterology Insights* 2010; 21-26 [DOI: 10.4081/gi.2010.e6]
27 **Jarrett M**, Heitkemper MM, Bond EF, Georges J. Comparison of diet composition in women with and without functional bowel disorder. *Gastroenterol Nurs* 1994; **16**: 253-258 [PMID: 8075160 DOI: 10.1097/00001610-199406000-00004]
28 **Saito YA**, Locke GR, Weaver AL, Zinsmeister AR, Talley NJ. Diet and functional gastrointestinal disorders: a population-based case-control study. *Am J Gastroenterol* 2005; **100**: 2743-2748 [PMID: 16393229 DOI: 10.1111/j.1572-0241.2005.00288.x]
29 **El-Salhy M**, Gundersen D. Diet in irritable bowel syndrome. *Nutr J* 2015; **14**: 36 [PMID: 25880820 DOI: 10.1186/s12937-015-0022-3]

30 **El-Salhy M**, Hatlebakk JG, Gilja OH, Hausken T. The relation between celiac disease, nonceliac gluten sensitivity and irritable bowel syndrome. *Nutr J* 2015; **14**: 92 [PMID: 26345589 DOI: 10.1186/s12937-015-0080-6]
31 **El-Salhy M**, Gundersen D, Hatlebakk JG, Hausken T, Watson RR. Diet and irritable bowel syndrome, with a focus on appetite-regulating hormones. In: Watson RR. Nutrition in the prevention and treatment of abdominal obesity. San Diego: Elsevier. Watson RR. 2014; 5-16
32 **El-Salhy M**. Diet in the pathophysiology and management of irritable bowel syndrome. *Cleve Clin J Med* 2016; **83**: 663-664 [PMID: 27618354 DOI: 10.3949/ccjm.83a.16019]
33 **Dionne J**, Ford AC, Yuan Y, Chey WD, Lacy BE, Saito YA, Quigley EMM, Moayyedi P. A Systematic Review and Meta-Analysis Evaluating the Efficacy of a Gluten-Free Diet and a Low FODMAPs Diet in Treating Symptoms of Irritable Bowel Syndrome. *Am J Gastroenterol* 2018; **113**: 1290-1300 [PMID: 30046155 DOI: 10.1038/s41395-018-0195-4]
34 **Ellis A**, Linaker BD. Non-coeliac gluten sensitivity? *Lancet* 1978; **1**: 1358-1359 [PMID: 78118 DOI: 10.1016/s0140-6736(78)92427-3]
35 **Boettcher E**, Crowe SE. Dietary proteins and functional gastrointestinal disorders. *Am J Gastroenterol* 2013; **108**: 728-736 [PMID: 23567359 DOI: 10.1038/ajg.2013.97]
36 **Sapone A**, Bai JC, Ciacci C, Dolinsek J, Green PH, Hadjivassiliou M, Kaukinen K, Rostami K, Sanders DS, Schumann M, Ullrich R, Villalta D, Volta U, Catassi C, Fasano A. Spectrum of gluten-related disorders: consensus on new nomenclature and classification. *BMC Med* 2012; **10**: 13 [PMID: 22313950 DOI: 10.1186/1741-7015-10-13]
37 **Campanella J**, Biagi F, Bianchi PI, Zanellati G, Marchese A, Corazza GR. Clinical response to gluten withdrawal is not an indicator of coeliac disease. *Scand J Gastroenterol* 2008; **43**: 1311-1314 [PMID: 18609173 DOI: 10.1080/00365520802200036]
38 **Vazquez-Roque MI**, Camilleri M, Smyrk T, Murray JA, Marietta E, O'Neill J, Carlson P, Lamsam J, Janzow D, Eckert D, Burton D, Zinsmeister AR. A controlled trial of gluten-free diet in patients with irritable bowel syndrome-diarrhea: effects on bowel frequency and intestinal function. *Gastroenterology* 2013; **144**: 903-911.e3 [PMID: 23357715 DOI: 10.1053/j.gastro.2013.01.049]
39 **Kaukinen K**, Turjanmaa K, Mäki M, Partanen J, Venäläinen R, Reunala T, Collin P. Intolerance to cereals is not specific for coeliac disease. *Scand J Gastroenterol* 2000; **35**: 942-946 [PMID: 11063153 DOI: 10.1080/003655200750022995]
40 **Carroccio A**, Mansueto P, Iacono G, Soresi M, D'Alcamo A, Cavataio F, Brusca I, Florena AM, Ambrosiano G, Seidita A, Pirrone G, Rini GB. Non-celiac wheat sensitivity diagnosed by double-blind placebo-controlled challenge: exploring a new clinical entity. *Am J Gastroenterol* 2012; **107**: 1898-1906 [PMID: 22825366 DOI: 10.1038/ajg.2012.236]
41 **Biesiekierski JR**, Newnham ED, Irving PM, Barrett JS, Haines M, Doecke JD, Shepherd SJ, Muir JG, Gibson PR. Gluten causes gastrointestinal symptoms in subjects without celiac disease: a double-blind randomized placebo-controlled trial. *Am J Gastroenterol* 2011; **106**: 508-514 [PMID: 21224837 DOI: 10.1038/ajg.2010.487]
42 **Shahbazkhani B**, Sadeghi A, Malekzadeh R, Khatavi F, Etemadi M, Kalantri E, Rostami-Nejad M, Rostami K. Non-Celiac Gluten Sensitivity Has Narrowed the Spectrum of Irritable Bowel Syndrome: A Double-Blind Randomized Placebo-Controlled Trial. *Nutrients* 2015; **7**: 4542-4554 [PMID: 26056920 DOI: 10.3390/nu7064542]
43 **Skodje GI**, Sarna VK, Minelle IH, Rolfsen KL, Muir JG, Gibson PR, Veierød MB, Henriksen C, Lundin KEA. Fructan, Rather Than Gluten, Induces Symptoms in Patients With Self-Reported Non-Celiac Gluten Sensitivity. *Gastroenterology* 2018; **154**: 529-539 [PMID: 29102613 DOI: 10.1053/j.gastro.2017.10.040]
44 **Thursby E**, Juge N. Introduction to the human gut microbiota. *Biochem J* 2017; **474**: 1823-1836 [PMID: 28512250 DOI: 10.1042/BCJ20160510]
45 **Hugon P**, Dufour JC, Colson P, Fournier PE, Sallah K, Raoult D. A comprehensive repertoire of prokaryotic species identified in human beings. *Lancet Infect Dis* 2015; **15**: 1211-1219 [PMID: 26311042 DOI: 10.1016/S1473-3099(15)00293-5]
46 **Ley RE**, Hamady M, Lozupone C, Turnbaugh PJ, Ramey RR, Bircher JS, Schlegel ML, Tucker TA, Schrenzel MD, Knight R, Gordon JI. Evolution of mammals and their gut microbes. *Science* 2008; **320**: 1647-1651 [PMID: 18497261 DOI: 10.1126/science.1155725]
47 **Kriss M**, Hazleton KZ, Nusbacher NM, Martin CG, Lozupone CA. Low diversity gut microbiota dysbiosis: drivers, functional implications and recovery. *Curr Opin Microbiol* 2018; **44**: 34-40 [PMID: 30036705 DOI: 10.1016/j.mib.2018.07.003]
48 **Wilson BC**, Vatanen T, Cutfield WS, O'Sullivan JM. The Super-Donor Phenomenon in Fecal Microbiota Transplantation. *Front Cell Infect Microbiol* 2019; **9**: 2 [PMID: 30719428 DOI: 10.3389/fcimb.2019.00002]
49 **El-Salhy M**, Mazzawi T. Fecal microbiota transplantation for managing irritable bowel syndrome. *Expert Rev Gastroenterol Hepatol* 2018; **12**: 439-445 [PMID: 29493330 DOI: 10.1080/17474124.2018.1447380]
50 **Casén C**, Vebø HC, Sekelja M, Hegge FT, Karlsson MK, Ciemniejewska E, Dzankovic S, Frøyland C, Nestestog R, Engstrand L, Munkholm P, Nielsen OH, Rogler G, Simrén M, Öhman L, Vatn MH, Rudi K. Deviations in human gut microbiota: a novel diagnostic test for determining dysbiosis in patients with IBS or IBD. *Aliment Pharmacol Ther* 2015; **42**: 71-83 [PMID: 25973666 DOI: 10.1111/apt.13236]
51 **Enck P**, Mazurak N. Dysbiosis in Functional Bowel Disorders. *Ann Nutr Metab* 2018; **72**: 296-306 [PMID: 29694952 DOI: 10.1159/000488773]
52 **El-Salhy M**, Seim I, Chopin L, Gundersen D, Hatlebakk JG, Hausken T. Irritable bowel syndrome: the role of gut neuroendocrine peptides. *Front Biosci (Elite Ed)* 2012; **4**: 2783-2800 [PMID: 22652678 DOI: 10.2741/e583]
53 **El-Salhy M**, Gundersen D, Hatlebakk JG, Hausken T. Irritable bowel syndrome: diagnosis, pathogenesis and treatment options. New York: Nova Science Publishers, 2012: 35-78
54 **El-Salhy M**, Hatlebakk JG, Hausken T. Diet in Irritable Bowel Syndrome (IBS): Interaction with Gut Microbiota and Gut Hormones. *Nutrients* 2019; **11**: pii: E1824 [PMID: 31394793 DOI: 10.3390/nu11081824]
55 **Mawe GM**, Coates MD, Moses PL. Review article: intestinal serotonin signalling in irritable bowel syndrome. *Aliment Pharmacol Ther* 2006; **23**: 1067-1076 [PMID: 16611266 DOI: 10.1111/j.1365-2036.2006.02858.x]
56 **Wade PR**, Chen J, Jaffe B, Kassem IS, Blakely RD, Gershon MD. Localization and function of a 5-HT transporter in crypt epithelia of the gastrointestinal tract. *J Neurosci* 1996; **16**: 2352-2364 [PMID: 8601815 DOI: 10.1523/JNEUROSCI.16-07-02352.1996]

57 **Gershon MD**, Tack J. The serotonin signaling system: from basic understanding to drug development for functional GI disorders. *Gastroenterology* 2007; **132**: 397-414 [PMID: 17241888 DOI: 10.1053/j.gastro.2006.11.002]
58 **Gershon MD**. 5-Hydroxytryptamine (serotonin) in the gastrointestinal tract. *Curr Opin Endocrinol Diabetes Obes* 2013; **20**: 14-21 [PMID: 23222853 DOI: 10.1097/MED.0b013e32835bc703]
59 **Gershon MD**. Serotonin is a sword and a shield of the bowel: serotonin plays offense and defense. *Trans Am Clin Climatol Assoc* 2012; **123**: 268-280 [PMID: 23303993]
60 **El-Salhy M**, Mazzawi T, Gundersen D, Hatlebakk JG, Hausken T. The role of peptide YY in gastrointestinal diseases and disorders (review). *Int J Mol Med* 2013; **31**: 275-282 [PMID: 23292145 DOI: 10.3892/ijmm.2012.1222]
61 **Dubrasquet M**, Bataille D, Gespach C. Oxyntomodulin (glucagon-37 or bioactive enteroglucagon): a potent inhibitor of pentagastrin-stimulated acid secretion in rats. *Biosci Rep* 1982; **2**: 391-395 [PMID: 6125221 DOI: 10.1007/bf01119301]
62 **Schjoldager BT**, Baldissera FG, Mortensen PE, Holst JJ, Christiansen J. Oxyntomodulin: a potential hormone from the distal gut. Pharmacokinetics and effects on gastric acid and insulin secretion in man. *Eur J Clin Invest* 1988; **18**: 499-503 [PMID: 3147901 DOI: 10.1111/j.1365-2362.1988.tb01046.x]
63 **Schjoldager B**, Mortensen PE, Myhre J, Christiansen J, Holst JJ. Oxyntomodulin from distal gut. Role in regulation of gastric and pancreatic functions. *Dig Dis Sci* 1989; **34**: 1411-1419 [PMID: 2670487 DOI: 10.1007/bf01538078]
64 **Dakin CL**, Small CJ, Batterham RL, Neary NM, Cohen MA, Patterson M, Ghatei MA, Bloom SR. Peripheral oxyntomodulin reduces food intake and body weight gain in rats. *Endocrinology* 2004; **145**: 2687-2695 [PMID: 15001546 DOI: 10.1210/en.2003-1338]
65 **Wynne K**, Park AJ, Small CJ, Patterson M, Ellis SM, Murphy KG, Wren AM, Frost GS, Meeran K, Ghatei MA, Bloom SR. Subcutaneous oxyntomodulin reduces body weight in overweight and obese subjects: a double-blind, randomized, controlled trial. *Diabetes* 2005; **54**: 2390-2395 [PMID: 16046306 DOI: 10.2337/diabetes.54.8.2390]
66 **Camilleri M**. Peripheral mechanisms in irritable bowel syndrome. *N Engl J Med* 2012; **367**: 1626-1635 [PMID: 23094724 DOI: 10.1056/NEJMra1207068]
67 **Jianu MCS**, Fossmark R, Syversen U, Hauso Ø, Waldum HL. A meal test improves the specificity of chromogranin A as a marker of neuroendocrine neoplasia. *Tumour Biol* 2010; **31**: 373-380 [PMID: 20480408 DOI: 10.1007/s13277-010-0045-5]
68 **Gunawardene AR**, Corfe BM, Staton CA. Classification and functions of enteroendocrine cells of the lower gastrointestinal tract. *Int J Exp Pathol* 2011; **92**: 219-231 [PMID: 21518048 DOI: 10.1111/j.1365-2613.2011.00767.x]
69 **May CL**, Kaestner KH. Gut endocrine cell development. *Mol Cell Endocrinol* 2010; **323**: 70-75 [PMID: 20025933 DOI: 10.1016/j.mce.2009.12.009]
70 **Sandström O**, El-Salhy M. Ageing and endocrine cells of human duodenum. *Mech Ageing Dev* 1999; **108**: 39-48 [PMID: 10366038 DOI: 10.1016/s0047-6374(98)00154-7]
71 **El-Salhy M**. Ghrelin in gastrointestinal diseases and disorders: a possible role in the pathophysiology and clinical implications (review). *Int J Mol Med* 2009; **24**: 727-732 [PMID: 19885611 DOI: 10.3892/ijmm_00000285]
72 **Tolhurst G**, Reimann F, Gribble FM. Intestinal sensing of nutrients. *Handb Exp Pharmacol* 2012; 309-335 [PMID: 22249821 DOI: 10.1007/978-3-642-24716-3_14]
73 **Lee J**, Cummings BP, Martin E, Sharp JW, Graham JL, Stanhope KL, Havel PJ, Raybould HE. Glucose sensing by gut endocrine cells and activation of the vagal afferent pathway is impaired in a rodent model of type 2 diabetes mellitus. *Am J Physiol Regul Integr Comp Physiol* 2012; **302**: R657-R666 [PMID: 22160540 DOI: 10.1152/ajpregu.00345.2011]
74 **Parker HE**, Reimann F, Gribble FM. Molecular mechanisms underlying nutrient-stimulated incretin secretion. *Expert Rev Mol Med* 2010; **12**: e1 [PMID: 20047700 DOI: 10.1017/S146239940900132X]
75 **Raybould HE**. Nutrient sensing in the gastrointestinal tract: possible role for nutrient transporters. *J Physiol Biochem* 2008; **64**: 349-356 [PMID: 19391461 DOI: 10.1007/bf03174091]
76 **San Gabriel A**, Nakamura E, Uneyama H, Torii K. Taste, visceral information and exocrine reflexes with glutamate through umami receptors. *J Med Invest* 2009; **56** Suppl: 209-217 [PMID: 20224183 DOI: 10.2152/jmi.56.209]
77 **Rudholm T**, Wallin B, Theodorsson E, Näslund E, Hellström PM. Release of regulatory gut peptides somatostatin, neurotensin and vasoactive intestinal peptide by acid and hyperosmolal solutions in the intestine in conscious rats. *Regul Pept* 2009; **152**: 8-12 [PMID: 18992283 DOI: 10.1016/j.regpep.2008.10.002]
78 **Sternini C**, Anselmi L, Rozengurt E. Enteroendocrine cells: a site of 'taste' in gastrointestinal chemosensing. *Curr Opin Endocrinol Diabetes Obes* 2008; **15**: 73-78 [PMID: 18185066 DOI: 10.1097/MED.0b013e3282f43a73]
79 **Sternini C**. Taste receptors in the gastrointestinal tract. IV. Functional implications of bitter taste receptors in gastrointestinal chemosensing. *Am J Physiol Gastrointest Liver Physiol* 2007; **292**: G457-G461 [PMID: 17095755 DOI: 10.1152/ajpgi.00411.2006]
80 **Buchan AM**. Nutrient Tasting and Signaling Mechanisms in the Gut III. Endocrine cell recognition of luminal nutrients. *Am J Physiol* 1999; **277**: G1103-G1107 [PMID: 10600808 DOI: 10.1152/ajpgi.1999.277.6.G1103]
81 **Montero-Hadjadje M**, Elias S, Chevalier L, Benard M, Tanguy Y, Turquier V, Galas L, Yon L, Malagon MM, Driouich A, Gasman S, Anouar Y. Chromogranin A promotes peptide hormone sorting to mobile granules in constitutively and regulated secreting cells: role of conserved N- and C-terminal peptides. *J Biol Chem* 2009; **284**: 12420-12431 [PMID: 19179339 DOI: 10.1074/jbc.M805607200]
82 **Shooshtarizadeh P**, Zhang D, Chich JF, Gasnier C, Schneider F, Haïkel Y, Aunis D, Metz-Boutigue MH. The antimicrobial peptides derived from chromogranin/secretogranin family, new actors of innate immunity. *Regul Pept* 2010; **165**: 102-110 [PMID: 19932135 DOI: 10.1016/j.regpep.2009.11.014]
83 **Wendelbo I**, Mazzawi T, El-Salhy M. Increased serotonin transporter immunoreactivity intensity in the ileum of patients with irritable bowel disease. *Mol Med Rep* 2014; **9**: 180-184 [PMID: 24213511 DOI: 10.3892/mmr.2013.1784]
84 **El-Salhy M**, Wendelbo IH, Gundersen D. Reduced chromogranin A cell density in the ileum of patients with irritable bowel syndrome. *Mol Med Rep* 2013; **7**: 1241-1244 [PMID: 23426642 DOI: 10.3892/mmr.2013.1325]
85 **El-Salhy M**, Vaali K, Dizdar V, Hausken T. Abnormal small-intestinal endocrine cells in patients with

irritable bowel syndrome. *Dig Dis Sci* 2010; **55**: 3508-3513 [PMID: 20300845 DOI: 10.1007/s10620-010-1169-6]
86 **El-Salhy M**, Mazzawi T, Gundersen D, Hausken T. Chromogranin A cell density in the rectum of patients with irritable bowel syndrome. *Mol Med Rep* 2012; **6**: 1223-1225 [PMID: 22992886 DOI: 10.3892/mmr.2012.1087]
87 **El-Salhy M**, Lomholt-Beck B, Hausken T. Chromogranin A as a possible tool in the diagnosis of irritable bowel syndrome. *Scand J Gastroenterol* 2010; **45**: 1435-1439 [PMID: 20602602 DOI: 10.3109/00365521.2010.503965]
88 **El-Salhy M**, Lillebø E, Reinemo A, Salmelid L. Ghrelin in patients with irritable bowel syndrome. *Int J Mol Med* 2009; **23**: 703-707 [PMID: 19424595 DOI: 10.3892/ijmm_00000183]
89 **El-Salhy M**, Gilja OH, Gundersen D, Hausken T. Endocrine cells in the oxyntic mucosa of the stomach in patients with irritable bowel syndrome. *World J Gastrointest Endosc* 2014; **6**: 176-185 [PMID: 24891930 DOI: 10.4253/wjge.v6.i5.176]
90 **El-Salhy M**, Gundersen D, Hatlebakk JG, Hausken T. Chromogranin A cell density as a diagnostic marker for lymphocytic colitis. *Dig Dis Sci* 2012; **57**: 3154-3159 [PMID: 22699394 DOI: 10.1007/s10620-012-2249-6]
91 **Mazzawi T**, Hausken T, Gundersen D, El-Salhy M. Effects of dietary guidance on the symptoms, quality of life and habitual dietary intake of patients with irritable bowel syndrome. *Mol Med Rep* 2013; **8**: 845-852 [PMID: 23820783 DOI: 10.3892/mmr.2013.1565]
92 **El-Salhy M**, Gilja OH, Hatlebakk JG, Hausken T. Stomach antral endocrine cells in patients with irritable bowel syndrome. *Int J Mol Med* 2014; **34**: 967-974 [PMID: 25110039 DOI: 10.3892/ijmm.2014.1887]
93 **Sjölund K**, Ekman R, Wierup N. Covariation of plasma ghrelin and motilin in irritable bowel syndrome. *Peptides* 2010; **31**: 1109-1112 [PMID: 20338210 DOI: 10.1016/j.peptides.2010.03.021]
94 **Wang SH**, Dong L, Luo JY, Gong J, Li L, Lu XL, Han SP. Decreased expression of serotonin in the jejunum and increased numbers of mast cells in the terminal ileum in patients with irritable bowel syndrome. *World J Gastroenterol* 2007; **13**: 6041-6047 [PMID: 18023097 DOI: 10.3748/wjg.v13.45.6041]
95 **Park JH**, Rhee PL, Kim G, Lee JH, Kim YH, Kim JJ, Rhee JC, Song SY. Enteroendocrine cell counts correlate with visceral hypersensitivity in patients with diarrhoea-predominant irritable bowel syndrome. *Neurogastroenterol Motil* 2006; **18**: 539-546 [PMID: 16771769 DOI: 10.1111/j.1365-2982.2006.00771.x]
96 **Coates MD**, Mahoney CR, Linden DR, Sampson JE, Chen J, Blaszyk H, Crowell MD, Sharkey KA, Gershon MD, Mawe GM, Moses PL. Molecular defects in mucosal serotonin content and decreased serotonin reuptake transporter in ulcerative colitis and irritable bowel syndrome. *Gastroenterology* 2004; **126**: 1657-1664 [PMID: 15188158 DOI: 10.1053/j.gastro.2004.03.013]
97 **El-Salhy M**, Wendelbo I, Gundersen D. Serotonin and serotonin transporter in the rectum of patients with irritable bowel disease. *Mol Med Rep* 2013; **8**: 451-455 [PMID: 23778763 DOI: 10.3892/mmr.2013.1525]
98 **Soares RL**. Irritable bowel syndrome: a clinical review. *World J Gastroenterol* 2014; **20**: 12144-12160 [PMID: 25232249 DOI: 10.3748/wjg.v20.i34.12144]
99 **Weston AP**, Biddle WL, Bhatia PS, Miner PB. Terminal ileal mucosal mast cells in irritable bowel syndrome. *Dig Dis Sci* 1993; **38**: 1590-1595 [PMID: 8359068 DOI: 10.1007/BF01303164]
100 **O'Sullivan M**, Clayton N, Breslin NP, Harman I, Bountra C, McLaren A, O'Morain CA. Increased mast cells in the irritable bowel syndrome. *Neurogastroenterol Motil* 2000; **12**: 449-457 [PMID: 11012945 DOI: 10.1046/j.1365-2982.2000.00221.x]
101 **Barbara G**, De Giorgio R, Stanghellini V, Cremon C, Corinaldesi R. A role for inflammation in irritable bowel syndrome? *Gut* 2002; **51** Suppl 1: i41-i44 [PMID: 12077063 DOI: 10.1136/gut.51.suppl_1.i41]
102 **Barbara G**, Stanghellini V, De Giorgio R, Cremon C, Cottrell GS, Santini D, Pasquinelli G, Morselli-Labate AM, Grady EF, Bunnett NW, Collins SM, Corinaldesi R. Activated mast cells in proximity to colonic nerves correlate with abdominal pain in irritable bowel syndrome. *Gastroenterology* 2004; **126**: 693-702 [PMID: 14988823 DOI: 10.1053/j.gastro.2003.11.055]
103 **Montgomery RK**, Breault DT. Small intestinal stem cell markers. *J Anat* 2008; **213**: 52-58 [PMID: 18638070 DOI: 10.1111/j.1469-7580.2008.00925.x]
104 **Barker N**, Clevers H. Tracking down the stem cells of the intestine: strategies to identify adult stem cells. *Gastroenterology* 2007; **133**: 1755-1760 [PMID: 18054544 DOI: 10.1053/j.gastro.2007.10.029]
105 **Barker N**, van de Wetering M, Clevers H. The intestinal stem cell. *Genes Dev* 2008; **22**: 1856-1864 [PMID: 18628392 DOI: 10.1101/gad.1674008]
106 **Barker N**, van Es JH, Kuipers J, Kujala P, van den Born M, Cozijnsen M, Haegebarth A, Korving J, Begthel H, Peters PJ, Clevers H. Identification of stem cells in small intestine and colon by marker gene Lgr5. *Nature* 2007; **449**: 1003-1007 [PMID: 17934449 DOI: 10.1038/nature06196]
107 **Korinek V**, Barker N, Moerer P, van Donselaar E, Huls G, Peters PJ, Clevers H. Depletion of epithelial stem-cell compartments in the small intestine of mice lacking Tcf-4. *Nat Genet* 1998; **19**: 379-383 [PMID: 9697701 DOI: 10.1038/1270]
108 **Cheng H**, Leblond CP. Origin, differentiation and renewal of the four main epithelial cell types in the mouse small intestine. V. Unitarian Theory of the origin of the four epithelial cell types. *Am J Anat* 1974; **141**: 537-561 [PMID: 4440635 DOI: 10.1002/aja.1001410407]
109 **Le Douarin NM**, Teillet MA. The migration of neural crest cells to the wall of the digestive tract in avian embryo. *J Embryol Exp Morphol* 1973; **30**: 31-48 [PMID: 4729950]
110 **Rawdon BB**, Andrew A. Origin and differentiation of gut endocrine cells. *Histol Histopathol* 1993; **8**: 567-580 [PMID: 8358166]
111 **Hoffman J**, Kuhnert F, Davis CR, Kuo CJ. Wnts as essential growth factors for the adult small intestine and colon. *Cell Cycle* 2004; **3**: 554-557 [PMID: 15044853 DOI: 10.4161/cc.3.5.858]
112 **Lee CS**, Kaestner KH. Clinical endocrinology and metabolism. Development of gut endocrine cells. *Best Pract Res Clin Endocrinol Metab* 2004; **18**: 453-462 [PMID: 15533769 DOI: 10.1016/j.beem.2004.08.008]
113 **Potten CS**, Booth C, Tudor GL, Booth D, Brady G, Hurley P, Ashton G, Clarke R, Sakakibara S, Okano H. Identification of a putative intestinal stem cell and early lineage marker; musashi-1. *Differentiation* 2003; **71**: 28-41 [PMID: 12558601 DOI: 10.1046/j.1432-0436.2003.700603.x]
114 **Kayahara T**, Sawada M, Takaishi S, Fukui H, Seno H, Fukuzawa H, Suzuki K, Hiai H, Kageyama R, Okano H, Chiba T. Candidate markers for stem and early progenitor cells, Musashi-1 and Hes1, are expressed in crypt base columnar cells of mouse small intestine. *FEBS Lett* 2003; **535**: 131-135 [PMID: 12560091 DOI: 10.1016/S0014-5793(02)03896-6]
115 **He XC**, Yin T, Grindley JC, Tian Q, Sato T, Tao WA, Dirisina R, Porter-Westpfahl KS, Hembree M, Johnson T, Wiedemann LM, Barrett TA, Hood L, Wu H, Li L. PTEN-deficient intestinal stem cells initiate

intestinal polyposis. *Nat Genet* 2007; **39**: 189-198 [PMID: 17237784 DOI: 10.1038/ng1928]
116 **Fishbein TM**, Novitskiy G, Lough DM, Matsumoto C, Kaufman SS, Shetty K, Zasloff M. Rejection reversibly alters enteroendocrine cell renewal in the transplanted small intestine. *Am J Transplant* 2009; **9**: 1620-1628 [PMID: 19519821 DOI: 10.1111/j.1600-6143.2009.02681.x]
117 **Schonhoff SE**, Giel-Moloney M, Leiter AB. Minireview: Development and differentiation of gut endocrine cells. *Endocrinology* 2004; **145**: 2639-2644 [PMID: 15044355 DOI: 10.1210/en.2004-0051]
118 **Schonhoff SE**, Giel-Moloney M, Leiter AB. Neurogenin 3-expressing progenitor cells in the gastrointestinal tract differentiate into both endocrine and non-endocrine cell types. *Dev Biol* 2004; **270**: 443-454 [PMID: 15183725 DOI: 10.1016/j.ydbio.2004.03.013]
119 **El-Salhy M**, Hausken T, Gilja OH, Hatlebakk JG. The possible role of gastrointestinal endocrine cells in the pathophysiology of irritable bowel syndrome. *Expert Rev Gastroenterol Hepatol* 2017; **11**: 139-148 [PMID: 27927062 DOI: 10.1080/17474124.2017.1269601]
120 **Jenny M**, Uhl C, Roche C, Duluc I, Guillermin V, Guillemot F, Jensen J, Kedinger M, Gradwohl G. Neurogenin3 is differentially required for endocrine cell fate specification in the intestinal and gastric epithelium. *EMBO J* 2002; **21**: 6338-6347 [PMID: 12456641 DOI: 10.1093/emboj/cdf649]
121 **Wang J**, Cortina G, Wu SV, Tran R, Cho JH, Tsai MJ, Bailey TJ, Jamrich M, Ament ME, Treem WR, Hill ID, Vargas JH, Gershman G, Farmer DG, Reyen L, Martín MG. Mutant neurogenin-3 in congenital malabsorptive diarrhea. *N Engl J Med* 2006; **355**: 270-280 [PMID: 16855267 DOI: 10.1056/NEJMoa054288]
122 **Mazzawi T**, El-Salhy M. Changes in small intestinal chromogranin A-immunoreactive cell densities in patients with irritable bowel syndrome after receiving dietary guidance. *Int J Mol Med* 2016; **37**: 1247-1253 [PMID: 26987104 DOI: 10.3892/ijmm.2016.2523]
123 **Mazzawi T**, El-Salhy M. Dietary guidance and ileal enteroendocrine cells in patients with irritable bowel syndrome. *Exp Ther Med* 2016; **12**: 1398-1404 [PMID: 27588061 DOI: 10.3892/etm.2016.3491]
124 **Mazzawi T**, Gundersen D, Hausken T, El-Salhy M. Increased gastric chromogranin A cell density following changes to diets of patients with irritable bowel syndrome. *Mol Med Rep* 2014; **10**: 2322-2326 [PMID: 25174455 DOI: 10.3892/mmr.2014.2498]
125 **Mazzawi T**, Gundersen D, Hausken T, El-Salhy M. Increased chromogranin a cell density in the large intestine of patients with irritable bowel syndrome after receiving dietary guidance. *Gastroenterol Res Pract* 2015; 823897 [PMID: 25918524 DOI: 10.1155/2015/823897]
126 **Mazzawi T**, Hausken T, Gundersen D, El-Salhy M. Effect of dietary management on the gastric endocrine cells in patients with irritable bowel syndrome. *Eur J Clin Nutr* 2015; **69**: 519-524 [PMID: 25097003 DOI: 10.1038/ejcn.2014.151]
127 **Mazzawi T**, Hausken T, Gundersen D, El-Salhy M. Dietary guidance normalizes large intestinal endocrine cell densities in patients with irritable bowel syndrome. *Eur J Clin Nutr* 2016; **70**: 175-181 [PMID: 26603880 DOI: 10.1038/ejcn.2015.191]
128 **Mazzawi T**, Arslan G, El-Sahy M, Gilja OH, Hatlebakk JG, Hausken T. Effect of fecal microbiota transplantation on the symptoms and duodenal enteroendocrine cells in patients with irritable bowel syndrome. *United Eur Gastroe* 2016; **4**: 677-677 [DOI: 10.26226/morressier.57c53841d462b80296c9c83f]
129 **Chen S**, Xia Y, Zhu G, Yan J, Tan C, Deng B, Deng J, Yin Y, Ren W. Glutamine supplementation improves intestinal cell proliferation and stem cell differentiation in weanling mice. *Food Nutr Res* 2018; **62** [PMID: 30083086 DOI: 10.29219/fnr.v62.1439]
130 **Chen Y**, Tsai YH, Tseng BJ, Tseng SH. Influence of Growth Hormone and Glutamine on Intestinal Stem Cells: A Narrative Review. *Nutrients* 2019; **11** [PMID: 31426533 DOI: 10.3390/nu11081941]
131 **Chen Y**, Tseng SH, Yao CL, Li C, Tsai YH. Distinct Effects of Growth Hormone and Glutamine on Activation of Intestinal Stem Cells. *JPEN J Parenter Enteral Nutr* 2018; **42**: 642-651 [PMID: 28510488 DOI: 10.1177/0148607117709435]
132 **Kim MH**, Kim H. The Roles of Glutamine in the Intestine and Its Implication in Intestinal Diseases. *Int J Mol Sci* 2017; **18** [PMID: 28498331 DOI: 10.3390/ijms18051051]
133 **Wang B**, Wu G, Zhou Z, Dai Z, Sun Y, Ji Y, Li W, Wang W, Liu C, Han F, Wu Z. Glutamine and intestinal barrier function. *Amino Acids* 2015; **47**: 2143-2154 [PMID: 24965526 DOI: 10.1007/s00726-014-1773-4]
134 **Zhou Q**, Verne ML, Fields JZ, Lefante JJ, Basra S, Salameh H, Verne GN. Randomised placebo-controlled trial of dietary glutamine supplements for postinfectious irritable bowel syndrome. *Gut* 2019; **68**: 996-1002 [PMID: 30108163 DOI: 10.1136/gutjnl-2017-315136]
135 **Corcoba A**, Gruetter R, Do KQ, Duarte JMN. Social isolation stress and chronic glutathione deficiency have a common effect on the glutamine-to-glutamate ratio and myo-inositol concentration in the mouse frontal cortex. *J Neurochem* 2017; **142**: 767-775 [PMID: 28664650 DOI: 10.1111/jnc.14116]
136 **Harnett NG**, Wood KH, Ference EW, Reid MA, Lahti AC, Knight AJ, Knight DC. Glutamate/glutamine concentrations in the dorsal anterior cingulate vary with Post-Traumatic Stress Disorder symptoms. *J Psychiatr Res* 2017; **91**: 169-176 [PMID: 28478230 DOI: 10.1016/j.jpsychires.2017.04.010]
137 **El-Salhy M**, Umezawa K, Hatlebakk JG, Gilja OH. Abnormal differentiation of stem cells into enteroendocrine cells in rats with DSS-induced colitis. *Mol Med Rep* 2017; **15**: 2106-2112 [PMID: 28259987 DOI: 10.3892/mmr.2017.6266]
138 **El-Salhy M**, Mazzawi T, Umezawa K, Gilja OH. Enteroendocrine cells, stem cells and differentiation progenitors in rats with TNBS-induced colitis. *Int J Mol Med* 2016; **38**: 1743-1751 [PMID: 27779708 DOI: 10.3892/ijmm.2016.2787]

World Journal of Gastroenterology

Submit a Manuscript: https://www.f6publishing.com

World J Gastroenterol 2020 April 7; 26(13): 1439-1449

DOI: 10.3748/wjg.v26.i13.1439

ISSN 1007-9327 (print) ISSN 2219-2840 (online)

MINIREVIEWS

Review of the diagnosis of gastrointestinal lanthanum deposition

Masaya Iwamuro, Haruo Urata, Takehiro Tanaka, Hiroyuki Okada

ORCID number: Masaya Iwamuro (0000-0002-1757-5754); Haruo Urata (0000-0002-0268-6187); Takehiro Tanaka (0000-0002-1509-5706); Hiroyuki Okada (0000-0003-2814-7146).

Author contributions: Iwamuro M designed the research study and wrote the paper; Urata H and Tanaka T critically reviewed the manuscript for important intellectual content; Okada H approved the manuscript.

Conflict-of-interest statement: There is no conflict of interest associated with any of the senior author or other coauthors contributed their efforts in this manuscript.

Manuscript source: Invited manuscript

Received: December 21, 2019
Peer-review started: December 21, 2019
First decision: January 3, 2020
Revised: January 20, 2020
Accepted: March 9, 2020
Article in press: March 9, 2020

Masaya Iwamuro, Hiroyuki Okada, Department of Gastroenterology and Hepatology, Okayama University Graduate School of Medicine, Dentistry, and Pharmaceutical Sciences, Okayama 7008558, Japan

Haruo Urata, Central Research Laboratory, Okayama University Medical School, Okayama 7008558, Japan

Takehiro Tanaka, Department of Pathology, Okayama University Hospital, Okayama 7008558, Japan

Corresponding author: Masaya Iwamuro, MD, PhD, Assistant Professor, Doctor, Department of Gastroenterology and Hepatology, Okayama University Graduate School of Medicine, Dentistry, and Pharmaceutical Sciences, 2-5-1 Shikata-cho, Kita-Ku, Okayama 7008558, Japan. iwamuromasaya@yahoo.co.jp

Abstract

Lanthanum carbonate is used for treatment of hyperphosphatemia mostly in patients with chronic renal failure. Although lanthanum carbonate is safe, recently, lanthanum deposition in the gastrointestinal mucosa of patients has been reported in the literature. This review provides an overview of gastroduodenal lanthanum deposition and focuses on disease's endoscopic, radiological, and histological features, prevalence, and outcome, by reviewing relevant clinical studies, case reports, and basic research findings, to better understand the endoscopic manifestation of gastrointestinal lanthanum deposition. The possible relationship between gastric lanthanum deposition pattern and gastric mucosal atrophy is also illustrated; in patients without gastric mucosal atrophy, gastric lanthanum deposition appears as diffuse white lesions in the posterior wall and lesser curvature of the gastric body. In the gastric mucosa with atrophy, lanthanum-related lesions likely appear as annular or granular whitish lesions. Moreover, these white lesions are probably more frequently observed in the lower part of the stomach, where intestinal metaplasia begins.

Key words: Lanthanum carbonate; Hyperphosphatemia; Gastrointestinal endoscopy; Lanthanum phosphate; Scanning electron microscopy; Energy-dispersive X-ray spectrometry

Core tip: This review provides an overview of the endoscopic and pathological diagnosis of gastroduodenal lanthanum deposition. Previously reported case reports, case series, and retrospective studies are reviewed, focusing on disease's endoscopic, histological,

Published online: April 7, 2020

P-Reviewer: Casadesus D, Chow WK
S-Editor: Zhang L
L-Editor: A
E-Editor: Ma YJ

and computed tomography features, prevalence, and outcome. Although gastroduodenal deposition presents with white appearance at esophagogastroduodenoscopy, macroscopic features and locations of gastric lesions possibly vary depending on the presence or absence of mucosal atrophy. Our hypotheses are also related to the pattern of lanthanum deposition in the gastric mucosa with/without atrophy, which will aid endoscopists to understand this disease entity.

Citation: Iwamuro M, Urata H, Tanaka T, Okada H. Review of the diagnosis of gastrointestinal lanthanum deposition. *World J Gastroenterol* 2020; 26(13): 1439-1449
URL: https://www.wjgnet.com/1007-9327/full/v26/i13/1439.htm
DOI: https://dx.doi.org/10.3748/wjg.v26.i13.1439

INTRODUCTION

Lanthanum carbonate (Fosrenol®) is used for treatment of hyperphosphatemia and in the management of chronic renal failure, especially in dialysis patients[1-3]. Since patients with chronic renal failure generally have a reduced ability to excrete phosphorus from the bloodstream, the levels of serum phosphorus increase as their kidney function deteriorates, resulting in hyperphosphatemia. Persistent hyperphosphatemia causes osteoporosis and deposition of calcium phosphate on the blood vessel walls, leading to arteriosclerosis[4,5]. Moreover, hyperphosphatemia is associated with an increased risk of cardiovascular events and mortality[6]. Therefore, serum phosphorus levels should be controlled within their normal ranges during the management of dialysis patients.

For the treatment of hyperphosphatemia in dialysis patients, aluminum-containing agents have long been used as phosphate binders since the 1970s. However, chronic administration of aluminum salts results in accumulation of aluminum in the central nervous system, bone and hematopoietic cells, leading to encephalopathy, osteomalacia, myopathy, and microcytic anemia[7]. Due to these severe toxic effects, long-term use of aluminum salts is not allowed for dialysis patients. Alternatively, calcium carbonate, calcium acetate, polymers such as sevelamer hydrochloride, and lanthanum carbonate have been developed and used in clinical practice. Among these, calcium carbonate occasionally increases serum calcium levels and causes extraskeletal calcification. Sevelamer hydrochloride also exhibits adverse events such as digestive symptoms mainly due to constipation. In contrast, lanthanum carbonate has been widely used for patients with chronic renal failure because it is safe and well-tolerated by the patients.

After ingestion of lanthanum carbonate, the lanthanum ion (La^{3+}) is released in the stomach and binds to dietary phosphate in the intestinal tract. Lanthanum phosphate is an insoluble complex in the gut that is not absorbed by the digestive tract, thereby it is excreted from the body together with feces. The absorption rate of lanthanum carbonate from the gastrointestinal tract into the blood is less than 0.002%[8]. Because the slightly absorbed lanthanum is reportedly excreted from the body *via* bile[9], lanthanum carbonate can be safely used even in patients with impaired renal function. Although absorbed lanthanum is known to deposit in the bones and liver, the amount of deposition is quite small and does not cause any damage to the organs[10,11]. However, more recently, patients with lanthanum deposition in the gastrointestinal mucosa have been reported in the literature. Here, we review relevant clinical studies, case reports, and basic research findings, including our articles, to better understand the endoscopic manifestation of gastrointestinal lanthanum deposition.

PATHOLOGICAL FEATURES

Light microscopy observation

Hematoxylin and eosin staining of biopsy specimens containing lanthanum showed deposition of fine, amorphous, eosinophilic material (Figure 1A). Deposited materials have been variably described as inclusion-like materials with irregularly branching or coiled configurations[12], granular, brown material, sometimes needle-shaped or crystalloid and irregular eosinophilic material with slit-like clefts[13,14], variably dense

and granular deposits[15], many colorless and coarse granular materials[16], gray or brown pigments or crystal-like structures[17], amphophilic and/or yellowish-brown fine granules, and amphophilic and/or brownish rods or curly strings[18]. Deposited materials are generally phagocytosed by macrophages in the lamina propria in the stomach and duodenum, which are more clearly visualized with immunohistochemical staining, such as anti-CD68 staining (Figure 1B). Nakamura *et al*[19] revealed that the macrophages are positive for both CD68 and CD206 staining and speculated that M2 macrophages potentially play a role in the clearance of lanthanum from the gastroduodenal mucosa[19].

Diagnosis of lanthanum deposition can be made with (1) conventional light microscopy observation of the fine, amorphous, eosinophilic material; and (2) medication information of patient's current or past use of lanthanum carbonate. Analysis of elements by energy-dispersive X-ray spectrometry (EDX) is not always required, unless the amount of lanthanum deposition is subtle or pathological features are atypical[20-24].

Electron microscopy observation

In scanning electron microscopy (SEM), deposited lanthanum is visible as bright areas (Figure 2A). Higher magnification shows that the deposition is composed of aggregates of particles, measuring 0.5–3 m in diameter (Figure 2B). Elemental mapping by energy dispersive X-ray spectroscopy is useful to visualize distribution of lanthanum (Figure 2C) and phosphate (Figure 2D), which is identical to that of the bright areas. EDX also shows presence of lanthanum and phosphate elements (Figure 2E). Since both lanthanum and phosphate are generally detected simultaneously, deposited material is considered as lanthanum phosphate. SEM observation and EDX analysis enable analysis of the elemental composition and distribution of elements, leading to direct proof of lanthanum deposition. In contrast to light microscopy, deposited lanthanum is easily identified as bright areas with SEM[22].

COMPUTED TOMOGRAPHY FINDINGS OF LANTHANUM DEPOSITION

Because lanthanum carbonate is not transparent to X-rays, it has a radiopaque appearance in plain abdominal radiography and computed tomography (CT) scanning images[25]. Figure 3A shows ingested lanthanum carbonate in the stomach (arrow) and colon (arrowhead) that is displayed as high-density substance. In this patient, lanthanum carbonate and food contents are separated in the stomach, while lanthanum carbonate in the colon is combined with digested materials and forms a lump of feces. In another patient, deposited lanthanum in the stomach is observed as a high-density layer within the gastric mucosa (Figure 3B). Namie *et al*[26] reported the identification of a high-density layer in the stomach in 42 out of 70 (60%) patients treated with lanthanum carbonate.

ENDOSCOPIC MANIFESTATION

Lanthanum deposition in the stomach

Lanthanum carbonate has been marketed as a phosphate binder since 2005 in United States and was released in Japan in 2009. Despite its general tolerance and safety profile, lanthanum deposition in the gastroduodenal mucosa of lanthanum carbonate users was first reported in 2015. The endoscopic features of the gastric lesions were initially portrayed as numerous small, irregular white spots[13], scattered ulcerations[15], polyp, erosions, ulcer[12,14], white thickenings of annular shape or those on the gastric folds[26], slightly granular, white mucosa[20], granular white depositions in reddish mucosa[21], white spots[27], mucosal irregularity with reddish and/or whitish color, and even nonremarkable mucosa[18]. Based on the accumulation of cases reported in the literature and clinical practice, typical endoscopic findings of gastric lanthanum deposition have been currently recognized as white lesions.

In our earlier work, we reviewed four patients showing gastric white lesions (Bw) and peripheral mucosa where the white substance was not endoscopically observed (Bp) during biopsy[28]. We performed SEM analysis and EDX spectrometry to quantify the lanthanum elements (wt%) in the biopsy specimens. We showed that the amount of lanthanum was significantly higher in Bw than in Bp (0.15–0.31 wt% *vs* 0.00–0.13 wt%) ($P < 0.05$), revealing that pathological lanthanum deposition coincides with endoscopically observed white lesions in the gastric mucosa. On the other hand, although its deposited amount was small, lanthanum was detectable in EDX analysis

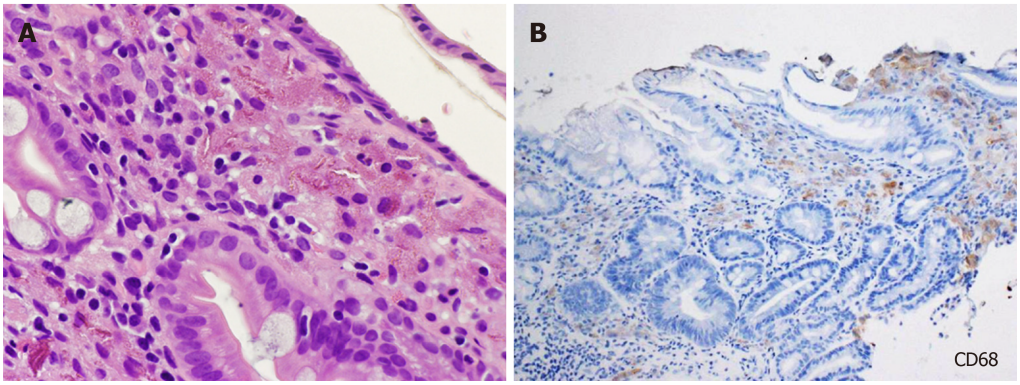

Figure 1 Light microscopy images of gastric lanthanum deposition. A: Fine, amorphous, eosinophilic material is observed in hematoxylin and eosin staining; B: Deposited material is generally phagocytosed by macrophages.

of the gastric mucosa where the white substance was not endoscopically visible[22,28]. Consequently, a subtle amount of lanthanum deposition is not detected under endoscopic observation, while it can be detected with optical microscopy or electron microscopy.

We also reviewed gastric lesions of lanthanum deposition and subclassified endoscopic features into "whitish spots" (Figure 4A and B), "annular whitish mucosa" (Figure 4C and D), and "diffuse whitish mucosa" (Figure 4E and F)[29]. Subsequently we added "fine granular whitish deposition" as a new subtype of endoscopic features (Figure 4G and H), because we noticed that whitish spots are relatively infrequent compared with the other three subtypes, while small amount of lanthanum deposition often appears as fine, granular white lesions[23]. We defined annular whitish mucosa as a lesion (s) ≤ 20 mm in diameter with a white color in the periphery. A diffuse whitish mucosa presents a white area > 20 mm in diameter, where reddish areas may be intermixed. Fine granular whitish deposition is a tiny or faint whitish lesion (s) ≤ 1 mm in diameter. Whitish spot is a whitish lesion ≤ 20 mm in diameter with a uniform white color, resembling gastric xanthoma. Generally, diffuse whitish mucosa is observed in the non-atrophic mucosa of the gastric body, whereas annular whitish mucosa and fine granular whitish deposition are observed in the atrophic mucosa. In the following sections, we discuss endoscopic features of lanthanum deposition focusing on gastric mucosal atrophy.

Lanthanum deposition in the atrophic gastric mucosa

Possible association with gastric lanthanum deposition and underlying regenerative changes, intestinal metaplasia, and/or foveolar hyperplasia has been reported in 2015. Makino *et al*[13] reported that macrophages containing lanthanum existed in the gastric mucosa with atrophic pyloric glands and foveolar epithelium fully replaced by intestinal metaplasia. Tonooka *et al*[30] also found atrophic mucosa with metaplastic epithelia in their patient. They speculated that altered mucosal structure resulted in increased epithelial permeability, finally leading to lanthanum deposition in the stomach. Ban *et al*[18] found a significant correlation between deposition grade of lanthanum and mucosal alterations such as regenerative changes, intestinal metaplasia, or foveolar hyperplasia, reinforcing the tendency of lanthanum deposition in higher degree in the microscopically altered gastric mucosa. Ji *et al*[31] investigated the mucosal barrier defects in patients with intestinal metaplasia using laser confocal endomicroscopy. *In vivo* functional imaging revealed that lanthanum nitrate did not permeated normal gastric epithelium, whereas it permeated gastric mucosa with intestinal metaplasia. These results indicated that gastric mucosa with regenerative changes, intestinal metaplasia, and/or foveolar hyperplasia allows permeation of lanthanum.

We recently reviewed endoscopic features of gastric lanthanum deposition in 10 patients with gastric atrophy (under review). Although gastric lanthanum deposition appears as whitish lesions, this presentation was not observed in 1 out of 10 patients. In the gastric mucosa with atrophy, the antrum (n = 5) and angle (n = 5) were most frequently involved and lanthanum deposition presented with annular and/or granular whitish lesions. Whitish lesions were also found in the gastric body with mucosal atrophy that appeared as annular (n = 1), granular (n = 1), and diffuse whitish lesions (n = 1). Consequently, we speculate that, in the atrophic gastric mucosa, lanthanum-related lesions typically present with annular or granular whitish lesions. In our earlier study, we investigated pathological features of four patients

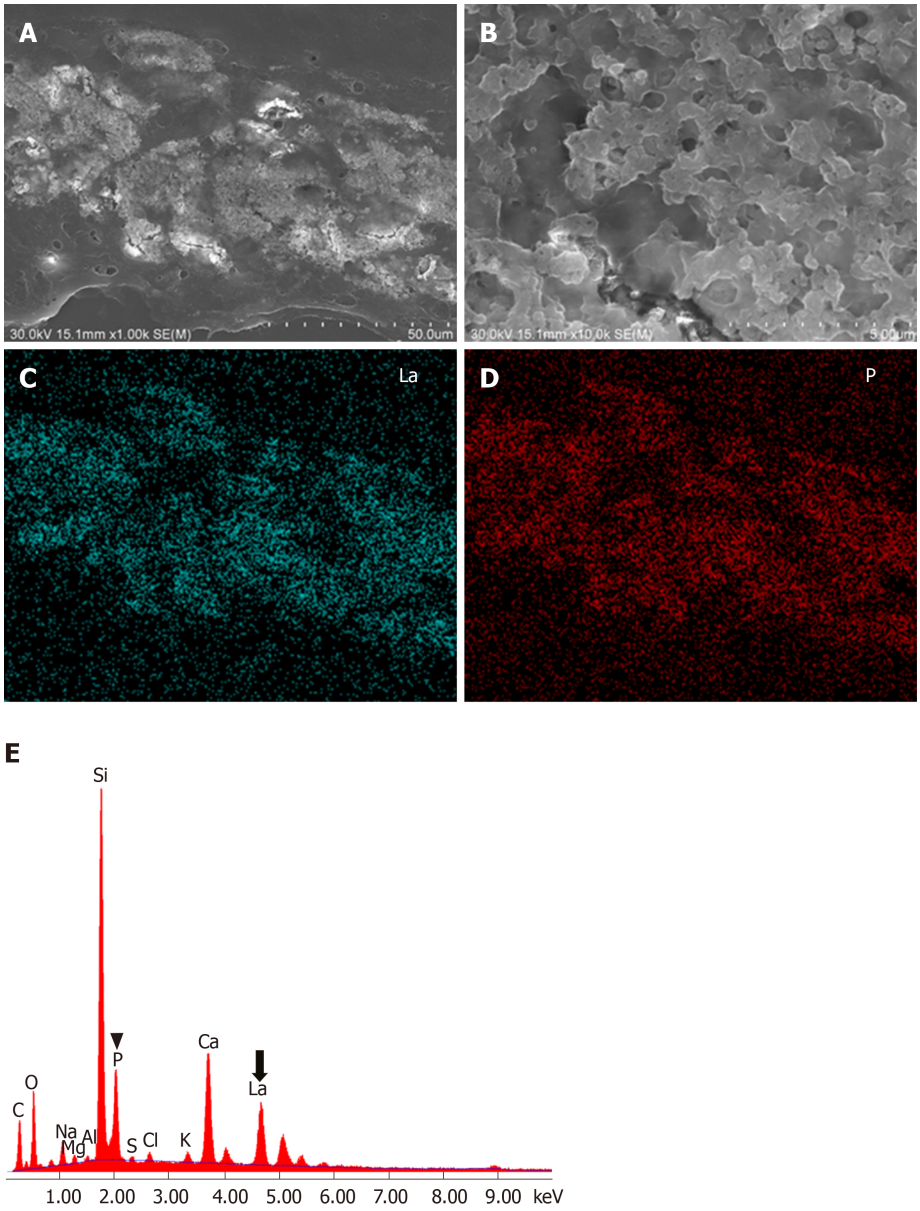

Figure 2 Electron microscopy analysis of gastric lanthanum deposition. A: In scanning electron microscopy, deposited lanthanum is visible as bright areas; B: Deposited lanthanum is composed of aggregates of particles; C: Elemental mapping with energy dispersive X-ray spectroscopy shows that the distribution of lanthanum; D: Phosphate is identical to that of the bright areas; E: Energy dispersive X-ray spectroscopy shows presence of lanthanum (La) and phosphate elements (P).

with annular whitish lesions[28]. We took one biopsy sample from white lesions and the other sample from the surrounding mucosa approximately 5 mm away from the white lesions. Intestinal metaplasia was identified in 3 out of 4 samples acquired from the annular whitish lesion, whereas the surrounding mucosa contained no intestinal metaplasia (Figure 5). Thus, we speculate that lanthanum deposition appears as "annular" or "granular" lesions in the atrophic mucosa, because intestinal metaplasia unevenly exists in the background gastric mucosa and is susceptible to lanthanum deposition. In addition, lanthanum-related lesions are probably more frequently observed in the gastric antrum and angle, because intestinal metaplasia generally appears at the lower part of the stomach.

We postulate that in the atrophic mucosa, particularly in areas with intestinal metaplasia, lanthanum deposition presents with annular and/or granular whitish lesions, predominantly in the gastric antrum and angle. As the intestinal metaplasia expands, the size of the areas with lanthanum deposition may increase (Figure 6A).

Lanthanum deposition in the gastric mucosa without atrophy

As described above, several reports have revealed that lanthanum deposition

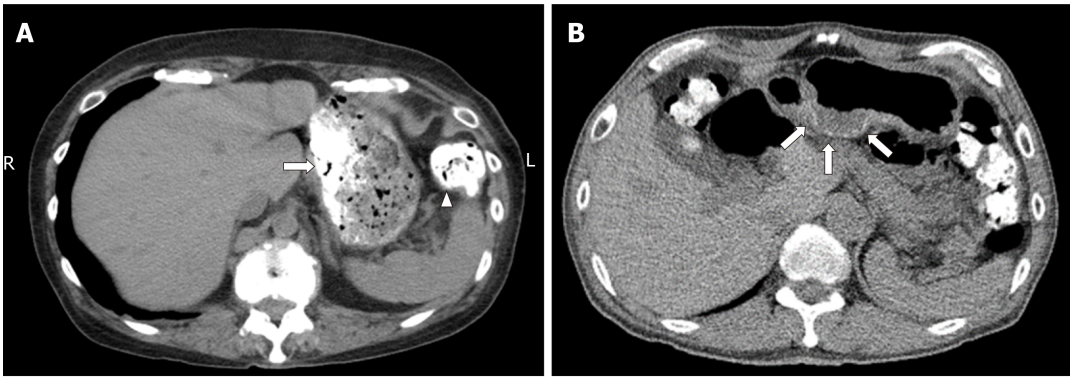

Figure 3 Computed tomography images. A: Computed tomography scanning shows ingested lanthanum carbonate in the stomach (arrow) and colon (arrowhead) as high-density substances; B: In another patient, deposited lanthanum in the stomach is observed as a high-density layer within the gastric mucosa (arrows).

develops within the gastric mucosa showing regenerative changes, intestinal metaplasia, and/or foveolar hyperplasia. Because all these histopathological features generally arise as *Helicobacter pylori (H. pylori)*-induced mucosal alterations, lanthanum deposition had been considered to occur in the stomach in close association with *H. pylori*-infection. In contrast, we previously reported two patients with lanthanum deposition in the stomach who were serologically and histopathologically negative for *H. pylori*[32]. In our patients, lanthanum deposition was identified as diffuse whitish lesions, which were predominantly observed in the lesser curvature and posterior wall of the gastric body, rather than in the antrum or angle. Based on this observation, we hypothesized that in the gastric mucosa without atrophy, lanthanum primarily deposits in the lesser curvature and posterior wall of the gastric body and presents diffuse whitish lesions (Figure 6B). The area of lanthanum deposition probably expands as time elapses unless the patient stops lanthanum carbonate.

We speculate that gastric body-predominant lanthanum deposition occurs because of the direct physical contact between ingested lanthanum carbonate and the gastric body mucosa[32]. Figure 3A shows a CT image of a patient, who had been administered lanthanum carbonate. Even after abstinence from food and medicine for 10 h, a substantial amount of lanthanum was observed as a high-density substance (Figure 3A, arrow), predominantly in the gastric body. Thus, the gastric body is expected to be involved in lanthanum deposition due to prolonged contact with ingested lanthanum.

Lanthanum deposition in the duodenum

Although several authors have described various endoscopic features of lanthanum-related duodenal lesions as duodenal ulcer[12], granular and micronodular mucosa[33], granular mucosa[34], and duodenitis[27], we first reported white villi as a characteristic appearance of duodenal lanthanum deposition[35]. Subsequently, we retrospectively reviewed endoscopic and pathological features in patients with pathologically proven lanthanum deposition in the gastrointestinal tract[36]. We revealed that, among 19 patients who underwent biopsy from the duodenum, lanthanum deposition was detected in 17 patients (89.5%). Moreover, white villi were observed in 15 patients (88.2%). These results indicate that the duodenum is often involved in lanthanum deposition, which generally presents with white villi (Figure 7). However, these deposits may not be detected during esophagogastroduodenoscopy in some cases due to the subtle degree of deposition. We consider that endoscopic biopsy should be performed in the duodenum as well as in the stomach, regardless of the presence or absence of white villi, for accurate determination of lanthanum deposition in the gastrointestinal tract[36].

Lanthanum deposition in other organs

Deposition of lanthanum in organs other than the stomach and duodenum has scarcely been reported. In 2009, Davis *et al*[37]reported lanthanum deposition in the mesenteric lymph nodes in postmortem examination of a dialysis patient. Yabuki *et al*[17] and Tonooka *et al*[30] also described involvement of the gastric regional lymph nodes in patients who underwent gastrectomy for gastric cancer. Goto *et al*[14] reported lanthanum deposition in a tubular adenoma of the transverse colon.

In animal models, Lacour *et al*[38] investigated lanthanum concentrations in various rat tissues after oral administration for 28 d. Although lanthanum concentration did

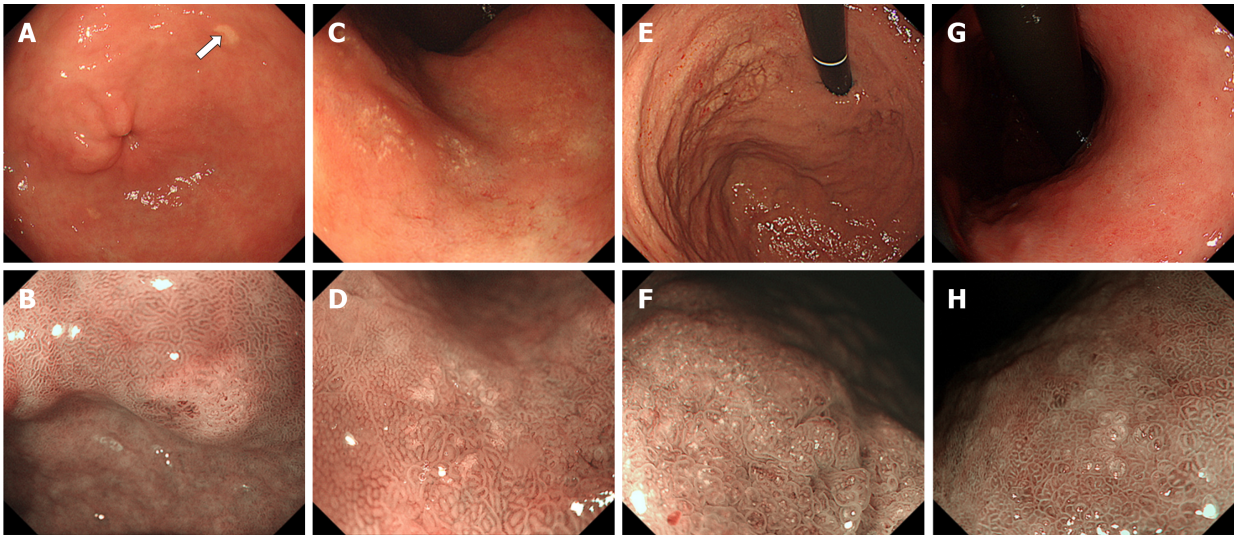

Figure 4 Typical endoscopic features of gastric lanthanum deposition during conventional white-light (upper row) and magnified observation with narrow-band imaging (lower row). A, B: "Whitish spot" is defined as a whitish lesion ≤ 20 mm in diameter with a uniform white color; C, D: "Annular whitish mucosa" are lesion (s) ≤ 20 mm in diameter with white color in the periphery; E, F: "Diffuse whitish mucosa" appears with a white area > 20 mm in diameter; G, H: "Fine granular whitish deposition" is a tiny or faint whitish lesion (s) ≤ 1 mm in diameter.

not increase in the brain and heart of rats, significantly elevated levels of lanthanum concentration were observed in the liver, lungs, femur, muscles, and kidneys of lanthanum-treated rats. Of note, compared with lanthanum-treated rats with normal kidney function, rats with impaired kidney function showed significantly higher tissue lanthanum concentration in the brain, liver, heart, lungs, femur, and muscles. Therefore, in patients with chronic kidney disease, a long period of careful observation may be required to reveal organ-specific properties of lanthanum accumulation.

GASTRIC CANCER AND LANTHANUM DEPOSITION

Coexistence of gastric cancer and lanthanum deposition in the gastric mucosa has been reported by several authors[13,17,30,39]. Makino *et al*[13] reported lanthanum-related gastric lesions as numerous small, irregular white spots, which exist in the periphery of the area with gastric cancer. Yabuki *et al*[17] also described lanthanum deposition in non-neoplastic area, while deposition was not significant in the gastric adenocarcinoma lesion. The authors speculated that different permeability between adenocarcinoma and background mucosa resulted in the uneven distribution of lanthanum deposition. Tonooka *et al*[30] and Takatsuna *et al*[39] also described quite small amounts of lanthanum deposition in gastric cancer lesions. Based on these observations, the area with gastric cancer is probably spared from lanthanum deposition. Although understanding this phenomenon will help endoscopists to easily identify gastric cancer lesions in the lanthanum-deposited stomach, this concept requires further investigation.

PREVALENCE

The actual prevalence of gastroduodenal lanthanum deposition among end-stage renal disease patients treated with lanthanum carbonate has not yet been clarified. Murakami *et al*[29] performed endoscopic biopsy in 9 out of 90 patients with lanthanum carbonate prescription. Gastric lanthanum deposition was histologically diagnosed in seven patients (7/9, 77.8%). Goto *et al*[14] reported that lanthanum was detected in the stomach of 12 out of 14 patients who received lanthanum carbonate and underwent endoscopic biopsy (12/14, 85.7%). Namie *et al*[26] found high-density lesions within the gastric mucosa on CT scanning in 42 out of 70 patients who were administered lanthanum carbonate (42/70, 60.0%). Therefore, prevalence of lanthanum deposition in the stomach is estimated to be 60%–85%. However, because only retrospective studies have been performed, sampling biases are inevitable and prospective studies are required to address this issue.

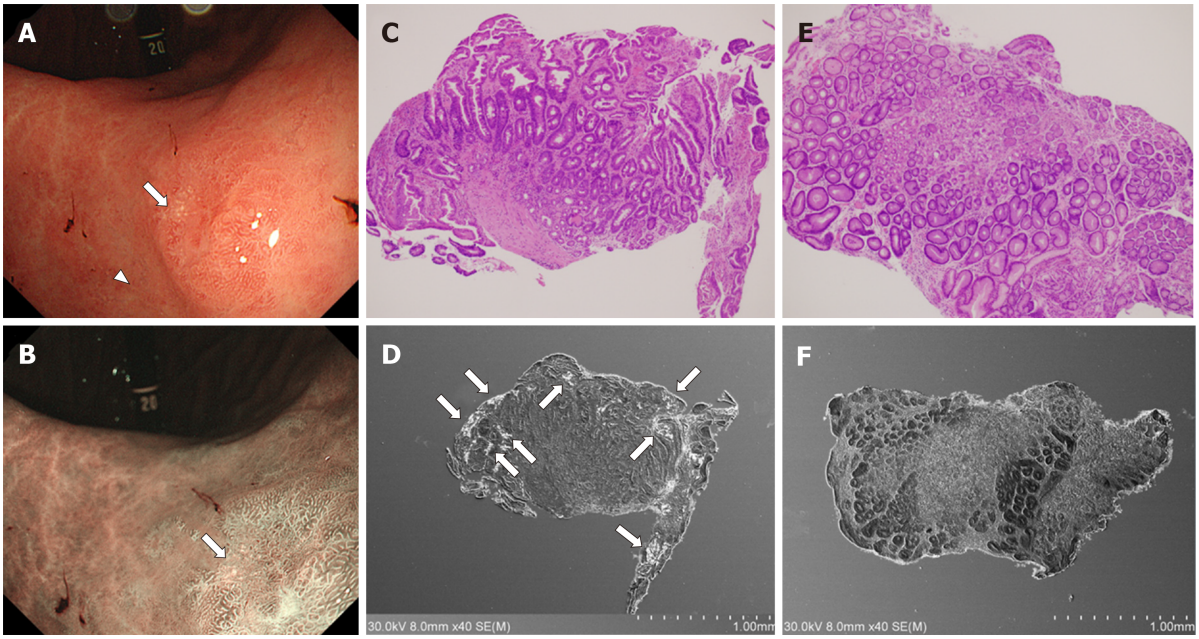

Figure 5 Correlation between intestinal metaplasia and lanthanum deposition in the stomach. A: Esophagogastroduodenoscopy shows an annular whitish lesion in the gastric antrum (white light observation); B: Esophagogastroduodenoscopy shows an annular whitish lesion in the gastric antrum (narrow-band imaging); C, D: Biopsy sample acquired from a white lesion (A, B, arrows) contains intestinal metaplasia (C) and lanthanum deposition (D); E, F: In contrast, the sample acquired from the surrounding mucosa approximately 5 mm away from the white lesions (A, arrowhead) contains no intestinal metaplasia (E) and lanthanum deposition is subtle (F).

OUTCOME OF THE GASTRODUODENAL LANTHANUM DEPOSITION

Our retrospective study revealed that, during continuous lanthanum carbonate use, lanthanum-related lesions in the stomach were endoscopically unchanged in two patients, whereas whitish lesions became apparent and spread in three patients[29], indicating that gastric lanthanum deposition progresses in several patients in a time-dependent manner. In contrast, Rothenberg *et al*[15] reported resolution of histiocytosis in the stomach and significant decrease in the duodenum three months after cessation of lanthanum carbonate in a patient with gastroduodenal lanthanum deposition. However, Namie *et al*[26] reported that CT and pathological findings of lanthanum-related gastric lesions were unchanged eight months after discontinuation of lanthanum carbonate. Awad *et al*[40] also noted that lanthanum-related lesions remained unchanged six months after drug cessation. Moreover, Hoda *et al*[33] detected lanthanum deposition in a biopsy specimen from the stomach acquired seven years after stopping lanthanum carbonate intake. It has not been clarified to date whether lanthanum deposition in tissues is reversible or not.

The pathological significance of lanthanum deposition in the gastrointestinal mucosa has not been clarified, and there is no consensus on whether to stop administration of lanthanum carbonate in such cases. Yabuki *et al*[17] investigated histological changes in the gastric mucosa of lanthanum carbonate-consuming rats. The authors found a variety of alterations including glandular atrophy, stromal fibrosis, proliferation of mucous neck cells, intestinal metaplasia, squamous cell papilloma, erosion, and ulcer in the stomach of rats. They speculated that deposited lanthanum was able to cause mucosal injury and abnormal cell proliferation, leading to structural changes in the mucosa and neoplastic lesions in the stomach. In this context, we consider that endoscopists should accurately diagnose lanthanum deposition in the gastroduodenal tract in lanthanum-carbonate users and recommend them to undergo regular endoscopy examinations in order to track progression of white lesions and elucidate whether lanthanum deposition is related to health problems.

CONCLUSION

Lanthanum deposition in the stomach and duodenum is recognized as whitish lesions during endoscopy examination. Accurate diagnosis and keeping track of the health of

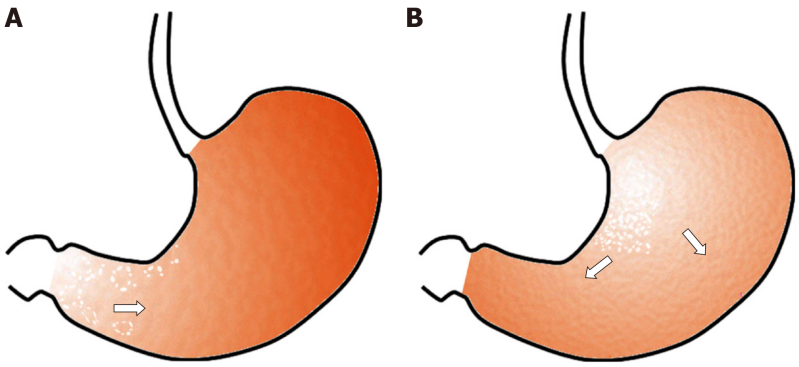

Figure 6 Hypothesis regarding the pattern of lanthanum deposition in the gastric mucosa with or without atrophy. A: In the atrophic mucosa, particularly in areas with intestinal metaplasia, lanthanum deposition probably presents with annular and/or granular white lesions, predominantly in the gastric antrum and angle. As intestinal metaplasia expands, the size of the areas with lanthanum deposition may increase; B: In the gastric mucosa without atrophy, lanthanum primarily deposits in the lesser curvature and posterior wall of the gastric body and presents diffuse whitish lesions. The area of lanthanum deposition probably expands as time elapses unless the patient stops lanthanum carbonate.

patients with gastroduodenal lanthanum deposition are essential to elucidate pathogenicity of lanthanum deposition in the gastrointestinal tract.

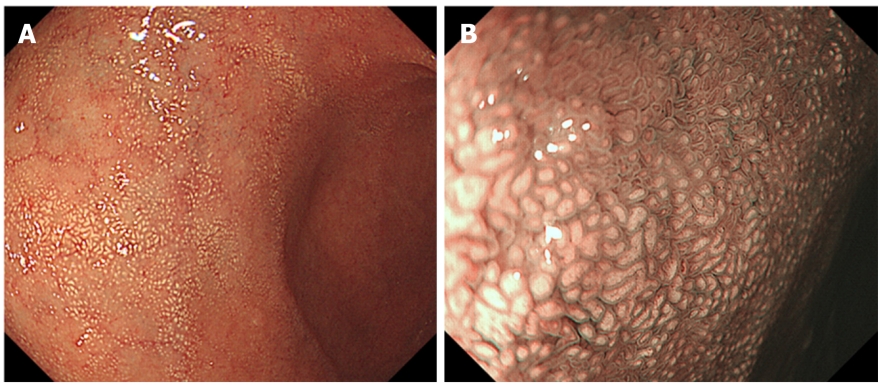

Figure 7 Endoscopic images of the duodenal lanthanum deposition. A: A lanthanum-related lesion in the duodenum presents with white mucosa; B: Magnified image with narrow-band imaging shows white depositions within the duodenal villi.

REFERENCES

1 **Shinoda T**, Yamasaki M, Chida Y, Takagi M, Tanaka Y, Ando R, Suzuki T, Tagawa H. Improvement of MBD parameters in dialysis patients by a switch to, and combined use of lanthanum carbonate: Josai Dialysis Forum collaborative study. *Ther Apher Dial* 2013; **17** Suppl 1: 29-34 [PMID: 23586510 DOI: 10.1111/1744-9987.12041]

2 **Kasai S**, Sato K, Murata Y, Kinoshita Y. Randomized crossover study of the efficacy and safety of sevelamer hydrochloride and lanthanum carbonate in Japanese patients undergoing hemodialysis. *Ther Apher Dial* 2012; **16**: 341-349 [PMID: 22817122 DOI: 10.1111/j.1744-9987.2012.01071.x]

3 **Shigematsu T**; Lanthanum Carbonate Research Group. One year efficacy and safety of lanthanum carbonate for hyperphosphatemia in Japanese chronic kidney disease patients undergoing hemodialysis. *Ther Apher Dial* 2010; **14**: 12-19 [PMID: 20438515 DOI: 10.1111/j.1744-9987.2009.00697.x]

4 **Lau WL**, Festing MH, Giachelli CM. Phosphate and vascular calcification: Emerging role of the sodium-dependent phosphate co-transporter PiT-1. *Thromb Haemost* 2010; **104**: 464-470 [PMID: 20664908 DOI: 10.1160/TH09-12-0814]

5 **Giachelli CM**. The emerging role of phosphate in vascular calcification. *Kidney Int* 2009; **75**: 890-897 [PMID: 19145240 DOI: 10.1038/ki.2008.644]

6 **Kendrick J**, Kestenbaum B, Chonchol M. Phosphate and cardiovascular disease. *Adv Chronic Kidney Dis* 2011; **18**: 113-119 [PMID: 21406296 DOI: 10.1053/j.ackd.2010.12.003]

7 **Salusky IB**. A new era in phosphate binder therapy: what are the options? *Kidney Int Suppl* 2006; S10-S15 [PMID: 17136110 DOI: 10.1038/sj.ki.5001997]

8 **Giotta N**, Marino AM. Pharmacoeconomic analysis: Analysis of cost-effectiveness of lanthanum-carbonate (Lc) in uncontrolled hyperphosphatemia in dialysis. *Value Health* 2015; **18**: A511 [DOI: 10.1016/j.jval.2015.09.1474]

9 **Pennick M**, Dennis K, Damment SJ. Absolute bioavailability and disposition of lanthanum in healthy human subjects administered lanthanum carbonate. *J Clin Pharmacol* 2006; **46**: 738-746 [PMID: 16809799 DOI: 10.1177/0091270006289846]

10 **Spasovski GB**, Sikole A, Gelev S, Masin-Spasovska J, Freemont T, Webster I, Gill M, Jones C, De Broe ME, D'Haese PC. Evolution of bone and plasma concentration of lanthanum in dialysis patients before, during 1 year of treatment with lanthanum carbonate and after 2 years of follow-up. *Nephrol Dial Transplant* 2006; **21**: 2217-2224 [PMID: 16595583 DOI: 10.1093/ndt/gfl146]

11 **Damment SJ**, Pennick M. Clinical pharmacokinetics of the phosphate binder lanthanum carbonate. *Clin Pharmacokinet* 2008; **47**: 553-563 [PMID: 18698878 DOI: 10.2165/00003088-200847090-00001]

12 **Haratake J**, Yasunaga C, Ootani A, Shimajiri S, Matsuyama A, Hisaoka M. Peculiar histiocytic lesions with massive lanthanum deposition in dialysis patients treated with lanthanum carbonate. *Am J Surg Pathol* 2015; **39**: 767-771 [PMID: 25602800 DOI: 10.1097/PAS.0000000000000385]

13 **Makino M**, Kawaguchi K, Shimojo H, Nakamura H, Nagasawa M, Kodama R. Extensive lanthanum deposition in the gastric mucosa: the first histopathological report. *Pathol Int* 2015; **65**: 33-37 [PMID: 25413959 DOI: 10.1111/pin.12227]

14 **Goto K**, Ogawa K. Lanthanum Deposition Is Frequently Observed in the Gastric Mucosa of Dialysis Patients with Lanthanum Carbonate Therapy: A Clinicopathologic Study of 13 Cases, Including 1 Case of Lanthanum Granuloma in the Colon and 2 Nongranulomatous Gastric Cases. *Int J Surg Pathol* 2016; **24**: 89-92 [PMID: 26490721 DOI: 10.1177/1066896915613434]

15 **Rothenberg ME**, Araya H, Longacre TA, Pasricha PJ. Lanthanum-Induced Gastrointestinal Histiocytosis. *ACG Case Rep J* 2015; **2**: 187-189 [PMID: 26157959 DOI: 10.14309/crj.2015.50]

16 **Yasunaga C**, Haratake J, Ohtani A. Specific Accumulation of Lanthanum Carbonate in the Gastric Mucosal Histiocytes in a Dialysis Patient. *Ther Apher Dial* 2015; **19**: 622-624 [PMID: 26420000 DOI: 10.1111/1744-9987.12325]

17 **Yabuki K**, Shiba E, Harada H, Uchihashi K, Matsuyama A, Haratake J, Hisaoka M. Lanthanum deposition in the gastrointestinal mucosa and regional lymph nodes in dialysis patients: Analysis of surgically excised specimens and review of the literature. *Pathol Res Pract* 2016; **212**: 919-926 [PMID: 27515549 DOI: 10.1016/j.prp.2016.07.017]

18 **Ban S**, Suzuki S, Kubota K, Ohshima S, Satoh H, Imada H, Ueda Y. Gastric mucosal status susceptible to lanthanum deposition in patients treated with dialysis and lanthanum carbonate. *Ann Diagn Pathol* 2017; **26**: 6-9 [PMID: 28038714 DOI: 10.1016/j.anndiagpath.2016.10.001]

19 **Nakamura T**, Tsuchiya A, Kobayashi M, Naito M, Terai S. M2-polarized macrophages relate the clearance of gastric lanthanum deposition. *Clin Case Rep* 2019; **7**: 570-572 [PMID: 30899497 DOI:

10.1002/ccr3.1989]
20 **Iwamuro M**, Sakae H, Okada H. White Gastric Mucosa in a Dialysis Patient. *Gastroenterology* 2016; **150**: 322-323 [PMID: 26724264 DOI: 10.1053/j.gastro.2015.11.013]
21 **Iwamuro M**, Kanzaki H, Tanaka T, Kawano S, Kawahara Y, Okada H. Lanthanum phosphate deposition in the gastric mucosa of patients with chronic renal failure. *Nihon Shokakibyo Gakkai Zasshi* 2016; **113**: 1216-1222 [PMID: 27383105 DOI: 10.11405/nisshoshi.113.1216]
22 **Iwamuro M**, Urata H, Tanaka T, Ando A, Nada T, Kimura K, Yamauchi K, Kusumoto C, Otsuka F, Okada H. Lanthanum Deposition in the Stomach: Usefulness of Scanning Electron Microscopy for Its Detection. *Acta Med Okayama* 2017; **71**: 73-78 [PMID: 28238013 DOI: 10.18926/AMO/54828]
23 **Iwamuro M**, Kanzaki H, Kawano S, Kawahara Y, Tanaka T, Okada H. Endoscopic features of lanthanum deposition in the gastroduodenal mucosa. *Gastroenterol Endosc* 2017; **59**: 1428-1434 [DOI: 10.11280/gee.59.1428]
24 **Iwamuro M**, Urata H, Tanaka T, Okada H. Gastric lanthanum phosphate deposition masquerading as white globe appearance. *Dig Liver Dis* 2019; **51**: 168 [PMID: 30145054 DOI: 10.1016/j.dld.2018.07.031]
25 **Cerny S**, Kunzendorf U. Images in clinical medicine. Radiographic appearance of lanthanum. *N Engl J Med* 2006; **355**: 1160 [PMID: 16971722 DOI: 10.1056/NEJMicm050535]
26 **Namie S**, Hamabe S, Kawatomi M, Kawatomi M, Oda H, Nakazawa M, Nishino T. Investigation of deposition of lanthanum on gastric mucosa in hemodialysis patients with lanthanum therapy. *J Jpn Soc Dial Ther* 2015; **48**: 169-177 [DOI: 10.4009/jsdt.48.169]
27 **Hattori K**, Maeda T, Nishida S, Imanishi M, Sakaguchi M, Amari Y, Moriya T, Hirose Y. Correlation of lanthanum dosage with lanthanum deposition in the gastroduodenal mucosa of dialysis patients. *Pathol Int* 2017; **67**: 447-452 [PMID: 28799264 DOI: 10.1111/pin.12564]
28 **Iwamuro M**, Urata H, Tanaka T, Kawano S, Kawahara Y, Kimoto K, Okada H. Lanthanum deposition corresponds to white lesions in the stomach. *Pathol Res Pract* 2018; **214**: 934-939 [PMID: 29843926 DOI: 10.1016/j.prp.2018.05.024]
29 **Murakami N**, Yoshioka M, Iwamuro M, Nasu J, Nose S, Shiode J, Okada H, Yamamoto K. Clinical Characteristics of Seven Patients with Lanthanum Phosphate Deposition in the Stomach. *Intern Med* 2017; **56**: 2089-2095 [PMID: 28781325 DOI: 10.2169/internalmedicine.8720-16]
30 **Tonooka A**, Uda S, Tanaka H, Yao A, Uekusa T. Possibility of lanthanum absorption in the stomach. *Clin Kidney J* 2015; **8**: 572-575 [PMID: 26413283 DOI: 10.1093/ckj/sfv062]
31 **Ji R**, Zuo XL, Yu T, Gu XM, Li Z, Zhou CJ, Li YQ. Mucosal barrier defects in gastric intestinal metaplasia: in vivo evaluation by confocal endomicroscopy. *Gastrointest Endosc* 2012; **75**: 980-987 [PMID: 22325805 DOI: 10.1016/j.gie.2011.12.016]
32 **Iwamuro M**, Urata H, Tanaka T, Kawano S, Kawahara Y, Kimoto K, Okada H. Lanthanum Deposition in the Stomach in the Absence of Helicobacter pylori Infection. *Intern Med* 2018; **57**: 801-806 [PMID: 29225268 DOI: 10.2169/internalmedicine.9665-17]
33 **Hoda RS**, Sanyal S, Abraham JL, Everett JM, Hundemer GL, Yee E, Lauwers GY, Tolkoff-Rubin N, Misdraji J. Lanthanum deposition from oral lanthanum carbonate in the upper gastrointestinal tract. *Histopathology* 2017; **70**: 1072-1078 [PMID: 28134986 DOI: 10.1111/his.13178]
34 **Komatsu-Fujii T**, Onuma H, Miyaoka Y, Ishikawa N, Araki A, Ishikawa N, Yamamoto T, Mishiro T, Adachi K, Kinoshita Y, Tauchi-Nishi P, Maruyama R. A Combined Deposition of Lanthanum and β2-Microglobulin-Related Amyloid in the Gastroduodenal Mucosa of Hemodialysis-Dependent Patients: An Immunohistochemical, Electron Microscopic, and Energy Dispersive X-Ray Spectrometric Analysis. *Int J Surg Pathol* 2017; **25**: 674-683 [PMID: 28675980 DOI: 10.1177/1066896917718623]
35 **Iwamuro M**, Tanaka T, Urata H, Kimoto K, Okada H. Lanthanum phosphate deposition in the duodenum. *Gastrointest Endosc* 2017; **85**: 1103-1104 [PMID: 27339946 DOI: 10.1016/j.gie.2016.06.012]
36 **Iwamuro M**, Urata H, Tanaka T, Kawano S, Kawahara Y, Okada H. Frequent Involvement of the Duodenum with Lanthanum Deposition: A Retrospective Observational Study. *Intern Med* 2019; **58**: 2283-2289 [PMID: 31118380 DOI: 10.2169/internalmedicine.2398-18]
37 **Davis RL**, Abraham JL. Lanthanum deposition in a dialysis patient. *Nephrol Dial Transplant* 2009; **24**: 3247-3250 [PMID: 19625369 DOI: 10.1093/ndt/gfp364]
38 **Lacour B**, Lucas A, Auchère D, Ruellan N, de Serre Patey NM, Drüeke TB. Chronic renal failure is associated with increased tissue deposition of lanthanum after 28-day oral administration. *Kidney Int* 2005; **67**: 1062-1069 [PMID: 15698446 DOI: 10.1111/j.1523-1755.2005.00171.x]
39 **Takatsuna M**, Takeuchi M, Usuda H, Terai S. Case of early-stage gastric cancer identified in the gastric mucosa with lanthanum phosphate deposition. *Endosc Int Open* 2019; **7**: E893-E895 [PMID: 31281874 DOI: 10.1055/a-0918-5804]
40 **Awad C**, Gilkison K, Shaw E. Lanthanum phosphate binder-induced iron deficiency anaemia. *BMJ Case Rep* 2019; 12 [PMID: 30878952 DOI: 10.1136/bcr-2018-226157]

World Journal of Gastroenterology

Submit a Manuscript: https://www.f6publishing.com

World J Gastroenterol 2020 April 7; 26(13): 1450-1462

DOI: 10.3748/wjg.v26.i13.1450

ISSN 1007-9327 (print) ISSN 2219-2840 (online)

ORIGINAL ARTICLE

Basic Study

Calpain-2 activity promotes aberrant endoplasmic reticulum stress-related apoptosis in hepatocytes

Ru-Jia Xie, Xiao-Xia Hu, Lu Zheng, Shuang Cai, Yu-Si Chen, Yi Yang, Ting Yang, Bing Han, Qin Yang

ORCID number: Ru-Jia Xie (0000-0001-5991-2678); Xiao-Xia Hu (0000-0001-9674-6277); Lu Zheng (0000-0003-3851-0607); Shuang Cai (0000-0001-8169-0485); Yu-Si Chen (0000-0003-2566-8878); Yi Yang (0000-0003-2756-6955); Ting Yang (0000-0001-5174-7575); Bing Han (0000-0002-9577-293X); Qin Yang (0000-0003-1479-6700).

Author contributions: Xie RJ, Han B and Zheng L performed the experiments; Hu XX, Cai S, Chen YS, Yang Y and Yang T analyzed the data; Xie RJ and Yang Q designed the study; Xie RJ wrote the manuscript; all authors approved the final manuscript. Xie RJ and Hu XX contributed equally to this work.

Supported by the National Natural Science Foundation of China, No. 81560105; the Department of Science and Technology of Guizhou Province, No. LH (2014) 7074.

Institutional animal care and use committee statement: All animal experiments conformed to the internationally accepted principles for the care and use of laboratory animals.

Conflict-of-interest statement: The authors declare no competing interests.

Data sharing statement: The datasets in the present study are available upon reasonable request.

ARRIVE guidelines statement: The authors have read the ARRIVE guidelines, and the manuscript was prepared and revised

Ru-Jia Xie, Lu Zheng, Shuang Cai, Yu-Si Chen, Yi Yang, Ting Yang, Bing Han, Qin Yang, Guizhou Provincial Key Laboratory of Pathogenesis and Drug Research on Common Chronic Diseases, College of Basic Medical Sciences, Guizhou Medical University, Guiyang 550025, Guizhou Province, China

Ru-Jia Xie, Lu Zheng, Shuang Cai, Yu-Si Chen, Yi Yang, Ting Yang, Bing Han, Qin Yang, Department of Pathophysiology, College of Basic Medical Sciences, Guizhou Medical University, Guiyang 550025, Guizhou Province, China

Xiao-Xia Hu, Department of Physiology, College of Basic Medical Sciences, Guizhou Medical University, Guiyang 550025, Guizhou Province, China

Corresponding author: Bing Han, MD, Academic Research, Department of Pathophysiology, College of Basic Medical Sciences, Guizhou Medical University, Dongqing Road, Guiyang 550025, Guizhou Province, China. 47569390@qq.com

Abstract

BACKGROUND

Calpain-2 is a Ca^{2+}-dependent cysteine protease, and high calpain-2 activity can enhance apoptosis mediated by multiple triggers.

AIM

To investigate whether calpain-2 can modulate aberrant endoplasmic reticulum (ER) stress-related apoptosis in rat hepatocyte BRL-3A cells.

METHODS

BRL-3A cells were treated with varying doses of dithiothreitol (DTT), and their viability and apoptosis were quantified by 3-[4, 5-dimethyl-2-thiazolyl]-2, 5-diphenyl-2-H-tetrazolium bromide and flow cytometry. The expression of ER stress- and apoptosis-related proteins was detected by Western blot analysis. The protease activity of calpain-2 was determined using a fluorescent substrate, *N*-succinyl-Leu-Leu-Val-Tyr-AMC. Intracellular Ca^{2+} content, and ER and calpain-2 co-localization were characterized by fluorescent microscopy. The impact of calpain-2 silencing by specific small interfering RNA on caspase-12 activation and apoptosis of BRL-3A cells was quantified.

RESULTS

DTT exhibited dose-dependent cytotoxicity against BRL-3A cells and treatment with 2 mmol/L DTT triggered BRL-3A cell apoptosis. DTT treatment significantly upregulated 78 kDa glucose-regulated protein, activating transcription factor 4, C/EBP-homologous protein expression by >2-fold, and

according to the ARRIVE guidelines.

Manuscript source: Unsolicited manuscript

Received: December 2, 2019
Peer-review started: December 2, 2019
First decision: December 12, 2019
Revised: February 20, 2020
Accepted: March 9, 2020
Article in press: March 9, 2020
Published online: April 7, 2020

P-Reviewer: Aureliano M, Abdulnour-Nakhoul SM, El-Bendary M, Marickar F
S-Editor: Zhang L
L-Editor: Filipodia
E-Editor: Zhang YL

enhanced PRKR-like ER kinase phosphorylation, caspase-12 and caspase-3 cleavage in BRL-3A cells in a trend of time-dependence. DTT treatment also significantly increased intracellular Ca^{2+} content, calpain-2 expression, and activity by >2-fold in BRL-3A cells. Furthermore, immunofluorescence revealed that DTT treatment promoted the ER accumulation of calpain-2. Moreover, calpain-2 silencing to decrease calpain-2 expression by 85% significantly mitigated DTT-enhanced calpain-2 expression, caspase-12 cleavage, and apoptosis in BRL-3A cells.

CONCLUSION
The data indicated that Ca^{2+}-dependent calpain-2 activity promoted the aberrant ER stress-related apoptosis of rat hepatocytes by activating caspase-12 in the ER.

Key words: Calcium; Calpain-2; Caspase-12; Endoplasmic reticulum stress; Apoptosis; Hepatocyte

Core tip: Hepatocyte apoptosis is associated with many liver diseases. During the process of apoptosis, calpain-2 can cleave several apoptosis-related proteins. However, the regulatory mechanisms by which calpain-2 regulates the endoplasmic reticulum (ER) stress-mediated hepatocyte apoptosis remain unclear. In this study, the effect of calpain-2 on ER stress-mediated hepatocyte apoptosis and the underlying regulatory mechanisms was investigated. Our data indicate that calpain-2 is crucial for the aberrant ER stress-induced apoptosis of hepatocytes and may be a novel therapeutic target for liver diseases.

Citation: Xie RJ, Hu XX, Zheng L, Cai S, Chen YS, Yang Y, Yang T, Han B, Yang Q. Calpain-2 activity promotes aberrant endoplasmic reticulum stress-related apoptosis in hepatocytes. *World J Gastroenterol* 2020; 26(13): 1450-1462
URL: https://www.wjgnet.com/1007-9327/full/v26/i13/1450.htm
DOI: https://dx.doi.org/10.3748/wjg.v26.i13.1450

INTRODUCTION

Hepatocyte apoptosis participates in the pathogenesis of many types of liver diseases. Actually, apoptotic hepatocytes are observed in the liver of patients with acute liver injury, non-alcoholic fatty liver diseases, hepatic fibrosis, and liver cirrhosis[1-5]. However, the regulatory mechanisms underlying hepatocyte apoptosis remains elusive. It is notable that aberrant endoplasmic reticulum (ER) stress can trigger hepatocyte apoptosis[6,7]. While the ER is physiologically responsible for the control of protein proper folding and function, many factors such as the unfolded protein response, ER overload response and others can disturb ER function, leading to ER stress[8,9]. During the process of ER stress, the ER chaperon glucose-regulated protein (GRP78) changes its binding from ER transmembrane protein PRKR-like endoplasmic reticulum kinase (PERK) to unfolded/misfolded proteins to release PERK[10]. The released PERK is subjected to self-phosphorylation, which promotes the expression of transcription factors of activating transcription factor 4 (ATF4) and C/EBP-homologous protein (CHOP) in cells[11]. The upregulated ATF4 and CHOP can enter the nucleus to regulate the transcription of related genes[12]. Such compensative responses may reduce the accumulation of unfolded proteins, leading to the re-establishment of cellular homeostasis. However, if the ER stress cannot be alleviated, aberrant ER stress can trigger cell apoptosis, particularly by activating caspase-12[13-15]. However, how aberrant ER stress induces caspase-12 activation to trigger cell apoptosis has not been clarified in hepatocytes.

Calpain-2 is a Ca^{2+}-dependent cysteine protease that can cleave its protein substrates. Calpain-2 can regulate cell cycle, differentiation, and apoptosis[16]. Previous studies have revealed that calpains promote ER stress-related apoptosis by activating caspase-12[17-19]. Actually, our previous studies indicated that ER stress occurred in hepatocytes in a rat model of carbon tetrachloride-induced hepatic fibrosis, which was associated with increased calpain-2 and caspase-12 expression and hepatocyte apoptosis[20,21]. However, it is unclear whether calpain-2 can modulate caspase-12

activation and ER stress-related apoptosis in hepatocytes.

This study explored the importance of calpain-2 in regulating caspase-12 activation and dithiothreitol (DTT)-induced ER stress-related apoptosis in hepatocytes. The results indicated that calpain-2 activity was crucial for DTT-induced ER stress-related hepatocyte apoptosis by activating caspase-12 *in vitro*.

MATERIALS AND METHODS

Special reagents included rat non-tumor BRL-3A cells (Number: KCB92013YJ, Kunming Cell Bank of Chinese Academy of Sciences, China), fetal bovine serum, Dulbecco's modified Eagle's medium (DMEM; GIBCO, New York, NY, United States), Acrylamide, bisacrylamide, ammonium peroxydisulfate, glycine, Tri-hydroxymethyl aminomethane, 3-[4, 5-dimethyl-2-thiazolyl]-2, 5-diphenyl-2-H- tetrazolium bromide (MTT), Tween 20, DTT, dimethyl sulfoxide (Genview, League City, TX, United States), *N*-succinyl-Leu-Leu-Val-Tyr-AMC, antibodies against GRP78, PERK, ATF4, CHOP, and caspase-12 (Abcam, Cambridge, United Kingdom), antibodies against p-PERK (Affinity Biosciences, Cincinnati, OH, United States), calpain-2 and β-actin (Cell Signaling Technologies, Danvers, MA, United States), caspase-3 and secondary antibodies (Boster Biological Engineering, Wuhan, China), polyvinylidene difluoride membranes and enhanced chemiluminescence kit (Millipore, Burlington, MA, United States). Calpain-2-specific and control small interfering RNAs (siRNAs) and siRNA dilution buffer were produced by Santa Cruz Biotechnology (Santa Cruz, CA, United States), and the Annexin V-FITC Detection Kit, ER-tracker Red, and Fluo-3 AM were obtained from Beyotime Institute of Biotechnology (Nanjing, China).

Cell culture and treatment

Rat non-tumor hepatocyte BRL-3A cells were cultured in high-glucose DMEM supplemented with 10% fetal bovine serum, 100 units/mL penicillin, and 100 μg/mL streptomycin at 37 °C in a humidified atmosphere of 5% CO_2. When the cells reached 80% confluency, the cells were treated with DTT, an inhibitor of disulfide bond formation, to induce ER stress.

MTT assay

We examined the impact of DTT on the BRL-3A cell viability by MTT. Briefly, BRL-3A cells (5×10^3 cells/well) were treated in triplicate with 0-10 mmol/L of DTT for 24 h. During the last 4-h culture, the cells were treated with 0.5 mg/mL MTT reagent. The resulting formazan in individual wells was dissolved with 150 μL dimethyl sulfoxide, and the absorbance at 570 nmol/L in individual wells was measured using a microplate reader.

Flow cytometry

The effect of DTT on the apoptosis of BRL-3A cells was quantified by flow cytometry using the Annexin V/propidium (PI) kit per the manufacturer's protocol. Briefly, BRL-3A cells (5×10^5 cells/flask) were treated in triplicate with vehicle or 2.0 mmol/L DTT, a sub-toxic dose, for varying time periods[22]. After being washed twice with phosphate-buffered saline, the cells were stained with FITC-Annexin-V and PI. The percentages of apoptotic cells in individual groups were quantified by flow cytometry in a FACSCalibur™ (BD Biosciences, Franklin Lakes, NJ, United States).

Western blotting

After treatment with 2.0 mmol/L DTT for varying time periods, BRL-3A cells were lysed in a RIPA buffer and centrifuged, followed by quantifying the protein concentrations. The cell lysates (50 μg/lane) were separated by sodium dodecyl sulfate polyacrylamide gel electrophoresis (SDS-PAGE) on 10%-12% gels and transferred onto polyvinylidene difluoride membranes. After being blocked in 5% non-fat dry milk in Tris-buffered saline with Tween-20, the membranes were probed overnight at 4°C with primary antibodies against GRP78 (1:1500), PERK (1:1500), p-PERK (1:1500), ATF4 (1:1500), CHOP (1:1500), calpain-2 (1:1000), caspase-12 (1:1000), cleaved capase-3 (1:500), and β-actin (1:1000). The bound antibodies were detected with horseradish peroxidase-conjugated secondary antibodies and visualized using enhanced chemiluminescence reagents. The signal intensity was measured using Bio-Rad imaging system (Bio-Rad, Hercules, CA, United States) and analyzed by Quantity One software (Bio-Rad).

Microscopy analysis of intracellular Ca^{2+} content

The intracellular Ca^{2+} content in BRL-3A cells was detected by microscopy after staining with a Ca^{2+}-sensitive fluorescent dye, Fluo-3 AM[23]. In brief, BRL-3A cells

were treated in triplicate with 2.0 mmol/L DTT for 0, 6, 12, and 24 h. After being washed with Hank's balanced salt solution, the cells were stained with Fluo-3 AM at 37 °C for 45 min. The morphology and fluorescent signals in individual wells of cells were examined under a light and fluorescent microscope (FV1000; Olympus, Tokyo, Japan).

Calpain activity assay

We measured cellular calpain enzymatic activity using a fluorescence substrate *N*-succinyl-Leu-Leu-Val-Tyr-AMC, as previously described[24]. In brief, individual cell lysates were reacted at 37°C with 40 μmol/L *N*-succinyl-Leu-Leu-Val-Tyr-AMC for 1 h, and the fluorescent signals were measured using a fluorescence plate reader.

Immunofluorescent microscopy

BRL-3A cells were cultured on coverslips overnight, and treated with 2.0 mmol/L DTT for 0, 6, 12, and 24 h. The cells were stained with ER-tracker Red (ER fluorescent dye)[25,26], fixed in 2% paraformaldehyde, and permeabilized with 0.2% Triton X-100. Subsequently, the cells were stained with anti-calpain-2 and Alexa Fluor 488-conjugated secondary antibody. We photoimaged the fluorescent signals under a fluorescence microscope (IX71; Olympus).

Calpain-2 siRNA transfection

BRL-3A cells (5×10^5 cells/flask) were grown in antibiotic-free medium overnight and transfected with control or calpain-2 specific siRNA for 48 h. The efficacy of calpain-2 silencing was determined by Western blotting. Subsequently, the different groups of cells were treated in triplicate with 2.0 mmol/L DTT for 24 h and used for analysis of apoptosis, calpain-2, and cleaved caspase-12 expression.

Statistical analysis

Data are present as the mean ± SD. We compared the different groups of data by one-way analysis of variance and post hoc least significant difference test using SPSS 13.0 software. Statistical significance was defined at a P value < 0.05.

RESULTS

DTT exhibits cytotoxicity against BRL-3A cells in a dose-dependent manner

To determine the toxicity of DTT, BRL-3A cells were treated with 0-10 mmol/L DTT for 24 h and their viability was measured by MTT (Figure 1A). DTT had dose-dependent cytotoxicity against BRL-3A cells and the median lethal dose (LD50) value for BRL-3A cells was about 4 mmol/L in our experimental condition. Longitudinal analysis displayed that treatment with 2 mmol/L DTT for 6 h significantly increased the percentages of apoptotic BRL-3A cells by about 3-fold ($P < 0.01$), and treatment for a longer period did not significantly increase the frequency of apoptotic BRL-3A cells (Figure 1B and C). Hence, DTT exhibited dose-dependent cytotoxicity against BRL-3A cells by increasing their apoptosis *in vitro*.

DTT induces ER stress in BRL-3A cells

DTT can induce ER stress in many types of cells[27,28]. To understand the role of DTT in decreasing viability, BRL-3A cells were treated with 2.0 mmol/L DTT for varying time periods and their ER stress-related proteins were quantified by Western blot (Figure 2). DTT treatment for 6 h upregulated GRP78, ATF4, and CHOP expression and PERK phosphorylation by about 2-fold in BRL-3A cells and treatment with DTT for a longer period further increased its effects. The effects of DTT on upregulating GRP78 expression and PERK phosphorylation appeared to have a trend of time-dependence. Thus, DTT induced ER stress in BRL-3A cells *in vitro*.

DTT enhances caspase-12 and caspase-3 activation and calpain-2 activity in BRL-3A cells

Aberrant ER stress can promote sensitive cell apoptosis by inducing caspase-12 and caspase-3 activation, and calpain-2 participates in the process of ER-stress-related apoptosis[18,19,25]. To understand the consequence of ER stress induced by DTT, the relative levels of caspase-3, and caspase-12 cleavage, and calpain-2 activity were quantified. Treatment with 2 mmol/L DTT significantly induced time-dependent caspase-12 cleavage and increased the levels of cleaved caspase-3 in BRL-3A cells by 2-2.5 fold (Figure 3A and B). Similarly, DTT treatment significantly upregulated calpain-2 expression by more than 2-fold and enhanced calpain-2 activity in a trend of time-dependence in BRL-3A cells (Figure 3C and D). Given that calpain-2 activity is Ca^{2+}-dependent, we further quantified intracellular Ca^{2+} content in each group of cells

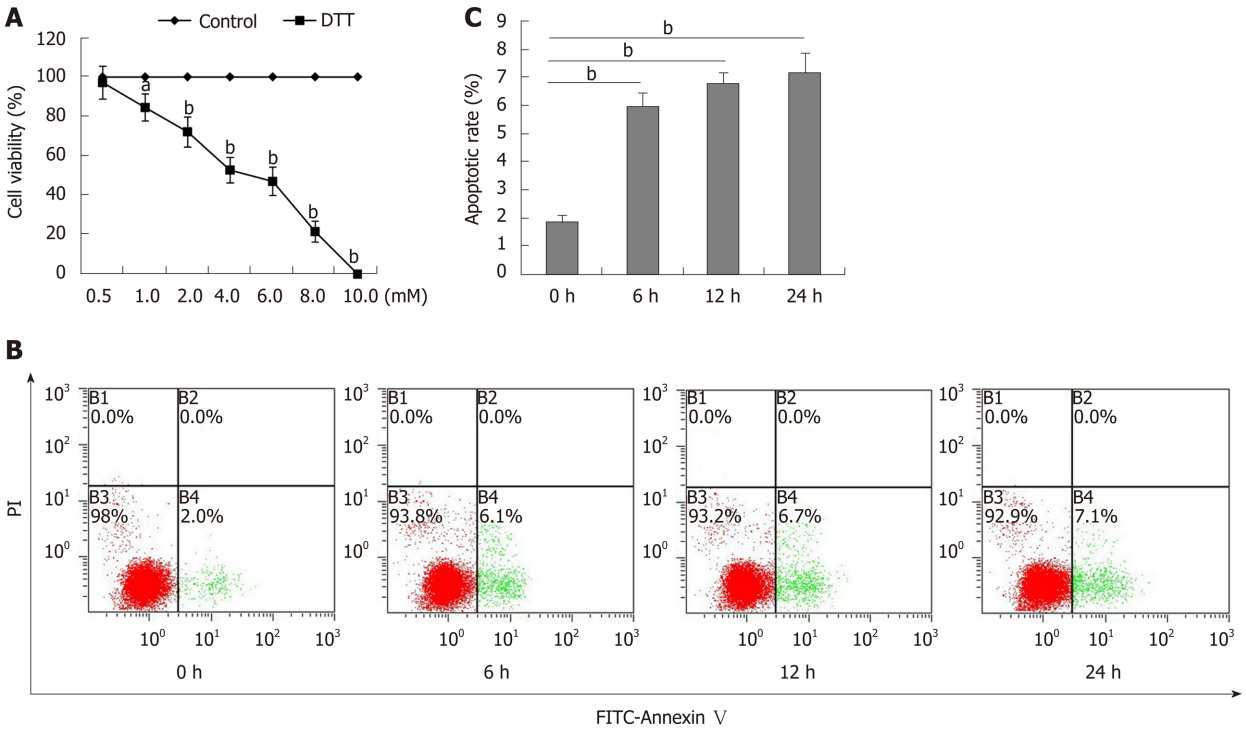

Figure 1 Dithiothreitol exhibits dose-dependent cytotoxicity against BRL-3A cells. A: BRL-3A cells were treated in triplicate with, or without, the indicated doses of dithiothreitol (DTT) for 24 h and their viability was examined by MTT. The percentages (y) of cell viability were calculated by the equation, y = -9.3654x + 95.744 with a correlation (R^2 = 0.9781), here x represents DTT concentration. Accordingly, the DTT LD_{50} = 4.88 mM; B, C: Subsequently, BRL-3A cells were treated with 2.0 mmol/L DTT for varying periods and stained with FITC-Annexin-V and PI. The percentages of mechanically damaged (B1 quadrant), healthy (B3), early (B4) and late apoptotic and necrotic (B2) cells were analyzed by flow cytometry. Data are representative flow cytometry charts or expressed as the mean ± SD of each group from three separate experiments. $^aP < 0.05$, $^bP < 0.01$.

by microscopy. After staining with Fluo-3 AM, we observed that DTT treatment time dependently increased the content of clustery Ca^{2+} by 2-3 fold in BRL-3A cells at 12 and 24 h post treatment (Figure 4). To identify additional evidence to demonstrate the importance of calpain-2 activity, we stained the different groups of cells with fluorescent anti-calpain-2 and ER-tracker Red, and observed the co-localization of red ER and green calpain-2 signals by fluorescent microscopy. As shown in Figure 5, there were obviously increased merged yellow signals in the DTT-treated cells, particularly at the later time point, while there was little merged signal in the cells without DTT treatment. Collectively, such data indicated that DTT-induced aberrant ER stress promoted the apoptosis of BRL-3A cells by activating caspase-12 and increasing calpain-2 activity.

Calpain-2 silencing mitigates DTT-induced caspase-12 activation and apoptosis in BRL-3A cells

Finally, we tested whether calpain-2 silencing could modulate the DTT-induced caspase-12 activation and apoptosis of BRL-3A cells. We found that transfection with calpain-2 specific siRNA, but not the control, significantly decreased calpain-2 expression by about 85%, demonstrating the efficacy of calpain-2 silencing ($P < 0.01$; Figure 6A). Calpain-2 silencing also significantly mitigated the DTT-upregulated calpain-2 expression near 80% ($P < 0.01$; Figure 6B). Although calpain-2 silencing did not alter the DTT-upregulated caspase-12 expression, it significantly reduced the caspase-12 cleavage near 63% in BRL-3A cells, relative to that in the control cells ($P < 0.01$; Figure 6C). More importantly, calpain-2 silencing significantly decreased the percentage of DTT-induced apoptosis of BRL-3A cells by 50% ($P < 0.05$; Figure 6D and E). Together, the significantly decreased caspase-12 activation and cell apoptosis indicated that calpain-2 activity was crucial for DTT-induced ER stress-related caspase-12 activation and apoptosis in BRL-3A cells.

DISCUSSION

Many factors can induce ER stress including chemical agents such as tunicamycin,

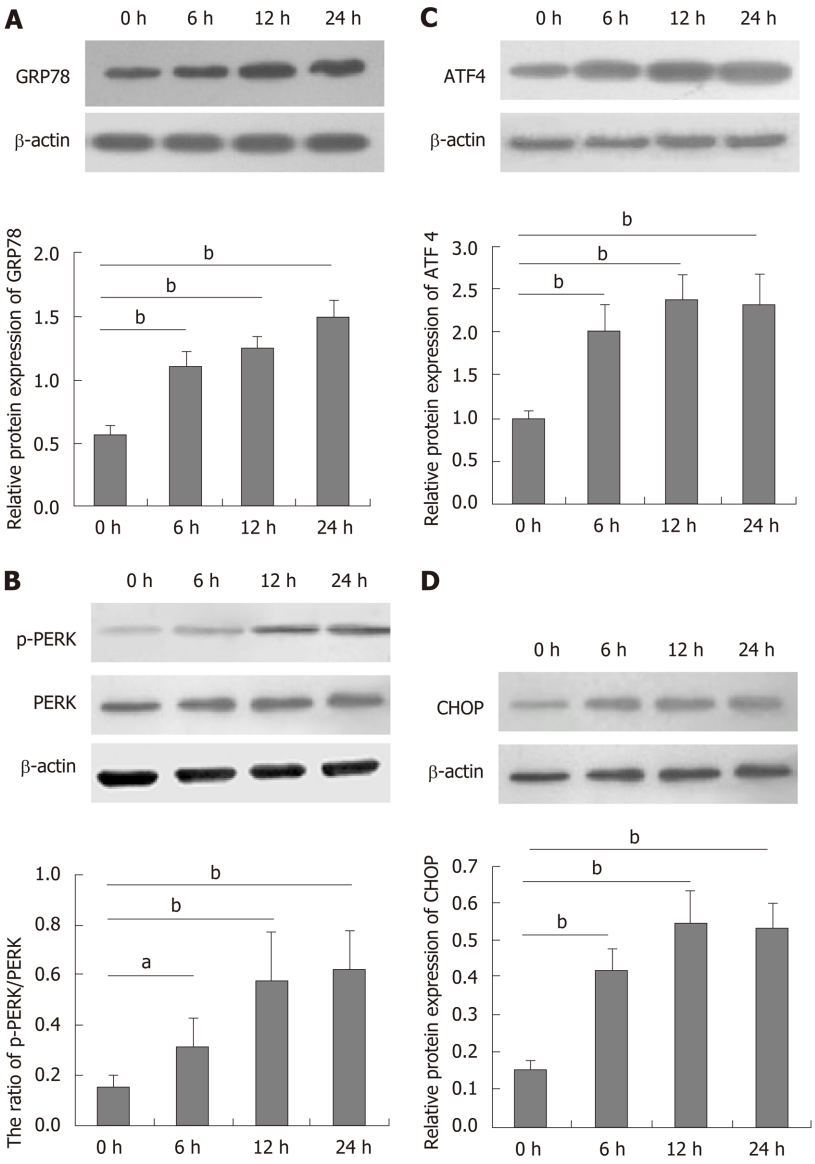

Figure 2 Dithiothreitol induces endoplasmic reticulum stress in BRL-3A cells. BRL-3A cells were treated in triplicate with, or without, 2.0 mmol/L dithiothreitol for the indicated time periods, and the relative levels of glucose-regulated protein 78, activating transcription factor 4 and C/EBP-homologous protein to β-actin expression and PERK phosphorylation in each group of cells were quantified by Western blot. Data are representative images or expressed as the mean ± SD of each group of cells from three separate experiments. A: Relative glucose-regulated protein 78 expression; B: Relative PERK phosphorylation; C: Relative activating transcription factor 4 expression; D: Relative C/EBP-homologous protein expression. $^{a}P < 0.05$, $^{b}P < 0.01$.

thapsigargin, and DTT[27,29]. In this study, we used a sub-toxic 2.0 mmol/L DTT to induce ER stress in BRL-3A cells, based on a previous report[22]. It is well known that DTT can inhibit the formation of disulfide bonds and result in the accumulation of unfolded proteins in the ER, leading to ER stress.

Aberrant ER stress-induced apoptosis of hepatocytes participates in the pathogenesis of several types of liver diseases[30-32]. In this study, we found that DTT had strong cytotoxicity against rat hepatocyte BRL-3A cells and its cytotoxicity was dose-dependent. Furthermore, treatment with DTT induced ER stress in BRL-3A cells by significantly upregulating GRP78, ATF4, and CHOP expression and PERK phosphorylation. More importantly, DTT treatment significantly increased the frequency of apoptotic BRL-3A cells, supporting that aberrant ER stress promotes the apoptosis of hepatocytes[33,34]. Given that hepatocyte apoptosis participates in the pathogenesis of several types of liver diseases, inhibition of ER stress may be valuable for protecting hepatocytes from apoptosis.

ER stress-related apoptosis is independent of mitochondria and death receptors, and is thought to be mediated by activating caspase-12, an ER-anchored caspase[35,36]. A previous study has reported that the caspase-12 gene is mutated in most human

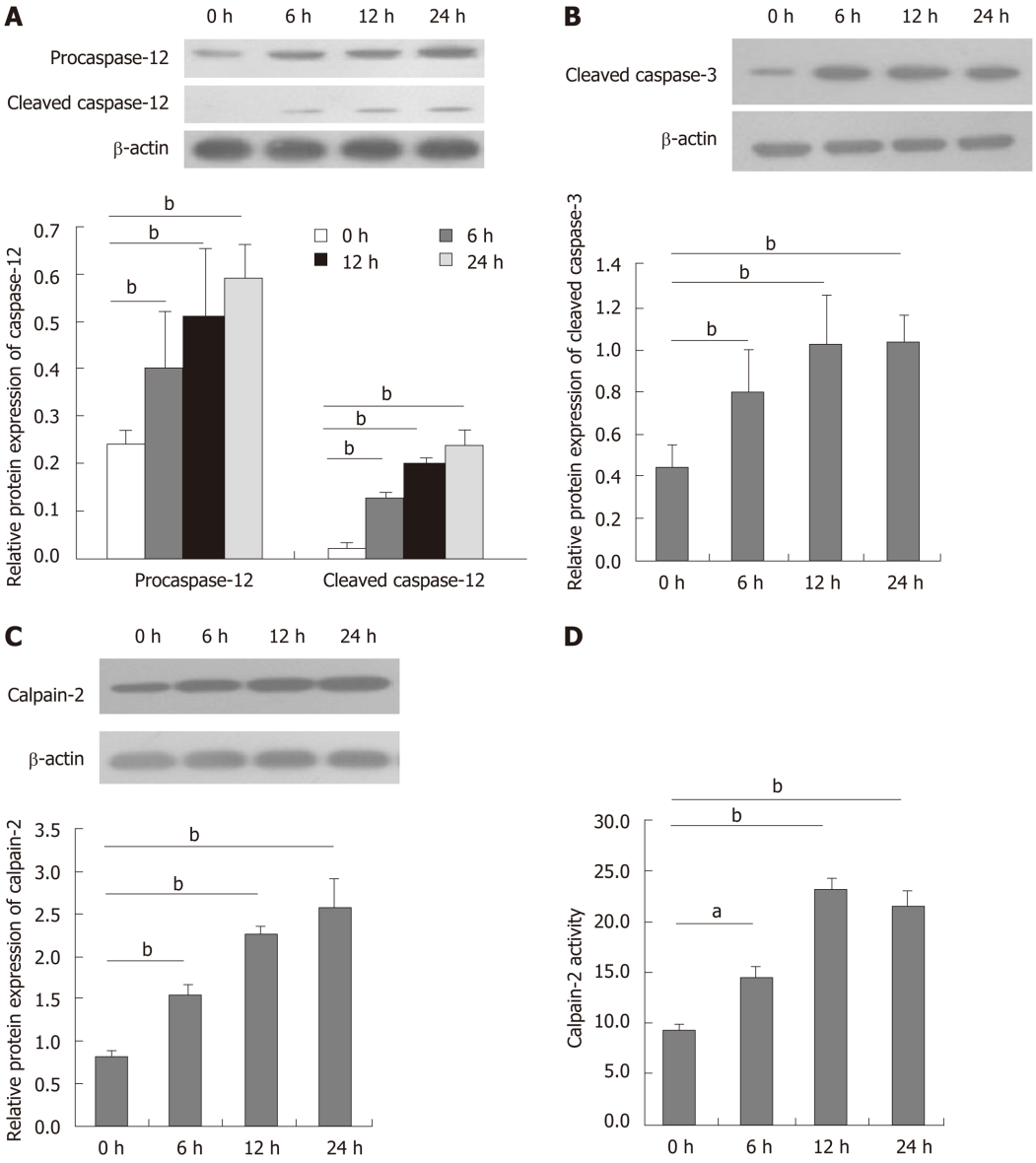

Figure 3 Dithiothreitol induces caspase-12 and caspase-3 activation and increases calpain-2 activity in BRL-3A cells. After treatment with 2.0 mmol/L dithiothreitol for varying periods, the relative levels of caspase-12, cleaved caspase-12 and cleaved caspase-3 as well as calpain-2 expression in each group of BRL-3A cells were quantified by Western blotting. Furthermore, the activity of calpain-2 in each group of cells was measured. Data are representative images or expressed as the mean ± SD of each group of cells from three separate experiments. A: Caspase-12 activation; B: Caspase-3 activation; C: Calpain-2 expression; D: Calpain-2 activity. $^{a}P < 0.05$, $^{b}P < 0.01$.

hepatocyte lines[23], so we chose rat non-tumor hepatocyte BRL-3A cells as a cell model in this study. Similar to other caspases, procaspase-12 has to be activated by cleaving a short inhibitory peptide, and cleaved caspase-12 can activate the downstream effector caspase-3, leading to apoptosis[37]. Actually, caspase-12-/- cells are resistant to ER stress-induced apoptosis[38]. In this study, we found that DTT treatment significantly induced caspase-12 and caspase-3 cleavage in BRL-3A cells. Such data indicated that activated caspase-12 and caspase-3 contributed to the ER stress-related apoptosis of BRL-3A cells, although the precise mechanisms underlying caspase-12 activation in hepatocytes remain incompletely understood. A recent study revealed that enhanced calpain-2 activity is crucial for caspase-12 activation[39]. Calpain-2 is a Ca^{2+}-dependent cysteine protease, and its activity and function depend on the concentrations of intracellular Ca^{2+}[40]. As the ER holds the major pool of Ca^{2+}, ER stress can promote Ca^{2+} efflux from the ER, which may be responsible for enhancing calpain-2 activity and its ER accumulation[41]. Interestingly, we found that DTT treatment significantly increased intracellular Ca^{2+} content and calpain-2 activity in BRL-3A cells. Furthermore, DTT treatment promoted the accumulation of calpain-2 in the ER of BRL-3A cells. More importantly, calpain-2 silencing not only significantly

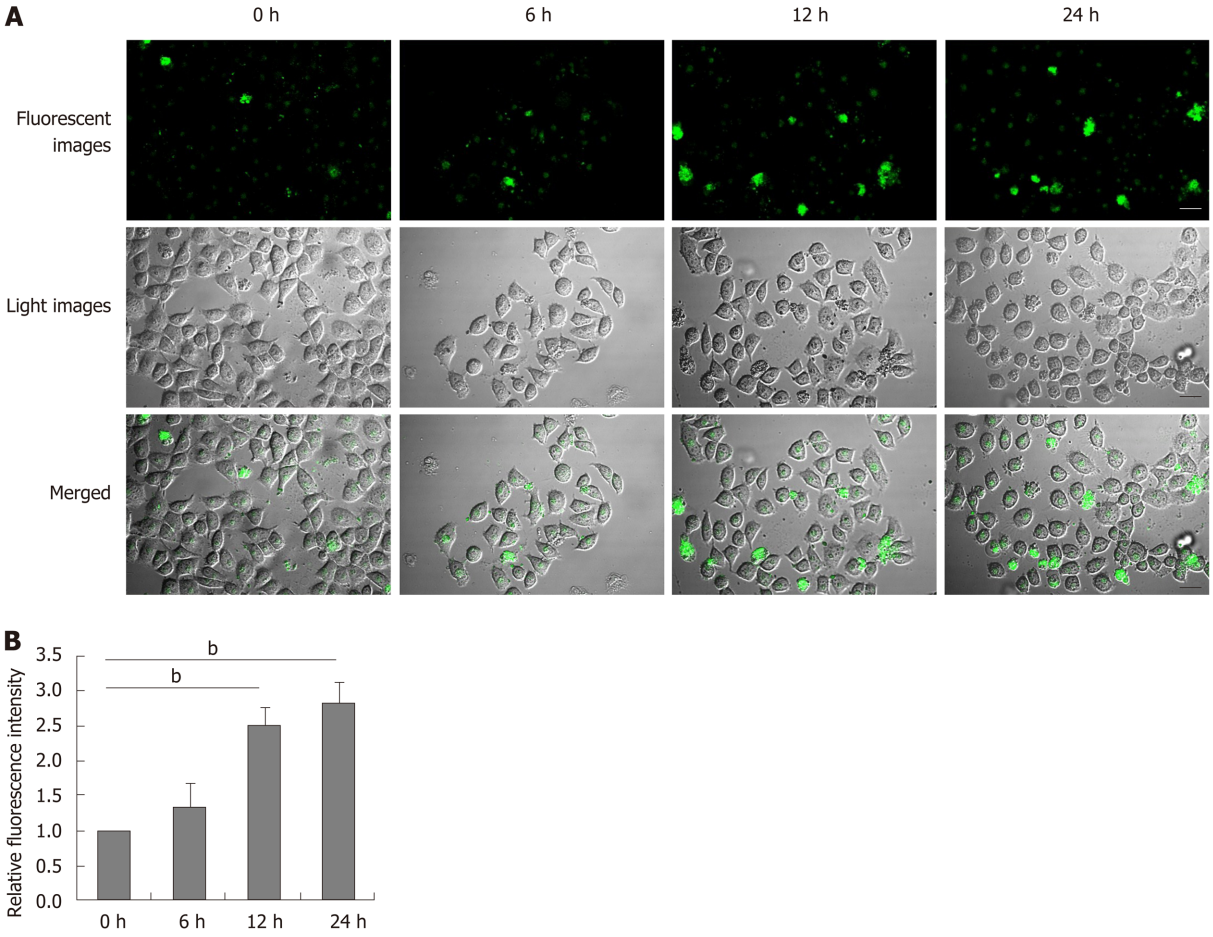

Figure 4 Dithiothreitol increases the levels of intracellular Ca^{2+} in BRL-3A cells. After treatment with 2.0 mmol/L dithiothreitol for varying time periods, the cells were labeled by Fluo-3 AM. The cell morphology and fluorescent signals in cells were observed by microscopy. A: Representative images of Fluo-3 fluorescence and morphology in BRL-3A cells following dithiothreitol treatment (Scale bars: 25 μm); B: Quantification of fluorescence intensity in BRL-3A cells. Data are representative images (magnification 200 ×) or expressed as the mean ± SD of each group of cells from three separate experiments. $^{b}P < 0.01$.

mitigated DTT-upregulated calpain-2 expression and caspase-12 activation, but also decreased the DTT-triggered apoptosis of BRL-3A cells. Hence, the DTT-induced ER stress increased intracellular Ca^{2+} content and calpain-2 expression, leading to calpain-2 activation, which cleaved caspase-12 to trigger apoptosis of BRL-3A cells. In our recent preliminary studies, we found that treatment with Z-LLY-fmk, a specific inhibitor of calpain, significantly mitigated the DTT-induced hepatocyte apoptosis by more than 90% (Chen *et al*[11], unpublished data). Such novel findings may provide new evidence to demonstrate that the Ca^{2+}-dependent calpain-2 activity is crucial for promoting the ER stress-related apoptosis in hepatocytes.

In conclusion, our data indicated that DTT exhibited dose-dependent cytotoxicity against rat hepatocytes, and induced ER stress and apoptosis in BRL-3A cells. Evidently, DTT treatment significantly upregulated GRP78, ATF4, and CHOP expression and PERK phosphorylation; increased intracellular Ca^{2+} content and calpain-2 activity; and induced caspase-12 and caspase-3 activation in BRL-3A cells. Furthermore, calpain-2 silencing significantly mitigated DTT-upregulated calpain-2 expression and DTT-induced caspase-12 activation as well as apoptosis of BRL-3A cells. The results indicated that enhanced calpain-2 activity promoted aberrant ER stress-mediated apoptosis of hepatocytes. Our data suggest that ER stress may induce Ca^{2+} release from the ER and lead to the recruitment and activation of calpain-2 in the ER, where calpain-2 activates caspase-12 and caspase-3 and triggers apoptosis in hepatocytes. Therefore, ER stress may be a novel therapeutic target and our findings may provide new evidence to demonstrate the importance of Ca^{2+}-dependent calpain-2 in caspase-12 activation and ER stress-related apoptosis in hepatocytes.

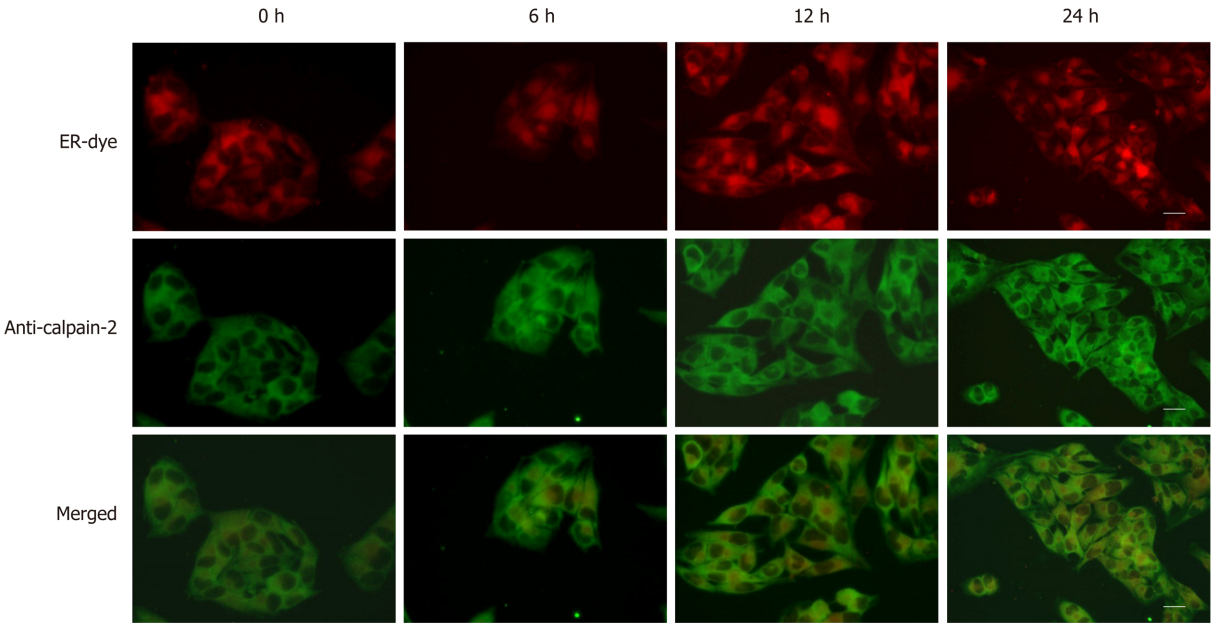

Figure 5 Dithiothreitol promotes the accumulation of calpain-2 in the endoplasmic reticulum of BRL-3A cells. After treatment with 2.0 mmol/L dithiothreitol for varying time periods, the cells were labeled with endoplasmic reticulum-tracker red dye, fixed, permeabilized, followed by staining with fluorescent-anti-calpain-2 (green). The cells were examined by fluorescent microscopy, scale bars, 25 μm. Data are representative images (magnification 200 ×) of each group of cells from three separate experiments.

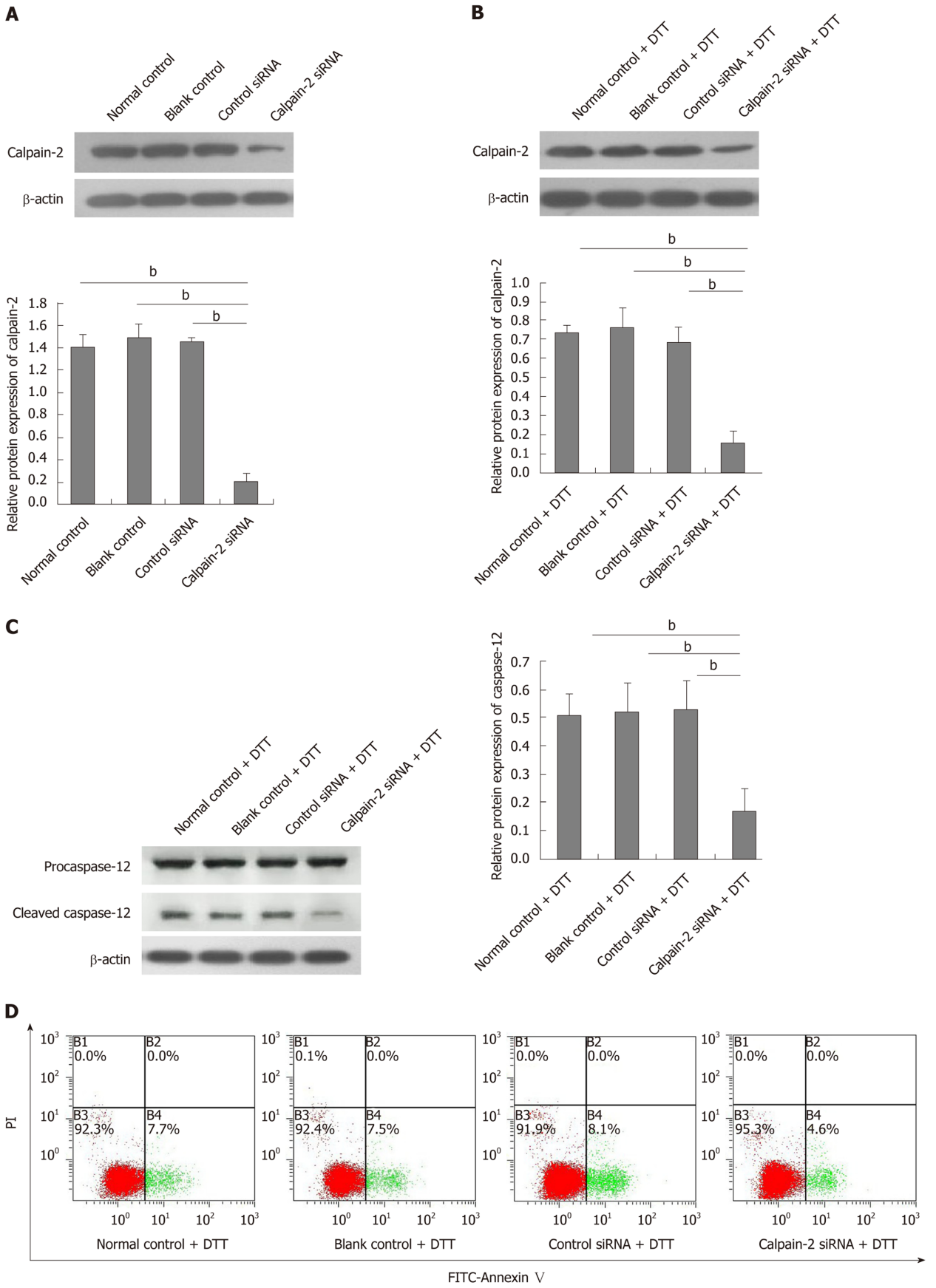
A
Normal control
Blank control
Control siRNA
Calpain-2 siRNA
Calpain-2
β-actin
Relative protein expression of calpain-2
b
B
Normal control + DTT
Blank control + DTT
Control siRNA + DTT
Calpain-2 siRNA + DTT
C
Procaspase-12
Cleaved caspase-12
Relative protein expression of caspase-12
D
PI
FITC-Annexin V
B1 0.0%
B2 0.0%
B3 92.3%
B4 7.7%
B1 0.1%
B2 0.0%
B3 92.4%
B4 7.5%
B1 0.0%
B2 0.0%
B3 91.9%
B4 8.1%
B1 0.0%
B2 0.0%
B3 95.3%
B4 4.6%

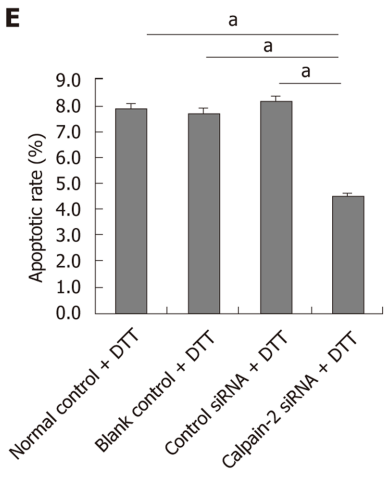

Figure 6 Calpain-2 silencing mitigates dithiothreitol-upregulated calpain-2 expression, caspase-12 activation and apoptosis of BRL-3A cells. BRL-3A cells were transfected with, or without, control or calpain-2 specific siRNA for 48 h and treated with, or without, dithiothreitol (DTT). The relative levels of calpain-2 expression and caspase-12 activation were quantified by Western blot. The percentages of apoptotic cells were quantified by flow cytometry. Data are representative images or expressed as the mean ± SD of each group of cells from three separate experiments. A: Calpain-2 silencing; B: Calpain-2 silencing mitigates DTT-upregulated calpain-2 expression; C: Calpain-2 silencing decreases DTT-induced caspase-12 activation; D, E: Calpain-2 silencing mitigates DTT-triggered apoptosis of BRL-3A cells. $^{a}P < 0.05$, $^{b}P < 0.01$.

ARTICLE HIGHLIGHTS

Research background

Endoplasmic reticulum (ER) stress-mediated hepatocyte apoptosis is associated with many liver diseases, however, the underlying mechanisms remain unknown. Calpain-2 is a Ca^{2+}-dependent cysteine protease, which can cleave several apoptosis-related proteins and mediate the process of apoptosis. Our data indicate that calpain-2 is crucial for the aberrant ER stress-induced apoptosis of hepatocytes and may be a novel therapeutic target for liver diseases.

Research motivation

Calpain-2 protease is involved in multiple signaling pathways mediating apoptotic processes, including the mitochondrial pathway. However, the regulatory mechanisms by which calpain-2 regulates ER stress-mediated hepatocyte apoptosis remain unclear. Our study further assessed its potential as a therapeutic target for inhibiting hepatocyte apoptosis.

Research objectives

In this study, the effect of calpain-2 on ER stress-mediated hepatocyte apoptosis and the underlying regulatory mechanisms were investigated. Our data indicates that ER stress may be a novel therapeutic target, and our findings provide new evidence to demonstrate the importance of Ca^{2+}-dependent calpain-2 in caspase-12 activation and ER stress-related apoptosis in hepatocytes.

Research methods

Our study employed Western blotting, flow cytometry, confocal microscopy, and calpain-2 small interfering RNA to elucidate the mechanism of calpain-2-mediated activation of caspase-12, a key molecule in ER stress-related apoptosis. These research methods are relatively mature technically, thus ensuring the reliability of the results from this study.

Research results

The ER stress inducer dithiothreitol can significantly increase intracellular Ca^{2+}content, calpain-2 expression and activity in hepatocytes and promote caspase-12 cleavage and apoptosis in hepatocytes. Moreover, calpain-2 silencing can mitigate dithiothreitol-enhanced calpain-2 expression, caspase-12 cleavage, and apoptosis in hepatocytes. These results indicated that enhanced calpain-2 activity promoted aberrant ER stress-mediated apoptosis of hepatocytes. In future studies, we will further investigate whether calpain-2 can mediate hepatocyte death through other mechanisms, such as regulating autophagy.

Research conclusions

Ca^{2+}-dependent calpain-2 activity promoted the aberrant ER stress-related apoptosis of rat hepatocytes by activating caspase-12 in the ER. ER stress may be a novel therapeutic target and our findings may provide new evidence to demonstrate the importance of Ca^{2+}-dependent calpain-2 in caspase-12 activation and ER stress-related apoptosis in hepatocytes. ER stress may induce Ca^{2+} release from the ER and lead to the recruitment and activation of calpain-2 in the ER, where, calpain-2 activates caspase-12 and caspase-3, and triggers apoptosis in hepatocytes. Calpain-2 activity plays an important role in aberrant ER stress-related apoptosis in hepatocytes.

Inhibition of calpain-2 expression and activity is expected to be an effective way to alleviate hepatocyte apoptosis and liver injury.

Research perspectives

Because calpain-2 is a protease, in addition to focusing on its expression, studies should also focus on its activity. In our recent preliminary studies, we found that treatment with Z-LLY-fmk, a specific inhibitor of calpain activity, significantly mitigated DTT-induced hepatocyte apoptosis by more than 90%.

ACKNOWLEDGEMENTS

We thank Hua Pei and Jinxingyi Wang for their technical advice in using flow cytometry and microscope in the Basic Medical Science Research Center of Guizhou Medical University. We would like to thank Dr. Tengxiang Chen for his comments on this manuscript.

REFERENCES

1 **Kanda T**, Matsuoka S, Yamazaki M, Shibata T, Nirei K, Takahashi H, Kaneko T, Fujisawa M, Higuchi T, Nakamura H, Matsumoto N, Yamagami H, Ogawa M, Imazu H, Kuroda K, Moriyama M. Apoptosis and non-alcoholic fatty liver diseases. *World J Gastroenterol* 2018; **24**: 2661-2672 [PMID: 29991872 DOI: 10.3748/wjg.v24.i25.2661]

2 **Akazawa Y**, Nakao K. To die or not to die: death signaling in nonalcoholic fatty liver disease. *J Gastroenterol* 2018; **53**: 893-906 [PMID: 29574534 DOI: 10.1007/s00535-018-1451-5]

3 **Iorga A**, Dara L, Kaplowitz N. Drug-Induced Liver Injury: Cascade of Events Leading to Cell Death, Apoptosis or Necrosis. *Int J Mol Sci* 2017; 18 [PMID: 28486401 DOI: 10.3390/ijms18051018]

4 **Luedde T**, Kaplowitz N, Schwabe RF. Cell death and cell death responses in liver disease: mechanisms and clinical relevance. *Gastroenterology* 2014; **147**: 765-783.e4 [PMID: 25046161 DOI: 10.1053/j.gastro.2014.07.018]

5 **Mehal W**, Imaeda A. Cell death and fibrogenesis. *Semin Liver Dis* 2010; **30**: 226-231 [PMID: 20665375 DOI: 10.1055/s-0030-1255352]

6 **Tagawa R**, Kawano Y, Minami A, Nishiumi S, Yano Y, Yoshida M, Kodama Y. β-hydroxybutyrate protects hepatocytes against endoplasmic reticulum stress in a sirtuin 1-independent manner. *Arch Biochem Biophys* 2019; **663**: 220-227 [PMID: 30664838 DOI: 10.1016/j.abb.2019.01.020]

7 **Wang H**, Chen L, Zhang X, Xu L, Xin B, Shi H, Duan Z, Zhang H, Ren F. Kaempferol protects mice from d-GalN/LPS-induced acute liver failure by regulating the ER stress-Grp78-CHOP signaling pathway. *Biomed Pharmacother* 2019; **111**: 468-475 [PMID: 30594786 DOI: 10.1016/j.biopha.2018.12.105]

8 **Mahfoudh-Boussaid A**, Zaouali MA, Hauet T, Hadj-Ayed K, Miled AH, Ghoul-Mazgar S, Saidane-Mosbahi D, Rosello-Catafau J, Ben Abdennebi H. Attenuation of endoplasmic reticulum stress and mitochondrial injury in kidney with ischemic postconditioning application and trimetazidine treatment. *J Biomed Sci* 2012; **19**: 71 [PMID: 22853733 DOI: 10.1186/1423-0127-19-71]

9 **Bonilla M**, Nastase KK, Cunningham KW. Essential role of calcineurin in response to endoplasmic reticulum stress. *EMBO J* 2002; **21**: 2343-2353 [PMID: 12006487 DOI: 10.1093/emboj/21.10.2343]

10 **Song S**, Tan J, Miao Y, Li M, Zhang Q. Crosstalk of autophagy and apoptosis: Involvement of the dual role of autophagy under ER stress. *J Cell Physiol* 2017; **232**: 2977-2984 [PMID: 28067409 DOI: 10.1002/jcp.25785]

11 **Chen Y**, Gui D, Chen J, He D, Luo Y, Wang N. Down-regulation of PERK-ATF4-CHOP pathway by Astragaloside IV is associated with the inhibition of endoplasmic reticulum stress-induced podocyte apoptosis in diabetic rats. *Cell Physiol Biochem* 2014; **33**: 1975-1987 [PMID: 25012492 DOI: 10.1159/000362974]

12 **B'chir W**, Maurin AC, Carraro V, Averous J, Jousse C, Muranishi Y, Parry L, Stepien G, Fafournoux P, Bruhat A. The eIF2α/ATF4 pathway is essential for stress-induced autophagy gene expression. *Nucleic Acids Res* 2013; **41**: 7683-7699 [PMID: 23804767 DOI: 10.1093/nar/gkt563]

13 **Nakagawa T**, Zhu H, Morishima N, Li E, Xu J, Yankner BA, Yuan J. Caspase-12 mediates endoplasmic-reticulum-specific apoptosis and cytotoxicity by amyloid-beta. *Nature* 2000; **403**: 98-103 [PMID: 10638761 DOI: 10.1038/47513]

14 **Zhang Q**, Liu J, Chen S, Liu J, Liu L, Liu G, Wang F, Jiang W, Zhang C, Wang S, Yuan X. Caspase-12 is involved in stretch-induced apoptosis mediated endoplasmic reticulum stress. *Apoptosis* 2016; **21**: 432-442 [PMID: 26801321 DOI: 10.1007/s10495-016-1217-6]

15 **Zou X**, Qu Z, Fang Y, Shi X, Ji Y. Endoplasmic reticulum stress mediates sulforaphane-induced apoptosis of HepG2 human hepatocellular carcinoma cells. *Mol Med Rep* 2017; **15**: 331-338 [PMID: 27959410 DOI: 10.3892/mmr.2016.6016]

16 **Qiu K**, Su Y, Block ER. Use of recombinant calpain-2 siRNA adenovirus to assess calpain-2 modulation of lung endothelial cell migration and proliferation. *Mol Cell Biochem* 2006; **292**: 69-78 [PMID: 16733798 DOI: 10.1007/s11010-006-9219-2]

17 **Martinez JA**, Zhang Z, Svetlov SI, Hayes RL, Wang KK, Larner SF. Calpain and caspase processing of caspase-12 contribute to the ER stress-induced cell death pathway in differentiated PC12 cells. *Apoptosis* 2010; **15**: 1480-1493 [PMID: 20640600 DOI: 10.1007/s10495-010-0526-4]

18 **Bajaj G**, Sharma RK. TNF-alpha-mediated cardiomyocyte apoptosis involves caspase-12 and calpain. *Biochem Biophys Res Commun* 2006; **345**: 1558-1564 [PMID: 16729970 DOI: 10.1016/j.bbrc.2006.05.059]

19 **Cheng C**, Dong W. Aloe-Emodin Induces Endoplasmic Reticulum Stress-Dependent Apoptosis in Colorectal Cancer Cells. *Med Sci Monit* 2018; **24**: 6331-6339 [PMID: 30199885 DOI: 10.12659/msm.908400]

20 **Xie RJ**, Han B, Yang T, Yang Q. Activation of Caspase-12, a key molecule in endoplasmic reticulum

stress related apoptosis pathway, induces apoptosis of hepatocytes in rats with hepatic fibrosis. *World Chinese Journal of Digestology* 2016; **24**: 2470-2477 [DOI: 10.11569/wcjd.v24.i16.2470]
21 **Xie RJ**, Han B, Yang T, Wen JJ, Yang Q. Expression of calpain-2 and Bax in rat fibrotic liver tissues. *Chinese Journal of Pathophysiology* 2013; **29**: 1603-1608 [DOI: 10.3969/j.issn.1000-4718.2013.09.011]
22 **Smith MD**, Harley ME, Kemp AJ, Wills J, Lee M, Arends M, von Kriegsheim A, Behrends C, Wilkinson S. CCPG1 Is a Non-canonical Autophagy Cargo Receptor Essential for ER-Phagy and Pancreatic ER Proteostasis. *Dev Cell* 2018; **44**: 217-232.e11 [PMID: 29290589 DOI: 10.1016/j.devcel.2017.11.024]
23 **Zuo S**, Kong D, Wang C, Liu J, Wang Y, Wan Q, Yan S, Zhang J, Tang J, Zhang Q, Lyu L, Li X, Shan Z, Qian L, Shen Y, Yu Y. CRTH2 promotes endoplasmic reticulum stress-induced cardiomyocyte apoptosis through m-calpain. *EMBO Mol Med* 2018; 10 [PMID: 29335338 DOI: 10.15252/emmm.201708237]
24 **Luo X**, Han B, Tian T, Yu L, Zheng L, Tang L, Yang T, Yang Q, Xin RJ, Huang JZ. Dithiothreitol induces of apoptosis of BRL-3A cells by activation of calpain-2/caspase-12 signaling pathway. *Zhongguo Bingli Shengli Zazhi* 2018; **34**: 1820-1826 [DOI: 10.3969/j.issn.1000-4718.2018.10.014]
25 **Tan Y**, Dourdin N, Wu C, De Veyra T, Elce JS, Greer PA. Ubiquitous calpains promote caspase-12 and JNK activation during endoplasmic reticulum stress-induced apoptosis. *J Biol Chem* 2006; **281**: 16016-16024 [PMID: 16597616 DOI: 10.1074/jbc.M601299200]
26 **Phaniraj S**, Gao Z, Rane D, Peterson BR. Hydrophobic resorufamine derivatives: potent and selective red fluorescent probes of the endoplasmic reticulum of mammalian cells. *Dyes Pigm* 2016; **135**: 127-133 [PMID: 27765999 DOI: 10.1016/j.dyepig.2016.05.007]
27 **Xiang XY**, Yang XC, Su J, Kang JS, Wu Y, Xue YN, Dong YT, Sun LK. Inhibition of autophagic flux by ROS promotes apoptosis during DTT-induced ER/oxidative stress in HeLa cells. *Oncol Rep* 2016; **35**: 3471-3479 [PMID: 27035858 DOI: 10.3892/or.2016.4725]
28 **Ren B**, Wang Y, Wang H, Wu Y, Li J, Tian J. Comparative proteomics reveals the neurotoxicity mechanism of ER stressors tunicamycin and dithiothreitol. *Neurotoxicology* 2018; **68**: 25-37 [PMID: 30003905 DOI: 10.1016/j.neuro.2018.07.004]
29 **Deegan S**, Saveljeva S, Logue SE, Pakos-Zebrucka K, Gupta S, Vandenabeele P, Bertrand MJ, Samali A. Deficiency in the mitochondrial apoptotic pathway reveals the toxic potential of autophagy under ER stress conditions. *Autophagy* 2014; **10**: 1921-1936 [PMID: 25470234 DOI: 10.4161/15548627.2014.981790]
30 **He C**, Qiu Y, Han P, Chen Y, Zhang L, Yuan Q, Zhang T, Cheng T, Yuan L, Huang C, Zhang S, Yin Z, Peng XE, Liang D, Lin X, Lin Y, Lin Z, Xia N. ER stress regulating protein phosphatase 2A-B56γ, targeted by hepatitis B virus X protein, induces cell cycle arrest and apoptosis of hepatocytes. *Cell Death Dis* 2018; **9**: 762 [PMID: 29988038 DOI: 10.1038/s41419-018-0787-3]
31 **Wang N**, Tan HY, Li S, Feng Y. Atg9b Deficiency Suppresses Autophagy and Potentiates Endoplasmic Reticulum Stress-Associated Hepatocyte Apoptosis in Hepatocarcinogenesis. *Theranostics* 2017; **7**: 2325-2338 [PMID: 28740555 DOI: 10.7150/thno.18225]
32 **Takahara I**, Akazawa Y, Tabuchi M, Matsuda K, Miyaaki H, Kido Y, Kanda Y, Taura N, Ohnita K, Takeshima F, Sakai Y, Eguchi S, Nakashima M, Nakao K. Toyocamycin attenuates free fatty acid-induced hepatic steatosis and apoptosis in cultured hepatocytes and ameliorates nonalcoholic fatty liver disease in mice. *PLoS One* 2017; **12**: e0170591 [PMID: 28278289 DOI: 10.1371/journal.pone.0170591]
33 **Zhang Y**, Miao L, Zhang H, Wu G, Zhang Z, Lv J. Chlorogenic acid against palmitic acid in endoplasmic reticulum stress-mediated apoptosis resulting in protective effect of primary rat hepatocytes. *Lipids Health Dis* 2018; **17**: 270 [PMID: 30486828 DOI: 10.1186/s12944-018-0916-0]
34 **Yang FW**, Fu Y, Li Y, He YH, Mu MY, Liu QC, Long J, Lin SD. Prostaglandin E1 protects hepatocytes against endoplasmic reticulum stress-induced apoptosis via protein kinase A-dependent induction of glucose-regulated protein 78 expression. *World J Gastroenterol* 2017; **23**: 7253-7264 [PMID: 29142472 DOI: 10.3748/wjg.v23.i40.7253]
35 **Sanges D**, Marigo V. Cross-talk between two apoptotic pathways activated by endoplasmic reticulum stress: differential contribution of caspase-12 and AIF. *Apoptosis* 2006; **11**: 1629-1641 [PMID: 16820963 DOI: 10.1007/s10495-006-9006-2]
36 **Szegezdi E**, Fitzgerald U, Samali A. Caspase-12 and ER-stress-mediated apoptosis: the story so far. *Ann N Y Acad Sci* 2003; **1010**: 186-194 [PMID: 15033718 DOI: 10.1196/annals.1299.032]
37 **Yan Z**, He JL, Guo L, Zhang HJ, Zhang SL, Zhang J, Wen YJ, Cao CZ, Wang J, Wang J, Zhang MS, Liang F. Activation of caspase-12 at early stage contributes to cardiomyocyte apoptosis in trauma-induced secondary cardiac injury. *Sheng Li Xue Bao* 2017; **69**: 367-377 [PMID: 28825094]
38 **Morishima N**, Nakanishi K, Takenouchi H, Shibata T, Yasuhiko Y. An endoplasmic reticulum stress-specific caspase cascade in apoptosis. Cytochrome c-independent activation of caspase-9 by caspase-12. *J Biol Chem* 2002; **277**: 34287-34294 [PMID: 12097332 DOI: 10.1074/jbc.M204973200]
39 **Chan SL**, Culmsee C, Haughey N, Klapper W, Mattson MP. Presenilin-1 mutations sensitize neurons to DNA damage-induced death by a mechanism involving perturbed calcium homeostasis and activation of calpains and caspase-12. *Neurobiol Dis* 2002; **11**: 2-19 [PMID: 12460542 DOI: 10.1006/nbdi.2002.0542]
40 **Chen B**, Tang J, Guo YS, Li Y, Chen ZN, Jiang JL. Calpains are required for invasive and metastatic potentials of human HCC cells. *Cell Biol Int* 2013; **37**: 643-652 [PMID: 23733271 DOI: 10.1002/cbin.10062]
41 **Cui W**, Ma J, Wang X, Yang W, Zhang J, Ji Q. Free fatty acid induces endoplasmic reticulum stress and apoptosis of β-cells by Ca2+/calpain-2 pathways. *PLoS One* 2013; **8**: e59921 [PMID: 23527285 DOI: 10.1371/journal.pone.0059921]

World Journal of Gastroenterology

Submit a Manuscript: https://www.f6publishing.com

World J Gastroenterol 2020 April 7; 26(13): 1463-1473

DOI: 10.3748/wjg.v26.i13.1463

ISSN 1007-9327 (print) ISSN 2219-2840 (online)

ORIGINAL ARTICLE

Clinical and Translational Research

Clinical relevance of increased serum preneoplastic antigen in hepatitis C-related hepatocellular carcinoma

Satoyoshi Yamashita, Akira Kato, Toshitaka Akatsuka, Takashi Sawada, Tomohide Asai, Noriyuki Koyama, Kiwamu Okita

ORCID number: Satoyoshi Yamashita (0000-0002-7795-9960); Akira Kato (0000-0002-2242-2787); Toshitaka Akatsuka (0000-0002-3719-1205); Takashi Sawada (0000-0002-6055-8183); Tomohide Asai (0000-0002-7878-1404); Noriyuki Koyama (0000-0002-7509-6583); Kiwamu Okita (0000-0001-7368-8609).

Author contributions: Okita K, Sawada T, Asai T, and Koyama N developed the original idea for this study and designed the research protocol; Akatsuka T, Sawada T, and Asai T contributed to isolating specific antibodies and developing specific assays for this study; Yamashita S and Kato A contributed to patient enrollment and collecting clinical data; Sawada T, Asai T and Koyama N contributed to data analysis; All authors contributed to the interpretation of data and preparation of the manuscript.

Institutional review board statement: The study protocol was approved by the Human Ethics Committee of JCHO Shimonoseki Medical Center (Approval date: May 29, 2015).

Informed consent statement: The study participants, or their legal guardian, provided informed written consent prior to study enrollment.

Conflict-of-interest statement: The authors SawadaT and Asai T are employees of Sekisui Medical Co., Ltd. Koyama N is an employee of Eisai Co., Ltd. Yamashita S, Kato

Satoyoshi Yamashita, Akira Kato, Department of Gastroenterology and Hepatology, Japan Community Health Care Organization Shimonoseki Medical Center, Shimonoseki, Yamaguchi 7500061, Japan

Toshitaka Akatsuka, Department of Physiology, Faculty of Medicine, Saitama Medical University, Iruma-gun, Saitama 3500495, Japan

Takashi Sawada, Tomohide Asai, Research and Development Division, Sekisui Medical Company Limited, Ryugasaki, Ibaraki 3010852, Japan

Noriyuki Koyama, Clinical Research Department, Eidia Company Limited, Chiyoda-ku, Tokyo 1010032, Japan

Noriyuki Koyama, Eisai Company Limited, Shinjuku-ku, Tokyo 1620812, Japan

Kiwamu Okita, Department of Internal Medicine, Shunan Memorial Hospital, Kudamatsu, Yamaguchi 7440033, Japan

Corresponding author: Kiwamu Okita, MD, PhD, Honorary Director, Department of Internal Medicine, Shunan Memorial Hospital, Ikunoya Minami 1-10-1, Kudamatsu, Yamaguchi 7440033, Japan. okita@hcsdojinkai.or.jp

Abstract

BACKGROUND

The prognosis of hepatocellular carcinoma (HCC) patients remains poor despite advances in treatment modalities and diagnosis. It is important to identify useful markers for the early detection of HCC in patients. Preneoplastic antigen (PNA), originally reported in a rat carcinogenesis model, is increased in the tissues and serum of HCC patients.

AIM

To determine the diagnostic value of PNA for discriminating HCC and to characterize PNA-positive HCC.

METHODS

Patients with hepatitis C virus (HCV)-related hepatic disorders were prospectively enrolled in this study, which included patients with hepatitis, with cirrhosis, and with HCC. A novel enzyme-linked immunosorbent assay was developed to measure serum PNA concentrations in patients.

RESULTS

A, Akatsuka T, and Okita K have no conflicts of interest to declare.

Data sharing statement: The datasets analyzed during the current study are available from the corresponding author on reasonable request.

Manuscript source: Unsolicited manuscript

Received: December 16, 2019
Peer-review started: December 16, 2019
First decision: February 18, 2020
Revised: March 6, 2020
Accepted: March 19, 2020
Article in press: March 19, 2020
Published online: April 7, 2020

P-Reviewer: Mrzljak A
S-Editor: Zhang L
L-Editor: Webster JR
E-Editor: Liu JH

Serum PNA concentrations were measured in 89 controls and 141 patients with HCV infections (50 hepatitis, 44 cirrhosis, and 47 HCC). Compared with control and non-HCC patients, PNA was increased in HCC. On receiver operating characteristic curve analysis, the sensitivity of PNA was similar to the HCC markers des-γ-carboxy-prothrombin (DCP) and α-fetoprotein (AFP), but the specificity of PNA was lower. There was no correlation between PNA and AFP and a significant but weak correlation between PNA and DCP in HCC patients. Importantly, the correlations with biochemical markers were completely different for PNA, AFP, and DCP; glutamyl transpeptidase was highly correlated with PNA, but not with AFP or DCP, and was significantly higher in PNA-high patients than in PNA-low patients with HCV-related HCC.

CONCLUSION

PNA may have the potential to diagnose a novel type of HCC in which glutamyl transpeptidase is positively expressed but AFP or DCP is weakly or negatively expressed.

Key words: Serum preneoplastic antigen; Hepatitis C virus; Hepatocellular carcinoma; Des-γ-carboxy-prothrombin; α-Fetoprotein; Sensitivity; Specificity

Core tip: Despite advances in treatment modalities and diagnosis, the prognosis of hepatocellular carcinoma (HCC) patients remains poor. It is important to identify useful markers for the early detection of HCC. Preneoplastic antigen (PNA) is increased in the tissues and serum of HCC patients. Therefore, we investigated the diagnostic value of PNA to discriminate HCC. We found that PNA had a comparable diagnostic value to α-fetoprotein and des-γ-carboxy-prothrombin. PNA may have the potential to diagnose a novel type of HCC in which glutamyl transpeptidase is positively expressed, but α-fetoprotein or des-γ-carboxy-prothrombin is weakly or negatively expressed.

Citation: Yamashita S, Kato A, Akatsuka T, Sawada T, Asai T, Koyama N, Okita K. Clinical relevance of increased serum preneoplastic antigen in hepatitis C-related hepatocellular carcinoma. *World J Gastroenterol* 2020; 26(13): 1463-1473
URL: https://www.wjgnet.com/1007-9327/full/v26/i13/1463.htm
DOI: https://dx.doi.org/10.3748/wjg.v26.i13.1463

INTRODUCTION

Hepatocellular carcinoma (HCC) is one of the most common cancers worldwide, and the primary risk factors for HCC include chronic infection by hepatitis B virus (HBV) or hepatitis C virus (HCV) and nonalcoholic fatty liver disease[1,2]. The overall survival rate of HCC patients has improved with advances in treatment modalities and diagnosis[3,4]. The surveillance rate for HCC patients has increased in Japan; thus, patients are more likely to be diagnosed in the earlier stage of the disease, and the survival rate has increased[5]. The HCC markers α-fetoprotein (AFP) and des-γ-carboxy-prothrombin (DCP), also known as PIVKA-II, have been used for the early-stage screening and diagnosis of HCC[6].

Although HCC treatment modalities and diagnosis have developed and improved, the prognosis of HCC patients at advanced stages remains poor[7,8]. Therefore, it is important to develop useful markers for the early detection of HCC.

The expression of preneoplastic antigen (PNA) was originally reported in a study of hyperplastic nodules in a rat experimental carcinogenesis model[9]. Immunostaining approaches showed that PNA was present in the cytoplasm of hepatocytes in hyperplastic nodules and in primary hepatomas[9,10]. Purification and biochemical characterization indicated that PNA was composed of microsomal epoxide hydrolase (mEH) and other binding proteins[11,12]. The mEH gene was hypomethylated in nodules and hepatomas induced by chemical carcinogens[13].

Evidence that PNA expression in human liver tissues is increased in pathological states has been accumulating. Immunohistochemical analysis of human tissues showed that mEH was positive in normal hepatocytes and HCC tissues, but less or

negatively expressed in other tumors, even if they metastasized to liver tissues[14,15]. Localization of mEH in the membrane changed during liver pathogenesis, such as neoplasia[16] or hepatitis infection[17]. An autoantibody response to mEH was detected in the serum of patients infected with HCV[18]. PNA was also detected in the culture medium of human HCC cell lines[19]. These data suggest that immunological detection of PNA may be a promising diagnostic tool for HCC.

To gain insight into PNA expression in liver diseases, we developed a highly sensitive enzyme-linked immunosorbent assay (ELISA) to measure PNA and determined serum PNA concentrations in patients with HCV-related hepatitis, cirrhosis, or HCC. The characteristics of PNA-positive HCC are also discussed in relation to biochemical markers.

MATERIALS AND METHODS

Patients

In Japan Community Health Care Organization (JCHO) Shimonoseki Medical Center, patients with HCV-related hepatic disorders were prospectively enrolled in this study, which included patients with hepatitis, with cirrhosis, and with HCC. All subjects fulfilled the criteria for a diagnosis of hepatitis, cirrhosis, or HCC with HCV infection, regardless of treatment history. The study protocol was approved by the Human Ethics Committee of JCHO Shimonoseki Medical Center (Approval date: May 29, 2015). Informed consent was obtained from all patients in accordance with the Declaration of Helsinki.

Clinical and laboratory assessments

Blood samples were collected from patients after written, informed consent was confirmed. Biochemical markers were assessed routinely in JCHO Shimonoseki Medical Center including albumin, serum aspartate aminotransferase (AST), alanine aminotransferase, alkaline phosphatase (ALP), γ-glutamyl transpeptidase (γ-GTP), and total bilirubin levels, as well as HCC markers including DCP and AFP. A fibrosis marker of type IV collagen was measured with a latex immunoassay by Sekisui Medical Co., Ltd. (Tokyo, Japan).

Preparation of monoclonal antibodies and measurement of serum PNA

Human mEH, a component of PNA, was produced in a recombinant baculovirus system[20], and the solubilized form of mEH was purified with sequential steps by column chromatography[16]. The development of anti-mEH monoclonal antibody 2G2 has been previously described[19]. For preparation of the PNA-specific antibody, PNA fractions were purified from the culture medium of Huh.1 (human HCC) and LN-71 (human glioblastoma) cells by ammonium sulfate precipitation followed by the same methods for mEH purification. Female BALB/c mice aged 6 wk, purchased from Tokyo Laboratory Animal Science Co., Ltd. (Tokyo, Japan), were injected s.c. with 2 μg of PNA four times, along with Freund's complete adjuvant for the first injection, with incomplete adjuvant for the second injection, and no adjuvant for the third and fourth injections. Their spleen cells were harvested and hybridized with NS-1 myeloma cells, as described previously[21]. Hybridoma clone 6G2 producing PNA-specific antibody was selected by screening each culture supernatant by ELISA against mEH and PNA. The mEH-specific 2G2 antibody (IgG1) was purified using an IgG Purification Kit-A (Chemical Dojin Co., Ltd., Tokyo, Japan), and PNA-specific antibody 6G2 (IgM) was purified using a HiTrap IgY Purification HP column (GE Healthcare Japan, Tokyo, Japan).

The ELISA for PNA was developed using a combination of anti-PNA antibody fixed on the plate and horseradish peroxidase-conjugated anti-mEH antibody for detection. Sera from control individuals were collected from healthy volunteers in Japan or purchased from BioreclamationIVT (Westbury, NY, United States).

Receiver operating characteristic curves for assessing the diagnosis of HCC

The receiver operating characteristic (ROC) curve was obtained by calculating the sensitivity and specificity of the assay at every possible cut-off point and plotting sensitivity against [1-specificity] in SPSS for Windows (SPSS Japan, Tokyo, Japan). The area under the ROC curve (AUROC) was calculated to determine the diagnostic accuracy of the assay. Appropriate cut-off points were examined for balancing the sensitivity and specificity of the ROC curve, and the optimal cut-off point was identified as that yielding the minimal value for $[(1 - \text{sensitivity})^2 + (1 - \text{specificity})^2]$ or the maximal value for [sensitivity + specificity - 1][22].

Statistical analysis

Statistical analysis was performed using SPSS for Windows (SPSS Japan, Tokyo, Japan). Differences in mean values between groups were assessed by the Mann-Whitney *U* test. χ^2 tests were used to compare univariate associations of categorical variables. Correlations between two parameters were analyzed using Spearman's rank correlation coefficient. A statistical review of this study was performed by a biomedical statistician.

RESULTS

Of the 141 patients diagnosed as HCV-positive, 50 had hepatitis, 44 had cirrhosis, and 47 had HCC (Table 1). Compared with patients with hepatitis and cirrhosis, HCC patients had higher percentages of male and older patients. The percentage of male patients was 40% (20/50) in the hepatitis group, 41% (18/44) in the cirrhosis group, and 53% (25/47) in the HCC group. The median age was 70.2 years, 71.7 years, and 75.3 years in the three groups, respectively. The results of biochemical markers differed among the groups (Table 1). With the progression of hepatic disorders from hepatitis to cirrhosis, serum albumin decreased, whereas ALP, total bilirubin, and type IV collagen increased significantly. With the progression to HCC, AST and GTP increased significantly. It is important to note that no biological markers differed between cirrhosis and HCC, suggesting no significant deterioration of liver functions in HCV-related HCC.

Next, serum PNA was measured in patients with hepatitis, cirrhosis, and HCC, and the results were compared with those of 89 control subjects (Figure 1). Serum PNA did not differ between control and hepatitis patients, but it was slightly higher in cirrhosis than in control ($P = 0.004$) and hepatitis patients ($P = 0.017$). In contrast, PNA increased significantly in HCC compared with control ($P < 0.001$) and hepatitis patients ($P < 0.001$). PNA concentrations were over 10 times higher in HCC patients than in cirrhosis patients, although the difference between the two groups was not significant ($P = 0.077$) due to the wide variations in data, especially in HCC patients.

The diagnostic value of serum PNA in HCC was determined and compared with the two HCC markers AFP and DCP (Figure 2). The ROC curves were obtained by calculating the sensitivity and specificity of these markers to differentiate HCC from hepatitis. The AUROC was 0.745 for PNA, 0.824 for AFP, and 0.793 for DCP. The ROC curve was also obtained to differentiate HCC from hepatitis and cirrhosis, and the AUROC was 0.680 for PNA and 0.754 for AFP and DCP. These data indicate that the diagnostic value of PNA was comparable to AFP and DCP to differentiate HCC from hepatitis or from hepatitis and cirrhosis.

Balancing sensitivity and specificity of the ROC curve indicated that the optimal cut-off point of serum PNA for predicting HCC was 5 ng/mL. Using this cut-off point, the sensitivity and specificity of PNA were determined and compared with those of AFP and DCP (Table 2). In differentiating HCC from hepatitis, the sensitivity and specificity were 63.8% and 78.0% for PNA, 61.7% and 88.0% for AFP, and 61.7% and 94.0% for DCP, respectively. In differentiating HCC from hepatitis and cirrhosis, the sensitivity and specificity were 63.8% and 66.0% for PNA, 61.7% and 75.5% for AFP, and 61.7% and 83.0% for DCP, respectively. These data suggest that the sensitivity of PNA was similar to AFP and DCP, but the specificity of PNA was lower than of AFP and DCP.

The correlations of PNA with AFP and DCP in the serum of HCC patients were evaluated (Figure 3). Spearman's correlation analysis clearly indicated no correlation between PNA and AFP, with a correlation index of 0.229 ($P = 0.121$). A significant but weak correlation was seen between PNA and DCP, with a correlation index of 0.313 ($P = 0.032$). These data indicated that PNA was positive in many patients who were negative for AFP or DCP.

To determine the differences in disease characteristics, the correlations of PNA, AFP, and DCP with biochemical markers in the sera of HCC patients were compared (Table 3). Spearman's correlation analysis indicated significant correlations of PNA with AST, ALP, and GTP. The highest correlation was seen between PNA and GTP, with a correlation index of 0.666 ($P < 0.001$). In contrast, AFP was significantly correlated with all biochemical markers with the exception of GTP. DCP was significantly correlated only with albumin and ALP. These data indicate that the correlations with biochemical markers were completely different for PNA, AFP, and DCP in HCC patients, and that GTP was highly correlated with PNA, but not with AFP or DCP. HCC patients were then divided into PNA-high and PNA-low patients by the cut-off of the median PNA value (8 ng/mL), and biochemical markers were compared between PNA-high and PNA-low patients (Table 4). Statistical analyses indicated that AST, ALP, and GTP were significantly higher in PNA-high patients

Table 1 Characteristics of patients with hepatitis C virus-related hepatitis, cirrhosis, and hepatocellular carcinoma

	1: Hepatitis (n = 50)		2: Cirrhosis (n = 44)		3: HCC (n = 47)		1 *vs* 2	1 *vs* 3	2 *vs* 3
	Mean	SD	Mean	SD	Mean	SD	*P* value	*P* value	*P* value
Sex (male/female)	20/30		18/26		25/22		0.360	0.048	0.101
Age (yr)	70.2	(11.7)	71.8	(10.4)	75.3	(9.0)	0.558	0.018	0.102
Albumin (g/L)	4.2	(0.3)	3.7	(0.6)	3.7	(0.9)	< 0.001	< 0.001	0.962
AST (U/L)	44	(35)	46	(20)	60	(51)	0.056	0.033	0.861
ALT (U/L)	41	(42)	33	(20)	45	(48)	0.967	0.667	0.674
ALP (U/L)	259	(60)	345	(141)	362	(312)	0.001	0.084	0.212
Bilirubin total (mg/dL)	0.8	(0.4)	1.2	(0.7)	1.2	(1.1)	0.001	0.003	0.477
GTP (U/L)	46	(61)	47	(44)	105	(212)	0.186	0.001	0.078
Type IV collagen (ng/mL)	159	(69)	237	(88)	207	(94)	< 0.001	0.003	0.075

Results are shown as means with SD. Differences in mean values between each group were assessed with Mann–Whitney *U* tests, and differences in the sex ratio were assessed with χ^2 tests. HCC: Hepatocellular carcinoma; AST: Aspartate aminotransferase; ALT: Alanine aminotransferase ; ALP: Alkaline phosphatase; GTP: Glutamyl tranpeptidase.

than in PNA-low patients with HCV-related HCC. The mean GTP value was 183.2 U/L in PNA-high patients, which was almost 6 times higher than the mean GTP value (31.0 U/L) in PNA-low patients (P < 0.0001).

DISCUSSION

HCC patients consist of heterogeneous populations, and the subtypes of HCC are characterized by clinical phenotypes such as cell differentiation and tumor size, and molecular phenotypes associated with gene mutations and transcriptional modification[23,24]. In addition, the immune microenvironment, which is affected by both clinical and molecular phenotypes, may have a large impact on patient prognosis[25] and be activated in a certain population of HCC patients[26]. Therefore, the development of a novel biomarker that can diagnose HCC and further characterize its phenotype in the clinical setting is warranted.

In this study, PNA was aberrantly increased in the serum of HCV-related HCC patients. The mechanism and function of the PNA increase in the serum of HCC patients are unclear. A component of PNA, mEH, is a drug metabolizing enzyme on the endoplasmic reticulum membrane that catalyzes the hydration of reactive epoxide. In addition, mEH plays a role in bile acid transport on the plasma membrane of hepatocytes[27], and bile acid regulates hepatic tumor development[28]. Studies with a number of monoclonal antibodies recognizing different portions of mEH showed that mEH was located predominantly inside hepatocytes, while located abundantly on the surface of HCC cells[19,29]. Recent studies have shown that mEH plays a key role in the hydrolysis of fatty acids such as epoxyeicosatrienoic acid (EET)[30,31]. As EET regulates tumor cell growth, metastasis, angiogenesis, and inflammation in cancer[30,32,33], the induction of mEH in HCC may reflect the dynamic change of localization and functions of mEH during carcinogenesis. The present data showing that serum PNA was increased in a limited number of non-HCC cirrhotic patients may suggest the change of mEH in preneoplastic stages.

The early detection of HCC allows patients to receive curative treatment and achieve long-term survival. The routine practice of screening high-risk patients for HCC contributes to the detection of HCC nodules in the early stages in more than 60% of patients in Japan[34]. The HCC markers AFP and DCP have been used to screen and diagnose HCC at an earlier stage. An immunohistochemical study of small HCC tissues showed that AFP-positive HCCs were more malignant than AFP-negative and DCP-positive HCCs[35]. DCP was more efficient than AFP for the diagnosis of early HCC and for the prediction of microvascular invasion[36]. The combined use of AFP and DCP was useful for predicting the aggressiveness of early-stage HCC in patients given local treatment[37,38]. However, their sensitivity and specificity are lower for early-stage HCC than for advanced stage HCC[6]. It appears that PNA has the potential to diagnose a novel population of HCC patients in which AFP or DCP is weakly or negatively expressed. Further analysis of PNA may clarify its potential for the detection of HCC nodules in the early stage.

In the present study, serum GTP was highly correlated with PNA, but not with

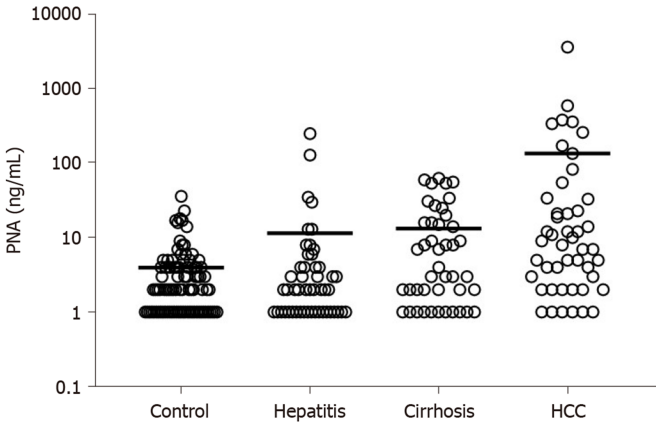

Mean	4.0	11.5	13.2	134.9
SD	5.4	38.8	18.0	532.8
P vs control		0.877	0.004	< 0.001
P vs hepatitis			0.017	< 0.001
P vs cirrhosis				0.077

Figure 1 Serum preneoplastic antigen concentrations in controls and in patients with hepatitis C virus-related hepatitis, cirrhosis, or hepatocellular carcinoma. Serum preneoplastic antigen concentrations were measured by ELISA. The results from each patient are plotted, and the means are shown by horizontal bars. The differences between groups were evaluated by Mann-Whitney *U* tests. The mean with SD and *P* value for comparison are summarized in the table. *n* = 89 in control, 50 in hepatitis, 44 in cirrhosis, and 47 in hepatocellular carcinoma.

AFP or DCP, and it was significantly higher in PNA-high patients than in PNA-low patients with HCV-related HCC. Therefore, PNA could potentially be used to diagnose a novel type of HCC in which GTP is positively expressed, but AFP or DCP is weakly or negatively expressed.

HCC patients with elevated serum GTP had a lower survival rate after resection[39] and transarterial chemoembolization[40]. The increase of GTP in early-stage HCC and the aggressive phenotype of HCC highly expressing GTP have been examined. Immunohistochemical and enzyme histochemical analysis showed the localization of GTP in preneoplastic foci at the early stage in a rat carcinogenesis model[41] and in hepatocellular foci of HCC patients with HCV infection[42]. The meta-analysis indicated that pretreatment serum GTP was a predictor of poor overall survival, recurrence-free survival, and disease-free survival in HCC patients[43,44]. The ectopic expression of GTP accelerated tumor cell growth, metastasis, and resistance to chemotherapy[45,46]. Therefore, PNA-positive HCC may have an aggressive phenotype with a higher risk for disease progression and a poor prognosis. The prognostic value of PNA for survival will be determined in the follow-up evaluation of the patients enrolled in this study.

A limitation of this study is the etiologies of the hepatic disorders. The risk factors for hepatitis, cirrhosis, and HCC include chronic infection by HBV or HCV and hepatic steatosis and inflammation in nonalcoholic fatty liver disease. In the present study, however, only patients with HCV-related hepatic disorders were enrolled. Further studies are warranted to identify the changes of PNA in hepatitis, cirrhosis, and HCC with other etiologies.

In conclusion, the diagnostic value of PNA to discriminate HCC was comparable to AFP and DCP. PNA may have the potential to diagnose a novel type of HCC in which GTP is positively expressed, but AFP or DCP is weakly or negatively expressed. Further studies are needed to determine the diagnostic value of PNA for HCC patients in comparison with other HCC markers.

Table 2 Sensitivity and specificity of preneoplastic antigen, α-fetoprotein, and des-γ-carboxy-prothrombin in patients with hepatitis C virus-related hepatocellular carcinoma

	(A) HCC *vs* hepatitis		(B) HCC *vs* hepatitis/cirrhosis	
	Sensitivity (%)	Specificity (%)	Sensitivity (%)	Specificity (%)
PNA	63.8	78.0	63.8	66.0
AFP	61.7	88.0	61.7	75.5
DCP	61.7	94.0	61.7	83.0

The sensitivity and specificity of markers were determined to discriminate hepatocellular carcinoma patients from (A) hepatitis patients and (B) hepatitis and cirrhosis patients. The cut-off value for positivity was 5 ng/mL for preneoplastic antigen, 10 ng/mL for α-fetoprotein, and 40 mAU/mL for des-γ-carboxy-prothrombin. HCC: Hepatocellular carcinoma; PNA: Preneoplastic antigen; AFP: α-Fetoprotein; DCP: Des-γ-carboxy-prothrombin.

Table 3 Correlations of preneoplastic antigen, α-fetoprotein, and des-γ-carboxy-prothrombin with laboratory tests in patients with hepatitis C virus-related hepatocellular carcinoma

	PNA		AFP		DCP	
	r	*P* value	*r*	*P* value	*r*	*P* value
Albumin	-0.173	0.245	-0.416	0.004	-0.339	0.020
AST	0.325	0.026	0.626	< 0.001	0.232	0.117
ALT	0.227	0.125	0.438	0.002	-0.038	0.799
ALP	0.582	< 0.001	0.459	0.001	0.302	0.039
Bilirubin	0.226	0.130	0.366	0.012	0.030	0.841
GTP	0.666	< 0.001	0.274	0.062	0.082	0.585
Type IV collagen	0.107	0.476	0.498	< 0.001	0.246	0.095

The correlation index (*r*) and 2-sided *P* value were calculated by Spearman's correlation analysis. PNA: Preneoplastic antigen; AFP: α-Fetoprotein; DCP: Des-γ-carboxy-prothrombin; AST: Aspartate aminotransferase; ALT: Alanine aminotransferase; ALP: Alkaline phosphatase.

Table 4 Comparison of biochemical markers between preneoplastic antigen-high and preneoplastic antigen-low patients with hepatitis C virus-related hepatocellular carcinoma

	PNA-high patients (*n* = 23)		PNA-low patients (*n* = 24)		
	Mean	SD	Mean	SD	*P* value
Albumin (g/L)	3.5	0.7	3.9	1.1	0.1348
AST (U/L)	73.2	58.6	47.0	36.1	0.0247
ALT (U/L)	58.3	61.8	31.7	18.9	0.3025
ALP (U/L)	463.4	393.2	264.2	135.9	0.0004
Bilirubin total (mg/dL)	1.4	1.4	1.0	0.7	0.6345
GTP (U/L)	183.2	278.7	31.0	12.5	< 0.0001
Type IV collagen (ng/mL)	225.2	104.3	189.4	76.3	0.2133

Hepatocellular carcinoma patients were divided into preneoplastic antigen-high and preneoplastic antigen-low groups using the median preneoplastic antigen value (8 ng/mL) as the cut-off. Results are shown as means with SD. Differences in mean values between each group were assessed with Mann–Whitney *U* tests. PNA: Preneoplastic antigen; AST: Aspartate aminotransferase; ALT: Alanine aminotransferase; ALP: Alkaline phosphatase.

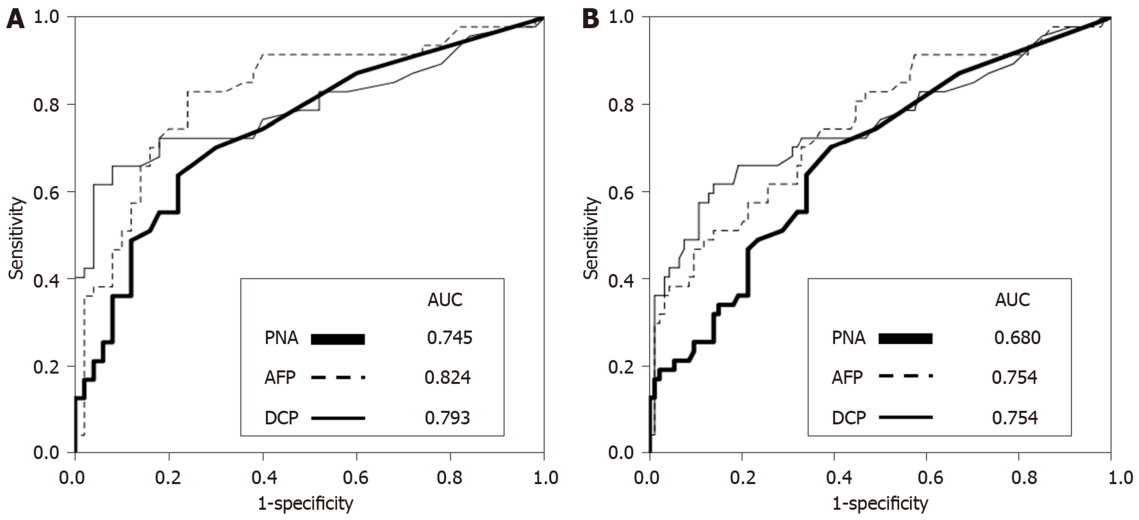

Figure 2 Receiver-operating characteristic analyses of preneoplastic antigen, α-fetoprotein and des-γ-carboxy-prothrombin in hepatitis C virus-related hepatocellular carcinoma. The sensitivity and specificity of markers were determined to discriminate hepatocellular carcinoma patients from hepatitis patients and cirrhosis patients. A: Hepatitis patients; B: Hepatitis and cirrhosis patients. The receiver–operating characteristic curve was obtained by plotting the sensitivity on the Y-axis against 1-specificity on the X-axis, and the area under the receiver–operating characteristic curve was calculated. PNA: Preneoplastic antigen; AFP: α-Fetoprotein; DCP: Des-γ-carboxy-prothrombin.

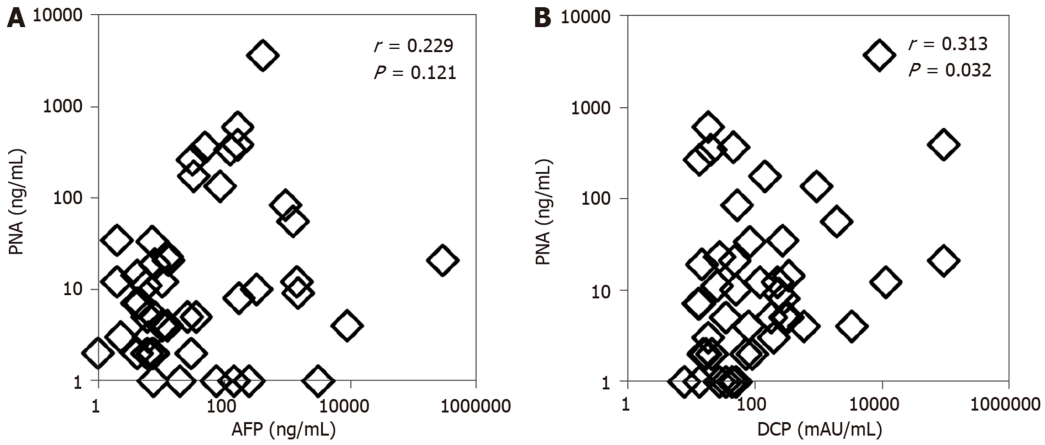

Figure 3 Correlation analysis of preneoplastic antigen with α-fetoprotein and des-γ-carboxy-prothrombin in sera of patients with hepatitis C virus-related hepatocellular carcinoma. The correlation index (*r*) and 2-sided *P* value were calculated by Spearman correlation analysis. AFP: α-Fetoprotein; DCP: Des-γ-carboxy-prothrombin; PNA: Preneoplastic antigen.

ARTICLE HIGHLIGHTS

Research background

The prognosis of hepatocellular carcinoma (HCC) patients remains poor despite advances in treatment modalities and diagnosis. The early detection of HCC allows patients to receive curative treatment and achieve long-term survival. It is important to identify useful markers for the early detection of HCC in patients.

Research motivation

Preneoplastic antigen (PNA), originally reported in a rat carcinogenesis model, is increased in the tissues and serum of HCC patients. However, the diagnostic value of PNA for discriminating HCC remains to be determined.

Research objectives

The objectives of this study are to determine the diagnostic value of PNA for discriminating HCC and to characterize PNA-positive HCC.

Research methods

Patients with hepatitis C virus-related hepatic disorders were prospectively enrolled in this study, which included patients with hepatitis, with cirrhosis, and with HCC. A novel enzyme-

linked immunosorbent assay was developed to measure serum PNA concentrations in patients.

Research results

Compared with control and non-HCC patients, PNA was increased in HCC. The sensitivity of PNA was similar to the HCC markers des-γ-carboxy-prothrombin (DCP) and αα-fetoprotein (AFP), but the specificity of PNA was lower. There was no correlation between PNA and AFP and a significant but weak correlation between PNA and DCP in HCC patients. Importantly, the correlations with biochemical markers indicated that GTP was highly correlated with PNA, but not with AFP or DCP, and that it was significantly higher in PNA-high patients than in PNA-low patients with hepatitis C virus-related HCC.

Research conclusions

PNA may have the potential to diagnose a novel type of HCC in which GTP is positively expressed but AFP or DCP is weakly or negatively expressed.

Research perspectives

Further studies are needed to determine the diagnostic value of PNA for HCC patients in comparison with other HCC markers and to determine its potential for the detection of HCC nodules in the early stage. PNA-positive HCC may have an aggressive phenotype with a higher risk for disease progression and a poor prognosis. The prognostic value of PNA for survival will be determined in a follow-up evaluation of the patients enrolled in this study.

ACKNOWLEDGEMENTS

The authors would like to thank all of the patients and their families who participated in this study.

REFERENCES

1 **Bray F**, Ferlay J, Soerjomataram I, Siegel RL, Torre LA, Jemal A. Global cancer statistics 2018: GLOBOCAN estimates of incidence and mortality worldwide for 36 cancers in 185 countries. *CA Cancer J Clin* 2018; **68**: 394-424 [PMID: 30207593 DOI: 10.3322/caac.21492.]

2 **Dimitroulis D**, Damaskos C, Valsami S, Davakis S, Garmpis N, Spartalis E, Athanasiou A, Moris D, Sakellariou S, Kykalos S, Tsourouflis G, Garmpi A, Delladetsima I, Kontzoglou K, Kouraklis G. From diagnosis to treatment of hepatocellular carcinoma: An epidemic problem for both developed and developing world. *World J Gastroenterol* 2017; **23**: 5282-5294 [PMID: 28839428 DOI: 10.3748/wjg.v23.i29.5282]

3 **Harris PS**, Hansen RM, Gray ME, Massoud OI, McGuire BM, Shoreibah MG. Hepatocellular carcinoma surveillance: An evidence-based approach. *World J Gastroenterol* 2019; **25**: 1550-1559 [PMID: 30983815 DOI: 10.3748/wjg.v25.i13.1550]

4 **Kudo M**, Izumi N, Sakamoto M, Matsuyama Y, Ichida T, Nakashima O, Matsui O, Ku Y, Kokudo N, Makuuchi M; Liver Cancer Study Group of Japan. Survival Analysis over 28 Years of 173,378 Patients with Hepatocellular Carcinoma in Japan. *Liver Cancer* 2016; **5**: 190-197 [PMID: 27493894 DOI: 10.1159/000367775]

5 **Johnson P**, Berhane S, Kagebayashi C, Satomura S, Teng M, Fox R, Yeo W, Mo F, Lai P, Chan SL, Tada T, Toyoda H, Kumada T. Impact of disease stage and aetiology on survival in hepatocellular carcinoma: implications for surveillance. *Br J Cancer* 2017; **116**: 441-447 [PMID: 28081537 DOI: 10.1038/bjc.2016.422]

6 **Tsuchiya N**, Sawada Y, Endo I, Saito K, Uemura Y, Nakatsura T. Biomarkers for the early diagnosis of hepatocellular carcinoma. *World J Gastroenterol* 2015; **21**: 10573-10583 [PMID: 26457017 DOI: 10.3748/wjg.v21.i37.10573]

7 **Désert R**, Nieto N, Musso O. Dimensions of hepatocellular carcinoma phenotypic diversity. *World J Gastroenterol* 2018; **24**: 4536-4547 [PMID: 30386103 DOI: 10.3748/wjg.v24.i40.4536]

8 **Akada K**, Koyama N, Taniguchi S, Miura Y, Aoshima K. Database analysis of patients with hepatocellular carcinoma and treatment flow in early and advanced stages. *Pharmacol Res Perspect* 2019; **7**: e00486 [PMID: 31249691 DOI: 10.1002/prp2.486]

9 **Okita K**, Kligman LH, Farber E. A new common marker for premalignant and malignant hepatocytes induced in the rat by chemical carcinogens. *J Natl Cancer Inst* 1975; **54**: 199-202 [PMID: 163316 DOI: 10.1093/jnci/54.1.199]

10 **Okita K**, Esaki T, Kurokawa F, Takemoto T, Fujikura Y, Fukumoto T. An antigen specific to hyperplastic liver nodules defined with monoclonal antibody: a new marker for preneoplastic cells in rat chemical hepatocarcinogenesis. *Tumour Biol* 1988; **9**: 170-177 [PMID: 3420373 DOI: 10.1159/000217559]

11 **Levin W**, Lu AY, Thomas PE, Ryan D, Kizer DE, Griffin MJ. Identification of epoxide hydrase as the preneoplastic antigen in rat liver hyperplastic nodules. *Proc Natl Acad Sci USA* 1978; **75**: 3240-3243 [PMID: 210455 DOI: 10.1073/pnas.75.7.3240]

12 **Ogino M**, Okita K, Tsubota W, Numa Y, Kodama T, Takemoto T. Some biochemical properties of the preneoplastic antigen in rat liver hyperplastic nodules. *Gan* 1982; **73**: 349-353 [PMID: 6813180]

13 **Ding VD**, Cameron R, Pickett CB. Regulation of microsomal, xenobiotic epoxide hydrolase messenger RNA in persistent hepatocyte nodules and hepatomas induced by chemical carcinogens. *Cancer Res* 1990; **50**: 256-260 [PMID: 2295064]

14 **Fritz P**, Behrle E, Zanger UM, Mürdter T, Schwarzmann P, Kroemer HK. Immunohistochemical assessment of human microsomal epoxide hydrolase in primary and secondary liver neoplasm: a quantitative approach. *Xenobiotica* 1996; **26**: 107-116 [PMID: 8851825 DOI: 10.3109/00498259609046692]

15 **Coller JK**, Fritz P, Zanger UM, Siegle I, Eichelbaum M, Kroemer HK, Mürdter TE. Distribution of microsomal epoxide hydrolase in humans: an immunohistochemical study in normal tissues, and benign and malignant tumours. *Histochem J* 2001; **33**: 329-336 [PMID: 11758809 DOI: 10.1023/a:1012414806166]

16 **Gill SS**, Ota K, Ruebner B, Hammock BD. Microsomal and cytosolic epoxide hydrolases in rhesus monkey liver, and in normal and neoplastic human liver. *Life Sci* 1983; **32**: 2693-2700 [PMID: 6855465 DOI: 10.1016/0024-3205(83)90362-4]

17 **Akatsuka T**, Tohmatsu J, Abe K, Shikata T, Ishikawa T, Nakajima K, Yoshihara N, Odaka T. Non-A, non-B hepatitis related AN6520 Ag is a normal cellular protein mainly expressed in liver. II. *J Med Virol* 1986; **20**: 43-56 [PMID: 2428929 DOI: 10.1002/jmv.1890200107]

18 **Akatsuka T**, Kobayashi N, Ishikawa T, Saito T, Shindo M, Yamauchi M, Yoshihara N, Odaka T. Autoantibody response to microsomal epoxide hydrolase in hepatitis C and A. *J Autoimmun* 2007; **28**: 7-18 [PMID: 17296285 DOI: 10.1016/j.jaut.2006.12.005]

19 **Duan H**, Yoshimura K, Kobayashi N, Sugiyama K, Sawada J, Saito Y, Morisseau C, Hammock BD, Akatsuka T. Development of monoclonal antibodies to human microsomal epoxide hydrolase and analysis of "preneoplastic antigen"-like molecules. *Toxicol Appl Pharmacol* 2012; **260**: 17-26 [PMID: 22310175 DOI: 10.1016/j.taap.2012.01.023]

20 **Morisseau C**, Newman JW, Dowdy DL, Goodrow MH, Hammock BD. Inhibition of microsomal epoxide hydrolases by ureas, amides, and amines. *Chem Res Toxicol* 2001; **14**: 409-415 [PMID: 11304129 DOI: 10.1021/tx0001732]

21 **Akatsuka T**, Tohmatsu J, Yoshihara N, Katsuhara N, Okamoto T, Shikata T, Odaka T. Detection of an antigen (AN6520), possibly related to non-A, non-B hepatitis, by monoclonal antibodies. I. *J Med Virol* 1986; **20**: 33-42 [PMID: 2428928 DOI: 10.1002/jmv.1890200106]

22 **Akobeng AK**. Understanding diagnostic tests 3: Receiver operating characteristic curves. *Acta Paediatr* 2007; **96**: 644-647 [PMID: 17376185 DOI: 10.1111/j.1651-2227.2006.00178.x]

23 **Hoshida Y**, Nijman SM, Kobayashi M, Chan JA, Brunet JP, Chiang DY, Villanueva A, Newell P, Ikeda K, Hashimoto M, Watanabe G, Gabriel S, Friedman SL, Kumada H, Llovet JM, Golub TR. Integrative transcriptome analysis reveals common molecular subclasses of human hepatocellular carcinoma. *Cancer Res* 2009; **69**: 7385-7392 [PMID: 19723656 DOI: 10.1158/0008-5472.CAN-09-1089]

24 **Calderaro J**, Couchy G, Imbeaud S, Amaddeo G, Letouzé E, Blanc JF, Laurent C, Hajji Y, Azoulay D, Bioulac-Sage P, Nault JC, Zucman-Rossi J. Histological subtypes of hepatocellular carcinoma are related to gene mutations and molecular tumour classification. *J Hepatol* 2017; **67**: 727-738 [PMID: 28532995 DOI: 10.1016/j.jhep.2017.05.014]

25 **Kurebayashi Y**, Ojima H, Tsujikawa H, Kubota N, Maehara J, Abe Y, Kitago M, Shinoda M, Kitagawa Y, Sakamoto M. Landscape of immune microenvironment in hepatocellular carcinoma and its additional impact on histological and molecular classification. *Hepatology* 2018; **68**: 1025-1041 [PMID: 29603348 DOI: 10.1002/hep.29904]

26 **Sadeghi M**, Lahdou I, Oweira H, Daniel V, Terness P, Schmidt J, Weiss KH, Longerich T, Schemmer P, Opelz G, Mehrabi A. Serum levels of chemokines CCL4 and CCL5 in cirrhotic patients indicate the presence of hepatocellular carcinoma. *Br J Cancer* 2015; **113**: 756-762 [PMID: 26270232 DOI: 10.1038/bjc.2015.227]

27 **Peng H**, Zhu QS, Zhong S, Levy D. Transcription of the Human Microsomal Epoxide Hydrolase Gene (EPHX1) Is Regulated by PARP-1 and Histone H1.2. Association with Sodium-Dependent Bile Acid Transport. *PLoS One* 2015; **10**: e0125318 [PMID: 25992604 DOI: 10.1371/journal.pone.0125318]

28 **Takahashi S**, Tanaka N, Fukami T, Xie C, Yagai T, Kim D, Velenosi TJ, Yan T, Krausz KW, Levi M, Gonzalez FJ. Role of Farnesoid X Receptor and Bile Acids in Hepatic Tumor Development. *Hepatol Commun* 2018; **2**: 1567-1582 [PMID: 30556042 DOI: 10.1002/hep4.1263]

29 **Duan H**, Takagi A, Kayano H, Koyama I, Morisseau C, Hammock BD, Akatsuka T. Monoclonal antibodies reveal multiple forms of expression of human microsomal epoxide hydrolase. *Toxicol Appl Pharmacol* 2012; **260**: 27-34 [PMID: 22306621 DOI: 10.1016/j.taap.2012.01.021]

30 **Rand AA**, Barnych B, Morisseau C, Cajka T, Lee KSS, Panigrahy D, Hammock BD. Cyclooxygenase-derived proangiogenic metabolites of epoxyeicosatrienoic acids. *Proc Natl Acad Sci USA* 2017; **114**: 4370-4375 [PMID: 28396419 DOI: 10.1073/pnas.1616893114]

31 **Marowsky A**, Meyer I, Erismann-Ebner K, Pellegrini G, Mule N, Arand M. Beyond detoxification: a role for mouse mEH in the hepatic metabolism of endogenous lipids. *Arch Toxicol* 2017; **91**: 3571-3585 [PMID: 28975360 DOI: 10.1007/s00204-017-2060-4]

32 **Panigrahy D**, Greene ER, Pozzi A, Wang DW, Zeldin DC. EET signaling in cancer. *Cancer Metastasis Rev* 2011; **30**: 525-540 [PMID: 22009066 DOI: 10.1007/s10555-011-9315-y]

33 **Panigrahy D**, Edin ML, Lee CR, Huang S, Bielenberg DR, Butterfield CE, Barnés CM, Mammoto A, Mammoto T, Luria A, Benny O, Chaponis DM, Dudley AC, Greene ER, Vergilio JA, Pietramaggiori G, Scherer-Pietramaggiori SS, Short SM, Seth M, Lih FB, Tomer KB, Yang J, Schwendener RA, Hammock BD, Falck JR, Manthati VL, Ingber DE, Kaipainen A, D'Amore PA, Kieran MW, Zeldin DC. Epoxyeicosanoids stimulate multiorgan metastasis and tumor dormancy escape in mice. *J Clin Invest* 2012; **122**: 178-191 [PMID: 22182838 DOI: 10.1172/JCI58128]

34 **Song P**, Gao J, Inagaki Y, Kokudo N, Hasegawa K, Sugawara Y, Tang W. Biomarkers: evaluation of screening for and early diagnosis of hepatocellular carcinoma in Japan and china. *Liver Cancer* 2013; **2**: 31-39 [PMID: 24159594 DOI: 10.1159/000346220]

35 **Fujioka M**, Nakashima Y, Nakashima O, Kojiro M. Immunohistologic study on the expressions of α-fetoprotein and protein induced by vitamin K absence or antagonist II in surgically resected small hepatocellular carcinoma. *Hepatology* 2001; **34**: 1128-1134 [PMID: 11732002 DOI: 10.1053/jhep.2001.29202]

36 **Poté N**, Cauchy F, Albuquerque M, Voitot H, Belghiti J, Castera L, Puy H, Bedossa P, Paradis V. Performance of PIVKA-II for early hepatocellular carcinoma diagnosis and prediction of microvascular invasion. *J Hepatol* 2015; **62**: 848-854 [PMID: 25450201 DOI: 10.1016/j.jhep.2014.11.005]

37 **Suh SW**, Lee KW, Lee JM, You T, Choi Y, Kim H, Lee HW, Lee JM, Yi NJ, Suh KS. Prediction of aggressiveness in early-stage hepatocellular carcinoma for selection of surgical resection. *J Hepatol* 2014; **60**: 1219-1224 [PMID: 24548529 DOI: 10.1016/j.jhep.2014.01.027]

38 **Park H**, Kim SU, Park JY, Kim DY, Ahn SH, Chon CY, Han KH, Seong J. Clinical usefulness of double biomarkers AFP and PIVKA-II for subdividing prognostic groups in locally advanced hepatocellular carcinoma. *Liver Int* 2014; **34**: 313-321 [PMID: 23895043 DOI: 10.1111/liv.12274]

39 **Xu XS**, Wan Y, Song SD, Chen W, Miao RC, Zhou YY, Zhang LQ, Qu K, Liu SN, Zhang YL, Dong YF,

Liu C. Model based on γ-glutamyltransferase and alkaline phosphatase for hepatocellular carcinoma prognosis. *World J Gastroenterol* 2014; **20**: 10944-10952 [PMID: 25152598 DOI: 10.3748/wjg.v20.i31.10944]

40 **Ventura Y**, Carr BI, Kori I, Guerra V, Shibolet O. Analysis of aggressiveness factors in hepatocellular carcinoma patients undergoing transarterial chemoembolization. *World J Gastroenterol* 2018; **24**: 1641-1649 [PMID: 29686471 DOI: 10.3748/wjg.v24.i15.1641]

41 **Satoh K**, Takahashi G, Miura T, Hayakari M, Hatayama I. Enzymatic detection of precursor cell populations of preneoplastic foci positive for γ-glutamyltranspeptidase in rat liver. *Int J Cancer* 2005; **115**: 711-716 [PMID: 15729699 DOI: 10.1002/ijc.20979]

42 **Paolicchi A**, Marchi S, Petruccelli S, Ciancia E, Malvaldi G, Pompella A. Gamma-glutamyltransferase in fine-needle liver biopsies of subjects with chronic hepatitis C. *J Viral Hepat* 2005; **12**: 269-273 [PMID: 15850467 DOI: 10.1111/j.1365-2893.2005.00579.x]

43 **Ou Y**, Huang J, Yang L. The prognostic significance of pretreatment serum γ-glutamyltranspeptidase in primary liver cancer: a meta-analysis and systematic review. *Biosci Rep* 2018; **38** [PMID: 30389711 DOI: 10.1042/BSR20181058]

44 **Sun P**, Li Y, Chang L, Tian X. Prognostic and clinicopathological significance of Gamma-Glutamyltransferase in patients with hepatocellular carcinoma: A PRISMA-compliant meta-analysis. *Medicine (Baltimore)* 2019; **98**: e15603 [PMID: 31083251 DOI: 10.1097/MD.0000000000015603]

45 **Hanigan MH**, Gallagher BC, Townsend DM, Gabarra V. γ-glutamyl transpeptidase accelerates tumor growth and increases the resistance of tumors to cisplatin in vivo. *Carcinogenesis* 1999; **20**: 553-559 [PMID: 10223181 DOI: 10.1093/carcin/20.4.553]

46 **Obrador E**, Carretero J, Ortega A, Medina I, Rodilla V, Pellicer JA, Estrela JM. γ-Glutamyl transpeptidase overexpression increases metastatic growth of B16 melanoma cells in the mouse liver. *Hepatology* 2002; **35**: 74-81 [PMID: 11786961 DOI: 10.1053/jhep.2002.30277]

World Journal of Gastroenterology

Submit a Manuscript: https://www.f6publishing.com

World J Gastroenterol 2020 April 7; 26(13): 1474-1489

DOI: 10.3748/wjg.v26.i13.1474

ISSN 1007-9327 (print) ISSN 2219-2840 (online)

ORIGINAL ARTICLE

Case Control Study

Effects of long non-coding RNA Opa-interacting protein 5 antisense RNA 1 on colon cancer cell resistance to oxaliplatin and its regulation of microRNA-137

Jing Liang, Xiao-Feng Tian, Wei Yang

ORCID number: Jing Liang (0000-0002-6207-0317); Xiao-Feng Tian (0000-0001-6676-9240); Wei Yang (0000-0003-0801-846X).

Author contributions: Yang W performed the majority of experiments and analyzed the data; Liang J performed the molecular investigations; Tian XF and Yang W designed and coordinated the research, and wrote the paper.

Institutional review board statement: This study was reviewed and approved by the China-Japan Union Hospital of Jilin University Ethics Committee.

Informed consent statement: All patients in our study provided informed consent.

Conflict-of-interest statement: The authors declare no conflict of interest.

Data sharing statement: No additional data are available.

STROBE statement: The authors have read the STROBE Statement-checklist of items, and the manuscript was prepared and revised according to the STROBE Statement-checklist of items.

Jing Liang, Department of Gastrointestinal Surgery, China-Japan Union Hospital of Jilin University, Changchun 130000, Jilin Province, China

Xiao-Feng Tian, Wei Yang, Department of Hepatopancreatobiliary Surgery, China-Japan Union Hospital of Jilin University, Changchun 130000, Jilin Province, China

Corresponding author: Wei Yang, MD, Chief Physician, Department of Hepatopancreatobiliary Surgery, China-Japan Union Hospital of Jilin University, No. 126 Xiantai Avenue, Changchun 130000, Jilin Province, China. 18345893430@163.com

Abstract

BACKGROUND

The incidence of colon cancer (CC) is currently high, and is mainly treated with chemotherapy. Oxaliplatin (L-OHP) is a commonly used drug in chemotherapy; however, long-term use can induce drug resistance and seriously affect the prognosis of patients. Therefore, this study investigated the mechanism of Opa-interacting protein 5 antisense RNA 1 (OIP5-AS1) on L-OHP resistance by determining the expression of OIP5-AS1 and microRNA-137 (miR-137) in CC cells and the effects on L-OHP resistance, with the goal of identifying new targets for the treatment of CC.

AIM

To study the effects of long non-coding RNA OIP5-AS1 on L-OHP resistance in CC cell lines and its regulation of miR-137.

METHODS

A total of 114 CC patients admitted to China-Japan Union Hospital of Jilin University were enrolled, and the expression of miR-137 and OIP5-AS1 in tumor tissues and corresponding normal tumor-adjacent tissues was determined. The influence of OIP5-AS1 and miR-137 on the biological behavior of CC cells was evaluated. Resistance to L-OHP was induced in CC cells, and their activity was determined and evaluated using cell counting kit-8. Flow cytometry was used to analyze the apoptosis rate, Western blot to determine the levels of apoptosis-related proteins, and dual luciferase reporter assay combined with RNA-binding protein immunoprecipitation to analyze the relationship between OIP5-AS1 and miR-137.

RESULTS

Manuscript source: Unsolicited manuscript

Received: December 4, 2019
Peer-review started: December 4, 2019
First decision: January 16, 2020
Revised: February 4, 2020
Accepted: March 9, 2020
Article in press: March 9, 2020
Published online: April 7, 2020

P-Reviewer: González-González R, Lieto E
S-Editor: Tang JZ
L-Editor: Webster JR
E-Editor: Xing YX

OIP5-AS1 was up-regulated in CC tissues and cells, while miR-137 was down-regulated in CC tissues and cells. OIP5-AS1 was inversely correlated with miR-137 ($P < 0.001$). Silencing OIP5-AS1 expression significantly hindered the proliferation, invasion and migration abilities of CC cells and markedly increased the apoptosis rate. Up-regulation of miR-137 expression also suppressed these abilities in CC cells and increased the apoptosis rate. Moreover, silencing OIP5-AS1 and up-regulating miR-137 expression significantly intensified growth inhibition of drug-resistant CC cells and improved the sensitivity of CC cells to L-OHP. OIP5-AS1 targetedly inhibited miR-137 expression, and silencing OIP5-AS1 reversed the resistance of CC cells to L-OHP by promoting the expression of miR-137.

CONCLUSION

Highly expressed in CC, OIP5-AS1 can affect the biological behavior of CC cells, and can also regulate the resistance of CC cells to L-OHP by mediating miR-137 expression.

Key words: Long non-coding RNA Opa-interacting protein 5 antisense RNA 1; MicroRNA-137; Colon cancer; Drug resistance; Oxaliplatin; Biological behavior

Core tip: Long non-coding RNA (lncRNA) has drug resistance in various diseases, which has become a research hotspot, and it can participate in the regulation of various biological functions in cells. In this study, the expression and regulation mechanism of lncRNA Opa-interacting protein 5 antisense RNA 1 (OIP5-AS1) in colon cancer were investigated, and it was found that OIP5-AS1 was up-regulated in colon cancer cells. Dual luciferase reporter gene and RNA-binding protein immunoprecipitation assays were carried out, and the relationship between microRNA-137 and OIP5-AS1 was determined. The results showed that OIP5-AS1 could mediate drug resistance to oxaliplatin in these cells by regulating microRNA-137.

Citation: Liang J, Tian XF, Yang W. Effects of long non-coding RNA Opa-interacting protein 5 antisense RNA 1 on colon cancer cell resistance to oxaliplatin and its regulation of microRNA-137. *World J Gastroenterol* 2020; 26(13): 1474-1489
URL: https://www.wjgnet.com/1007-9327/full/v26/i13/1474.htm
DOI: https://dx.doi.org/10.3748/wjg.v26.i13.1474

INTRODUCTION

Colon cancer (CC) is a common cancer and one of the main causes of mortality worldwide, especially in people over 50 years old. According to the statistics, there are more than 1000000 new CC patients every year, and this number is expected to be 2200000 in 2030[1,2]. At present, surgery and chemotherapy are the two main treatments for CC[3]. Due to the availability of various chemotherapy regimens, the overall survival rate of CC patients has improved in the past few decades[4]. However, even though the current response rate to systemic chemotherapy can reach 50%, almost all CC patients have reportedly developed drug resistance, which limits the efficacy of anticarcinogens and eventually leads to chemotherapy failure[4]. Oxaliplatin (L-OHP), a third generation platinum drug, is usually used as a first-line chemotherapy agent for metastatic CC, and is often administered with leucovorin (FOLFOX) and 5-fluorouracil. It can induce intrachain and interchain bridges between guanines, thus inhibiting DNA replication and synthesis[5,6]. However, the long-term use of L-OHP results in drug resistance and ultimately limits its therapeutic effect[7]. Therefore, understanding the molecular mechanism of L-OHP resistance is of great significance in order to obtain better therapeutic response predictions in CC patients and to achieve better therapeutic decision-making.

Long non-coding RNA (lncRNA) a non-coding RNA with a length greater than 200 bp, was reported to be strongly linked to drug resistance of tumor cells in recent years[8,9]. The Opa-interacting protein 5 antisense RNA 1 (OIP5-AS1) gene is a lncRNA on human chromosome 15q15.1, which is up-regulated in various cancers, and

promotes cancer development[10]. Kim *et al*[11] pointed out that OIP5-AS1 is a competitive endogenous RNA against HuR and can regulate the growth of cervical cancer (HeLa) cells. In addition, previous studies have found that OIP5-AS1 can affect cell apoptosis and proliferation in multiple myeloma by regulating various pathways[12]. MicroRNAs, a group of non-coding RNAs approximately 19-24 nucleotides long, are involved in drug resistance in various tumor cells[13]. Bi *et al*[14] concluded that microRNA-137 (miR-137) could suppress the migration, proliferation, and invasion of CC cell lines by targeting TCF4. One study demonstrated that miR-137 could suppress the development of lung carcinoma and enhance the sensitivity of cells to paclitaxel and cisplatin[15]. At present, there is no study on the role of OIP5-AS1 in CC, and the mechanism of OIP5-AS1 in regulating L-OHP resistance in CC requires further research.

The present study investigated the role of OIP5-AS1 and miR-137 in the biological behavior and L-OHP resistance in CC cells, and determined the mechanism of OIP5-AS1 on L-OHP resistance in these cells, with the goal of identifying new targets for the treatment of CC.

MATERIALS AND METHODS

Data collection

A total of 114 CC patients admitted to China-Japan Union Hospital of Jilin University from January 2017 to December 2018 were enrolled, including 63 males and 51 females, with an average age of 61.56 ± 7.09 years. CC tissue specimens (n = 114) and corresponding tumor-adjacent tissue specimens (n = 114) were obtained from the patients following their permission for later analysis. This study was carried out with permission from the Ethics Committee of China-Japan Union Hospital of Jilin University, and each subject signed an informed consent form after understanding the study in detail. The inclusion criteria were as follows: Patients diagnosed with CC based on pathology and imaging examination, patients with detailed clinical data, patients with good compliance, and those without a family history of mental diseases or other malignant tumors. The exclusion criteria were as follows: Patients not accompanied by their families at admission, patients with autoimmune diseases or severe liver or kidney dysfunction, and patients reluctant to receive treatment or cooperate during the study.

Cell culture

Human CC cell lines (HCT116, LOVO, HT29, and SW480), and a human normal colon epithelial cell line (FHC) obtained from Nanjing Cobioer Biosciences Co., Ltd. were cultured in RPMI 1640 containing 100 μg/mL penicillin, 100 μg/mL streptomycin, and 10% fetal bovine serum under 5% CO_2 and saturated humidity at 37°C. When the confluency of adherent cell growth reached 85%, 25% pancreatin was added to the cells for digestion, and the cells were continually cultured in the medium for passage after digestion. The lncRNA OIP5-AS1 and miR-137 expression in each cell line was subsequently determined. HCT116 and SW480 cells in logarithmic growth phase were then selected and transfected with blank control (Vector), targetedly inhibited OIP5-AS1 (si-OIP5-AS1), targetedly overexpressed OIP5-AS1 (sh-OIP5-AS1), miR-137-mimics (overexpressed sequence), miR negative control (miR-NC), and miR-137-inhibitor (inhibited sequence) using a Lipofectamine™ 2000 Kit (Invitrogen) in strict accordance with the kit instructions.

Construction of drug-resistant cell lines

HCT116 and SW480 cells in the logarithmic growth phase with a cell density of 1×10^5 cells /mL were cultured for 48 h after the addition of L-OHP at the concentration of 1.6 μg/mL (Shanghai Yuanye Biotechnology Co., Ltd., China). After 48 h, the solution was discarded and the cells were continuously cultured in fresh solution without L-OHP. When the cells resumed normal growth, they were digested for passage. If the cells grew well, the above step was repeated once by increasing the concentration of L-OHP to 2.4 μg/mL. Drug-resistant cell lines (SW480/L-OHP and HCT116/L-OHP) were finally obtained by changing the solution and gradually increasing the concentration of L-OHP. L-OHP treatment of the cells obtained for future analysis was stopped one week before the experiment.

Determination of drug sensitivity

The cell counting kit-8 (Nanjing Enogene Biotech. Co., Ltd., China) was employed to analyze the inhibition rate of cells. Drug-resistant cell lines and parental cell lines in logarithmic growth phase with the concentration adjusted to 1×10^5 cells/mL were seeded into a 96-well plate at 1×10^4 cells/well. The plate included three replicates of

each treatment, and each well was cultured for 48 h after the addition of L-OHP at different concentrations. The plate was cultured for another 2 h or 3 h after the addition of 10 μL of cell counting kit-8 solution to each well. The optical density of each well at the wavelength of 450 nm was then measured. The experiment was repeated three times, and the 50% inhibitory concentration (IC50) of the drugs in the cells from each group was calculated.

Real-time polymerase chain reaction assay

Total RNA was extracted from the tissues and cells using a Trizol Extraction Kit (Invitrogen, CA, United States), and its purity, concentration, and integrity were determined using an ultraviolet spectrophotometer and agarose gel electrophoresis. Reverse transcription was carried out to change RNA into cDNA according to the operating instructions of the reverse transcription kit. A 7500 real-time polymerase chain reaction (PCR) instrument (ABI Company) and SYBR Premix Ex Taq kit (TaKaRa) were employed. GAPD was taken as an internal reference for lncRNA OIP5-AS1, and U6 as an internal reference for miR-137 in the experiment. The specific sequences were as follows: OIP5-AS1: Upstream 5'-GGTCGTGAAACACCGTCG-3′ and downstream 5'-GTGGGGCATCCAGGGT-3′; GAPDH: Upstream 5'-CAGTCACTACTCAGCTGCCA-3′ and downstream 5'-GAGGGTGCTCC GGTAG-3; miR-137: Upstream 5'-GAAATCCGACAGCTTAAGGAGGTTTGA-3′ and downstream 5'-CATTGCACAGATAGGATTTGATTTACT-3′; and U6: Upstream 5'-CTCGCTTCGGCAGCACA-3′ and downstream 5'-AACGCTTCAC GAATTTGCGT-3′. PCR amplification was carried out at 95°C for 30 s, followed by 40 cycles at 95°C for 5 s and 60°C for 30 s. Data were obtained after three repeated experiments, and the calculated results were expressed using the $2^{\Delta\Delta ct}$ method.

Western blotting assay

Radio immunoprecipitation assay buffer (Thermo Scientific Company, United States) was adopted for lysis, and a Bicinchoninic Acid Kit (Thermo Scientific Company, United States) was adopted for protein concentration determination. The protein with an adjusted concentration of 4 μg/μL was transferred to a polyvinylidene fluoride membrane (Millipore Company) after being separated by 12% sodium dodecyl sulfate-polyacrylamide gel electrophoresis (SDS-PAGE). Subsequently, the membrane was sealed with 5% skim milk for later immune response. The membrane was incubated with primary antibody (Santa Cruz Biotechnology, United States) (1: 1000) overnight at 4°C, and the primary antibody was then removed. The membrane and horseradish peroxidase labeled goat anti-rabbit secondary antibody (Abcam, United States) (1: 1000) were then incubated at 37°C for 1 h, and cleaned with phosphate buffered saline (PBS) 3 times, for 5 min each time. After incubation, the protein was developed and immobilized with an electrochemiluminescence agent. The image was obtained by the Quantity One infrared imaging system, and the relative protein expression level was recorded as the gray value of the band/gray value of the reference.

Cell proliferation experiment

The transfected cells in each group were seeded into a 96-well plate at 5×10^3 cells/well, respectively. The cells were incubated under 5% CO_2 at 37°C. At 0 h, 24 h, 48 h, and 72 h after incubation, 20 μL of 3-(4,5-dimethylthiazol-2-yl)-2,5-diphenyltetrazolium bromide solution and 150 μL of dimethyl sulfoxide were added to each well, respectively, and the plate was shaken for 5-10 min to completely dissolve the purple crystals. The optical density of each well at 450 nm wavelength was measured using the Multiskan™ GO microplate spectrophotometer (Thermo Fisher Scientific, China) to analyze cell proliferation, and then growth curves of the cells were drawn. The experiment was repeated three times. The MTT assay kit was purchased from Thermo Fisher Scientific (China).

Cell apoptosis assay

An Annexin V-FITC/PI Apoptosis Assay Kit (Invitrogen Company, United States) was used to assess cell apoptosis. The cells were digested with trypsin, followed by washing twice with PBS. The 1×10^6 cells /mL cells were centrifuged for 5 min, and the supernatant discarded. Annexin-V-FITC labeling solution (20 μL) and PI reagent (20 μL) were successively added into 1 mL of buffer containing the cells, and incubated at room temperature in the dark for 5 min. A Beckman Coulter CytoFLEX LX Flow Cytometry System was employed to measure cell apoptosis. The experiment was repeated three times, and the data were averaged.

Cell migration and invasion assay

Both the scratch-wound healing assay and Transwell assay were performed to

evaluate cell migration and invasion. The cells were scratched perpendicularly using sterilized 100 μL disposable pipette tips to ensure consistent width of each scratch wound as far as possible. The cell culture medium was removed, and the plate was washed three times with PBS to wash off cell debris generated by the scratches. The cells were placed in serum-free medium, and the scratch in each group was analyzed using a microscope at 0 h and 24 h after cell scratching, to evaluate cell migration. A Transwell Kit (Shanghai Fanke Biotechnology Co., Ltd., FK-lk019) was used for the invasion assay. First, 200 μL of RPMI 1640 culture medium was placed in the upper compartment, and 500 mL of RPMI 1640 with 10% FBS was placed in the lower compartment. After 48 h of culture at 37°C, the matrix gelatin and cells in the upper compartment were wiped off. The plate was cleaned three times with PBS, immobilized with paraformaldehyde for 10 min, cleaned three times with double distilled water, dried, followed by staining with 0.1% crystal violet, and cell invasion was assessed by microscopy.

Dual luciferase assay

StarBase 3.0 was used to predict lncRNA and miRNA target genes. PmirGLO reporter vectors carrying pmir-miR-137-3' untranslated region wild type (Wt) and pmir-miR-137-3' untranslated region mutant (Mut), sh-OIP5-AS1, and sh-NC were co-transfected into CC cells. After 48 h, luciferase activity was determined using the dual luciferase reporter gene determination kit (Solarbio, China).

RNA-binding protein immunoprecipitation assay

A RNA-binding protein immunoprecipitation (RIP) kit (Beijing Biomars Technology Development Co., Ltd., China) was used to carry out the RIP assay following the manufacturer's instructions. The cells were cleaned with pre-cooled PBS, and then the supernatant was discarded. An equal volume of RIP lysate was added to lyse the cells, and the whole cell protein extract was incubated with RIP washing buffer containing magnetic beads bound to Ago2 antibody or immunoglobulin G controls. The immunoprecipitated RNA was extracted from the samples after protein digestion by proteinase K. Finally, the purified RNA was analyzed by qRT-PCR to prove the existence of binding targets.

Statistical analysis

In this study, the collected data were analyzed statistically using SPSS20.0, and visualized by figures using GraphPad 7. Inter-group comparisons were conducted using the *t* test, and multi-group comparisons were performed using one-way ANOVA. In addition, post hoc pairwise comparison was carried out by the LSD-*t* test. Receiver operating characteristic curves were used to analyze the diagnostic value of OIP5-AS1 and miR-137 in CC, and Pearson's correlation analysis was carried out to analyze the relationship between OIP5-AS1 and miR-137. $P < 0.05$ indicated statistically significant differences.

RESULTS

The expression of lncRNA OIP5-AS1 and miR-137 in CC

The results showed that OIP5-AS1 expression in CC tissues was significantly higher than that in corresponding tumor-adjacent tissues ($P < 0.05$) and miR-137 expression was low in cancer tissues ($P < 0.05$). In addition, correlation coefficient analysis revealed that there was a negative correlation between OIP5-AS1 expression and miR-137 expression in CC tissues ($r = -0.7123$, $P < 0.001$) (Figure 1). Receiver operating characteristic curve results showed that OIP5-AS1 and miR-137 had high diagnostic value in CC patients. Further determination of the expression of these two factors in CC cells revealed that OIP5-AS1 expression in normal CC cell lines (HCT116, SW480, HT29, and LOVO) was significantly higher than that in the normal colon epithelial cell line (FHC), and miR-137expression was low in all CC cell lines.

Influence of lncRNA OIP5-AS1 on the biological function of CC cells

Vector, si-OIP5-AS1, and sh-OIP5-AS1 were transfected into CC cells (HCT116 and SW480), respectively. It was shown that compared with HCT116 and SW480 cells transfected with Vector, those transfected with sh-OIP5-AS1 showed significantly increased expression of OIP5-AS1, while those transfected with si-OIP5-AS1 showed significantly decreased OIP5-AS1 expression. Evaluation of the biological function of cells revealed that compared with the Vector group, HCT116 and SW480 cells transfected with si-OIP5-AS1 showed significantly suppressed proliferation, migration, and invasion abilities, and a significantly increased apoptosis rate (all $P <$ 0.05), while those transfected with sh-OIP5-AS1 showed significantly enhanced

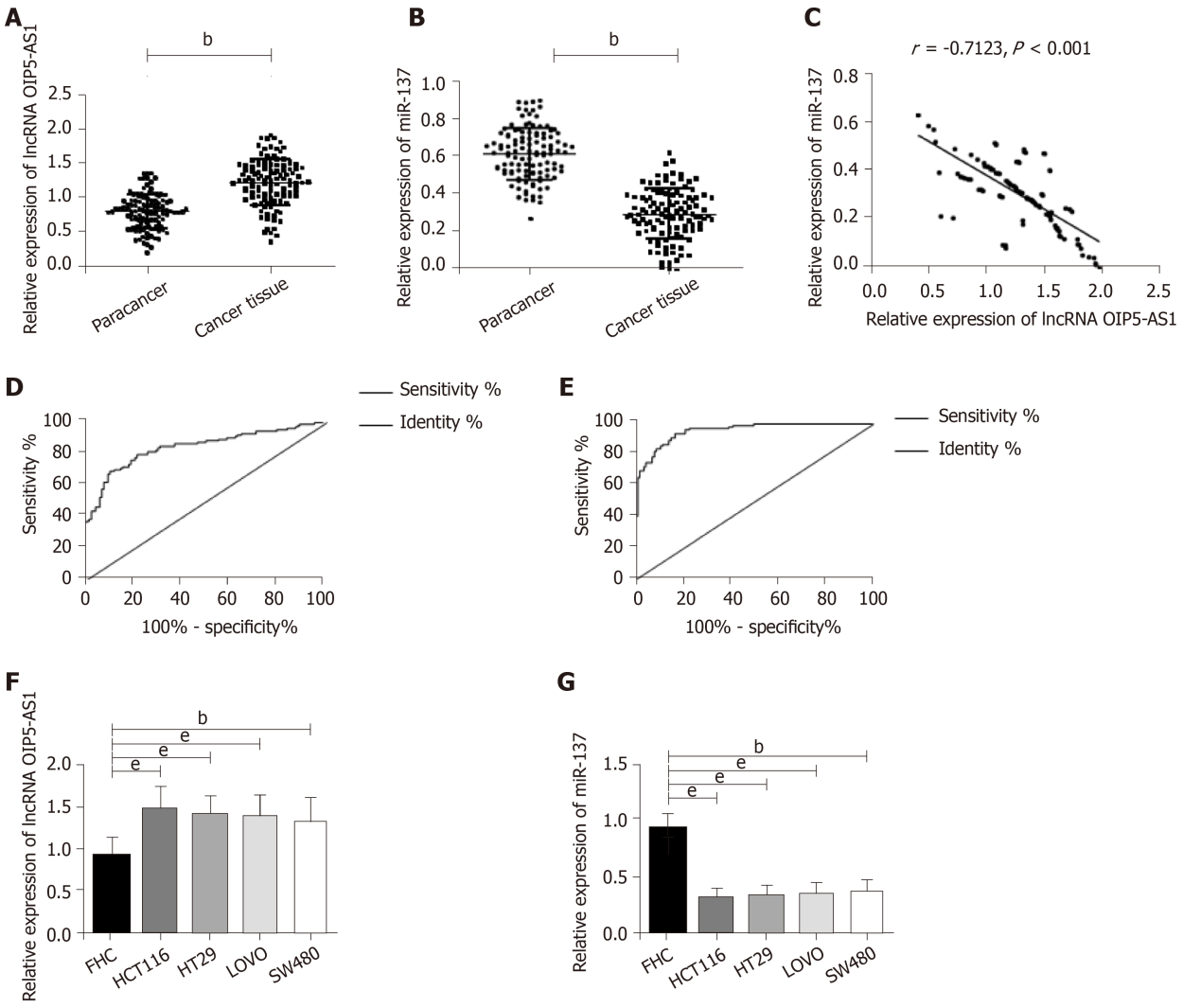

Figure 1 The expression of long non-coding RNA Opa-interacting protein 5 antisense RNA 1 and microRNA-137 in colon cancer. A: Opa-interacting protein 5 antisense RNA 1 (OIP5-AS1) was highly expressed in cancer tissues; B: miR-137 showed low expression in cancer tissues; C: The expression of OIP5-AS1 was negatively correlated with that of miR-137 in cancer tissues (r = - 0.7123); D: The value of OIP5-AS1 in diagnosing colon cancer (CC) patients; E: The value of miR-137 in diagnosing CC patients; F: The expression of OIP 5-AS1 in CC cell lines was much higher than that in the normal colon epithelial cell line; G: The expression of miR-137 in CC cell lines was significantly lower than that in the normal colon epithelial cell line. $^{b}P < 0.01$, $^{e}P < 0.001$ for between-group comparisons. OIP5-AS1: Opa-interacting protein 5 antisense RNA 1; LncRNA: Long non-coding RNA.

proliferation, migration, and invasion abilities, and a significantly decreased apoptosis rate (all $P < 0.05$). In addition, compared with the Vector group, the si-OIP5-AS1 group showed significantly increased expression of apoptosis-related proteins (Bax and Caspase-3), and significantly decreased expression of Bcl-2 protein (all $P < 0.05$), while the sh-OIP5-AS1 group showed significantly decreased expression of apoptosis-related proteins (Bax and Caspase-3), and significantly increased expression of Bcl-2 protein (all $P < 0.05$) (Figure 2).

Influence of lncRNA OIP5-AS1 on CC cell resistance to L-OHP

The OIP5-AS1 level in constructed drug-resistant cell lines was determined, and it was demonstrated that the OIP5-AS1 level in drug-resistant cell lines (HCT116/L-OHP and SW480/L-OHP) was significantly higher than that in the HCT116 and SW480 cell lines ($P < 0.05$). The inhibitory effect of L-OHP at different concentrations on cell growth was determined, and it was calculated that the IC50 of HCT116 and SW480 cells was 20.20 μg/mL and 19.40 μg/mL, respectively, while that of drug-resistant cell lines HCT116/L-OHP and SW480/L-OHP was 114.9 μg/mL and 109.8 μg/mL, respectively. Thus, after L-OHP treatment, the cell activity of drug-resistant cell lines was significantly higher than that of parent cell lines. The inhibitory effect of L-OHP at different concentrations on the growth of transfected drug-resistant cells was also determined, and it was found that the IC50 of HCT116/L-OHP cells transfected with Vector, those transfected with si-OIP5-AS1, and those transfected with sh-OIP5-AS1 was 116.5 μg/mL, 54.96 μg/mL, and 196.6 μg/mL, respectively,

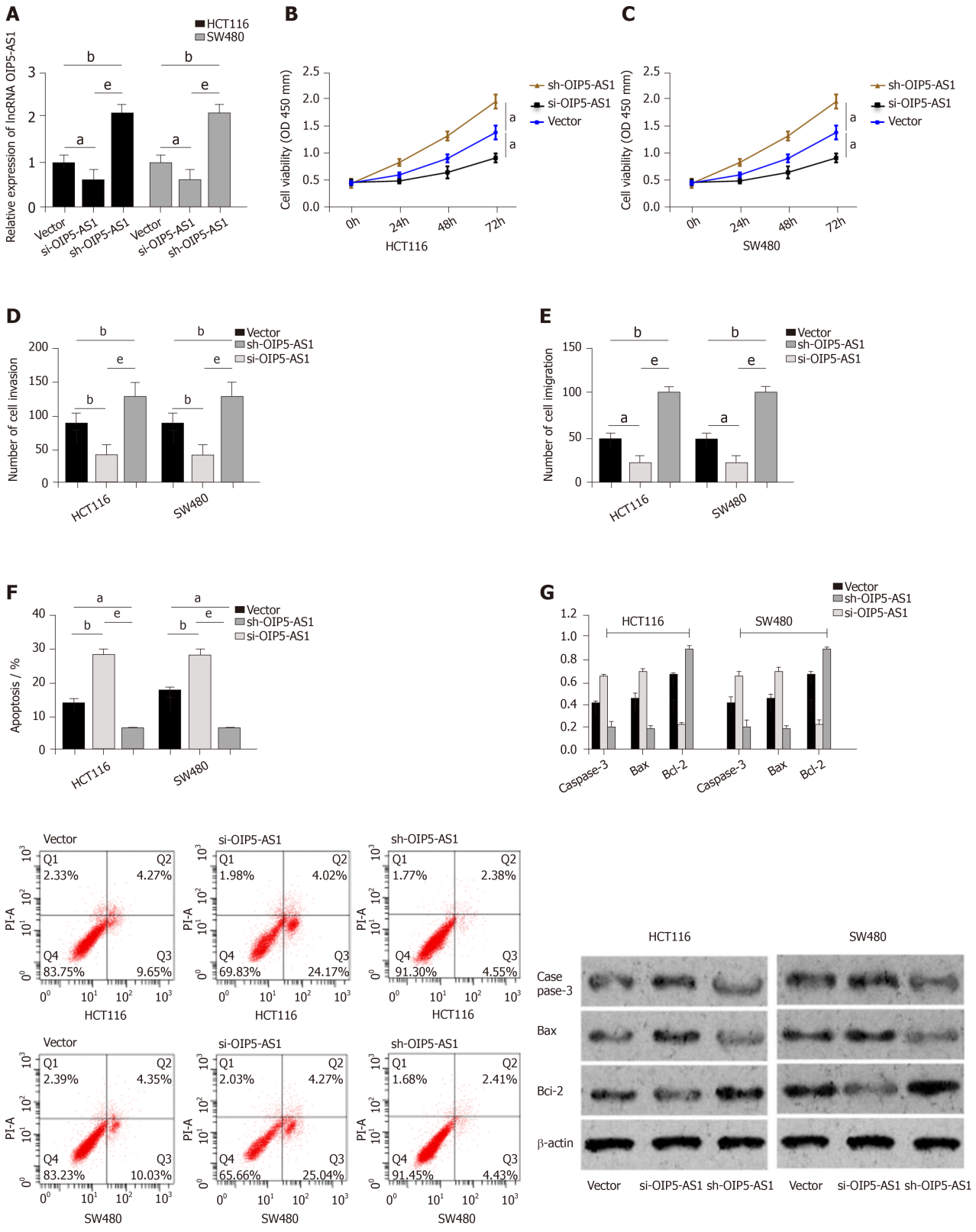

Figure 2 Influence of long non-coding RNA Opa-interacting protein 5 antisense RNA 1 on the biological function of colon cancer cells. A: The Opa-interacting protein 5 antisense RNA 1 expression in transfected colon cancer cell lines; B: Comparison of proliferation activity of HCT116 cells among different groups after transfection; C: Comparison of cell proliferation activity of SW480 cells among different groups after transfection; D: Comparison of invasion ability among different groups after transfection; E: Comparison of migration ability among different groups after transfection; F: Comparison of apoptosis ability among different groups after transfection, and apoptosis map; G: Comparison of apoptosis-related proteins among different groups after transfection and protein map. $^{a}P < 0.05$, $^{b}P < 0.01$, $^{e}P < 0.001$ for between-group comparisons. OIP5-AS1: Opa-interacting protein 5 antisense RNA 1; LncRNA: Long non-coding RNA; OD: Optical density.

and the IC50 of SW480/L-OHP cells transfected with Vector, those transfected with si-OIP5-AS1, and those transfected with sh-OIP5-AS1 was 114.1 μg/mL, 52.33 μg/mL,

and 186.7 μg/mL, respectively. Therefore, these findings indicated that silencing OIP5-AS1 expression significantly intensified the inhibition of drug-resistant cell growth. The IC50 of each drug-resistant cell line was used as the concentration of added L-OHP to observe the apoptosis of drug-resistant cells. It was found that compared with the cells transfected with Vector, those transfected with si-OIP5-AS1 showed significantly intensified apoptosis and significantly increased expression of apoptosis-related proteins (Bax and Caspase-3), and significantly decreased expression of Bcl-2 (all $P < 0.05$), while those transfected with sh-OIP5-AS1 showed the opposite trend (all $P < 0.05$) (Figure 3).

Influence of miR-137 on the biological function of CC cells

MiR-NC, miR-137-mimics, and miR-137-inhibitor were transfected into CC cells (HCT116 and SW48), respectively. It was shown that compared with HCT116 and SW480 cells transfected with miR-NC, those transfected with miR-137-mimics showed significantly up-regulated expression of miR-137, while those transfected with miR-137-inhibitor showed significantly decreased expression of miR-137. Assessment of the biological function of cells revealed that compared with the miR-NC group, HCT116 and SW480 cells transfected with miR-137-mimics showed significantly suppressed proliferation, migration, and invasion abilities, and significantly intensified apoptosis (all $P < 0.05$), while those transfected with miR-137-inhibitor showed the opposite trend (all $P < 0.05$). In addition, compared with the miR-NC group, the miR-137-mimics group showed significantly increased expression of apoptosis-related proteins (Bax and Caspase-3), and significantly decreased expression of Bcl-2 protein (all $P < 0.05$), while the miR-137-inhibitor group showed markedly down-regulated expression of apoptosis-related proteins (Bax and Caspase-3), and significantly up-regulated expression of Bcl-2 protein (all $P < 0.05$) (Figure 4).

Effects of miR-137 on CC cell resistance to L-OHP

The miR-137 level in constructed drug-resistant cell lines was determined, and it was found that the miR-137 level in drug-resistant cell lines (HCT116/L-OHP and SW480/L-OHP) was significantly lower than that in HCT116 and SW480 cell lines (all $P < 0.05$). The inhibition of L-OHP at different concentrations on the growth of transfected drug-resistant cells was determined, and the results showed that the IC50 of HCT116/L-OHP cells transfected with miR-NC, those transfected with miR-137-mimics, and those transfected with miR-137-inhibitor was 117.3 μg/mL, 52.87 μg/mL, and 202.0 μg/mL, respectively, and the IC50 of SW480/L-OHP cells transfected with miR-NC, those transfected with miR-137-mimics, and those transfected with miR-137-inhibitor was 112.5 μg/mL, 48.62 μg/mL, and 196.1 μg/mL, respectively. These findings indicated that overexpression of miR-137 could significantly intensify the growth inhibition of drug-resistant cells. The IC50 of each drug-resistant cell line was used as the concentration of added L-OHP to observe the apoptosis of drug-resistant cells. It was found that compared with the miR-NC group, the miR-137-mimics group showed significantly intensified apoptosis, significantly up-regulated apoptosis-related proteins (Bax and Caspase-3), and significantly down-regulated Bcl-2 protein, while the miR-137-inhibitor group showed the opposite trend (Figure 5).

Effects of OIP 5-AS1 on the expression of miR-137 in L-OHP-resistant CC cell lines

Bioinformatics analysis revealed binding sites between miR-137 and OIP5-AS1. Therefore, RIP and dual luciferase assay were carried out, and showed that the fluorescence activity of miR-137-Wt decreased significantly. The RIP assay revealed that compared with immunoprecipitation with anti-IgG, the immunoprecipitation with anti-Ago2 antibody contributed to significantly increased enrichment content of miR-137 and OIP5-AS1. In order to further verify that OIP5-AS1 affects the resistance of CC cells by regulating miR-137, we co-transfected Si-OIP5-AS1 and miR-137-inhibitor into HCT116/L-OHP and SW480/L-OHP cells. It was found that Si-OIP5-AS1 could enhance the drug resistance sensitivity of HCT116/L-OHP and SW480/L-OHP cells to L-OHP, increase the apoptosis rate, significantly up-regulate the expression of Bax and Caspase-3 proteins, and significantly down-regulate the expression of Bcl-2 protein, but miR-137-inhibitor did not reverse this effect. The increased IC50 of L-OHP lowered the apoptosis rate, reduced the expression of Bax and Caspase-3 proteins in cells, and further increased the expression of Bcl-2 protein (Figure 6).

DISCUSSION

CC is a common malignant tumor in the gastrointestinal tract, its associated morbidity is rising year by year, and its incidence and mortality among men are higher than

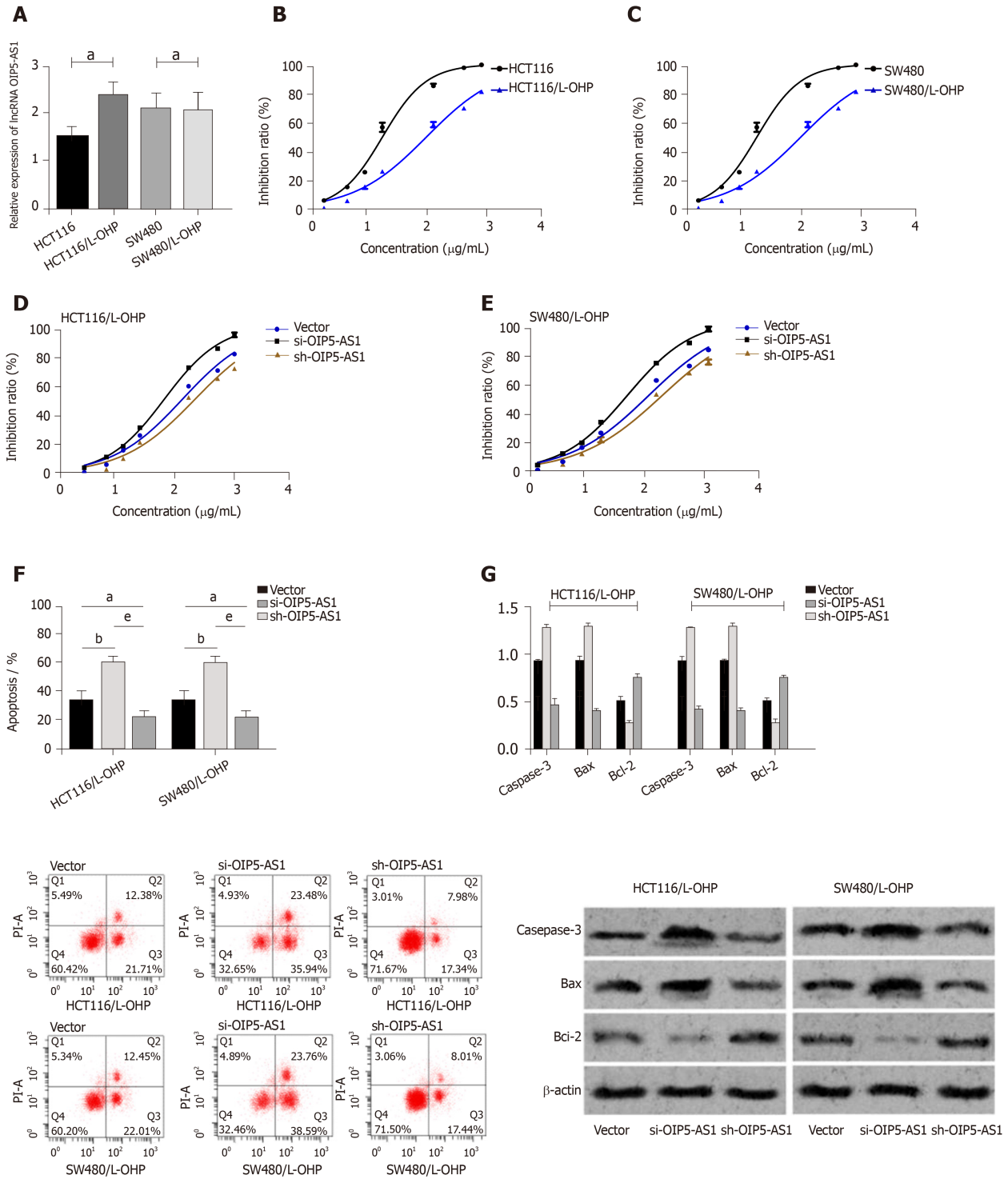

Figure 3 Effects of long non-coding RNA Opa-interacting protein 5 antisense RNA 1 on colon cancer cell resistance to oxaliplatin. A: Determined Opa-interacting protein 5 antisense RNA 1 expression in constructed drug-resistant cell lines; B: Effects of oxaliplatin (L-OHP) at different concentrations on growth inhibition of HCT116 and HCT116/L-OHP cells; C: Effects of L-OHP at different concentrations on growth inhibition of SW480 and SW480/L-OHP cells; D: Effects of L-OHP at different concentrations on growth inhibition of HCT116/L-OHP cells in each group after transfection; E: Influence of L-OHP at different concentrations on growth inhibition of SW480/L-OHP cells in each group after transfection; F: Comparison of apoptosis rate of drug-resistant cells among different groups after transfection and apoptosis map; G: Comparison of drug-resistant cell apoptosis among different groups after transfection and apoptotic protein map. SW480/L-OHP indicates SW480 cell line with L-OHP resistance. HCT116/L-OHP indicates HCT116 cell line with L-OHP resistance. $^{a}P < 0.05$, $^{b}P < 0.01$, $^{e}P < 0.001$ for between-group comparisons. OIP5-AS1: Opa-interacting protein 5 antisense RNA 1; L-OHP: Oxaliplatin.

those among women[16-18]. At present, the most effective clinical treatment for CC is chemotherapy. With low renal toxicity, L-OHP has been widely used as a first-line chemotherapy drug in CC patients[19,20]. However, chemotherapy is often accompanied by drug resistance, which limits the clinical application of L-OHP and seriously compromises the effectiveness of platinum-containing chemotherapy regimens[21,22].

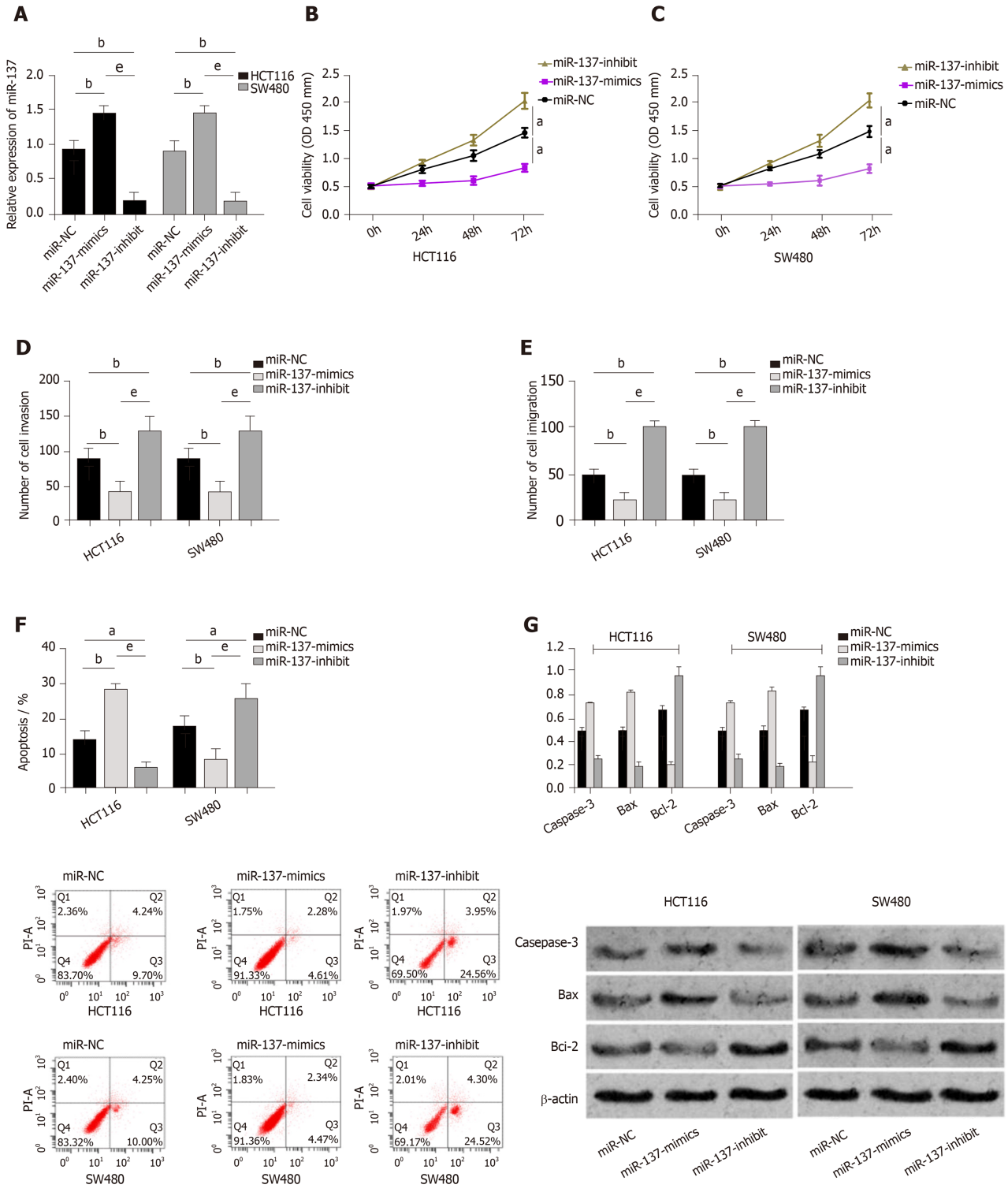

Figure 4 Influence of miR-137 on the biological function of colon cancer cells. A: The miR-137 expression in transfected colon cancer cell lines; B: Comparison of proliferation activity of HCT116 cells among different groups after transfection; C: Comparison of proliferation activity of SW480 cells among different groups after transfection; D: Comparison of invasion ability among different groups after transfection; E: Comparison of migration ability among different groups after transfection; F: Comparison of apoptosis ability among different groups after transfection and apoptosis map; G: Comparison of apoptosis-related proteins among different groups after transfection and protein map. $^{a}P < 0.05$, $^{b}P < 0.01$, $^{e}P < 0.001$ for between-group comparisons. OIP5-AS1: Opa-interacting protein 5 antisense RNA 1; OD: Optical density.

Therefore, finding a solution for L-OHP drug resistance has become the key to the treatment of tumors. At present, the correlation between cell resistance and specific genes during CC chemotherapy at the molecular biology level requires further clarification.

LncRNAs have gradually become key regulators of cellular processes and

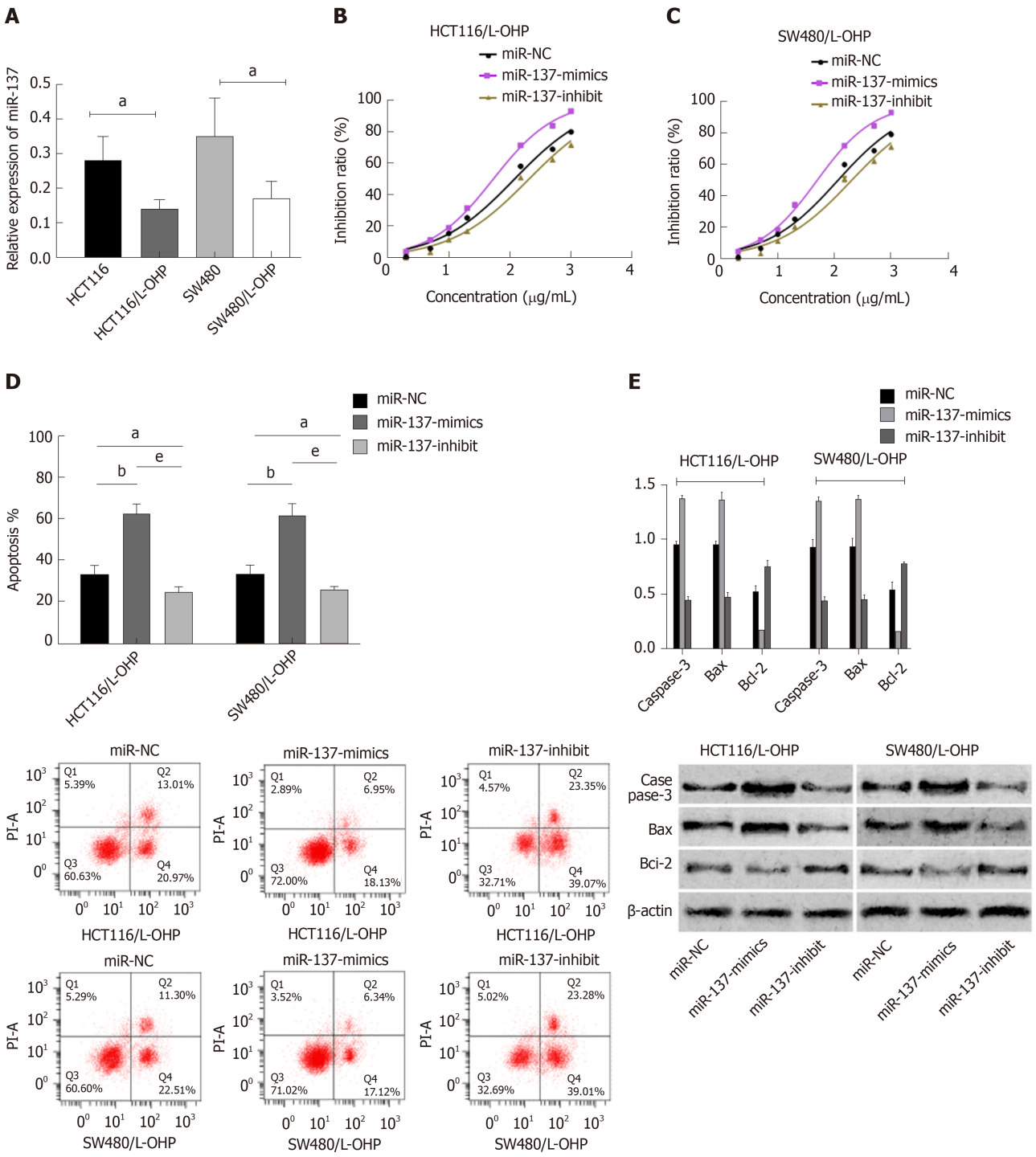

Figure 5 Influence of microRNA-137 on colon cancer cell resistance to oxaliplatin. A: Determined miR-137 expression in constructed drug-resistant cell lines; B: Influence of oxaliplatin (L-OHP) at different concentrations on growth inhibition of HCT116/L-OHP cells in each group after transfection; C: Effects of L-OHP at different concentrations on growth inhibition of SW480/L-OHP cells in each group after transfection; D: Comparison of apoptosis rate of drug-resistant cells among different groups after transfection and apoptosis map; E: Comparison of apoptotic protein of drug-resistant cells among different groups after transfection and apoptotic protein map. SW480/L-OHP indicates SW480 cell line with L-OHP resistance. HCT116/L-OHP indicates HCT116 cell line with resistance L-OHP resistance. $^{a}P < 0.05$, $^{b}P < 0.01$, $^{e}P < 0.001$ for between-group comparisons. L-OHP: Oxaliplatin; miR-NC: MiR negative control; OIP5-AS1: Opa-interacting protein 5 antisense RNA 1.

physiological and pathological processes[11]. OIP5-AS1 is highly expressed in various diseases and participates in the development and progression of diseases[11,12]. Earlier studies revealed that OIP5-AS1 can regulate the expression of miR-410 and can also regulate its target KLF10/PTEN/AKT to mediate the cellular behavior of multiple myeloma[12]. Wang *et al*[23] pointed out that OIP5-AS1, with low expression in lung cancer, could intensify the proliferation of lung cancer cells by targeting miR-378a-3p, resulting in poor prognosis. However, there are few studies on OIP5-AS1 in CC. In this study, OIP5-AS1 was up-regulated in CC tissues and cells, and silencing OIP5-

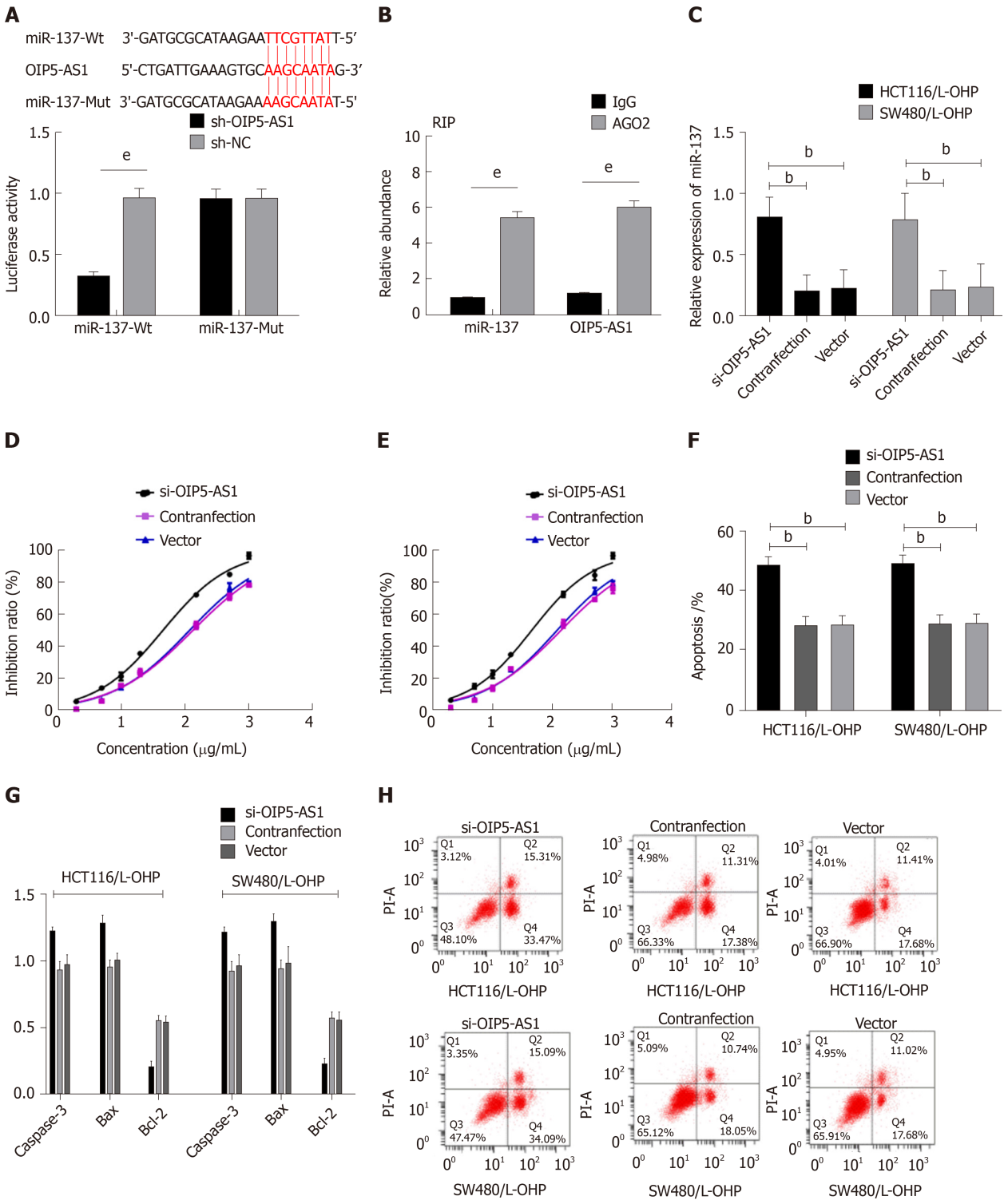
A
miR-137-Wt 3'-GATGCGCATAAGAATTCGTTATT-5'
OIP5-AS1 5'-CTGATTGAAAGTGCAAGCAATAG-3'
miR-137-Mut 3'-GATGCGCATAAGAAAAGCAATAT-5'
sh-OIP5-AS1
sh-NC
Luciferase activity
miR-137-Wt
miR-137-Mut
B
IgG
AGO2
RIP
Relative abundance
miR-137
OIP5-AS1
C
HCT116/L-OHP
SW480/L-OHP
Relative expression of miR-137
si-OIP5-AS1
Contranfection
Vector
D
si-OIP5-AS1
Contranfection
Vector
Inhibition ratio (%)
Concentration (μg/mL)
E
si-OIP5-AS1
Contranfection
Vector
Inhibition ratio(%)
Concentration (μg/mL)
F
si-OIP5-AS1
Contranfection
Vector
Apoptosis /%
HCT116/L-OHP
SW480/L-OHP
G
si-OIP5-AS1
Contranfection
Vector
HCT116/L-OHP
SW480/L-OHP
Caspase-3
Bax
Bcl-2
H
si-OIP5-AS1
Contranfection
Vector
PI-A
HCT116/L-OHP
SW480/L-OHP
Q1 3.12%
Q2 15.31%
Q3 48.10%
Q4 33.47%
Q1 4.98%
Q2 11.31%
Q3 66.33%
Q4 17.38%
Q1 4.01%
Q2 11.41%
Q3 66.90%
Q4 17.68%
Q1 3.35%
Q2 15.09%
Q3 47.47%
Q4 34.09%
Q1 5.09%
Q2 10.74%
Q3 65.12%
Q4 18.05%
Q1 4.95%
Q2 11.02%
Q3 65.91%
Q4 17.68%

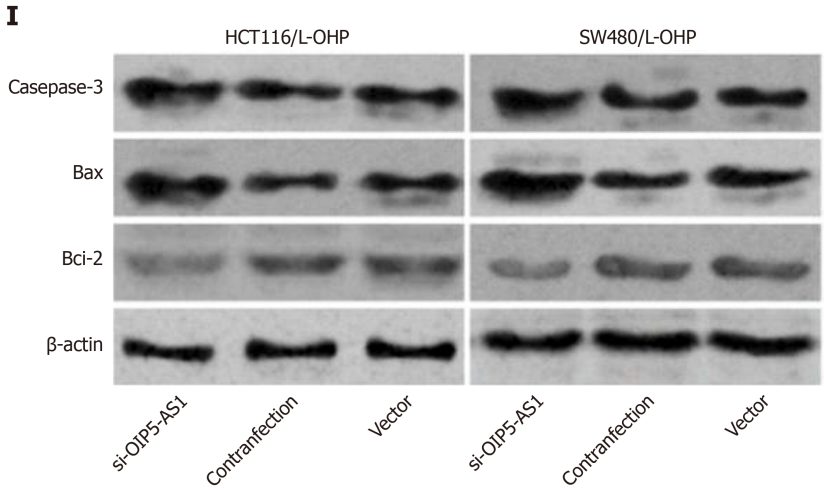

Figure 6 Effects of Opa-interacting protein 5 antisense RNA 1 on the expression of miR-137 in oxaliplatin-resistant colon cancer cell lines. A: Binding sites between OIP 5-AS1 and miR-137 and dual luciferase reporter assay; B: Verification of the relation between Opa-interacting protein 5 antisense RNA 1 and miR-137 by the RIP assay; C: The miR-137 expression in drug-resistant cell lines after co-transfection; D: Growth inhibition of HCT116/oxaliplatin (L-OHP) cell lines after co-transfection; E: Growth inhibition of SW480/L-OHP cell lines after co-transfection; F: Comparison of apoptosis rate of cell lines among different groups after co-transfection; G: Comparison of apoptosis protein level in drug resistant cell lines among different groups after co-transfection; H: Apoptosis of drug-resistant cell lines in each group after co-transfection; I: Apoptosis-related protein in drug-resistant cell lines in each group after co-transfection. SW480/L-OHP indicates SW480 cell line with L-OHP resistance. HCT116/L-OHP indicates HCT116 cell line with L-OHP resistance. $^{b}P < 0.01$, $^{e}P < 0.001$ for between-group comparisons. L-OHP: Oxaliplatin; miR-NC: MiR negative control; Wt: Wild type; Mut: Mutant.

AS1 expression significantly inhibited the invasion, proliferation, and migration abilities of CC cells and significantly increased the apoptosis rate. However, up-regulation of OIP5-AS1 resulted in the opposite effects. These results indicated that OIP5-AS1 promoted the development of CC, which was inconsistent with previous studies[11]. Subsequently, we constructed L-OHP resistant cells, and found that silencing the expression of OIP5-AS1 strongly intensified the growth inhibition of drug-resistant cells, and decreased the IC50 of L-OHP, significantly increased the apoptosis rate, up-regulated apoptosis-related proteins (Caspase-3 and Bax), and significantly down-regulated Bcl-2 protein. Similarly, up-regulation of the expression of OIP5-AS1 resulted in the opposite effects. This suggested that silencing OIP5-AS1 can improve the sensitivity of CC cells to L-OHP, and can also reverse the resistance of CC cells to L-OHP, thus improving chemotherapy efficacy. Recent studies have shown that silencing OIP5-AS1 inhibits the development of osteosarcoma cells *in vitro* and *in vivo* and promotes cell apoptosis, and it can also strengthen the drug resistance sensitivity of osteosarcoma cells to cisplatin[24]. These findings are similar to the results of this study. However, the mechanism of OIP5-AS1 in drug-resistant CC cells requires further study.

In recent years, more and more studies have found that a lncRNA can act as a miR response element and a competitive platform in a variety of tumors, and can also act as a miR molecular sponge by binding to miR, thus affecting miRNA expression and the regulation of cell function[25,26]. Some studies have revealed that lncRNA FOXD2-AS1 can promote drug resistance to gemcitabine in bladder cancer by regulating miR-143[27]. Moreover, one study concluded that lncRNA BLACAT1 could regulate ABCB1 through miR-361 to promote drug resistance to L-OHP in gastric cancer[28]. In this study, we found targeted binding sites between OIP5-AS1 and miR-137 through online tool analysis, and verified the results using dual luciferase reporter assay. We also found enrichment between OIP5-AS1 and miR-137 using the RIP assay. These findings further confirmed the competitive endogenous RNA relationship between OIP5-AS1 and miR-137. MiR-137 has low expression in various cancers and can participate in the regulation of cell biological behavior[29]. In this study, it was found that miR-137 expression was low in CC, and up-regulation of miR-137 expression could inhibit proliferation, invasion and migration of CC cells and increase the apoptosis rate, which was similar to the results of the study by Bi *et al*[14]. Previous studies revealed that down-regulation of miR-137 induced resistance to L-OHP in parent CC cells, while over-expression of miR-137 induced sensitivity to L-OHP in drug-resistant cells[30], which was similar to the results in this study and further proved the influence of miR-137 in drug-resistant cells. In this study, it was also found that the expression of OIP5-AS1 was negatively correlated with that of miR-137 in CC tissues. Finally, CC cells were co-transfected with Si-OIP5-AS1 and miR-137-inhibitor

in this study, and it was found that the inhibitory effect on CC cells and the inhibitory effect on L-OHP drug resistance were offset. Therefore, the results of this study confirmed that OIP5-AS1 can mediate the expression of miR-137 to regulate drug resistance to L-OHP in CC cells.

This study investigated the effects of OIP5-AS1 and miR-137 on biological behaviors and L-OHP drug resistance in CC cells from many aspects. However, there are still some limitations in this study. No study has been conducted in nude mice, and whether OIP5-AS1 is involved in the prognosis of CC still requires further research and verification. Moreover, the regulatory network of OIP5-AS1 in CC remains unclear, and further research is needed to determine whether OIP5-AS1 can affect the development and progression of tumors in other ways. In future research, we will carry out more experiments to verify these results.

To sum up, OIP5-AS1 is highly expressed in CC and can affect the biological behaviors of CC cells, and can regulate drug resistance to L-OHP in CC cells by mediating miR-137 expression.

ARTICLE HIGHLIGHTS

Research background

Recently, colon cancer (CC) has displayed a high incidence, and the main treatment of CC is chemotherapy. Oxaliplatin (L-OHP) is a common drug used in chemotherapy, but long-term use can result in drug resistance, seriously affecting the prognosis of patients.

Research motivation

Long non-coding RNA Opa-interacting protein 5 antisense RNA 1 (OIP5-AS1) appears to be up-regulated, which plays a tumor-promoting role in a number of cancers. It is speculated that miR-137 may be effective in mediating drug resistance in CC cells.

Research objectives

To determine the effect of long non-coding RNA OIP5-AS1 on drug resistance in CC cell lines and its role in regulating miR-137.

Research methods

We not only analyzed the expression levels of OIP5-AS1 and miR-137 in surgical CC tissue samples, but also observed their effects on the biological behavior of CC cells as well as L-OHP resistance.

Research results

We noted high expression of OIP5-AS in CC tissues and cells and low expression of miR-137. In cytological studies, it was found that reducing OIP5-AS1 expression or increasing miR-137 expression controlled the proliferation, invasion and migration of CC cells, promoting the apoptosis rate of tumor cells by regulating the expression of apoptosis-related proteins.

Research conclusions

OIP5-AS1 is highly expressed in CC, which contributes to regulation of the biological behavior of CC cells as well as drug resistance to L-OHP in CC cells *via* mediation of miR-137 expression.

Research perspectives

This study reveals the mechanism of OIP5-AS1 in drug resistance to L-OHP in CC cells, which provides a new method to improve the sensitivity of CC cells to L-OHP.

REFERENCES

1 **Gangireddy VGR**, Coleman T, Kanneganti P, Talla S, Annapureddy AR, Amin R, Parikh S. Polypectomy versus surgery in early colon cancer: size and location of colon cancer affect long-term survival. *Int J Colorectal Dis* 2018; **33**: 1349-1357 [PMID: 29938362 DOI: 10.1007/s00384-018-3101-z]

2 **Lawler M**, Alsina D, Adams RA, Anderson AS, Brown G, Fearnhead NS, Fenwick SW, Halloran SP, Hochhauser D, Hull MA, Koelzer VH, McNair AGK, Monahan KJ, Näthke I, Norton C, Novelli MR, Steele RJC, Thomas AL, Wilde LM, Wilson RH, Tomlinson I; Bowel Cancer UK Critical Research Gaps in Colorectal Cancer Initiative. Critical research gaps and recommendations to inform research prioritisation for more effective prevention and improved outcomes in colorectal cancer. *Gut* 2018; **67**: 179-193 [PMID: 29233930 DOI: 10.1136/gutjnl-2017-315333]

3 **Stein A**, Atanackovic D, Bokemeyer C. Current standards and new trends in the primary treatment of colorectal cancer. *Eur J Cancer* 2011; **47** Suppl 3: S312-S314 [PMID: 21943995 DOI: 10.1016/S0959-8049(11)70183-6]

4 **Hu T**, Li Z, Gao CY, Cho CH. Mechanisms of drug resistance in colon cancer and its therapeutic strategies. *World J Gastroenterol* 2016; **22**: 6876-6889 [PMID: 27570424 DOI: 10.3748/wjg.v22.i30.6876]

5 **Brungs D**, Aghmesheh M, de Souza P, Carolan M, Clingan P, Rose J, Ranson M. Safety and Efficacy of Oxaliplatin Doublet Adjuvant Chemotherapy in Elderly Patients With Stage III Colon Cancer. *Clin Colorectal Cancer* 2018; **17**: e549-e555 [PMID: 29861156 DOI: 10.1016/j.clcc.2018.05.004]

6 **Ray B**, Gupta B, Mehrotra R. Binding of platinum derivative, oxaliplatin to deoxyribonucleic acid: structural insight into antitumor action. *J Biomol Struct Dyn* 2019; **37**: 3838-3847 [PMID: 30282523 DOI: 10.1080/07391102.2018.1531059]

7 **Huang H**, Aladelokun O, Ideta T, Giardina C, Ellis LM, Rosenberg DW. Inhibition of PGE_2/EP4 receptor signaling enhances oxaliplatin efficacy in resistant colon cancer cells through modulation of oxidative stress. *Sci Rep* 2019; **9**: 4954 [PMID: 30894570 DOI: 10.1038/s41598-019-40848-4]

8 **Majidinia M**, Yousefi B. Long non-coding RNAs in cancer drug resistance development. *DNA Repair (Amst)* 2016; **45**: 25-33 [PMID: 27427176 DOI: 10.1016/j.dnarep.2016.06.003]

9 **Saeinasab M**, Bahrami AR, González J, Marchese FP, Martinez D, Mowla SJ, Matin MM, Huarte M. SNHG15 is a bifunctional MYC-regulated noncoding locus encoding a lncRNA that promotes cell proliferation, invasion and drug resistance in colorectal cancer by interacting with AIF. *J Exp Clin Cancer Res* 2019; **38**: 172 [PMID: 31014355 DOI: 10.1186/s13046-019-1169-0]

10 **Sun WL**, Kang T, Wang YY, Sun JP, Li C, Liu HJ, Yang Y, Jiao BH. Long noncoding RNA OIP5-AS1 targets Wnt-7b to affect glioma progression via modulation of miR-410. *Biosci Rep* 2019; **39** [PMID: 30498093 DOI: 10.1042/BSR20180395]

11 **Kim J**, Abdelmohsen K, Yang X, De S, Grammatikakis I, Noh JH, Gorospe M. LncRNA OIP5-AS1/cyrano sponges RNA-binding protein HuR. *Nucleic Acids Res* 2016; **44**: 2378-2392 [PMID: 26819413 DOI: 10.1093/nar/gkw017]

12 **Yang N**, Chen J, Zhang H, Wang X, Yao H, Peng Y, Zhang W. LncRNA OIP5-AS1 loss-induced microRNA-410 accumulation regulates cell proliferation and apoptosis by targeting KLF10 via activating PTEN/PI3K/AKT pathway in multiple myeloma. *Cell Death Dis* 2017; **8**: e2975 [PMID: 28796257 DOI: 10.1038/cddis.2017.358]

13 **Samuel P**, Pink RC, Brooks SA, Carter DR. miRNAs and ovarian cancer: a miRiad of mechanisms to induce cisplatin drug resistance. *Expert Rev Anticancer Ther* 2016; **16**: 57-70 [PMID: 26567444 DOI: 10.1586/14737140.2016.1121107]

14 **Bi WP**, Xia M, Wang XJ. miR-137 suppresses proliferation, migration and invasion of colon cancer cell lines by targeting TCF4. *Oncol Lett* 2018; **15**: 8744-8748 [PMID: 29805612 DOI: 10.3892/ol.2018.8364]

15 **Shen H**, Wang L, Ge X, Jiang CF, Shi ZM, Li DM, Liu WT, Yu X, Shu YQ. MicroRNA-137 inhibits tumor growth and sensitizes chemosensitivity to paclitaxel and cisplatin in lung cancer. *Oncotarget* 2016; **7**: 20728-20742 [PMID: 26989074 DOI: 10.18632/oncotarget.8011]

16 **Cerdán Santacruz C**, Frasson M, Flor-Lorente B, Ramos Rodríguez JL, Trallero Anoro M, Millán Scheiding M, Maseda Díaz O, Dujovne Lindenbaum P, Monzón Abad A, García-Granero Ximenez E; ANACO Study Group. Laparoscopy may decrease morbidity and length of stay after elective colon cancer resection, especially in frail patients: results from an observational real-life study. *Surg Endosc* 2017; **31**: 5032-5042 [PMID: 28455773 DOI: 10.1007/s00464-017-5548-3]

17 **Eaglehouse YL**, Georg MW, Richard P, Shriver CD, Zhu K. Costs for Colon Cancer Treatment Comparing Benefit Types and Care Sources in the US Military Health System. *Mil Med* 2019; **184**: e847-e855 [PMID: 30941433 DOI: 10.1093/milmed/usz065]

18 **Manceau G**, Mege D, Bridoux V, Lakkis Z, Venara A, Voron T, Sielezneff I, Karoui M; French Surgical Association Working Group. Emergency Surgery for Obstructive Colon Cancer in Elderly Patients: Results of a Multicentric Cohort of the French National Surgical Association. *Dis Colon Rectum* 2019; **62**: 941-951 [PMID: 31283592 DOI: 10.1097/DCR.0000000000001421]

19 **Witzig TE**, Johnston PB, LaPlant BR, Kurtin PJ, Pederson LD, Moore DF, Nabbout NH, Nikcevich DA, Rowland KM, Grothey A. Long-term follow-up of chemoimmunotherapy with rituximab, oxaliplatin, cytosine arabinoside, dexamethasone (ROAD) in patients with relapsed CD20+ B-cell non-Hodgkin lymphoma: Results of a study of the Mayo Clinic Cancer Center Research Consortium (MCCRC) MC0485 now known as academic and community cancer research united (ACCRU). *Am J Hematol* 2017; **92**: 1004-1010 [PMID: 28614905 DOI: 10.1002/ajh.24824]

20 **Gallois C**, Taieb J, Le Corre D, Le Malicot K, Tabernero J, Mulot C, Seitz JF, Aparicio T, Folprecht G, Lepage C, Mini E, Van Laethem JL, Emile JF, Laurent-Puig P; PETACC8 investigators. Prognostic Value of Methylator Phenotype in Stage III Colon Cancer Treated with Oxaliplatin-based Adjuvant Chemotherapy. *Clin Cancer Res* 2018; **24**: 4745-4753 [PMID: 29921730 DOI: 10.1158/1078-0432.CCR-18-0866]

21 **Uppada SB**, Gowrikumar S, Ahmad R, Kumar B, Szeglin B, Chen X, Smith JJ, Batra SK, Singh AB, Dhawan P. MASTL induces Colon Cancer progression and Chemoresistance by promoting Wnt/β-catenin signaling. *Mol Cancer* 2018; **17**: 111 [PMID: 30068336 DOI: 10.1186/s12943-018-0848-3]

22 **El Khoury F**, Corcos L, Durand S, Simon B, Le Jossic-Corcos C. Acquisition of anticancer drug resistance is partially associated with cancer stemness in human colon cancer cells. *Int J Oncol* 2016; **49**: 2558-2568 [PMID: 27748801 DOI: 10.3892/ijo.2016.3725]

23 **Wang M**, Sun X, Yang Y, Jiao W. Long non-coding RNA OIP5-AS1 promotes proliferation of lung cancer cells and leads to poor prognosis by targeting miR-378a-3p. *Thorac Cancer* 2018; **9**: 939-949 [PMID: 29897167 DOI: 10.1111/1759-7714.12767]

24 **Song L**, Zhou Z, Gan Y, Li P, Xu Y, Zhang Z, Luo F, Xu J, Zhou Q, Dai F. Long noncoding RNA OIP5-AS1 causes cisplatin resistance in osteosarcoma through inducing the LPAATβ/PI3K/AKT/mTOR signaling pathway by sponging the miR-340-5p. *J Cell Biochem* 2019; **120**: 9656-9666 [PMID: 30548308 DOI: 10.1002/jcb.28244]

25 **Deguchi S**, Katsushima K, Hatanaka A, Shinjo K, Ohka F, Wakabayashi T, Zong H, Natsume A, Kondo Y. Oncogenic effects of evolutionarily conserved noncoding RNA ECONEXIN on gliomagenesis. *Oncogene* 2017; **36**: 4629-4640 [PMID: 28368417 DOI: 10.1038/onc.2017.88]

26 **Liu T**, Chi H, Chen J, Chen C, Huang Y, Xi H, Xue J, Si Y. Curcumin suppresses proliferation and in vitro invasion of human prostate cancer stem cells by ceRNA effect of miR-145 and lncRNA-ROR. *Gene* 2017; **631**: 29-38 [PMID: 28843521 DOI: 10.1016/j.gene.2017.08.008]

27 **An Q**, Zhou L, Xu N. Long noncoding RNA FOXD2-AS1 accelerates the gemcitabine-resistance of bladder cancer by sponging miR-143. *Biomed Pharmacother* 2018; **103**: 415-420 [PMID: 29674277 DOI: 10.1016/j.biopha.2018.03.138]

28 **Wu X**, Zheng Y, Han B, Dong X. Long noncoding RNA BLACAT1 modulates ABCB1 to promote oxaliplatin resistance of gastric cancer via sponging miR-361. *Biomed Pharmacother* 2018; **99**: 832-838 [PMID: 29710482 DOI: 10.1016/j.biopha.2018.01.130]

29 **Wang M**, Gao H, Qu H, Li J, Liu K, Han Z. MiR-137 suppresses tumor growth and metastasis in clear cell renal cell carcinoma. *Pharmacol Rep* 2018; **70**: 963-971 [PMID: 30107346 DOI: 10.1016/j.pharep.2018.04.006]

30 **Guo Y**, Pang Y, Gao X, Zhao M, Zhang X, Zhang H, Xuan B, Wang Y. MicroRNA-137 chemosensitizes colon cancer cells to the chemotherapeutic drug oxaliplatin (OXA) by targeting YBX1. *Cancer Biomark* 2017; **18**: 1-9 [PMID: 28035913 DOI: 10.3233/CBM-160650]

World Journal of Gastroenterology

Submit a Manuscript: https://www.f6publishing.com

World J Gastroenterol 2020 April 7; 26(13): 1490-1500

DOI: 10.3748/wjg.v26.i13.1490

ISSN 1007-9327 (print) ISSN 2219-2840 (online)

ORIGINAL ARTICLE

Retrospective Study

Effectiveness and safety of a laparoscopic training system combined with modified reconstruction techniques for total laparoscopic distal gastrectomy

Shun Zhang, Hajime Orita, Hiroyuki Egawa, Ryota Matsui, Suguru Yamauchi, Yukinori Yube, Sanae Kaji, Toru Takahashi, Shinichi Oka, Noriyuki Inaki, Tetsu Fukunaga

ORCID number: Shun Zhang (0000-0002-3493-1247); Hajime Orita (0000-0002-8263-7069); Hiroyuki Egawa (0000-0003-1934-9918); Ryota Matsui (0000-0003-3185-3332); Suguru Yamauchi (0000-0003-3185-3333); Yukinori Yube (0000-0002-0289-8892); Sanae Kaji (0000-0002-1372-4468); Toru Takahashi (0000-0002-8476-9751); Shinichi Oka (0000-0002-3820-3394); Noriyuki Inaki (0000-0002-4241-5015); Tetsu Fukunaga (0000-0003-4802-8945).

Author contributions: All authors performed the research; Zhang S and Orita H contributed to manuscript writing, performing procedures and data analysis; Egawa H, Matsui R, Yube Y, Kaji S, Takahashi T and Oka S contributed to performing procedures and data analysis; Egawa H and Matsui R contributed to writing the manuscript; Zhang S, Yamauchi S and Inaki N contributed to data analysis and statistical review; Orita H and Fukunaga T contributed to writing the manuscript and drafting the conception and design of this work.

Supported by Japan China Sasakawa Medical Fellowship and the China Scholarship Council, No. 201908310012.

Institutional review board statement: This study was reviewed and approved by the Institutional Review Committee of

Shun Zhang, Hajime Orita, Hiroyuki Egawa, Ryota Matsui, Suguru Yamauchi, Yukinori Yube, Sanae Kaji, Toru Takahashi, Shinichi Oka, Noriyuki Inaki, Tetsu Fukunaga, Department of Gastroenterology and Minimally Invasive Surgery, Juntendo University Hospital, Tokyo 113-8431, Japan

Shun Zhang, Department of Gastrointestinal Surgery, Shanghai East Hospital, Tongji University, Shanghai 200120, China

Ryota Matsui, Toru Takahashi, Noriyuki Inaki, Department of Surgery, Juntendo Urayasu Hospital, Juntendo University, Chiba 2790021, Japan

Corresponding author: Hajime Orita, MD, PhD, Associate Professor, Department of Gastroenterology and Minimally Invasive Surgery, Juntendo University Hospital, 3-1-3 Hongo, Bunkyo-ku, Tokyo 113-8431, Japan. oriori@juntendo.ac.jp

Abstract

BACKGROUND

Total laparoscopic distal gastrectomy (TLDG) is increasing due to some advantages over open surgery, which has generated interest in gastrointestinal surgeons. However, TLDG is technically demanding especially for lymphadenectomy and gastrointestinal reconstruction. During the course of training, trainee surgeons have less chances to perform open gastrectomy compared with that of senior surgeons.

AIM

To evaluate an appropriate, efficient and safe laparoscopic training procedures suitable for trainee surgeons.

METHODS

Ninety-two consecutive patients with gastric cancer who underwent TLDG plus Billroth I reconstruction using an augmented rectangle technique and involving trainees were reviewed. The trainees were taught a laparoscopic view of surgical anatomy, standard operative procedures and practiced essential laparoscopic skills. The TLDG procedure was divided into regional lymph node dissections and gastrointestinal reconstruction for analyzing trainee skills. Early surgical outcomes were compared between trainees and trainers to clarify the feasibility and safety of TLDG performed by trainees. Learning curves were used to assess

Juntendo University Hospital.

Informed consent statement: Patients were not required to give informed consent to the study because our study was done retrospectively. Data for study were obtained after each patient agreed to treatment.

Conflict-of-interest statement: The authors have no conflicts of interest to disclose.

Manuscript source: Unsolicited manuscript

Received: December 12, 2019
Peer-review started: December 12, 2019
First decision: January 19, 2020
Revised: February 14, 2020
Accepted: March 5, 2020
Article in press: March 5, 2020
Published online: April 7, 2020

P-Reviewer: Fabozzi M
S-Editor: Tang JZ
L-Editor: Filipodia
E-Editor: Liu JH

the utility of our training system.

RESULTS

Five trainees performed a total of 52 TLDGs (56.5%), while 40 TLDGs were conducted by two trainers (43.5%). Except for depth of invasion and pathologic stage, there were no differences in clinicopathological characteristics. Trainers performed more D2 gastrectomies than trainees. The total operation time was significantly longer in the trainee group. The time spent during the lesser curvature lymph node dissection and the Billroth I reconstruction were similar between the two groups. No difference was found in postoperative complications between the two groups. The learning curve of the trainees plateaued after five TLDG cases.

CONCLUSION

Preparing trainees with a laparoscopic view of surgical anatomy, standard operative procedures and practice in essential laparoscopic skills enabled trainees to perform TLDG safely and feasibly.

Key words: Gastric cancer; Total laparoscopic gastrectomy; Education system; Trainees; Augmented rectangle technique; Standard procedure

Core tip: The rapid expansion of total laparoscopic distal gastrectomy has led to concern about education for young surgeons. Laparoscopic training for young surgeons differs from training experienced previously due to fewer opportunities to perform open gastrectomy and higher technical demands. We introduced our laparoscopic training system and found that making a standard laparoscopic procedure and using the easy reconstruction method are useful in the success of the training system.

Citation: Zhang S, Orita H, Egawa H, Matsui R, Yamauchi S, Yube Y, Kaji S, Takahashi T, Oka S, Inaki N, Fukunaga T. Effectiveness and safety of a laparoscopic training system combined with modified reconstruction techniques for total laparoscopic distal gastrectomy. *World J Gastroenterol* 2020; 26(13): 1490-1500
URL: https://www.wjgnet.com/1007-9327/full/v26/i13/1490.htm
DOI: https://dx.doi.org/10.3748/wjg.v26.i13.1490

INTRODUCTION

Laparoscopic assisted distal gastrectomy was first reported by Kitano *et al*[1] in 1991. Since then, the use of laparoscopic surgery has rapidly become popular due to improving patients' quality of life and improving efficacy outcomes. The Japan Society of Endoscopic Surgery performs a national survey every 2 years that indicates that the number of laparoscopic procedures for gastric cancer is increasing. According to the 13th Japan Society of Endoscopic Surgery survey, laparoscopic distal gastrectomy accounted for the highest proportion of laparoscopic gastrectomies[2]. Nevertheless, laparoscopic distal gastrectomy involves technically complex elements and requires dedicated skills especially in the procedures of lymphadenectomy and gastrointestinal (GI) reconstruction. Adequate harvesting of lymph nodes (LNs) is necessary for the quality of gastrectomy and now is mentioned in most gastric cancer guidelines[3]. GI reconstructions were initially performed extracorporeally by laparoscopy assisted procedures. However, it is sometimes difficult in patients with a small remnant stomach or in obese patients with thick abdominal walls[4]. With the development of laparoscopic devices and improvement of the anastomosis method, the reconstruction procedures can be completed laparoscopically[5].

The rapid expansion of laparoscopic surgery has led to concern about education for young surgeons. Experienced surgeons learned, developed and introduced laparoscopic gastrectomy after mastering conventional open surgery. However, training and learning may differ for young surgeons who have less experience with open surgery[6]. The feasibility of laparoscopic gastrectomy operated by trainees is still debatable. To our knowledge, there are few studies describing the safety of

laparoscopic assisted distal gastrectomy performed by trainee surgeons and even fewer studies on total laparoscopic distal gastrectomy (TLDG).

Our department was founded in May 2015 and mainly focuses on minimally invasive surgery. One experienced laparoscopic surgeon started performing laparoscopic gastrectomy in April 2004. About 100 cases were conducted yearly. TLDG is the standard procedure for distal gastrectomy. For those needing Billroth I reconstruction, the augmented rectangle technique (ART) is applied[7]. We established an education system for TLDG to help young surgeons master the technique quickly.

This study reports the technical feasibility and short-term surgical outcomes of TLDG combined with modified reconstruction techniques performed by trainee gastric surgeons using our training system

MATERIALS AND METHODS

Patients

We retrospectively studied patients with gastric cancer, who underwent TLDG plus Billroth I reconstruction at Juntendo University Hospital, Tokyo, Japan from June 2016 to June 2019. Clinical, surgical and pathological data of these patients were collected and analyzed. The clinicopathological variables included age, gender, body mass index, American Society of Anesthesiologists physical status classification, medical history, pathological record and duration of postoperative hospital stay. The surgical variables included operation time, LN dissection time, estimated blood loss and number of harvested LNs. Histological results were described according to the Japanese Classification of Gastric Carcinoma[8]. Intraoperative and postoperative complications were stratified using the Clavien–Dindo classification system[9].

Laparoscopic techniques

Laparoscopic gastrectomy was performed using a five trocar system. LN dissection was done according to the Japanese gastric cancer treatment guidelines[3]. Dissection was conducted in the following order: Infrapyloric LNs (No. 6), suprapyloric LNs (No. 5), great curvature LNs (No. 4 or plus 12a), suprapancreatic LNs (No. 8a, 7, 9 or plus 11p) and along lesser curvature LNs (No. 1 or 3). The operator stood on the left side of the patient for infrapyloric LN dissection and on the right side for other LN dissection. Concomitant cholecystectomy was performed during the operation for patients with symptomatic gallbladder stones. Concomitant appendectomy was performed for patients with recurrent appendicitis.

Billroth I reconstruction using ART

ART was applied for Billroth I reconstruction, and all the procedures were created laparoscopically. The operator performed this technique on the left side of the patient. Three automatic laparoscopic linear staplers were used to create the gastro-duodenostomy. The duodenum was transected from the greater curvature to the lesser curvature. Small incisions were made on the greater curvature side, for each of the duodenal stumps and the remnant stomach. One jaw of the stapler was pressed against the posterior wall of the stomach 2 cm away from the gastric resection margin, and then the remnant stomach was rotated clockwise to the duodenal side. The duodenal stump was inserted by another jaw of stapler and then rotated externally by 90°. After the initial suturing between the remnant stomach and the duodenum, the posterior wall and caudal wall formed a V-shape. A 30 mm linear stapler was then applied to close the insertion holes up to the closest side of the duodenal resection margin, creating the third side of a rectangle. After gastric and duodenal resection margins were ensured to be close together, the 60 mm linear stapler was used to transect the duodenal resection margin to create the fourth side of the rectangle. After the above steps, all the previous linear staplers were removed from duodenal resection margin, and the augmented rectangular gastroduodenal anastomosis was completed.

Trainer and trainees

Seven operators were involved in this study. There were two trainers and five trainees. Two trainers were Endoscopic Surgical Skill Qualification System for gastric cancer accredited surgeons. Trainees had at least 7 years of experience as a surgeon after graduation. The surgical outcomes of five trainees who had performed more than five TLDG procedures were compared with the other two trainers.

Education system for laparoscopic gastrectomy

Trainees received systematic education about laparoscopic gastrectomy in four components (Figure 1).

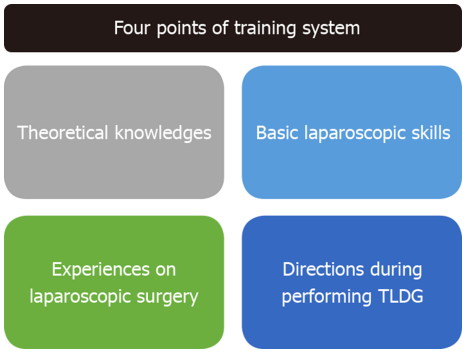

Figure 1 Four points of our training system. TLDG: Total laparoscopic distal gastrectomy.

The first component was understanding the anatomy and standard procedures of TLDG: (1) Study basic theoretical knowledge of vascular and lymphatic drainage anatomy especially in laparoscopy; and (2) Watch non-edited video from operations by the trainers as well as trainees repeatedly.

The second component was to master and improve the basic laparoscopic skills: (1) Develop hand-eye coordination, practice laparoscopic knot-tying and suturing techniques using training box; (2) Strengthen basic skills using computer simulator with programs for laparoscopic surgery; and (3) Participate in training sessions, such as hands-on training using porcine laboratory training organized by the Department of Minimally Invasive Surgery of Juntendo University Hospital and educational seminars organized by the Juntendo University Medical Technology and Simulation Center and other organizations.

The third component was experiences during laparoscopic surgery: (1) Complete simple laparoscopic surgery such as laparoscopic cholecystectomy and laparoscopic partial gastrectomy; and (2) Be a scope operator and then an assistant to understand the standard procedure of TLDG.

The fourth component was to receive direction during real TLDG. When a trainee performed the TLDG, the trainer surgeon was usually the first assistant to give guidance.

Learning curve of the trainees

Two variables, operation time and intraoperative estimated blood loss, from patients who underwent TLDG by trainees were used to define the learning curve. Variables in each group were calculated as mean ± standard deviation and then compared with that of those performed by the trainer surgeons. Continuous curves were plotted for each variable to identify any plateau effect. Plateau was defined as variable with < 5% change. The patient number at which a < 5% change occurred within the variable gave the minimum number of cases needed to reach the learning curve for that variable.

Statistical analysis

Continuous data are presented as median and ranges. Independent-sample *t* test was used to analyze continuous data, and χ^2 or Fisher's exact tests was used to assess differences in categorical data. Statistical analysis was performed using the SPSS statistical software program (version 23). A $P < 0.05$ was considered significant.

RESULTS

Ratio of the operator cases of TLDG by the trainees

A total of 92 patients received TLDG with ART between June 2016 and June 2019. Among them, 52 patients were operated by the trainee group while the remaining 40 patients were operated by the trainer group (Figure 2). Compared with trainers, trainees performed more than 50% of the TLDG except for the first year.

Clinicopathological characteristics of the patients

Patient clinicopathological characteristics are summarized in Table 1. There were no significant differences between the two groups in patient characteristics, including age, sex, body mass index, American society of anesthesiologists status and pathology staging. The trainer group tended to perform operations for patients with higher depth of invasion ($P = 0.004$) and higher pathology stage ($P = 0.017$).

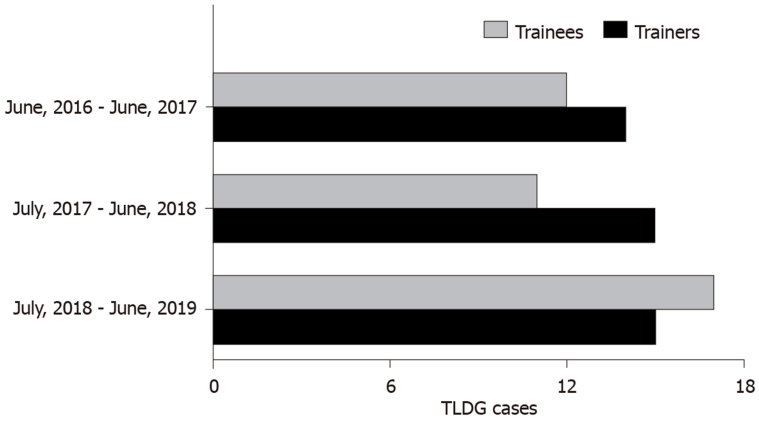

Figure 2 The number of patients who underwent total laparoscopic distal gastrectomy in our department each year. TLDG: Total laparoscopic distal gastrectomy.

Surgical outcomes

The surgical outcomes, including intraoperative blood loss and harvested number of LNs, were not significantly different between the trainee and trainer groups (Table 2). The trainer group performed more D2 gastrectomies than the trainee group (P = 0.034). The operation time was significantly longer in the trainee group compared with the trainer group (P = 0.002). No patients required conversion to open gastrectomy in either group. The postoperative stay was almost equivalent. The results of lymphadenectomy and GI reconstruction time are shown in Table 3. There were significant differences between the groups in the infrapyloric, suprapyloric, greater curvature and suprapancreatic LN dissection times. The times for lesser curvature LN dissection and GI reconstruction were similar between the two groups.

Postoperative complications

Four patients in the trainee group (7.7%) and two patients in the trainer group (5%) had complications (Table 4). The most frequent complication was intra-abdominal abscess (3.8%) in the trainee group. No complication needed surgical intervention. There was no mortality associated with surgery in either group.

Learning curve of the trainees

Among the 52 patients resected by trainees, the mean value of operation time is shown in Figure 3. The average operating time decreased from 315 min in cohort 1 to 253 min in cohort 10. The average operation time for the trainee group plateaued at around 260 min after five cases. There was less than 5% change in average operation time after cohort 5 up to cohort 10 but still a big gap compared with that of the trainer group. The average operative blood loss was similar for the two groups.

DISCUSSION

Gastric cancer ranks the fifth most common cancer and the third most common cause in cancer-related deaths worldwide with the highest incidence rate in Eastern Asia[10]. Radical resection is the only curative modality for patients with resectable gastric cancer. Introduction of laparoscopic gastrectomy has shown promising results in early gastric cancer[11] and even comparable outcomes in advanced gastric cancer[12,13] when compared with open surgery. Laparoscopic gastrectomy has therefore rapidly gained popularity in the world. With the developments in anastomosis devices and modification in anastomotic techniques[5,14], more and more cases can be performed by total laparoscopic gastrectomy[2]. Intracorporeal GI reconstruction showed some benefits especially in the setting of narrow spaces in obese patients and small remnant stomachs from high location of tumor.

Total laparoscopic gastrectomy has generated interest and desire not only in experienced surgeons but also in trainee surgeons. In this context, many efforts for research and education on laparoscopic surgery have been made. The Japan Society of Endoscopic Surgery established the Endoscopic Surgical Skill Qualification System and provides the educational environment for the training of qualified surgeons[15]. Some high-volume centers also reported their experiences of educating young surgeons on laparoscopic assisted distal gastrectomy[16-19]. However, most studies

Table 1 Patient clinicopathological characteristics

Characteristics	Trainee surgeon	Trainer surgeon	*P* value
Age in yr			
Median	68.5 (37-83)	69.6 (42-90)	0.630
< 80	44 (84.6%)	31 (77.5%)	0.794
≥ 80	8 (15.4%)	9 (22.5%)	
Sex			
Male	32 (61.5%)	23 (57.5%)	0.830
Female	20 (38.5%)	17 (42.5%)	
BMI in kg/m			
Median	22.01 (14.98-36.00)	23.11 (18.67-32.56)	0.145
< 25	43 (82.7%)	30 (75.0%)	0.440
≥ 25	9 (17.3%)	10 (25.0%)	
ASA			
1	20 (38.5%)	13 (32.5%)	0.793
2	29 (55.8%)	24 (60.0%)	
3	3 (5.7%)	3 (7.5%)	
Previous abdominal surgery			
Yes	14 (26.9%)	8 (20%)	0.472
No	38 (73.1%)	32 (80%)	
pT			
T1	42 (80.8%)	22 (55.0%)	0.004
T2	3 (5.8%)	5 (12.5%)	
T3	6 (11.5%)	4 (10%)	
T4	1 (1.9%)	9 (22.5%)	
pStage			
IA	35 (67.3%)	17 (42.5%)	0.017
IB	7 (13.5%)	6 (15%)	
IIA	5 (9.6%)	3 (7.5%)	
IIB	4 (7.7%)	3 (7.5%)	
IIIA	1 (1.9%)	8 (20%)	
IIIB	0	1 (2.5%)	
IIIC	0	2 (5%)	

Data are expressed as the median (range) or number of patients. BMI: Body mass index; ASA: American Society of Anesthesiologists.

mixed different kinds of gastrectomy and even different reconstruction methods, which may cause bias of the results. In order to limit the influence of different techniques on results, we only focused on TLDG using the same surgical procedures and reconstruction methods for each patient in this study.

Our department was founded in 2015, and laparoscopic surgeries represent most of our surgeries. More than 90% of gastrectomies were performed by laparoscopy, and most GI reconstructions are done intracorporeally. The advantage of our volume is more opportunities for trainee surgeons to perform such surgeries. However, shortcomings of this are also evident in less opportunity to learn open surgery and higher technical skills. These characteristics make laparoscopic training procedures for young surgeons different from what experience surgeons experienced previously by placing higher educational and technical demands on residents[20]. Appropriate and efficient training systems suitable for the current situation need to be urgently established. One experienced surgeon in our department has performed laparoscopic surgery since 2004 and has been concentrating on laparoscopic training[16,21]. When starting laparoscopic gastrectomy in our newly founded department, an educational and training system for young surgeon was set up at the same time.

Our training system covers four parts: understanding anatomy and standard procedures, practicing basic laparoscopic skills, performing simple laparoscopic surgery and providing focal points during laparoscopic gastrectomy. It is useful to use a dry box to help trainees practice laparoscopic suturing techniques and improve

Table 2 Surgical outcomes

Items	Trainee surgeon	Trainer surgeon	*P* value
LN dissection			
D1+	43 (82.7%)	25 (62.5%)	0.034
D2	9 (17.3%)	15 (37.5%)	
Combined organ resection	4 (7.7%)	2 (5%)	0.568
Cholecystectomy	4	0	
Appendicectomy	0	1	
Colectomy	0	1	
Blood loss	26 (5-170)	23 (3-125)	0.566
Conversion to open procedure	0	0	
Operation time in min			
Median (range)	270 (199-512)	239 (154-375)	0.002
Harvested LNs, number			
Median (range)	39 (14-86)	39 (14-70)	0.989
Postoperative hospital stays in d			
Median (range)	13.38 (7-60)	12.70 (7-27)	0.720

Data are expressed as the median (range) or number of patients. LN: Lymph node.

hand-eye coordination[19,22]. However, the camera in the box is usually fixed to a particular point, which is different from practical surgery. In order to create a more realistic laparoscopic environment, we also use computer simulators to train young surgeons. Computer simulators with laparoscopic programs and magnetic feedback systems can strengthen basic skills and surgical training more than a traditional dry box.

Using a video recording system and online video websites, trainees can watch operative videos before operating and can analyze each step of their own surgery repeatedly after operation. Before becoming an operator, experiences gained from watching laparoscopic gastrectomy videos, performing simple laparoscopic surgeries, being a scope assistant, and being the first assistant helps trainees master laparoscopy-specific anatomical views, acquire skills of handling of laparoscopic energy devices and cooperating closely with other surgeons. Trainers play an important role, especially during the trainee's actual operation. In our department, trainers usually worked as the first assistant when trainees performed TLDG. Trainers could not help the trainee's procedure because the assistant's hands were always occupied for exposing the operative field of vision[16]. But the first assistant trainers could directly provide direction, give confidence and control the quality of surgery.

The technically challenging component of TLDG for trainees mainly centers on lymphadenectomy and GI reconstruction. Trainees performed TLDG with longer time compared to trainers. After splitting the whole procedure of TLDG into lymphadenectomy for each station and GI reconstruction, we found that lymphadenectomy in the infrapyloric and suprapancreatic areas took longer in the trainee group. However, reconstruction time was similar between the two groups. Standardizing operative procedures is useful for surgical education[22-24]. Paying more attention to the details of lymphadenectomy could improve surgical efficiency, reduce unnecessary injury and result in less bleeding. In our department, D1 + LN dissection is normally performed in the following order: "No. 6 → No. 5 (plus 12a in D2) → No. 4sa, 4d → No. 8a, 7, 9 (plus 11p in D2) → No. 3, 1." The total procedure is just like page-turning, which may make a good field of vision and avoid repeated clamping of the diseased gastric wall. Our results show there is a positive relationship between infrapyloric and suprapancreatic lymphadenectomy time. LN dissection in infrapyloric and suprapancreatic areas requires delicate manipulations especially in obese patients. More adipose tissue makes it difficult to identify the correct anatomical planes. We developed an intracorporeal reconstruction technique named ART, which is easily performed[7]. Two 60 mm and one 30 mm laparoscopic linear staplers are used to create a larger 4-sided anastomosis. Stay sutures are canceled and less (even no) intersection angle sutures are needed, which makes the technique easy and time-saving especially for trainees. Our results showed that the reconstruction time of trainees is similar to that of trainers. No anastomosis-related complications were found between the two groups. These results may indicate that this

Table 3 Lymphadenectomy and reconstruction outcome

Items	Trainee surgeon	Trainer surgeon	*P* value
Lymphadenectomy			
Infrapyloric LNs	58.8 (27-135)	42.0 (19-85)	0.004
Suprapyloric LNs	18.8 (4-40)	10.6 (3-24)	0.001
Great Curvature LNs	17.7 (8-34)	12.3 (6-32)	0.004
Suprapancreatic LNs	41.0 (23-82)	28.4 (17-51)	0.001
Along lesser curvature LNs	16.6 (7-36)	14.1 (7-34)	0.213
GI reconstruction	19.0 (11-37)	18.9 (11-39)	0.988

Data are expressed as the median (range). LN: Lymph node; GI: Gastrointestinal.

reconstruction method is easy and safe to perform for young surgeons.

In this study, we compared early outcomes of TLDG between trainees and trainers to clarify whether our training system was useful in maintaining the quality of trainee operations. The number of harvested LNs and intraoperative bleeding were not significantly different between the two groups. The incidence of postoperative complications was similar between the trainee and trainer groups. These results indicated that TLDG performed by trainees is safe and feasible. Some studies indicated pancreatic fistula occurred much more in trainee surgeries[17,23,24]. However, our results showed the incidence of pancreatic fistula was similar between the two groups. Much attention was paid to the dissection of the infrapyloric and suprapancreatic LNs. During operations we normally compress the adjacent tissues at the inferior border of the pancreas instead of directly touching the pancreas itself. The postoperative hospital stays are relatively long compared with other reported studies. One reason is that more older patients were included in our series[7].

The trainees in our department have less chance to perform open gastrectomies. However, the learning curve for TLDG showed that the average operative time of the trainees reached a plateau after five cases, especially in older and advanced stage patients, compared with other studies[17,23]. The learning curve showed no difference in blood loss in the two groups. All the results may support that our educational and training system may enable trainees to quickly learn to perform TLDG. The influence of patient selection on the learning curve should also be evaluated. In our department, trainees usually performed surgery for lower stage gastric cancer *vs* trainers. Careful patient selection for trainees might be one important factor for a successful initial experience with TLDG. We should take cognizance of the situation clearly that there is still a big gap between the two groups after trainees reach the plateau, which may be accounted for the technical complexity of lymphadenectomy needing a longer learning time.

There are some limitations in our study. Its retrospective nature may induce some bias. Because of the length of follow up, our study did not provide enough data to show conclusions about oncologic safety and long-term outcomes. LNs dissection number may be prognostic factor for survival of patients. In our study, 97.8% of patients had more than 15 LNs harvested. We still need further follow up on these patients. The number of patients in our study is limited, but the study interval was shorter than other studies and only focused on TLDG with the same procedure and reconstruction method. These may reduce the impacts of surgical techniques.

In conclusion, trainees can perform TLDG safely and feasibly after receiving systematic training. Making laparoscopic procedures standard and using an easy reconstruction method are useful in the success of the training system.

Table 4 Postoperative complications

Items	Trainee surgeon	Trainer surgeon	*P* value
Anastomotic leakage	0	0	1.000
Anastomotic bleeding	1 (1.9%)	0	0.497
Anastomotic stenosis	0	0	1.000
Intra-abdominal abscess	2 (3.8%)	1 (2.4%)	0.683
Pancreatic fistula	1 (1.9%)	1 (2.4%)	1.000
Ileus	0	0	1.000
Mortality	0	0	1.000

Data are expressed as number of patients. Clavien–Dindo grade 2 or higher.

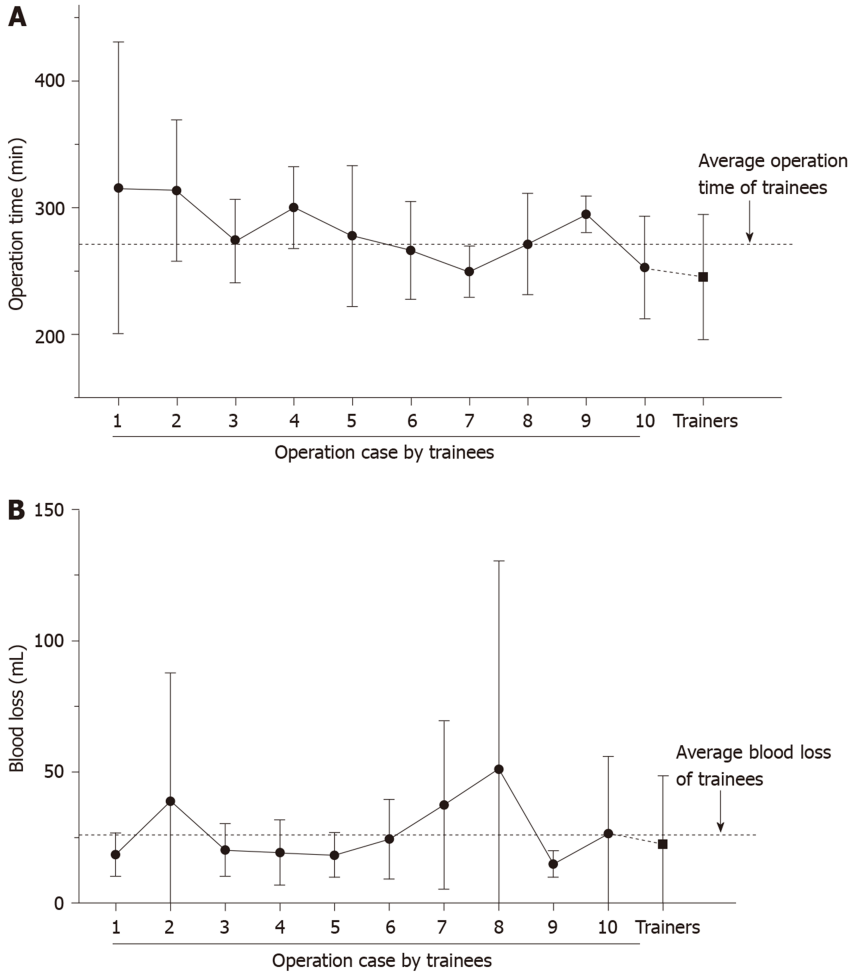

Figure 3 Learning curve of trainees. A: Average operation time for total laparoscopic distal gastrectomy performed by the trainees was compared among cases and that of trainers. After starting total laparoscopic distal gastrectomy as an operator, the average operative time reached a plateau after 5 cases; B: Average blood loss for total laparoscopic distal gastrectomy performed by the trainees was compared among cases and that of trainers.

ARTICLE HIGHLIGHTS

Research background

Total laparoscopic distal gastrectomy (TLDG), which involves technically complex elements and requires dedicated skills, has generated interest and desire not only in surgeon pioneers but also in trainee surgeons. The rapid expansion of TLDG has led to concern about education for young surgeons.

Research motivation

Fewer opportunities to perform open gastrectomy and higher technical demands has made laparoscopic training procedures for young surgeons differ from those of laparoscopic surgeon

pioneers. Appropriate and efficient training systems suitable for the current situation need to be urgently established.

Research objectives
The patients underwent TLDG plus Billroth I reconstruction from June 2016 to June 2019. Clinical, surgical and pathological data of these patients were collected and analyzed.

Research methods
This study assessed our laparoscopic training system for TLDG based on short-term surgical outcomes. We reviewed ninety-two consecutive patients with gastric cancer who underwent TLDG plus Billroth I reconstruction using the augmented rectangle technique. The trainees were required to receive systematic laparoscopic training. The total procedure of TLDG was divided into different regional lymph node dissection and gastrointestinal reconstruction for analyzing. Early surgical outcomes were compared between trainees and trainers to clarify the feasibility and safety of TLDG performed by trainees.

Research results
Five trainees performed a total of 52 TLDG (56.5%), while 40 TLDG were conducted by the two trainers (43.5%). Except for depth of invasion and pathology stage, there were no differences in patient clinicopathological characteristics. Trainers performed more D2 gastrectomies than trainees. The total operation time was significantly longer in the trainees. The time spent on less curvature lymph node dissection and Billroth I reconstruction was similar between the two groups. No difference was found in postoperative complications between the two groups. The learning curve of the trainees plateaued after five TLDG cases.

Research conclusions
Preparing trainees with a laparoscopic view of surgical anatomy, standard operative procedures and practice in essential laparoscopic skills enabled trainees to perform TLDG safely and feasibly.

Research perspectives
Making laparoscopic procedures standard and using an easy reconstruction method are useful in the success of the training system.

ACKNOWLEDGEMENTS

The authors thank Professor Mike Gibson (Vanderbilt University School of Medicine, United States) for his critical correction of the English language in the manuscript.

REFERENCES

1 **Kitano S**, Iso Y, Moriyama M, Sugimachi K. Laparoscopy-assisted Billroth I gastrectomy. *Surg Laparosc Endosc* 1994; **4**: 146-148 [PMID: 8180768]
2 **Shiroshita H**, Inomata M, Bandoh T, Uchida H, Akira S, Hashizume M, Yamaguchi S, Eguchi S, Wada N, Takiguchi S, Ieiri S, Endo S, Iwazaki M, Tamaki Y, Tabata M, Kanayama H, Mimata H, Hasegawa T, Onishi K, Yanaga K, Morikawa T, Terachi T, Matsumoto S, Yamashita Y, Kitano S, Watanabe M. Endoscopic surgery in Japan: The 13th national survey (2014-2015) by the Japan Society for Endoscopic Surgery. *Asian J Endosc Surg* 2019; **12**: 7-18 [PMID: 30681279 DOI: 10.1111/ases.12674]
3 **Japanese Gastric Cancer Association**. Japanese gastric cancer treatment guidelines 2014 (ver. 4). *Gastric Cancer* 2017; **20**: 1-19 [PMID: 27342689 DOI: 10.1007/s10120-016-0622-4]
4 **Kim MG**, Kim KC, Kim BS, Kim TH, Kim HS, Yook JH, Kim BS. A totally laparoscopic distal gastrectomy can be an effective way of performing laparoscopic gastrectomy in obese patients (body mass index≥30). *World J Surg* 2011; **35**: 1327-1332 [PMID: 21424875 DOI: 10.1007/s00268-011-1034-6]
5 **Zhang S**, Fukunaga T. Current status of technique for Billroth-I anastomosis in totally laparoscopic distal gastrectomy for gastric cancer. *Mini-invasive Surg* 2019; **3**: 1-7 [DOI: 10.20517/2574-1225.2018.64]
6 **Kano N**, Takeshi A, Kusanagi H, Watarai Y, Mike M, Yamada S, Mishima O, Uwafuji S, Kitagawa M, Watanabe H, Kitahama S, Matsuda S, Endo S, Gremillion D. Current surgical training: simultaneous training in open and laparoscopic surgery. *Surg Endosc* 2010; **24**: 2927-2929 [PMID: 20669034 DOI: 10.1007/s00464-010-1238-0]
7 **Fukunaga T**, Ishibashi Y, Oka S, Kanda S, Yube Y, Kohira Y, Matsuo Y, Mori O, Mikami S, Enomoto T, Otsubo T. Augmented rectangle technique for Billroth I anastomosis in totally laparoscopic distal gastrectomy for gastric cancer. *Surg Endosc* 2018; **32**: 4011-4016 [PMID: 29915985 DOI: 10.1007/s00464-018-6266-1]
8 **Japanese Gastric Cancer Association**. Japanese classification of gastric carcinoma: 3rd English edition. *Gastric Cancer* 2011; **14**: 101-112 [PMID: 21573743 DOI: 10.1007/s10120-011-0041-5]
9 **Dindo D**, Demartines N, Clavien PA. Classification of surgical complications: a new proposal with evaluation in a cohort of 6336 patients and results of a survey. *Ann Surg* 2004; **240**: 205-213 [PMID: 15273542 DOI: 10.1097/01.sla.0000133083.54934.ae]
10 **Bray F**, Ferlay J, Soerjomataram I, Siegel RL, Torre LA, Jemal A. Global cancer statistics 2018: GLOBOCAN estimates of incidence and mortality worldwide for 36 cancers in 185 countries. *CA Cancer J Clin* 2018; **68**: 394-424 [PMID: 30207593 DOI: 10.3322/caac.21492]
11 **Katai H**, Mizusawa J, Katayama H, Takagi M, Yoshikawa T, Fukagawa T, Terashima M, Misawa K, Teshima S, Koeda K, Nunobe S, Fukushima N, Yasuda T, Asao Y, Fujiwara Y, Sasako M. Short-term

surgical outcomes from a phase III study of laparoscopy-assisted versus open distal gastrectomy with nodal dissection for clinical stage IA/IB gastric cancer: Japan Clinical Oncology Group Study JCOG0912. *Gastric Cancer* 2017; **20**: 699-708 [PMID: 27718137 DOI: 10.1007/s10120-016-0646-9]

12 **Lee HJ**, Hyung WJ, Yang HK, Han SU, Park YK, An JY, Kim W, Kim HI, Kim HH, Ryu SW, Hur H, Kong SH, Cho GS, Kim JJ, Park DJ, Ryu KW, Kim YW, Kim JW, Lee JH, Kim MC; Korean Laparo-endoscopic Gastrointestinal Surgery Study (KLASS) Group. Short-term Outcomes of a Multicenter Randomized Controlled Trial Comparing Laparoscopic Distal Gastrectomy With D2 Lymphadenectomy to Open Distal Gastrectomy for Locally Advanced Gastric Cancer (KLASS-02-RCT). *Ann Surg* 2019; **270**: 983-991 [PMID: 30829698 DOI: 10.1097/SLA.0000000000003217]

13 **Yu J**, Huang C, Sun Y, Su X, Cao H, Hu J, Wang K, Suo J, Tao K, He X, Wei H, Ying M, Hu W, Du X, Hu Y, Liu H, Zheng C, Li P, Xie J, Liu F, Li Z, Zhao G, Yang K, Liu C, Li H, Chen P, Ji J, Li G; Chinese Laparoscopic Gastrointestinal Surgery Study (CLASS) Group. Effect of Laparoscopic vs Open Distal Gastrectomy on 3-Year Disease-Free Survival in Patients With Locally Advanced Gastric Cancer: The CLASS-01 Randomized Clinical Trial. *JAMA* 2019; **321**: 1983-1992 [PMID: 31135850 DOI: 10.1001/jama.2019.5359]

14 **Shim JH**, Yoo HM, Oh SI, Nam MJ, Jeon HM, Park CH, Song KY. Various types of intracorporeal esophagojejunostomy after laparoscopic total gastrectomy for gastric cancer. *Gastric Cancer* 2013; **16**: 420-427 [PMID: 23097123 DOI: 10.1007/s10120-012-0207-9]

15 **Tanigawa N**, Lee SW, Kimura T, Mori T, Uyama I, Nomura E, Okuda J, Konishi F. The Endoscopic Surgical Skill Qualification System for gastric surgery in Japan. *Asian J Endosc Surg* 2011; **4**: 112-115 [PMID: 22776273 DOI: 10.1111/j.1758-5910.2011.00082.x]

16 **Tokunaga M**, Hiki N, Fukunaga T, Miki A, Nunobe S, Ohyama S, Seto Y, Yamaguchi T. Quality control and educational value of laparoscopy-assisted gastrectomy in a high-volume center. *Surg Endosc* 2009; **23**: 289-295 [PMID: 18398642 DOI: 10.1007/s00464-008-9902-3]

17 **Yamada T**, Kumazu Y, Nakazono M, Hara K, Nagasawa S, Shimoda Y, Hayashi T, Rino Y, Masuda M, Shiozawa M, Morinaga S, Ogata T, Oshima T. Feasibility and safety of laparoscopy-assisted distal gastrectomy performed by trainees supervised by an experienced qualified surgeon. *Surg Endosc* 2020; **34**: 429-435 [PMID: 30969360 DOI: 10.1007/s00464-019-06786-y]

18 **Kuroda S**, Kikuchi S, Hori N, Sakamoto S, Kagawa T, Watanabe M, Kubota T, Kuwada K, Ishida M, Kishimoto H, Uno F, Nishizaki M, Kagawa S, Fujiwara T. Training system for laparoscopy-assisted distal gastrectomy. *Surg Today* 2017; **47**: 802-809 [PMID: 27830364 DOI: 10.1007/s00595-016-1439-9]

19 **Kinoshita T**, Kanehira E, Matsuda M, Okazumi S, Katoh R. Effectiveness of a team participation training course for laparoscopy-assisted gastrectomy. *Surg Endosc* 2010; **24**: 561-566 [PMID: 19597775 DOI: 10.1007/s00464-009-0607-z]

20 **Debes AJ**, Aggarwal R, Balasundaram I, Jacobsen MB. A tale of two trainers: virtual reality versus a video trainer for acquisition of basic laparoscopic skills. *Am J Surg* 2010; **199**: 840-845 [PMID: 20079480 DOI: 10.1016/j.amjsurg.2009.05.016]

21 **Hiki N**, Fukunaga T, Yamaguchi T, Nunobe S, Tokunaga M, Ohyama S, Seto Y, Yoshiba H, Nohara K, Inoue H, Muto T. The benefits of standardizing the operative procedure for the assistant in laparoscopy-assisted gastrectomy for gastric cancer. *Langenbecks Arch Surg* 2008; **393**: 963-971 [PMID: 18633638 DOI: 10.1007/s00423-008-0374-7]

22 **Kaito A**, Kinoshita T. Educational system of laparoscopic gastrectomy for trainee-how to teach, how to learn. *J Vis Surg* 2017; **3**: 16 [PMID: 29078579 DOI: 10.21037/jovs.2016.12.13]

23 **Nunobe S**, Hiki N, Tanimura S, Nohara K, Sano T, Yamaguchi T. The clinical safety of performing laparoscopic gastrectomy for gastric cancer by trainees after sufficient experience in assisting. *World J Surg* 2013; **37**: 424-429 [PMID: 23052817 DOI: 10.1007/s00268-012-1827-2]

24 **Kameda C**, Watanabe M, Suehara N, Watanabe Y, Nishihara K, Nakano T, Nakamura M. Safety of laparoscopic distal gastrectomy for gastric cancer when performed by trainee surgeons with little experience in performing open gastrectomy. *Surg Today* 2018; **48**: 211-216 [PMID: 28726166 DOI: 10.1007/s00595-017-1569-8]

World Journal of Gastroenterology

Submit a Manuscript: https://www.f6publishing.com

World J Gastroenterol 2020 April 7; 26(13): 1501-1512

DOI: 10.3748/wjg.v26.i13.1501

ISSN 1007-9327 (print) ISSN 2219-2840 (online)

ORIGINAL ARTICLE

Retrospective Study

Preoperative gamma-glutamyltransferase to lymphocyte ratio predicts long-term outcomes in intrahepatic cholangiocarcinoma patients following hepatic resection

Jin-Ju Wang, Hui Li, Jia-Xin Li, Lin Xu, Hong Wu, Yong Zeng

ORCID number: Jin-Ju Wang (0000-0003-1210-7676); Hui Li (0000-0001-7287-2690); Jia-Xin Li (0000-0002-6264-283X); Lin Xu (0000-0002-1595-5622); Hong Wu (0000-0001-5397-4800); Yong Zeng (0000-0002-7846-963X).

Author contributions: Wang JJ, Hui Li and Jia-Xin Li contributed equally to this work; Wang JJ, Wu H and Zeng Y designed the research; Li H and Xu L collected the data; Wang JJ and Li JX analyzed the data and wrote the paper.

Supported by the National Key Technologies RD Program, No. 2018YFC1106803; the Natural Science Foundation of China, No. 81972747, No. 81872004, No. 81770615 and No. 81672882; the Science and Technology Support Program of Sichuan Province, No. 2019YFQ0001 and No. 2017SZ0003.

Institutional review board statement: This work was reviewed and approved by the Ethics Committee of the West China Hospital.

Informed consent statement: Patients were not required to give informed consent to the study because the analysis used anonymous clinical data that were obtained after each patient agreed to treatment by written consent.

Conflict-of-interest statement: All authors declare no conflicts of interest.

Jin-Ju Wang, Hui Li, Jia-Xin Li, Hong Wu, Yong Zeng, Department of Liver Surgery and Liver Transplantation Center, West China Hospital, Sichuan University, Chengdu 610041, Sichuan Province, China

Lin Xu, Laboratory of Liver Surgery, West China Hospital, Sichuan University, Chengdu 610065, Sichuan Province, China

Corresponding author: Yong Zeng, MD, PhD, Professor, Doctor, Surgeon, Department of Liver Surgery and Liver Transplantation Center, West China Hospital of Sichuan University, No. 37 Guoxuexiang, Chengdu 610041, Sichuan Province, China. zengyong@medmail.com.cn

Abstract

BACKGROUND

Intrahepatic cholangiocarcinoma (ICC) is a heterogeneous hepatobiliary cancer with limited treatment options. A number of studies have illuminated the relationship between inflammation-based prognostic scores and outcomes in patients with ICC. However, the use of reliable and personalized prognostic algorithms in ICC after resection is pending.

AIM

To assess the prognostic value of the gamma-glutamyltransferase to lymphocyte ratio (GLR) in ICC patients following curative resection.

METHODS

ICC patients following curative resection (2009-2017) were divided into two cohorts: The derivation cohort and validation cohort. The derivation cohort was used to explore an optimal cut-off value, and the validation cohort was used to further evaluate the score. Overall survival (OS) and recurrence-free survival (RFS) were analyzed, and predictors of OS and RFS were determined.

RESULTS

A total of 527 ICC patients were included and randomly divided into the derivation cohort (264 patients) and the validation cohort (263 patients). The two patient cohorts had comparable baseline characteristics. The optimal cut-off value for the GLR was 33.7. Kaplan-Meier curves showed worse OS and RFS in the GLR > 33.7 group compared with GLR ≤ 33.7 group in both cohorts. After univariate and multivariate analysis, the results indicated that GLR was an independent prognostic factor of OS [derivation cohort: hazard ratio (HR) =

Data sharing statement: No additional data are available.

Manuscript source: Unsolicited manuscript

Received: November 30, 2019
Peer-review started: November 30, 2019
First decision: January 16, 2020
Revised: February 17, 2020
Accepted: March 5, 2020
Article in press: March 5, 2020
Published online: April 7, 2020

P-Reviewer: Farshadpour F, Talabnin C
S-Editor: Zhang L
L-Editor: Filipodia
E-Editor: Ma YJ

1.620, 95% confidence interval (CI): 1.066-2.462, P = 0.024; validation cohort: HR = 1.466, 95%CI: 1.033-2.142, P = 0.048] and RFS [derivation cohort: HR = 1.471, 95%CI: 1.029-2.103, P = 0.034; validation cohort: HR = 1.480, 95%CI: 1.057-2.070, P = 0.022].

CONCLUSION
The preoperative GLR is an independent prognostic factor for ICC patients following hepatectomy. A high preoperative GLR is associated with worse OS and RFS.

Key words: Gamma-glutamyltransferase; Lymphocyte ratio; Gamma-glutamyltransferase to lymphocyte ratio; Intrahepatic cholangiocarcinoma; Prognosis; Survival analysis

Core tip: This study investigated the clinical significance of preoperative gamma-glutamyltransferase to lymphocyte ratio (GLR) levels in intrahepatic cholangiocarcinoma (ICC) patients following hepatectomy. We retrospectively enrolled 527 ICC patients underwent curative hepatectomy at our center. The results showed that a higher GLR is associated with worse overall survival and recurrence-free survival in ICC patients after hepatectomy. Thus, the preoperative GLR is an independent prognostic factor for ICC patients following curative resection.

Citation: Wang JJ, Li H, Li JX, Xu L, Wu H, Zeng Y. Preoperative gamma-glutamyltransferase to lymphocyte ratio predicts long-term outcomes in intrahepatic cholangiocarcinoma patients following hepatic resection. *World J Gastroenterol* 2020; 26(13): 1501-1512
URL: https://www.wjgnet.com/1007-9327/full/v26/i13/1501.htm
DOI: https://dx.doi.org/10.3748/wjg.v26.i13.1501

INTRODUCTION

Intrahepatic cholangiocarcinoma (ICC), the second most type of common biliary malignancy, is a rare epithelial malignancy that results in poor prognosis[1]. An increasing incidence of ICC has been reported worldwide over the last few decades[2]. Surgical resection and liver transplantation may be the potentially curative method for patients with ICC. However, contemporary studies do not support the choice of liver transplantation for ICC patients as the preferred treatment. Despite advances in early detection and surgical techniques, the 5-year survival rate of ICC after curative resection is approximately 30%[3]. This poor outcome is mainly caused by tumor recurrence and metastasis[4-6]. Furthermore, the discovery of effective blood biomarkers or prognostic models for recurrence and survival in patients with ICC following curative resection remains an unmet need.

Accumulating evidence has demonstrated that a disordered inflammatory response plays an important role in carcinogenesis or tumor recurrence[7,8]. Recently, studies have suggested that inflammation-based prognostic indexes such as the platelet to lymphocyte ratio (PLR), neutrophil to lymphocyte ratio (NLR) or aspartate transaminase to lymphocyte ratio index can predict the risk and prognosis of various solid tumors; the gamma-glutamyltransferase (GGT) to lymphocyte ratio (GLR) is one of these prognostic indexes[9-12]. Previous studies have reported that the preoperative GLR has significant prognostic value for patients with nonfunctional pancreatic neuroendocrine tumor after curative resection[11]. However, the relationship between GLR and the prognosis of ICC patients following curative resection has not been reported.

Clinical practice needs to enhance the understanding of factors that underlie differences in prognosis observed among patients and to distinguish patients with a risk of recurrence for the development of personalized therapeutic approaches. Thus, we performed a retrospective study to assess the prognostic value of the GLR for ICC patients after curative resection.

MATERIALS AND METHODS

Patients

The study enrolled patients who underwent hepatic resection for ICC, between January 2009 and September 2017, at the West China Hospital of Sichuan University. This study was approved by the Medical Ethics Committee of the West China Hospital of Sichuan University. The included patients in this study met the following criteria: (1) Histologically confirmed ICC; and (2) Received curative hepatectomy. The exclusion criteria were as follows: (1) ICC accompanied by other lethal diseases or cancers; (2) Patients who received chemotherapy and/or radiotherapy; and (3) Metastasis. The patients were divided into a cohort and validation cohort. The derivation group was used to generate an optimal cut-off value, and the validation group was used to evaluate this cut-off value.

Follow up and data extraction

The follow-up time ended in October 2018. Informed consent was obtained from all patients. For each patient enrolled in our analysis, the following data were collected using electronic patient medical records: Age, sex, histological features, hepatitis virus infection, Child-Pugh levels, tumor-node-metastasis (TNM) stage, Barcelona Clinic Liver Cancer (BCLC) stage, preoperative serum GGT levels and neutrophil, platelet, and lymphocyte counts.

Statistical analysis

The primary and secondary endpoints were overall survival (OS) and recurrence-free survival (RFS), respectively. OS was defined as the time in months from resection to death or to the last follow-up. RFS was defined as the time in months from resection to recurrence or to the last follow-up. The NLR, PLR, and GLR were calculated by relevant laboratory parameters. The cut-off points for the inflammation-based prognostic scores were identified using receiver operating characteristic curve analysis, which was performed in the derivation cohort. Based on the optimal cut-off points, including the GLR, we divided the derivation and validation cohorts into two subgroups. Continuous variables were analyzed using the Student's *t*-test or Kruskal-Wallis test, and categorical variables were analyzed using Fisher's exact test or the χ^2 test. Univariate and multivariate analyses were conducted using logistic regression models. Variables with *P* values less than 0.10 in univariate regression analyses were selected for multivariate regression models. $P < 0.05$ was considered statistically significant. All analyses were performed using SPSS® software (version 23.0; Chicago, IL, United States) and Medcalc software (version 15.2.2.0; Ostend, Belgium).

RESULTS

Patient population

Of the 527 patients enrolled, 254 (48.2%) were men and 277 (51.8%) were women (Supplementary Table 1). These patients were diagnosed at a mean age of 57.26 ± 10.71 years and underwent a mean follow-up of 25 mo. Serum hepatitis B surface antigen (HBsAg) was positive in 151 patients (28.8%), hepatitis C virus infected 3 patients (0.6%) and hepatolithiasis existed in 88 patients (16.7%). Among them, 24 (4.6%) patients had Child-Pugh grade B liver function. Ascites existed in 50 patients (9.5%). Serum carbohydrate antigen 19-9 (CA19-9) < 22 U/mL were observed in 149 patients (28.3%). The mean value of NLR, PLR, and GLR were 2.73, 113, and 44.7, respectively. The numbers of patients classified into TNM stage IA, IB, II, IIIA, and IIIB were 63 (12%), 37 (7%), 55 (10.4%), 241 (45.7%), and 131 (24.9%), respectively. The numbers of patients classified into BCLC stage 0, A, B and C were 23 (4.4%), 141 (26.8%), 240 (45.5%), and 123 (23.3%), respectively. These patients were divided into a derivation cohort (n = 264) and a validation cohort (n = 263). There were no differences in sex, age, hepatitis virus infection, Child-Pugh grade, presence of ascites or serum CA19-9 levels (all $P > 0.05$). In addition, there were also no differences in histological features or the number of patients classified into TNM stages or BCLC stages (all $P > 0.05$).

Determination of optimal cut-off value

Using the 2-year overall survival rate as an endpoint, the optimal cut-off values were confirmed using receiver operating characteristic curve analyses. For all 264 ICC patients in the derivation cohort, a GLR cut-off value equal to 33.7 provided the best separation of the survival curves between the two groups. In addition, the cut-off values of the NLR and PLR were 2.62 and 103, respectively.

Relationships between GLR and patient characteristics

According to the cut-off value, 264 patients in the derivation cohort and 263 patients in the validation cohort were divided into the GLR > 33.7 group and the GLR ≤ 33.7 group, respectively. In the derivation cohort, the preoperative GLR was correlated with sex (P = 0.024), CA19-9 level (P = 0.005), tumor size (P < 0.001), solitary tumor (P = 0.001), macrovascular (P = 0.011) and microvascular invasion (MVI) (P = 0.026), node-positive (P = 0.005), perineural invasion (P = 0.044), TNM stage (P = 0.002), and BCLC stage (P < 0.001) (Table 1). Somewhat differently, in the validation cohort, the preoperative GLR was correlated with sex (P = 0.03), CA 19-9 level (P = 0.043), tumor size (P = 0.007), macrovascular invasion (P < 0.001), perineural invasion (P = 0.009), and BCLC stage (P < 0.001). In addition, no significant differences were observed between preoperative GLR and other clinicopathological variables such as age, HBsAg, hepatolithiasis, Child-Pugh grade B, ascites, well-differentiated tumors, MVI, liver capsule invasion, and cirrhosis (all P > 0.05).

Kaplan-Meier curves

The Kaplan-Meier curves suggested that the OS rates of the GLR > 33.7 group were markedly shorter than those of the GLR ≤ 33.7 group (P < 0.001) (Figure 1A), while the RFS rates of the GLR > 33.7 group were also shorter than those of the GLR ≤ 33.7 group in the derivation cohort (P < 0.001) (Figure 1B). The poorer outcome of those with GLR > 33.7 was demonstrated in the validation cohort, as those patients had shorter OS (P < 0.001) and RFS (P < 0.001) (Figure 2).

Previous studies have reported on the prognostic significance of NLR and PLR in ICC patients[13,14]. Therefore, based on the cutoff value of NLR, two cohorts were divided into the NLR ≤ 2.62 group and NLR > 2.62 group, respectively. The Kaplan-Meier curves showed that the OS rates of the NLR > 2.62 group were shorter than those of the NLR ≤ 2.62 group (derivation cohort: P = 0.002; validation cohort: P = 0.002) (Supplementary Figure 1), while the RFS rate of the NLR > 2.62 group was also shorter than that of the NLR ≤ 2.62 group (derivation cohort: P = 0.026; validation cohort: P < 0.001) (Supplementary Figure 2) in both cohorts. In the same way, two cohorts were divided into the PLR ≤ 103 group and PLR > 103 groups. However, PLR > 103 was associated with worse OS in the validation cohort but not in the derivation cohort (derivation cohort: P = 0.063; validation cohort: P = 0.028) (Supplementary Figure 3). Meanwhile, PLR > 103 was associated with a worse RFS in the derivation cohort but not in the validation cohort (derivation cohort: P = 0.043; validation cohort: P = 0.661) (Supplementary Figure 4).

Prognostic significance of GLR

Univariate analysis for OS revealed that preoperative GLR, CA19-9, tumor size, tumor number, MVI, node-positive, NLR, and PLR had P values of ≤ 0.10 in both cohorts (Tables 2 and 3). Similarly, univariate analysis for RFS identified that GLR, ascites, CA19-9 level, tumor size, tumor number, tumor differentiation, MVI, node-positive, TNM stage, BCLC stage, and NLR had P values of ≤ 0.10 in both cohorts (Tables 2 and 3).

The results of multivariate analysis are shown in Table 4. The results indicated that the GLR was an independent predictor of OS [derivation cohort: hazard ratio (HR) = 1.620, 95% confidence interval (CI): 1.066-2.462, P = 0.024; validation cohort: HR = 1.466, 95%CI: 1.033-2.142, P = 0.048] and RFS (derivation cohort: HR = 1.471, 95%CI: 1.029-2.103, P = 0.048; validation cohort: HR = 1.480, 95%CI: 1.057-2.070, P = 0.022). In addition, CA19-9 was also demonstrated to be an independent predictor of OS and RFS in both cohorts (all P < 0.05).

Prognostic values of GLR in different ICC subgroups

We further investigated the prognostic value of the GLR in various subgroups of ICC patients. The results suggested that the GLR was a prognostic factor for OS and RFS in patients age > 60 or ≤ 60, male or female, with or without cirrhosis, without ascites, with solitary tumor, with tumor size ≥ 5 cm or < 5 cm, with MVI-negative, with or without macrovascular invasion, with node-positive or node-negative, with or without perineural invasion, with BCLC stage 0-A or B-C and TNM stage I-II or III (all P < 0.05) (Figures 5 and 6). However, preoperative GLR was not a prognostic marker for OS and RFS in patients with ascites, multiple tumor and MVI-positive (all P > 0.05) (Figures 5 and 6).

DISCUSSION

It is clear that the poor prognosis and limited effective treatment options for ICC are common obstacles faced by clinicians[1,6]. Thus, a prognostic model to screen surgical

Table 1 Correlation between gamma-glutamyltransferase to lymphocyte ratio and clinicopathological characteristics in intrahepatic cholangiocarcinoma

Variables	Derivation		*P* value	Validation		*P* value
	GLR ≤ 33.7	GLR > 33.7		GLR ≤ 33.7	GLR > 33.7	
Total patients	107	157		97	166	
Age, yr	57.96 (11.48)	57.80 (10.35)	0.902	56.97 (10.69)	56.48 (10.56)	0.716
Male gender, *n* (%)	42 (39.3)	85 (54.1)	0.024[a]	38 (39.2)	89 (53.6)	0.030[a]
HBsAg, *n* (%)	36 (33.6)	37 (23.6)	0.073	31 (32.3)	47 (28.5)	0.575
Hepatolithiasis, *n* (%)	14 (13.1)	27 (17.2)	0.396	15 (15.5)	32 (19.3)	0.511
Child-Pugh grade B, *n* (%)	3 (2.8)	8 (5.1)	0.533	2 (2.1)	11 (6.6)	0.141
Ascites, *n* (%)	6 (5.6)	21 (13.4)	0.061	4 (4.1)	19 (11.4)	0.068
CA-199 < 22, *n* (%)	38 (36.5)	42 (27.5)	0.005[a]	29 (31.2)	40 (24.2)	0.043[a]
Tumor size, cm	5.14 (2.29)	6.51 (2.78)	< 0.001[a]	5.40 (2.22)	6.36 (2.97)	0.007[a]
Solitary tumor, *n* (%)	89 (83.2)	102 (65.0)	0.001[a]	67 (69.1)	113 (68.1)	0.895
Well tumor differentiation, *n* (%)	6 (5.6)	4 (2.5)	0.331	5 (5.2)	7 (4.2)	0.767
Macrovascular invasion, *n* (%)	17 (15.9)	45 (28.7)	0.011[a]	8 (8.2)	53 (31.9)	< 0.001[a]
Microvascular invasion, *n* (%)	6 (5.6)	23 (14.6)	0.026[a]	7 (7.2)	17 (10.2)	0.514
Liver capsule invasion, *n* (%)	67 (62.6)	107 (68.2)	0.362	64 (66.0)	97 (58.4)	0.248
Node-positive, *n* (%)	16 (15.0)	48 (30.6)	0.005[a]	18 (18.6)	47 (28.3)	0.107
Perineural invasion, *n* (%)	9 (8.4)	27 (17.2)	0.044[a]	8 (8.2)	35 (21.1)	0.009[a]
Cirrhosis, *n* (%)	27 (25.2)	53 (33.8)	0.174	19 (19.6)	46 (27.7)	0.182
TNM stage, *n* (%)			0.002[a]			0.107
IA	23 (21.5)	12 (7.6)		13 (13.4)	15 (9.0)	
IB	6 (5.6)	12 (7.6)		6 (6.2)	13 (7.8)	
II	6 (5.6)	13 (8.3)		10 (10.3)	26 (15.7)	
IIIA	55 (51.4)	72 (45.9)		50 (51.5)	64 (38.6)	
IIIB	17 (15.9)	48 (30.6)		18 (18.6)	48 (28.9)	
BCLC stage, *n* (%)			< 0.001[a]			< 0.001[a]
0	6 (5.6)	9 (5.7)		3 (3.1)	5 (3.0)	
A	44 (41.1)	25 (15.9)		34 (35.1)	38 (22.9)	
B	40 (37.4)	78 (49.7)		52 (53.6)	70 (42.2)	
C	17 (15.9)	45 (28.7)		8 (8.2)	53 (31.9)	

[a]*P* < 0.05. HBV: Hepatitis B virus; CA-199: Carbohydrate antigen-199; TNM: Tumor-node-metastasis; BCLC: BARCELONA Clinic Liver Cancer; GLR: Gamma-glutamyltransferase to lymphocyte ratio; ICC: Intrahepatic cholangiocarcinoma; HR: Hazard ratio; CI: Confidence interval.

patients with a high risk of recurrence or metastasis is of great value for developing additional personalized therapeutic approaches. The main finding of the present study relates to the identification of the GLR as a novel biomarker of prognosis in ICC patients undergoing curative resection. High preoperative GLR is associated with poor outcomes in patients with ICC after curative resection. In addition, we observed that a GLR > 33.7 was associated with the highly aggressive features of tumors, such as high CA19-9 levels and the presence of macrovascular invasion and perineural invasion.

GGT is a glycoprotein that is known as a marker of cardiovascular disease or bibulosity[15,16]. In addition, previous studies have confirmed the association of GGT with ICC and hepatocellular carcinoma[17-19]. It was previously reported that GGT plays a prooxidant role and is be associated with inflammation in carcinogenesis[20-22]. Similarly, lymphocytes can reflect systemic inflammation in various primary malignancies; thus, the lymphocyte count has been considered a prognostic predictor in patients with cancer. Accumulating evidence has highlighted the important role of systemic inflammation in tumor progression and aggressiveness[22,23]. In recent years, various inflammation-based scores have been considered as prognostic indicators in different solid cancers.

In 125 patients with nonfunctional pancreatic neuroendocrine tumor, the GLR was identified as an independent predictor for outcomes in multivariate analyses, with patients with preoperative a GLR > 10.3 demonstrating worse OS and disease-free survival compared with those with a GLR ≤ 10.3[11]. To the best of our knowledge, this

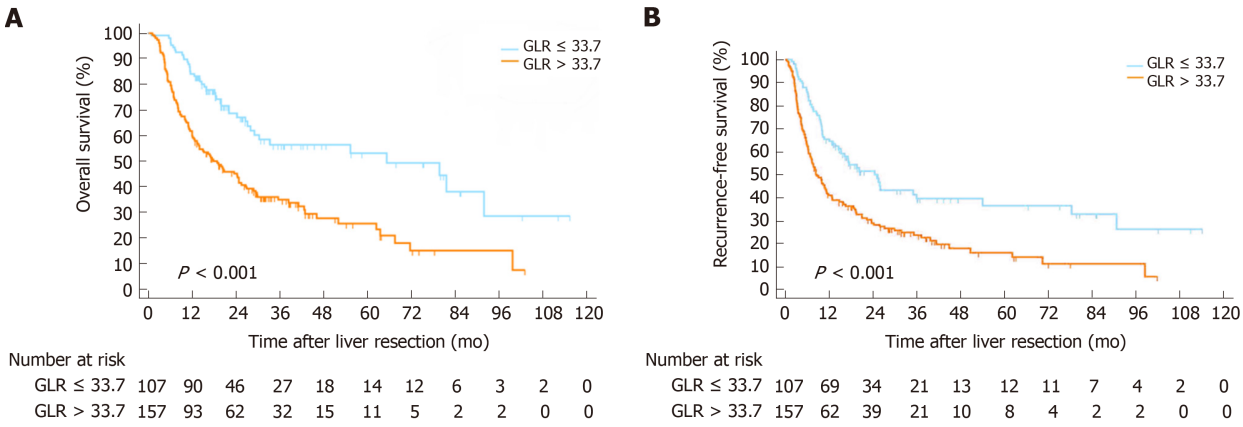

Figure 1 Kaplan-Meier survival curves and risk tables for overall survival and recurrence-free survival in the derivation cohort. A: Gamma-glutamyltransferase to lymphocyte ratio > 33.7 was correlated with shorter overall survival; B: Recurrence-free survival in intrahepatic cholangiocarcinoma patients following curative resection. OS: Overall survival; RFS: Recurrence-free survival; GLR: Gamma-glutamyltransferase to lymphocyte ratio; ICC: Intrahepatic cholangiocarcinoma.

is the first study to assess the prognostic significance of the GLR for ICC. The GLR index was developed using a cohort of 264 ICC patients and was validated in a validation cohort of 263 patients who underwent resection. There were no significant differences in the baseline characteristics. In this study, we first confirmed the optimal cut-off value of the preoperative GLR according to the receiver operating characteristic curve. We noticed that the elevated GLR was correlated with tumor size, the presence of macrovascular and perineural invasion and BCLC stage in both cohorts. Notably, all of these clinicopathological features indicated that the GLR might implicate the tumor burden. After further analysis, we identified that the GLR was a prognostic factor for OS and RFS in ICC patients after resection. Patients with a high GLR tended to have a poorer outcome. In addition, a high preoperative GLR could also predict worse OS and RFS in various subgroups. Hence, the preoperative GLR can be considered an independent prognostic factor for ICC patients after resection. Additionally, a high CA19-9 level could also act as an independent predictor of worse outcomes in ICC patients undergoing resection.

Previous studies have investigated the prognostic effects of the NLR and PLR in various cancers, including ICC[24-26]. These studies suggested that increased preoperative NLR and PLR values were independent risk factors for long-term outcomes. However, our results showed that NLR and PLR were not independent predictors of OS or RFS in ICC patients in our center.

There were several limitations in our study. First, the main limitation of this study is its retrospective nature. Second, the present study involved a single institution. Moreover, it identified the prognostic value of the GLR only in ICC patients who received curative resection. Given these limitations, future studies should include more centers and additional patients with various treatment modalities.

In conclusion, our study demonstrates that the preoperative GLR is an independent predictor of worse OS and RFS for ICC patients after resection. Therefore, as a readily available inflammatory marker, the preoperative GLR should be considered for incorporation into guiding selection of treatment methods by surgeons for ICC patients.

Table 2 Univariate analysis in the derivation cohort

Variables	Overall survival			Recurrence-free survival		
	HR	95%CI	*P* value	HR	95%CI	*P* value
Age	1.002	0.987-1.017	0.819	0.998	0.985-1.011	0.763
Gender, F/M	0.752	0.546-1.035	0.080[a]	0.846	0.633-1.132	0.262
HBsAg	1.210	0.853-1.717	0.285	1.274	0.924-1.756	0.139
Hepatolithiasis	1.593	1.061-2.393	0.025[a]	1.176	0.785-1.761	0.433
Child-Pugh grade, A /B	0.614	0.323-1.167	0.136	0.732	0.381-1.367	0.317
Ascites	1.639	1.011-2.658	0.045[a]	1.532	0.988-2.376	0.056[a]
CA-199 (≥ 22/< 22)	0.953	0.926-0.981	0.001[a]	1.546	1.259-1.899	< 0.001[a]
Tumor size	1.075	1.012-1.141	0.019[a]	1.123	1.063-1.187	< 0.001[a]
Tumor number, Multiple/Single	1.655	1.172-2.328	0.004[a]	1.893	1.388-2.582	< 0.001[a]
Tumor differentiation, Moderate-Poor/Well	1.891	0.699-5.115	0.209	3.277	1.045-10.274	0.042[a]
Macrovascular invasion	1.371	0.953-1.972	0.089[a]	1.277	0.913-1.787	0.153
Microvascular invasion	1.619	1.029-2.548	0.037[a]	1.983	1.306-3.012	0.001[a]
Liver capsule invasion	0.815	0.586-1.134	0.225	1.140	0.833-1.561	0.412
Node-positive	2.846	2.030-3.989	< 0.001[a]	2.484	1.810-3.409	< 0.001[a]
Perineural invasion	1.737	1.129-2.673	0.012[a]	1.245	0.821-1.887	0.302
Cirrhosis	1.526	1.094-2.130	0.013[a]	1.182	0.863-1.617	0.297
TNM stage, III/I-II	1.067	0.745-1.529	0.722	1.431	1.010-2.028	0.044[a]
BCLC, B-C/0-A	1.295	0.906-1.850	0.156	1.607	1.150-2.246	0.005[a]
NLR, > 2.62/≤ 2.62	1.701	1.221-2.371	0.002[a]	1.422	1.057-1.912	0.020[a]
PLR, > 103/≤ 103	1.366	0.983-1.897	0.063[a]	1.360	1.009-1.833	0.043[a]
GLR, > 33.7/≤ 33.7	2.316	1.617-3.316	< 0.001[a]	1.931	1.413-2.639	< 0.001[a]

[a]*P* < 0.10. M: male; F: Female; HBV: Hepatitis B virus; CA-199: Carbohydrate antigen-199; TNM: Tumor-node-metastasis; BCLC: Barcelona Clinic Liver Cancer; NLR: Neutrophil to lymphocyte ratio; PLR: Platelet to lymphocyte ratio; GLR: Gamma-glutamyltransferase to lymphocyte ratio; HR: Hazard ratio; CI: Confidence interval.

Table 3 Univariate analysis in the validation cohort

Variables	Overall survival			Recurrence-free survival		
	HR	95%CI	*P* value	HR	95%CI	*P* value
Age	0.996	0.981-1.011	0.594	0.990	0.976-1.004	0.148
Gender, F/M	0.907	0.667-1.233	0.534	0.920	0.695-1.218	0.560
HBsAg	1.004	0.717-1.405	0.982	1.110	0.819-1.505	0.500
Hepatolithiasis	1.092	0.744-1.602	0.654	0.799	0.551-1.158	0.236
Child-Pugh grade, A /B	0.852	0.435-1.671	0.642	0.751	0.418-1.350	0.339
Ascites	1.440	0.871-2.382	0.155	1.580	1.004-2.487	0.048[a]
CA-199, ≥ 22/< 22	1.744	1.390-2.188	< 0.001[a]	1.402	1.140-1.722	0.001[a]
Tumor size	1.054	0.997-1.115	0.064[a]	1.084	1.030-1.141	0.002[a]
Tumor number, Multiple/Single	1.845	1.344-2.531	< 0.001[a]	1.874	1.397-2.513	< 0.001[a]
Tumor differentiation, Moderate-Poor/Well	13.449	1.881-96.150	0.010	6.053	1.930-18.982	0.002[a]
Macrovascular invasion	1.050	0.730-1.511	0.792	1.009	0.718-1.418	0.959
Microvascular invasion	1.995	1.228-3.242	0.005[a]	2.023	1.290-3.172	0.002[a]
Liver capsule invasion	1.553	1.118-2.159	0.009[a]	1.280	0.955-1.716	0.099[a]
Node-positive	2.009	1.438-2.808	< 0.001[a]	1.525	1.115-2.085	0.008[a]
Perineural invasion	1.366	0.906-2.059	0.136	1.262	0.867-1.838	0.225
Cirrhosis	0.984	0.686-1.412	0.932	1.054	0.762-1.459	0.749
TNM stage, III/I-II	1.774	1.242-2.533	0.002[a]	1.413	1.035-1.929	0.029
BCLC, B-C/0-A	1.619	1.136-2.308	0.008[a]	1.849	1.335-2.562	< 0.001[a]
NLR, > 2.62/≤ 2.62	1.649	1.202-2.261	0.002[a]	1.635	1.226-2.180	0.001[a]
PLR, > 103/≤ 103	1.417	1.036-1.938	0.029[a]	1.065	0.803-1.414	0.661
GLR, > 33.7/≤ 33.7	1.826	1.300-2.565	0.001[a]	1.780	1.315-2.408	< 0.001[a]

[a]*P* < 0.10. M: Male; F: Female; HBV: Hepatitis B virus; CA-199: Carbohydrate antigen-199; TNM: Tumor-node-metastasis; BCLC: Barcelona Clinic Liver Cancer; NLR: Neutrophil to lymphocyte ratio; PLR: Platelet to lymphocyte ratio; GLR: Gamma-glutamyltransferase to lymphocyte ratio; HR: Hazard ratio; CI: Confidence interval.

Table 4 Multivariate analysis of prognostic factors for overall survival and recurrence-free survival

OS	Derivation cohort (*n* = 264)			Validation cohort (*n* = 263)		
	HR	95%CI	*P* value	HR	95%CI	*P* value
Gender, F/M	0.847	0.58-1.216	0.367	-		
Hepatolithiasis	1.073	0.677-1.699	0.765	-		
Child-Pugh grade, A /B	0.775	0.38-1.583	0.485	-		
Ascites	0.758	0.428-1.339	0.340	0.640	0.376-1.090	0.100
CA-199, ≥ 22/< 22	1.731	1.331-2.252	< 0.001[a]	1.612	1.252-2.075	< 0.001[a]
Tumor size	1.053	0.967-1.146	0.234	0.931	0.857-1.011	0.088
Tumor number, Multiple/Single	1.662	1.086-2.543	0.019[a]	1.677	1.189-2.366	0.003[a]
Tumor differentiation, Moderate-Poor/Well	-			7.927	1.083-58.02	0.042[a]
Macrovascular invasion	1.199	0.781-1.843	0.407	-		
Microvascular invasion	1.082	0.635-1.842	0.773	1.349	0.801-2.274	0.261
Liver capsule invasion	-			1.036	0.533-2.013	0.917
Node- positive	2.038	1.365-3.042	< 0.001[a]	1.269	0.835-1.928	0.265
Perineural invasion	1.252	0.773-1.116	0.169	0.973	0.591-1.603	0.914
Cirrhosis	1.589	1.074-2.351	0.020[a]	-		
TNM stage, III/I-II	-			1.294	0.607-2.761	0.505
BCLC, B-C/0-A	0.627	0.364-1.078	0.091	1.307	0.813-2.101	0.269
NLR, > 2.62/≤ 2.62	1.357	0.912-2.017	0.132	1.287	0.897-1.846	0.170
PLR, > 103/≤ 103	1.141	0.776-1.679	0.502	1.094	0.778-1.539	0.604
GLR, > 33.7/≤ 33.7	1.620	1.066-2.462	0.024[a]	1.466	1.033-2.142	0.048[a]
RFS						
Age	-			0.991	0.976-1.006	0.236
HBsAg	1.367	0.974-1.919	0.071	-		
Ascites	0.763	0.473-1.230	0.266	0.621	0.382-1.010	0.055
CA-199, ≥ 22/< 22	1.406	1.128-1.752	0.002[a]	1.319	1.050-1.656	0.017[a]
Tumor size	1.073	0.994-1.158	0.072	0.975	0.906-1.050	0.501
Tumor number, Multiple/Single	1.434	0.998-2.060	0.051	1.613	1.172-2.219	0.003[a]
Tumor differentiation, Moderate-Poor/Well	2.068	0.635-6.734	0.228	3.617	1.114-11.741	0.032[a]
Macrovascular invasion	1.149	0.785-1.682	0.475	-		
Microvascular invasion	1.643	1.031-2.618	0.037[a]	1.607	0.986-2.618	0.057
Liver capsule invasion	-			0.778	0.428-1.417	0.413
Node-positive	1.859	1.272-2.716	0.001[a]	0.972	0.664-1.421	0.882
TNM stage, III/I-II	0.892	0.559-1.328	0.572	1.524	0.778-2.988	0.220
BCLC, B-C/0-A	0.784	0.480-1.280	0.331	1.339	0.859-2.087	0.198
NLR, > 2.62/≤ 2.62	1.128	0.811-1.571	0.474	1.352	0.967-1.891	0.077
PLR, > 103/≤ 103	1.125	0.809-1.565	0.483	0.805	0.589-1.100	0.173
GLR, > 33.7/≤ 33.7	1.471	1.029-2.103	0.034[a]	1.480	1.057-2.070	0.022[a]

[a]*P* < 0.05. OS: Overall survival; RFS: Recurrence-free survival; HBV: Hepatitis B virus; CA-199: Carbohydrate antigen-199; TNM: Tumor-node-metastasis; BCLC: Barcelona Clinic Liver Cancer; GLR: Gamma-glutamyltransferase to lymphocyte ratio; HR: Hazard ratio; CI: Confidence interval.

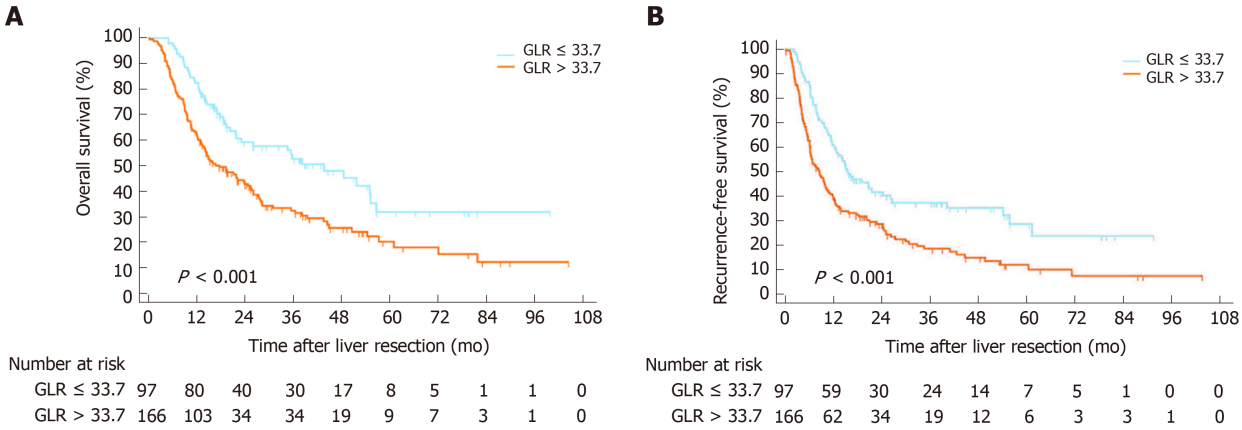

Figure 2 Kaplan-Meier survival curves and risk tables for overall survival and recurrence-free survival in the validation cohort. A: Gamma-glutamyltransferase to lymphocyte ratio > 33.7 was correlated with shorter overall survival; B: Recurrence-free survival in intrahepatic cholangiocarcinoma patients undergoing curative resection. OS: Overall survival; RFS: Recurrence-free survival; GLR: Gamma-glutamyltransferase to lymphocyte ratio; ICC: Intrahepatic cholangiocarcinoma.

ARTICLE HIGHLIGHTS

Research background

Intrahepatic cholangiocarcinoma (ICC) is a heterogeneous hepatobiliary cancer with limited treatment options and has a high mortality. Therefore, it is important to probe effective biomarkers or prognostic models for ICC patients following hepatic resection at risk of recurrence or metastasis. Accumulating studies has found that a system inflammatory response is important in tumor progression and recurrence. However, it is not yet clear whether neutrophil to lymphocyte ratio (NLR), platelet to lymphocyte ratio (PLR) or gamma-glutamyltransferase to lymphocyte ratio (GLR), can be used as a novel prognostic factor for ICC patients following hepatic resection.

Research motivation

Timely and effective establishment of prognostic models for ICC patients following curative resection is of great value for the long-term outcomes of these patients.

Research objectives

The main aim of our study was to examine the role of inflammation markers in ICC patients and evaluate the prognostic value of GLR in ICC patients following curative resection.

Research methods

We retrospectively enrolled ICC patients following curative resection between January 2009 and September 2017 at the West China Hospital of Sichuan University. The ICC patients were divided into a derivation cohort and a validation cohort. The derivation cohort was used to explore an optimal cut-off value, and the validation cohort was used to further evaluate the score.

Research results

In all, 527 ICC patients were included and divided into the derivation cohort (264 patients) and the validation cohort (263 patients). The two cohorts had comparable baseline characteristics. The optimal cut-off values for the NLR, PLR and GLR were 2.62, 103 and 33.7, respectively. The overall survival (OS) and recurrence-free survival (RFS) were shorter in the GLR > 33.7 group than GLR ≤ 33.7 group in both derivation cohort and validation cohort. Multivariate analysis revealed that the GLR was an independent predictor of OS [derivation cohort: hazard ratio (HR) = 1.620, 95% confidence interval (CI): 1.066-2.462, P = 0.024; validation cohort: HR = 1.466, 95%CI: 1.033-2.142, P = 0.048] and RFS (derivation cohort: HR = 1.471, 95%CI: 1.029-2.103, P = 0.048; validation cohort: HR = 1.480, 95%CI: 1.057-2.070, P = 0.022). Besides, CA19-9 also be demonstrated as an independent predictor of OS and RFS in both cohorts (all P < 0.05). However, our results showed that NLR and PLR were not independent predictors of OS or RFS in ICC patients in our center.

Research conclusions

The OS and RFS of ICC patients following curative resection are shorter in the GLR > 33.7 group than GLR ≤ 33.7 group. The preoperative GLR is an independent prognostic factor for ICC patients following hepatectomy. A high preoperative GLR is associated with worse OS and RFS.

Research perspectives

Because our study used a single-center retrospective design and enrolled limited patients. Future studies which included more centers and patients are needed to further verify our results.

REFERENCES

1 **Moeini A**, Sia D, Bardeesy N, Mazzaferro V, Llovet JM. Molecular Pathogenesis and Targeted Therapies for Intrahepatic Cholangiocarcinoma. *Clin Cancer Res* 2016; **22**: 291-300 [PMID: 26405193 DOI: 10.1158/1078-0432.CCR-14-3296]

2 **West J**, Wood H, Logan RF, Quinn M, Aithal GP. Trends in the incidence of primary liver and biliary tract cancers in England and Wales 1971-2001. *Br J Cancer* 2006; **94**: 1751-1758 [PMID: 16736026 DOI: 10.1038/sj.bjc.6603127]

3 **Razumilava N**, Gores GJ. Cholangiocarcinoma. *Lancet* 2014; **383**: 2168-2179 [PMID: 24581682 DOI: 10.1016/S0140-6736(13)61903-0]

4 **Rizvi S**, Khan SA, Hallemeier CL, Kelley RK, Gores GJ. Cholangiocarcinoma - evolving concepts and therapeutic strategies. *Nat Rev Clin Oncol* 2018; **15**: 95-111 [PMID: 28994423 DOI: 10.1038/nrclinonc.2017.157]

5 **Bridgewater J**, Galle PR, Khan SA, Llovet JM, Park JW, Patel T, Pawlik TM, Gores GJ. Guidelines for the diagnosis and management of intrahepatic cholangiocarcinoma. *J Hepatol* 2014; **60**: 1268-1289 [PMID: 24681130 DOI: 10.1016/j.jhep.2014.01.021]

6 **Poultsides GA**, Zhu AX, Choti MA, Pawlik TM. Intrahepatic cholangiocarcinoma. *Surg Clin North Am* 2010; **90**: 817-837 [PMID: 20637950 DOI: 10.1016/j.suc.2010.04.011]

7 **Shimizu T**, Marusawa H, Endo Y, Chiba T. Inflammation-mediated genomic instability: roles of activation-induced cytidine deaminase in carcinogenesis. *Cancer Sci* 2012; **103**: 1201-1206 [PMID: 22469133 DOI: 10.1111/j.1349-7006.2012.02293.x]

8 **Coussens LM**, Werb Z. Inflammation and cancer. *Nature* 2002; **420**: 860-867 [PMID: 12490959 DOI: 10.1038/nature01322]

9 **Sun X**, Liu X, Liu J, Chen S, Xu D, Li W, Zhan Y, Li Y, Chen Y, Zhou Z. Preoperative neutrophil-to-lymphocyte ratio plus platelet-to-lymphocyte ratio in predicting survival for patients with stage I-II gastric cancer. *Chin J Cancer* 2016; **35**: 57 [PMID: 27342313 DOI: 10.1186/s40880-016-0122-2]

10 **Ying HQ**, Deng QW, He BS, Pan YQ, Wang F, Sun HL, Chen J, Liu X, Wang SK. The prognostic value of preoperative NLR, d-NLR, PLR and LMR for predicting clinical outcome in surgical colorectal cancer patients. *Med Oncol* 2014; **31**: 305 [PMID: 25355641 DOI: 10.1007/s12032-014-0305-0]

11 **Zhou B**, Zhan C, Wu J, Liu J, Zhou J, Zheng S. Prognostic significance of preoperative gamma-glutamyltransferase to lymphocyte ratio index in nonfunctional pancreatic neuroendocrine tumors after curative resection. *Sci Rep* 2017; **7**: 13372 [PMID: 29042631 DOI: 10.1038/s41598-017-13847-6]

12 **Wang DS**, Ren C, Qiu MZ, Luo HY, Wang ZQ, Zhang DS, Wang FH, Li YH, Xu RH. Comparison of the prognostic value of various preoperative inflammation-based factors in patients with stage III gastric cancer. *Tumour Biol* 2012; **33**: 749-756 [PMID: 22198641 DOI: 10.1007/s13277-011-0285-z]

13 **Zhang C**, Wang H, Ning Z, Xu L, Zhuang L, Wang P, Meng Z. Prognostic nutritional index serves as a predictive marker of survival and associates with systemic inflammatory response in metastatic intrahepatic cholangiocarcinoma. *Onco Targets Ther* 2016; **9**: 6417-6423 [PMID: 27799789 DOI: 10.2147/OTT.S112501]

14 **Chen Q**, Dai Z, Yin D, Yang LX, Wang Z, Xiao YS, Fan J, Zhou J. Negative impact of preoperative platelet-lymphocyte ratio on outcome after hepatic resection for intrahepatic cholangiocarcinoma. *Medicine (Baltimore)* 2015; **94**: e574 [PMID: 25837750 DOI: 10.1097/MD.0000000000000574]

15 **Whitfield JB**. Gamma glutamyl transferase. *Crit Rev Clin Lab Sci* 2001; **38**: 263-355 [PMID: 11563810 DOI: 10.1080/20014091084227]

16 **Dillon JF**, Miller MH. Gamma glutamyl transferase 'To be or not to be' a liver function test? *Ann Clin Biochem* 2016; **53**: 629-631 [PMID: 27384446 DOI: 10.1177/0004563216659887]

17 **Lu Z**, Liu S, Yi Y, Ni X, Wang J, Huang J, Fu Y, Cao Y, Zhou J, Fan J, Qiu S. Serum gamma-glutamyl transferase levels affect the prognosis of patients with intrahepatic cholangiocarcinoma who receive postoperative adjuvant transcatheter arterial chemoembolization: A propensity score matching study. *Int J Surg* 2017; **37**: 24-28 [PMID: 27756646 DOI: 10.1016/j.ijsu.2016.10.015]

18 **Song P**, Inagaki Y, Wang Z, Hasegawa K, Sakamoto Y, Arita J, Tang W, Kokudo N. High Levels of Gamma-Glutamyl Transferase and Indocyanine Green Retention Rate at 15min as Preoperative Predictors of Tumor Recurrence in Patients With Hepatocellular Carcinoma. *Medicine (Baltimore)* 2015; **94**: e810 [PMID: 26020384 DOI: 10.1097/MD.0000000000000810]

19 **Yao D**, Jiang D, Huang Z, Lu J, Tao Q, Yu Z, Meng X. Abnormal expression of hepatoma specific gamma-glutamyl transferase and alteration of gamma-glutamyl transferase gene methylation status in patients with hepatocellular carcinoma. *Cancer* 2000; **88**: 761-769 [PMID: 10679644]

20 **Stark AA**, Russell JJ, Langenbach R, Pagano DA, Zeiger E, Huberman E. Localization of oxidative damage by a glutathione-gamma-glutamyl transpeptidase system in preneoplastic lesions in sections of livers from carcinogen-treated rats. *Carcinogenesis* 1994; **15**: 343-348 [PMID: 7906207 DOI: 10.1093/carcin/15.2.343]

21 **Everhart JE**, Wright EC. Association of γ-glutamyl transferase (GGT) activity with treatment and clinical outcomes in chronic hepatitis C (HCV). *Hepatology* 2013; **57**: 1725-1733 [PMID: 23258530 DOI: 10.1002/hep.26203]

22 **Yin X**, Zheng SS, Zhang BH, Zhou Y, Chen XH, Ren ZG, Qiu SJ, Fan J. Elevation of serum γ-glutamyltransferase as a predictor of aggressive tumor behaviors and unfavorable prognosis in patients with intrahepatic cholangiocarcinoma: analysis of a large monocenter study. *Eur J Gastroenterol Hepatol* 2013; **25**: 1408-1414 [PMID: 23839159 DOI: 10.1097/MEG.0b013e328364130f]

23 **Ma H**, Zhang L, Tang B, Wang Y, Chen R, Zhang B, Chen Y, Ge N, Wang Y, Gan Y, Ye S, Ren Z. γ-Glutamyltranspeptidase is a prognostic marker of survival and recurrence in radiofrequency-ablation treatment of hepatocellular carcinoma. *Ann Surg Oncol* 2014; **21**: 3084-3089 [PMID: 24748164 DOI: 10.1245/s10434-014-3724-4]

24 **Li J**, Liao Y, Suo L, Zhu P, Chen X, Dang W, Liao M, Qin L, Liao W. A novel prognostic index-neutrophil times γ-glutamyl transpeptidase to lymphocyte ratio (NγLR) predicts outcome for patients with hepatocellular carcinoma. *Sci Rep* 2017; **7**: 9229 [PMID: 28835713 DOI: 10.1038/s41598-017-09696-y]

25 **Hoshimoto S**, Hishinuma S, Shirakawa H, Tomikawa M, Ozawa I, Ogata Y. Association of Preoperative Platelet-to-Lymphocyte Ratio with Poor Outcome in Patients with Distal Cholangiocarcinoma. *Oncology* 2019; **96**: 290-298 [PMID: 30909286 DOI: 10.1159/000499050]

26 **Beal EW**, Wei L, Ethun CG, Black SM, Dillhoff M, Salem A, Weber SM, Tran T, Poultsides G, Son AY, Hatzaras I, Jin L, Fields RC, Buettner S, Pawlik TM, Scoggins C, Martin RC, Isom CA, Idrees K, Mogal HD, Shen P, Maithel SK, Schmidt CR. Elevated NLR in gallbladder cancer and cholangiocarcinoma -

making bad cancers even worse: results from the US Extrahepatic Biliary Malignancy Consortium. *HPB (Oxford)* 2016; **18**: 950-957 [PMID: 27683047 DOI: 10.1016/j.hpb.2016.08.006]

World Journal of Gastroenterology

Submit a Manuscript: https://www.f6publishing.com

World J Gastroenterol 2020 April 7; 26(13): 1513-1524

DOI: 10.3748/wjg.v26.i13.1513

ISSN 1007-9327 (print) ISSN 2219-2840 (online)

ORIGINAL ARTICLE

Observational Study

Evaluation of ^{177}Lu-Dotatate treatment in patients with metastatic neuroendocrine tumors and prognostic factors

Estephany Abou Jokh Casas, Virginia Pubul Núñez, Urbano Anido-Herranz, María del Carmen Mallón Araujo, Maria del Carmen Pombo Pasín, Miguel Garrido Pumar, José Manuel Cabezas Agrícola, José Manuel Cameselle-Teijeiro, Ashraf Hilal, Álvaro Ruibal Morell

ORCID number: Estephany Abou Jokh Casas (0000-0003-0193-828X); Virginia Pubul Núñez (0000-0002-4717-197X); Urbano Anido-Herranz (0000-0003-0376-5642); Maria del Carmen Mallón Araujo (0000-0001-5136-1592); Maria del Carmen Pombo Pasín (0000-0003-1347-0629); Miguel Garrido Pumar (0000-0003-2093-1286); José Manuel Cabezas Agrícola (0000-0003-4616-0512); José Manuel Cameselle-Teijeiro (0000-0002-5516-8914); Ashraf Hilal (0000-0002-4580-4366); Álvaro Ruibal Morell (0000-0002-6001-547X).

Author contributions: Abou Jokh Casas E, Pubul Núñez V, del Carmen Mallón Araujo M and del Carmen Pombo Pasín M designed the research and wrote the paper; Anido-Herranz U, Hilal A and Garrido Pumar M contributed new reagents/analytic tools; Cabezas Agrícola JM, Cameselle-Teijeiro JM and Ruibal Morell Á analyzed the data.

Institutional review board statement: The study was reviewed and approved by the ethics committee.

Informed consent statement: All study participants, or their legal guardian, provided informed written consent prior to study enrollment.

Conflict-of-interest statement:

Estephany Abou Jokh Casas, Virginia Pubul Núñez, María del Carmen Mallón Araujo, Maria del Carmen Pombo Pasín, Miguel Garrido Pumar, Álvaro Ruibal Morell, Department of Nuclear Medicine, Santiago de Compostela´s University Hospital, Santiago de Compostela 15706, A Coruña, Spain

Urbano Anido-Herranz, Department of Oncology, Santiago de Compostela´s University Hospital, Santiago de Compostela 15706, A Coruña, Spain

José Manuel Cabezas Agrícola, Department of Endocrinology, Santiago de Compostela´s University Hospital, Santiago de Compostela, 15706, A Coruña, Spain

José Manuel Cameselle-Teijeiro, Department of Pathology, Santiago de Compostela´s University Hospital, Santiago de Compostela 15706, A Coruña, Spain

Ashraf Hilal, Department of Statistics, University of Santiago de Compostela, Santiago de Compostela 15706, A Coruña, Spain

Corresponding author: Estephany Abou Jokh Casas, MD, Occupational Physician, Department of Nuclear Medicine, Santiago de Compostela´s University Hospital, Avenida Choupana, Santiago de Compostela 15706, A Coruña, Spain. estephanyaboujokh@gmail.com

Abstract

BACKGROUND

^{177}Lu peptide receptor radionuclide therapy (PRRT) is a recently approved therapy in Spain that has been demonstrated to be a well-tolerated therapy for positive somatostatin receptor advanced gastroenteropancreatic neuroendocrine tumors.

AIM

To determine the impact of PRRT on quality of life, radiologic and metabolic response, overall survival, prognostic factors and toxicity.

METHODS

Thirty-six patients treated with ^{177}Lu-PRRT from 2016 to 2019 were included. The most frequent location of the primary tumor was the gastrointestinal tract (52.8%), pancreas (27.8%), and nongastropancreatic neuroendocrine tumor (11.1%). The liver was the most common site of metastasis (91.7%), followed by distant nodes (50.0%), bone (27.8%), peritoneum (25.0%) and lung (11.1%). Toxicity was evaluated after the administration of each dose. Treatment efficacy

There are no conflicts of interest to report.

Data sharing statement: No additional data are available.

STROBE statement: The authors have read the STROBE Statement-checklist of items, and the manuscript was prepared and revised according to the STROBE Statement-checklist of items.

Manuscript source: Unsolicited manuscript

Received: December 8, 2019
Peer-review started: December 8, 2019
First decision: January 9, 2020
Revised: March 6, 2020
Accepted: March 19, 2020
Article in press: March 19, 2020
Published online: April 7, 2020

P-Reviewer: Gao BL, Khuroo MS, Yang ZH
S-Editor: Zhang L
L-Editor: Filipodia
E-Editor: Zhang YL

was evaluated by two parameters: stable disease and disease progression in response evaluation criteria in solid tumors 1.1 criterion and prognostic factors were tested.

RESULTS

From 36 patients, 55.6% were men, with a median age of 61.1 ± 11.8 years. Regarding previous treatments, 55.6% of patients underwent surgery of the primary tumor, 100% of patients were treated with long-acting somatostatin analogues, 66.7% of patients were treated with everolimus, 27.8% of patients were treated with tyrosine kinase inhibitor, and 27.8% of patients were treated with interferon. One patient received radioembolization, three patients received chemoembolization, six patients received chemotherapy. Hematological toxicity was registered in 14 patients (G1-G2: 55.5% and G3: 3.1%). Other events presented were intestinal suboclusion in 4 cases, cholestasis in 2 cases and carcinoid crisis in 1 case. The median follow-up time was 3 years. Currently, 24 patients completed treatment. Nineteen are alive with stable disease, two have disease progression, eight have died, and nine are still receiving treatment. The median overall survival was 12.5 mo (95% confidence interval range: 9.8–15.2), being inversely proportional to toxicity in previous treatments ($P < 0.02$), tumor grade ($P < 0.01$) and the presence of bone lesions ($P = 0.009$) and directly proportional with matching lesion findings between Octreoscan and computed tomography pre-PRRT ($P < 0.01$), , primary tumor surgery ($P = 0.03$) and metastasis surgery ($P = 0.045$). In a multivariate Cox regression analysis, a high Ki67 index ($P = 0.003$), a mismatch in the lesion findings between Octreoscan and computed tomography pre-PRRT ($P < 0.01$) and a preceding toxicity in previous treatments ($P < 0.05$) were risk factors to overall survival.

CONCLUSION

Overall survival was inversely proportional to previous toxicity, tumor grade and the presence of bone metastasis and directly proportional to matching lesion findings between Octreoscan and computed tomography pre-PRRT and primary tumor and metastasis surgery.

Key words: Peptide receptor radionuclide therapy; Gastropancreatic neuroendocrine tumors; Radiological response; Metabolic response

Core tip: Peptide receptor radionuclide therapy has been used successfully in patients diagnosed with metastatic gastroenteropancreatic somatostatin receptor positive tumors when cytoreductive options are limited. In this study we found that overall survival was inversely proportional to toxicity to previous treatments, tumor grade, bone metastasis and directly proportional to matching lesion findings between Octreoscan and computed tomography pre-peptide receptor radionuclide therapy and primary tumor and metastasis surgery. Also, pseudo-progression in the middle of the treatment was a common finding that should be taken into consideration by clinicians in daily practice.

Citation: Abou Jokh Casas E, Pubul Núñez V, Anido-Herranz U, del Carmen Mallón Araujo M, del Carmen Pombo Pasín M, Garrido Pumar M, Cabezas Agrícola JM, Cameselle-Teijeiro JM, Hilal A, Ruibal Morell Á. Evaluation of [177]Lu-Dotatate treatment in patients with metastatic neuroendocrine tumors and prognostic factors. *World J Gastroenterol* 2020; 26(13): 1513-1524
URL: https://www.wjgnet.com/1007-9327/full/v26/i13/1513.htm
DOI: https://dx.doi.org/10.3748/wjg.v26.i13.1513

INTRODUCTION

Neuroendocrine tumors (NETs) form a heterogeneous group of neoplasms with predominantly neuroendocrine differentiation that can develop in any place of the human body and that have the ability to secrete peptides and neuroamines[1].

Physiologically the transcription factors that direct fate and cell proliferation during embryological development maintain a balance between proliferation, cellular differentiation and apoptosis. Therefore, its disturbance plays a key role in oncogenesis[1]. This can lead to a malignant transformation of cells of the neuroendocrine system, which derives from the neural crest and endoderm and is characterized by its capacity to generate peptides that produce hormonal syndromes[1].

Although they can originate from any organ, gastroenteropancreatic endocrine tumors are the most numerous (67.5%) followed by bronchopulmonary tumors (25.3%)[2], and the remaining cases arise in other endocrine tissues. The most common site of gastroenteropancreatic endocrine tumors is the pancreas (30%-40%), the small intestine (15%-20%) and the rectum (5%-15%)[3].

NETs are an uncommon type of neoplasia; however, its prevalence is higher than other gastrointestinal cancers such as pancreatic, esophageal and hepatobiliary cancer, being exceeded only by colorectal neoplasms[2]. Its current incidence and prevalence increase are probably due to the extensive use of more developed routine radiological tests and endoscopic techniques[3]. According to the data from the Surveillance Epidemiology and End Results program of the National Cancer Institute, an increase in the incidence of gastric NETs in the latter was reported by 0.3 per 100000 in the last 30 years and that it is attributed to the routine use of endoscopic techniques. This increase in incidence was similar across sex and race[3]. According to the results of the national cancer registry in Spain, a substantial increase in the latest trends was reported, being the incidence of 2.5 to 5 cases per 100000 inhabitants in the Caucasian population[3].

An exclusive feature of well-differentiated gastropancreatic neuroendocrine tumor is the overexpression of somatostatin receptors, which is the basis for possible treatments with somatostatin analogues or with radionuclide-labeled peptides that bind to somatostatin receptors and for imaging tests[4,5]. In the past two decades, peptide receptor radionuclide therapy (PRRT) with radiolabeled somatostatin analogues ^{177}Lu-DOTA0-Tyr3-octreotate (^{177}Lu-Dotatate) has been used successfully in patients diagnosed with metastatic gastroenteropancreatic somatostatin receptor positive tumors when cytoreductive options are limited[6].

^{177}Lu-Dotatate is a radionuclide labeled peptide that binds to somatostatin receptors with high affinity for type 2 receptor and binds to the tumor cells that overexpress them. ^{177}Lu is a radionuclide that disintegrates into stable hafnium (^{177}Hf) by emission of β-particles. It also emits low energy gamma radiation with a half-life of 6.65 d and is indicated in adults for the treatment of gastroenteropancreatic endocrine tumors positive for somatostatin receptor, well differentiated (G1 and G2), progressive and unresectable or metastatic[7].

The aim of this study is to determine the impact of this treatment on the patient's quality of life, radiological and metabolic response, overall survival and possible prognostic factors and its toxicity.

MATERIALS AND METHODS

This is a retrospective longitudinal observational study in which impact on quality of life, radiological and metabolic response, overall survival, possible prognostic factors and toxicity were evaluated in patients diagnosed with advanced tumors expressing somatostatin receptors treated with PRRT. The information pertinent to this cohort of patients is collected through the clinical history, obtaining information about clinical data, treatment response and disease state. These data were treated confidentially and in an encrypted form for analysis. Written consent was obtained from all patients.

Patients

Patients diagnosed with advanced NET treated from May 2016 to November 2019 were included. All patients received ^{177}Lu-Dotatate treatment in the Nuclear Medicine department of the University Hospital Santiago de Compostela in Spain. These patients come from all the autonomous community of Galicia and have been previously evaluated by a committee of endocrine tumors in their own hospital center. Also, this study was evaluated and approved by the ethical committee of our medical center.

To evaluate the impact of PRRT over quality life of each patient, three parameters were used by means of a questionnaire after each dose, including "overall improvement," "pain assessment" and "evaluation of hormonal secretion symptoms" that included the assessment of diarrhea, flushing, and abdominal pain.

PRRT

The inclusion criteria were: Patients with advanced NET with a baseline tumor uptake on (111In-DTPA0) octreotide scintigraphy (Octreoscan®) in tumor cells at least as high as in normal liver tissue (Krenning score ≥ 2), tumor progression to previous treatments defined by response evaluation criteria in solid tumors (RECIST) in computed tomography (CT) or magnetic resonance imaging performed at least 3 mo before the treatment, a life expectancy of at least 6 mo, baseline serum hemoglobin ≥ 8 g/dL, white blood cell count > 3000/μL, platelet count ≥ 75.000/μL, creatinine clearance > 50 mL/min, bilirubin < 3 times the range limit, serum albumin > 30g/L (if the albumin < 30 g/L, then prothrombin time must be normal) and a Karnofsky performance status ≥ 60 or an ECOG < 2.

Patients were hospitalized for the administration of the treatment in which 30 min before the infusion of PRRT a capsule containing 300 mg of netupitant and 0.5 mg of palonosetron (Akynzeo®) was administrated orally. Later, an infusion of amino acids (2.5% arginine and 2.5% lysine, 1 L) was started 30 min before the administration of the radiopharmaceutical, lasting for 4-6 h. The radiopharmaceutical was co-administered using a second pump system. All cycle doses were 7.4 GBq (200 mCi) of ^{177}Lu-Dotatate, injected over 30 min completing 4 cycles of treatment. The intended interval between treatments cycles was 6–10 wk.

Between treatment cycles patients underwent blood analysis 4 and 6 wk after the dose administration to detect possible side effects. These blood tests included a hemogram and renal and liver function parameters. A full body scintigraphy was performed 24 h after each dose in an Optima 640 gamma camera from General Electric as well as a whole body CT following the second cycle to evaluate RECIST criterion. The follow-up included CT or magnetic resonance imaging performed 3-6 mo after the last treatment and thereafter every 6 mo.

Statistical analysis

Statistical analyses were performed using IBM SPSS® version 23.0 with the data obtained. A descriptive analysis was carried out describing the continuous variables as means, medians and standard deviation while the categorical variables were described as proportions, including 95% confidence intervals (CIs). The radiological, clinical and metabolic response variable was calculated as the percentage of patients that responded. Progression-free survival was calculated from the initiation date treatment with PRRT until disease progression, assessed by RECIST criteria or death from any cause. Overall survival was calculated from the start date of treatment with PRRT until the date of death of the patient for any reason and was estimated using Kaplan-Meier. Cox regression was used to evaluate the association with independent variables.

The study was conducted following the Declaration of Helsinki of the World Medical Association (1964) and ratifications of the following assemblies on ethical principles for medical research in humans (RD 1090/2015, of December 24, of clinical trials, specifically the provisions of article 38 on good clinical practice and the Convention on Human Rights and Biomedicine), made in Oviedo on April 4, 1997 and successive updates.

RESULTS

Baseline clinical characteristics

The median age was 61.1 ± 11.8 years (age range: 38-85 years), and 20 were men (55.6%). Regarding medical history, seven patients were diabetic (19.4%), fifteen were hypertensive (41.7%), nine had smoking habits prior to the diagnosis (25%), five had cancer history (13.9%), of which 3 received chemo-radiotherapy treatments, and one patient was a carrier of a mutation in the MEN-1 gene.

Regarding chief complaints, 33.3% consulted for abdominal pain, 16.67% for gastrointestinal and hormonal related symptoms, 12.5% for weight loss and 11.1% had no symptoms prior the diagnosis. In 58.3% of patients, the diagnosis was casual by an imaging test performed for other reasons, 30.6% guided by clinical suspicion and 5.6% during a surgical intervention for uterine leiomyomatosis.

The most common primary tumor was in the gastrointestinal tract (52.8%), followed by the pancreas (27.8%). A nongastropancreatic NET was diagnosed 11.1% of patients, including two endobronchial NETs, one thymic and three with unknown origin of the primary tumor. The vast majority of the patients (91.7%) had liver metastases followed by metastasis in the peritoneum (25.0%), lymph nodes (50.0%), bone (27.8%), lung (11.1%) and other locations including a lesion in the heart, in the suprarenal gland, in the kidney and in the ovary. Baseline characteristics are presented in Table 1.

Table 1 Demographic and baseline clinical characteristics of patients with neuroendocrine tumors, *n* = 36

Characteristics	Number of patients
Sex	
Male	20 (55.6%)
Female	16 (44.4%)
Comorbidities	
Hypertension	15 (41.7%)
DM	7 (19.4%)
Smoking habits	9 (25.0%)
Cancer history	5 (13.9%)
Symptoms prior to diagnosis	
Abdominal pain	12 (33.3%)
Gastrointestinal and carcinoid symptoms	6 (16.7%)
Weight loss	5 (12.5%)
Asymptomatic	4 (11.1%)
Primary tumor site	
Gastrointestinal tract	19 (52.8%)
Pancreas	10 (27.8%)
Nongastropancreatic NET	4 (11.1%)
Endobronchial NETs	2
Thymic	1
Histologic grade	
Grade 1	15 (41.7%)
Grade 2	18 (50.0%)
Grade 3 (2 NEC + 1 TNE)	3 (8.3%)
Site of metastasis	
Liver	33 (91.7%)
Lymph nodes	18 (50.0%)
Bone	10 (27.8%)
Peritoneum	9 (25.0%)
Lungs	4 (11.1%)
Primary tumor resection	20 (55.6%)
Metastasis resection	7 (19.4%)
Primary treatment before PRRT	
SSA	36 (100%)
Everolimus	24 (66.7%)
Sunitinib	10 (27.8%)
Interferon	10 (27.8%)
Chemotherapy	6 (16.7%)
Liver directed therapy	
Chemoembolization	3
Radioembolization	1

NEC: Neuroendocrine carcinoma; NET: Neuroendocrine tumors; PRRT: Peptide receptor radionuclide therapy; SSA: Somatostatin analogues.

Regarding anatomopathological characteristics, 41.7% were grade 1 (Ki67% ≤ 2), 50% were grade 2 (Ki67% = 3-20) and 8.3% were grade 3 (Ki67% > 20), of which two were poorly differentiated neuroendocrine carcinoma. Of the total number of patients, 63.9% completed treatment with PRRT, 25.0% patients are receiving treatment and 11.1% could not complete it due to death or complications of their underlying disease.

Treatment patterns before PRRT

More than half of the patients had surgically removed the primary tumor (55.6%), and 19.4% underwent surgery of the metastases. All patients were treated with

somatostatin analogues (SSA), 44.4% needed treatment with short-acting octreotide, 66.7% received everolimus, 27.8% received sunitinib, 27.8% received treatment with interferon, and 16.7% received chemotherapy. Four patients received liver directed therapy, three of which underwent chemoembolization and one underwent transarterial radioembolization of liver metastases.

Most patients (94.4%) had progression to previous treatments 12 mo after their start. Only 5.6% of patients had early progression of their disease according to RECIST criteria before 12 mo.

Metabolic and radiological imaging response

We assessed whether there was a matching coincidence between the lesions described in the CT evaluation and the Octreoscan® pre-PRRT. Twenty-six (72.2%) of the patients presented matching lesions in the two studies, 13.9% had lesions in the CT that did not express somatostatin receptors in Octreoscan®, and 13.9% presented metabolic lesions without anatomical correlate in the CT.

It was corroborated that 69.4% of the patients presented a greater number of lesions in the scintigraphy scan after the first dose of PRRT than in those described in the Octreoscan® pre-treatment. The most frequent localization was the liver (38.9%), bone (11.1%), lymph (5.6%), lung (2.8%) and spleen (2.8%).

At the end of the treatment, 23 patients completed the treatment. Of these patients, 11 (30.6%) presented a decrease in the number of lesions in the fourth post-dose scintigraphy compared to the first scan. The intensity of lesions decreased in 33.3% of patients, which changed the Krenning score from 4 to 3.

In the CT evaluation after the administration of the second dose, the radionuclide treatment was effective at achieving a radiological stability according to RECIST criteria in 20 patients (69%). However, there was an apparent radiological progression in nine cases (25%). Despite this, due to a significant clinical improvement and control of hormonal related symptoms, it was decided in a multidisciplinary committee to complete the treatment. Disease control was reached in the evaluation after the last dose in all cases. So far, nineteen patients (52.8%) are alive with stable disease, two (5.6%) have disease progression, eight (22.2%) have died and seven (25.0%) are still receiving treatment.

Quality of life

After the administration of the first and second doses, 75% of the patients presented an overall improvement that remained until the end of the treatment. Regarding the evaluation of pain, 15 patients (41.7%) reported a clear recovery after the first dose. Of these patients, ten (27%) were asymptomatic after the last dose. Of the 15 patients with hormonal secretion symptoms, 66.6% reported an amelioration of symptoms after the first dose, reaching control at the end of treatment in 26.6% of the patients.

Overall survival and prognostic factors

The median overall survival (OS) was 12.5 mo (95%CI: 9.8–15.2) (Figure 1). Eight patients (22.2%) died during follow-up. OS was inversely proportional to preceding toxicity in previous treatments ($P < 0.02$) with a hazard ratio (HR) of 0.09 (95%CI: 0.01–0.7; $P = 0.02$), tumor grade ($P < 0.01$, HR: 0.09, 95%CI: 0.014–0.676; $P = 0.018$) (Figure 2) and the presence of bone metastasis (BM) ($P = 0.009$, HR: 0.08, 95%CI: 0.015–0.446; $P = 0.004$) (Figure 4) and is directly proportional with matching lesion findings between Octreoscan and CT pre-PRRT ($P < 0.01$, HR: 0.36, 95%CI: 0.07–1.79; $P = 0.21$); primary tumor surgery ($P = 0.03$, HR: 1.7, 95%CI: 0.48–6.03; $P = 0.4$) and metastasis surgery ($P = 0.045$, HR: 26.2, 95%CI: 0.01–711; $P = 0.41$) (Figure 3). In a multivariate Cox regression analysis, a high Ki67 index ($P = 0.003$), a mismatch in the lesion findings between Octreoscan and CT pre-PRRT ($P < 0.01$) and a preceding toxicity in previous treatments ($P < 0.05$) were risk factors for OS.

OS was not significantly different by gender ($P = 0.74$, HR: 1.4, 95%CI: 0.39–5.47; $P = 0.56$); oncological history ($P = 0.091$, HR: 23.95, 95%CI: 0.00–316; $P = 0.51$); smoking ($P = 0.34$, HR: 5.07, 95%CI: 0.63–40.28; $P = 0.12$); treatment with SSA ($P = 0.959$, HR: 1.59, 95%CI: 0.32–7.71; $P = 0.56$); everolimus ($P = 0.97$, HR: 0.85, 95%CI: 0.21–3.35; $P = 0.82$); sunitinib ($P = 0.993$, HR: 0.85, 95%CI: 0.23–3.04; $P = 0.80$); interferon ($P = 0.945$, HR: 1.04, 95%CI: 0.21–5.17; $P = 0.95$); radioembolization ($P = 0.425$); quimioembolization ($P = 0.972$, HR: 0.25, 95%CI: 0.02–2.53; $P = 0.24$); and quimiotherapy ($P = 0.06$, HR: 0.42, 95%CI: 0.12–1.52; $P = 0.18$).

History of hypertension ($P = 0.06$), diabetes ($P = 0.83$), oncology diseases ($P = 0.31$), smoking ($P = 0.08$) as well as other factors such as the location of the primary tumor ($P = 0.426$), treatment with SSA ($P = 0.56$), everolimus ($P = 0.82$), sunitinib ($P = 0.80$) and interferon ($P = 0.95$) were not predictive risk factors.

Toxicity

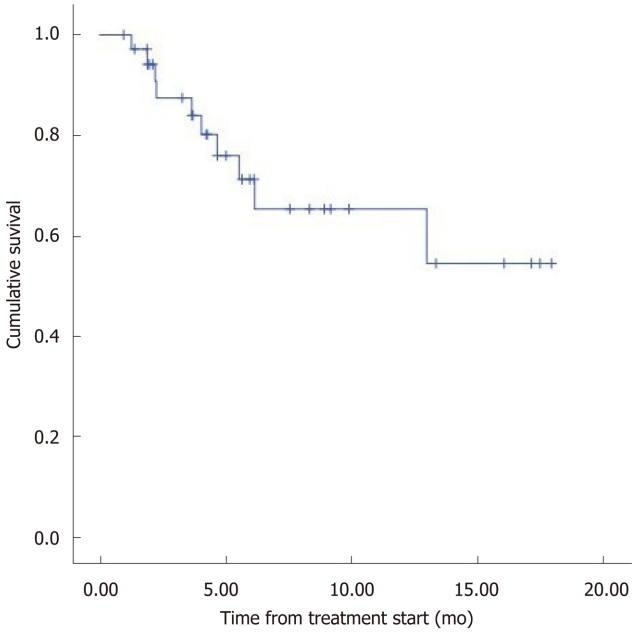

Figure 1 Graphical representation of overall survival in patients diagnosed with neuroendocrine tumors treated with peptide receptor radionuclide therapy. A median survival of 12.5 mo is shown (95% confidence interval: 9.8–15.2).

In this study, 44.4% of the patients presented toxicity to previous treatments before PRRT, of which 36.1% were due to everolimus and 8.3% to chemotherapy. Toxicity grade 1-2 was present in 71.4% of patients, and grade 3-4 was present in 28.6% of patients

During PRRT, acute adverse effects (< 24 h) were more frequent after the administration of the first dose, which manifested in 33.3% of the patients with sickness (25%), abdominal discomfort or pain (2.8%) and extravasation (2.8%). A hormone-related crisis in one patient resulted in hospitalization within 5 d after the administration dose. All recovered after adequate care.

During treatment, 55.6% of the patients suffered complications or toxicity. Hematological toxicity was present in 38.8% with one case being severe (CTCAE v.4 o v.5.)[8] with thrombocytopenia. Four patients (11.1%) suffered intestinal suboclusion in which only one had to be surgically operated, and three patients (8%) presented with cholestasis that corrected spontaneously. One patient with extensive liver metastasis presented with serious delayed liver toxicity. Liver functions deteriorated in the weeks following the first administration, and the patient died of hepatic failure 5 wk later.

DISCUSSION

In this study, the median OS obtained was 12.5 mo after 3 years of follow-up, and death presented in 21.8% of patients. Thomas *et al*[9] in a retrospective review with 273 patients diagnosed with advanced gastrointestinal NET for a similar period of time (41 mo) recorded 28% mortality during follow-up.

In this cohort of patients, OS was inversely proportional with respect to toxicity in previous treatments ($P < 0.05$) tumor grade and the presence of bone lesions, while it was directly proportional to matching lesion findings between Octreoscan and CT pre-PRRT ($P < 0.01$) and surgery of the primary tumor or its metastasis. These findings are confirmed by conducting a multivariate Cox regression analysis. A high Ki67 index ($P = 0.003$), a mismatch in lesion findings between Octreoscan and CT pre-PRRT ($P < 0.01$) and toxicity in previous treatments ($P < 0.05$) were risk factors to OS. Other contributing factors to OS were tumor grade and the presence of bone lesions. It is increasingly recognized that Ki-67 index and tumor grade are powerful determinants of survival. A study with 74 patients demonstrated the favorable response and long-term outcome of patients with G1/G2 gastroenteropancreatic NET after PRRT being the most powerful predictive factor in OS[10].

Regarding BM, there is little published data on the general prognostic impact of bone metastasis in NET in the context of PRRT, but it is well known that this outcome

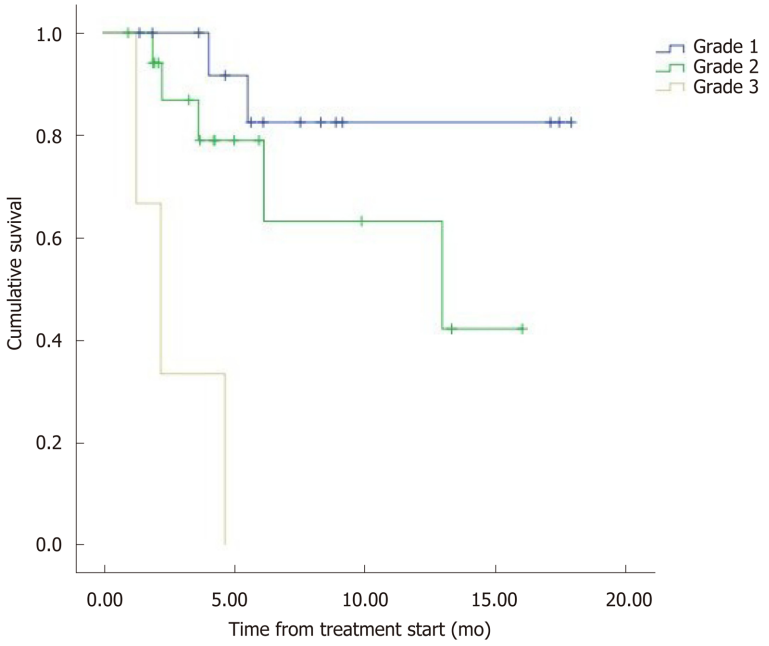

Figure 2 Representation of cumulative survival in the population studied according to the histological tumor grade. Grade 1 (blue), grade 2 (green) and grade 3 (gray) demonstrating that overall survival is inversely proportional to tumor grade.

is associated with pain and eventual decrease of bone marrow function[11]. It is difficult to evaluate the direct prognostic impact of BM in NET due to the incidence and the heterogeneity of these tumors as well as the frequent coexistence of multiple distant metastases. To the best of our knowledge, only retrospective studies and one systematic review have analyzed this topic. In the study by Strosberg *et al*[12], evaluating 146 cases of metastatic midgut NETs, BM represented a negative prognostic factor because patients with BMs (n = 35) had a median survival of 32 mo (95%CI: 28–35 mo) and a 5-year survival rate of 20%.

On the other hand, OS was similar and independent to other factors, such as the location of the primary tumor and the administration of previous treatments with SSA or others. However, a larger number of patients is needed to determine an accurate relationship between these variables.

Most patients (72.2%) presented with matching lesions identified in the CT evaluation and Octreoscan® pre-PRRT, while 13.9% had more lesions in the CT that did not express somatostatin receptors in Octreoscan® and 13.9% presented metabolic lesions without anatomical correlation in CT. Matching lesions between Octreoscan and CT pre-PRRT had a proportional relationship to OS, representing a prognostic factor (P < 0.05). This may be due to all lesions visualized on the CT expressing somatostatin receptors. Therefore, a greater number of tumor cells would be treated by the radionuclide and would respond well to treatment. However, in the case of a wide cellular heterogeneity and having lesions in the CT that are not visualized in the Octreoscan®, the scope of the radiopharmaceutical would be limited to the lesions with positive receptors, leaving the rest of the tumor cells untreated. This is the first study to our knowledge to report this important outcome. This result may help to evaluate individual prognostic factors to OS as well as for the need to conduct a ^{18}F-FDG positron emission tomography/CT to predict treatment response in patients with cellular heterogeneity. In addition, they demonstrate the need for more research with a greater number of patients assessing the importance of this and other prognostic factors that are yet to be described in order to improve patient management.

Another important result in this study was an apparent radiological progression in 20 cases (55.6%) in the CT evaluation after the second dose manifested as an increase in the lesion's diameter. Despite this, due to a significant clinical improvement and symptom control, it was decided to complete the treatment. Disease control was reached after the last dose in all cases. This transient increase was probably due to inflammation causing localized edematous tissue at the site of the metastases and not based on progression. This radiogenic edema has been described previously as possible pitfalls by Brabander *et al*[13], in which the phenomenon was called pseudo-progression. These findings were previously described in brain tumors and external

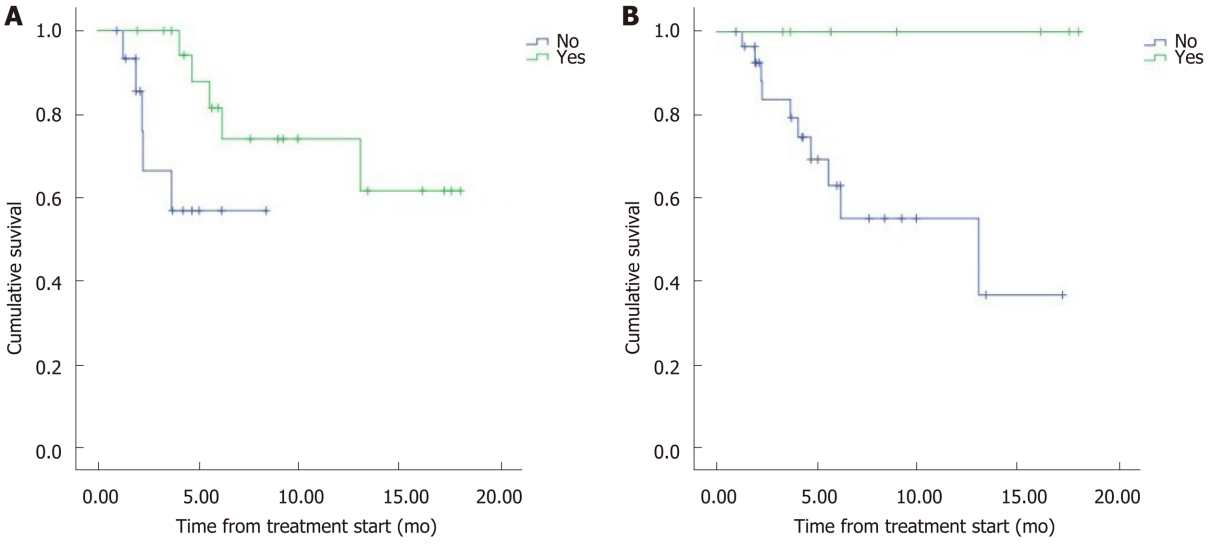

Figure 3 Representation of cumulative survival in patients treated with primary tumor surgery and metastases with peptide receptor radionuclide therapy (green) and patients treated only with peptide receptor radionuclide therapy (blue). A: For patients treated with primary tumor surgery, the probability of long-term survival is higher when treated with peptide receptor radionuclide therapy, showing the existence of a directly proportional relationship between survival and surgical treatment; B: The patients treated with metastases.

beam radiation, in cytokine studies, in monoclonal antibodies and in immunotherapy, where the increase in tumor size was probably related to infusion of lymphocytes and macrophages and was not always considered as disease progression. Therefore, in NET patients, clinicians should be aware and take into account in daily practice that an increase in tumor size is frequent due to radiation-induced inflammation and not always refers to tumor progression[13].

Currently, the only available curative treatment for NET is surgery, but for those patients who have an inoperable primary tumor, recurrent disease or metastatic disease, few therapeutic options are available. PRRT is commonly noncurative in patients diagnosed with NETs. Therefore, this systemic treatment should be focused on improving patient quality of life. Our results demonstrate an improvement in quality of life in 75% of our patients, better pain assessment in 41.7% and a better control of hormonal related symptoms in 66.6%, reaching full control at the end of the treatment in 26.6% of the population. Also, 41.6% of our patients were asymptomatic after the fourth dose. These results also prove the need for more research with a greater number of patients in assessing adverse events and effects on quality of life for NET therapies[14].

The NETTER-1 study showed a significant quality-of-life benefit for patients with midgut NETs who received ^{177}Lu-DOTATATE *vs* those treated with high dose long-acting octreotide specifically for diarrhea, flushing and abdominal pain[15,16]. Likewise, Tellestar is a Phase III, multicenter, randomized, double-blind, placebo-controlled study in which clinical outcomes were assessed. The study suggested a sustained improvement in bowel movement frequency in patients with carcinoid syndrome and a long-term effect on patient´s well-being[17]. Additionally, Martini *et al*[18] studied the impact of health-related quality of life (HRQoL) from the first PRRT to the first restaging and compared the scores with general population norms. They observed improvements from baseline to the first restaging for diarrhea in small-intestine NET patients and a clinically relevant decrease in appetite loss (for female small-intestine NET patients only). Compared with HRQoL general population norms, patients had impairments consisting of diarrhea, fatigue, appetite loss, reduced physical, social, and role functioning and reduced global HRQoL. In conclusion their findings supported overall stable HRQoL under PRRT. However, significant HRQoL impairments compared with the general population and potentially specific subgroup patterns need to be considered.

Side effects in our group were either related to the administration of the amino acids or due to the radio-peptide itself[19,20]. During the follow-up, half of the patients suffered some kind of complication or toxicity, in order of frequency: Nausea, discomfort or abdominal pain and a carcinoid crisis triggered by the massive release of bioactive substances. Similarly, the evaluation of toxicity in a group of 504 patients who were given four cycles of treatment at intervals of 6 to 10 wk revealed that the most common symptoms in the first 24 h were nausea (25%), vomiting (10%) and pain

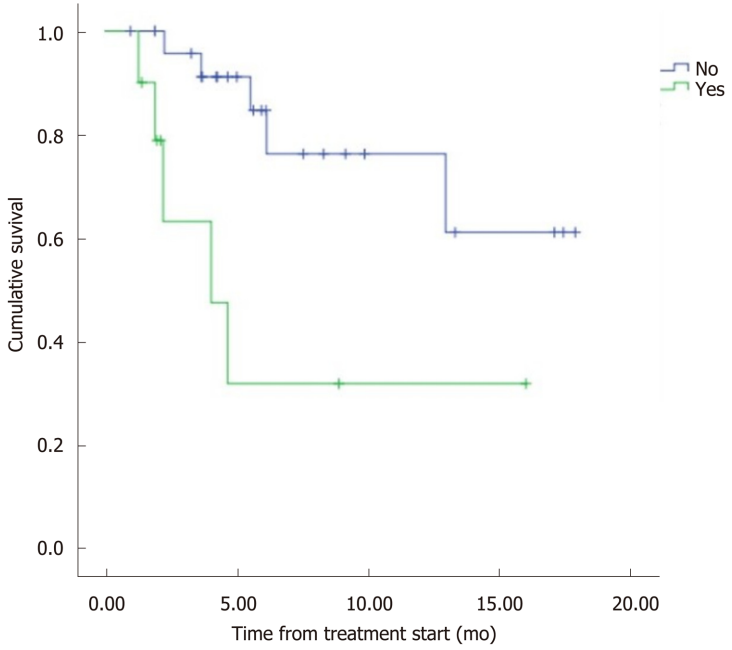

Figure 4 Representation of cumulative survival in patients with (green) and without (blue) bone metastasis. The probability of long-term survival is higher in the second group.

(10%)[21]. In a similar study, carried out in 479 patients, it was determined that only 1% with hormonally active neuroendocrine tumors had a clinical crisis after administration[22].

The development of hematological toxicity was found in almost half of the patients (38.8%), being severe (grade 3) in one case (2.8%) with thrombocytopenia. A recent study conducted with 450 patients treated with PRRT in five different centers stipulated that serious adverse events were rare with leukopenia and thrombocytopenia of grade 3 in 1.1% and 1.3% of patients respectively, and only one episode of grade 4 thrombocytopenia[23,24].

The most serious side effect in our study was observed in one patient with extensive liver metastasis who developed a severe deterioration of liver function. In patients with or without mild metastatic hepatic involvement, no significant liver toxicity has been reported. However, in patients with massive liver metastases and impaired hepatic function, hepatic toxicity may occur. This should be considered, along with pre-existing conditions affecting the liver, when deciding the appropriate dose[20].

Study limitations

This study has limitations. First, it is a retrospective observational study. The aim is to observe and describe and lacks an intervention in the natural course of patients. Therefore, one or more variables of interest could not be studied. As well, we are aware that the number of patients is scarce and limited, but this is the first study to our knowledge to describe that matching lesions in CT and Octreoscan® previous to PRRT treatment could be a prognostic factor that should be studied with a larger cohort of patients. If corroborated, this finding could be considered into treatment decisions and may result in major patient surveillance.

In this study we found that matching lesions in CT and Octreoscan® pre-PRRT, represent a prognostic factor to overall survival and that pseudo-progression is a common finding observed in the first stages of the treatment that should be taken into consideration by clinicians in daily practice.

ARTICLE HIGHLIGHTS

Research background

The incidence and prevalence of neuroendocrine tumors are currently increasing, probably due to the extensive use of more developed routine radiological tests and endoscopic techniques. In patients with limited cytoreductive options, peptide receptor radionuclide therapy (PRRT) with radiolabeled somatostatin analogues ^{177}Lu-DOTA0-Tyr3-octreotate (^{177}Lu-Dotatate) has been used successfully in patients diagnosed with metastatic gastroenteropancreatic somatostatin

receptor positive tumors in the past two decades.

Research motivation
The aim of this study was to determine the impact of this treatment on patient's quality of life, radiological and metabolic response, overall survival, prognostic factors and its toxicity.

Research objectives
The determination of prognostic factors that can modify the overall survival of these patients is of vital importance because it could allow a more specialized therapy and increase patient's surveillance when required. This might be an interesting approach in future research.

Research methods
This is a retrospective longitudinal observational study in which impact on quality of life, radiological and metabolic response, overall survival, prognostic factors and toxicity were evaluated in patients diagnosed with advanced tumors expressing somatostatin receptors treated with PRRT. The information pertinent to this cohort of patients was collected through the clinical history, obtaining information about clinical data, treatment response and disease state. These data were treated confidentially and in an encrypted form for analysis. Written consent was obtained from all patients.

Research results
In this cohort of patients, overall survival was inversely proportional with respect to toxicity in previous treatments ($P < 0.05$), tumor grade and the presence of bone lesions and was directly proportional to matching lesion findings between Octreoscan and computed tomography (CT) pre-PRRT ($P < 0.01$) andsurgery of the primary tumor or its metastasis. Also, we found that pseudo-progression is a common finding observed in the first stages of the treatment that should be taken into consideration by clinicians in daily practice. We consider that the matching lesions in CT and Octreoscan® before PRRT treatment could be a prognostic factor and should be studied with a greater cohort of patients. If corroborated, this finding could be considered in treatment decisions and may result in major patient surveillance.

Research conclusions
Overall survival was inversely proportional with respect to toxicity in previous treatments ($P < 0.05$) and was directly proportional to matching lesion findings between Octreoscan and CT pre-PRRT. Matching lesion findings between Octreoscan and CT pre-PRRT should be taken into consideration when treating these patients.

Research perspectives
This study reveals that prognostic factors should be taken into consideration because they modify the overall survival. Therefore, future research should focus on finding new prognostic factors that could allow specialized patient surveillance. In future studies, a larger number of patients should be included to extract more conclusive results that would allow the identification of new prognostic factors.

REFERENCES

1 **Fernández-Rañada Shaw I**, Arévalo MG, Martel IJ, Giménez DM, Valadés JIM, Martínez JM, Gárate CO, Salas NR, Sánchez JS. Guía Clínica de diagnóstico y tratamiento de Tumores Neuroendocrinos. OncoSur: Grupo de trabajo oncológico de centros hospitalarios del sur de Madrid 2011. Available from: https://cn.bing.com/search?q=Gu%C3%ADa+Cl%C3%ADnica+de+diagn%C3%B3stico+y+tratamiento+de+Tumores+Neuroendocrinos+2011&qs=n&form=QBRE&sp=-1&pq=&sc=8-0&sk=&cvid=DAC32997F9B64DFDBB72937861673A69

2 **Yao JC**, Hassan M, Phan A, Dagohoy C, Leary C, Mares JE, Abdalla EK, Fleming JB, Vauthey JN, Rashid A, Evans DB. One hundred years after "carcinoid": epidemiology of and prognostic factors for neuroendocrine tumors in 35,825 cases in the United States. *J Clin Oncol* 2008; **26**: 3063-3072 [PMID: 18565894 DOI: 10.1200/JCO.2007.15.4377]

3 **Garcia-Carbonero R**, Capdevila J, Crespo-Herrero G, Díaz-Pérez JA, Martínez Del Prado MP, Alonso Orduña V, Sevilla-García I, Villabona-Artero C, Beguiristain-Gómez A, Llanos-Muñoz M, Marazuela M, Alvarez-Escola C, Castellano D, Vilar E, Jiménez-Fonseca P, Teulé A, Sastre-Valera J, Benavent-Viñuelas M, Monleon A, Salazar R. Incidence, patterns of care and prognostic factors for outcome of gastroenteropancreatic neuroendocrine tumors (GEP-NETs): results from the National Cancer Registry of Spain (RGETNE). *Ann Oncol* 2010; **21**: 1794-1803 [PMID: 20139156 DOI: 10.1093/annonc/mdq022]

4 **Johnbeck CB**, Knigge U, Kjær A. PET tracers for somatostatin receptor imaging of neuroendocrine tumors: current status and review of the literature. *Future Oncol* 2014; **10**: 2259-2277 [PMID: 25471038 DOI: 10.2217/fon.14.139]

5 **Maxwell JE**, Howe JR. Imaging in neuroendocrine tumors: an update for the clinician. *Int J Endocr Oncol* 2015; **2**: 159-168 [PMID: 26257863 DOI: 10.2217/ije.14.40]

6 **Kendi AT**, Halfdanarson TR, Packard A, Dundar A, Subramaniam RM. Therapy With ^{177}Lu-DOTATATE: Clinical Implementation and Impact on Care of Patients With Neuroendocrine Tumors. *AJR Am J Roentgenol* 2019; **213**: 309-317 [PMID: 31039017 DOI: 10.2214/AJR.19.21123]

7 **Sanitarios agencia española de medicamentos**. Informe de Posicionamiento Terapéutico de lutecio (177Lu) oxodotreotida (Lutathera®) en el tratamiento de tumores neuroendocrinos gastroenteropancreáticos bien diferenciados. Informe De Posicionamiento Terapéutico. Madrid: Ministerio de Sanidad 2019. Available from: https://cn.bing.com/search?q=Informe+de+Posicionamiento+Terap%C3%A9utico+de+lutecio+%28177Lu

%29+oxodotreotida+%28Lutathera%C2%AE%29+en+el+tratamiento+de+tumores+neuroendocrinos+gastroenteropancre%C3%A1ticos+bien+diferenciados.&qs=n&form=QBLHCN&sp=-1&pq=&sc=8-0&sk=&cvid=78C09BCDE4C640F7B34FC5F3FD2A8138

8 **Cancer Therapy Evaluation Program**. Common Terminology Criteria for Adverse Events, Version 3.0, Department of Health and Human Services US 2006. Available from: http://ctep.cancer.gov

9 **Thomas KEH**, Voros BA, Boudreaux JP, Thiagarajan R, Woltering EA, Ramirez RA. Current Treatment Options in Gastroenteropancreatic Neuroendocrine Carcinoma. *Oncologist* 2019; **24**: 1076-1088 [PMID: 30635447 DOI: 10.1634/theoncologist.2018-0604]

10 **Ezziddin S**, Attassi M, Yong-Hing CJ, Ahmadzadehfar H, Willinek W, Grünwald F, Guhlke S, Biersack HJ, Sabet A. Predictors of long-term outcome in patients with well-differentiated gastroenteropancreatic neuroendocrine tumors after peptide receptor radionuclide therapy with 177Lu-octreotate. *J Nucl Med* 2014; **55**: 183-190 [PMID: 24434296 DOI: 10.2967/jnumed.113.125336]

11 **Ezziddin S**, Sabet A, Heinemann F, Yong-Hing CJ, Ahmadzadehfar H, Guhlke S, Höller T, Willinek W, Boy C, Biersack HJ. Response and long-term control of bone metastases after peptide receptor radionuclide therapy with (177)Lu-octreotate. *J Nucl Med* 2011; **52**: 1197-1203 [PMID: 21764798 DOI: 10.2967/jnumed.111.090373]

12 **Strosberg J**, Gardner N, Kvols, L. Survival and prognostic factor analysis of 146 metastatic neuroendocrine tumors of the mid-gut. *Neuroendocrinology* 2009; **89**: 471–476 [PMID: 19174605 DOI: 10.1159/000197899]

13 **Brabander T**, van der Zwan WA, Teunissen JJM, Kam BLR, de Herder WW, Feelders RA, Krenning EP, Kwekkeboom DJ. Pitfalls in the response evaluation after peptide receptor radionuclide therapy with [^{177}Lu-DOTA^{0},Tyr^{3}]octreotate. *Endocr Relat Cancer* 2017; **24**: 243-251 [PMID: 28320783 DOI: 10.1530/ERC-16-0524]

14 **Kaderli RM**, Spanjol M, Kollár A, Bütikofer L, Gloy V, Dumont RA, Seiler CA, Christ ER, Radojewski P, Briel M, Walter MA. Therapeutic Options for Neuroendocrine Tumors: A Systematic Review and Network Meta-analysis. *JAMA Oncol* 2019; **5**: 480-489 [PMID: 30763436 DOI: 10.1001/jamaoncol.2018.6720]

15 **Dash A**, Chakraborty S, Pillai MR, Knapp FF. Peptide receptor radionuclide therapy: an overview. *Cancer Biother Radiopharm* 2015; **30**: 47-71 [PMID: 25710506 DOI: 10.1089/cbr.2014.1741]

16 **Strosberg J**, El-Haddad G, Wolin E, Hendifar A, Yao J, Chasen B, Mittra E, Kunz PL, Kulke MH, Jacene H, Bushnell D, O'Dorisio TM, Baum RP, Kulkarni HR, Caplin M, Lebtahi R, Hobday T, Delpassand E, Van Cutsem E, Benson A, Srirajaskanthan R, Pavel M, Mora J, Berlin J, Grande E, Reed N, Seregni E, Öberg K, Lopera Sierra M, Santoro P, Thevenet T, Erion JL, Ruszniewski P, Kwekkeboom D, Krenning E; NETTER-1 Trial Investigators. Phase 3 Trial of ^{177}Lu-Dotatate for Midgut Neuroendocrine Tumors. *N Engl J Med* 2017; **376**: 125-135 [PMID: 28076709 DOI: 10.1056/NEJMoa1607427]

17 **Cella D**, Beaumont JL, Hudgens S, Marteau F, Feuilly M, Houchard A, Lapuerta P, Ramage J, Pavel M, Hörsch D, Kulke MH. Relationship Between Symptoms and Health-related Quality-of-life Benefits in Patients With Carcinoid Syndrome: Post Hoc Analyses From TELESTAR. *Clin Ther* 2018; **40**: 2006-2020.e2 [PMID: 30477789 DOI: 10.1016/j.clinthera.2018.10.008]

18 **Martini C**, Buxbaum S, Rodrigues M, Nilica B, Scarpa L, Holzner B, Virgolini I, Gamper EM. Quality of Life in Patients with Metastatic Gastroenteropancreatic Neuroendocrine Tumors Receiving Peptide Receptor Radionuclide Therapy: Information from a Monitoring Program in Clinical Routine. *J Nucl Med* 2018; **59**: 1566-1573 [PMID: 30042164 DOI: 10.2967/jnumed.117.204834]

19 **Maqsood MH**, Tameez Ud Din A, Khan AH. Neuroendocrine Tumor Therapy with Lutetium-177: A Literature Review. *Cureus* 2019; **11**: e3986 [PMID: 30972265 DOI: 10.7759/cureus.3986]

20 **Bodei L**, Mueller-Brand J, Baum RP, Pavel ME, Hörsch D, O'Dorisio MS, O'Dorisio TM, Howe JR, Cremonesi M, Kwekkeboom DJ, Zaknun JJ. The joint IAEA, EANM, and SNMMI practical guidance on peptide receptor radionuclide therapy (PRRNT) in neuroendocrine tumours. *Eur J Nucl Med Mol Imaging* 2013; **40**: 800-816 [PMID: 23389427 DOI: 10.1007/s00259-012-2330-6]

21 **Kwekkeboom DJ**, de Herder WW, Kam BL, van Eijck CH, van Essen M, Kooij PP, Feelders RA, van Aken MO, Krenning EP. Treatment with the radiolabeled somatostatin analog [177 Lu-DOTA 0,Tyr3]octreotate: toxicity, efficacy, and survival. *J Clin Oncol* 2008; **26**: 2124-2130 [PMID: 18445841 DOI: 10.1200/JCO.2007.15.2553]

22 **de Keizer B**, van Aken MO, Feelders RA, de Herder WW, Kam BL, van Essen M, Krenning EP, Kwekkeboom DJ. Hormonal crises following receptor radionuclide therapy with the radiolabeled somatostatin analogue [177Lu-DOTA0,Tyr3]octreotate. *Eur J Nucl Med Mol Imaging* 2008; **35**: 749-755 [PMID: 18210106 DOI: 10.1007/s00259-007-0691-z]

23 **Hicks RJ**, Kwekkeboom DJ, Krenning E, Bodei L, Grozinsky-Glasberg S, Arnold R, Borbath I, Cwikla J, Toumpanakis C, Kaltsas G, Davies P, Hörsch D, Tiensuu Janson E, Ramage J; Antibes Consensus Conference participants. ENETS Consensus Guidelines for the Standards of Care in Neuroendocrine Neoplasia: Peptide Receptor Radionuclide Therapy with Radiolabeled Somatostatin Analogues. *Neuroendocrinology* 2017; **105**: 295-309 [PMID: 28402980 DOI: 10.1159/000475526]

24 **Hörsch D**, Ezziddin S, Haug A, Gratz KF, Dunkelmann S, Miederer M, Schreckenberger M, Krause BJ, Bengel FM, Bartenstein P, Biersack HJ, Pöpperl G, Baum RP. Effectiveness and side-effects of peptide receptor radionuclide therapy for neuroendocrine neoplasms in Germany: A multi-institutional registry study with prospective follow-up. *Eur J Cancer* 2016; **58**: 41-51 [PMID: 26943056 DOI: 10.1016/j.ejca.2016.01.009]

World Journal of Gastroenterology

Submit a Manuscript: https://www.f6publishing.com

World J Gastroenterol 2020 April 7; 26(13): 1525-1539

DOI: 10.3748/wjg.v26.i13.1525

ISSN 1007-9327 (print) ISSN 2219-2840 (online)

ORIGINAL ARTICLE

Observational Study

Add-on pegylated interferon augments hepatitis B surface antigen clearance *vs* continuous nucleos(t)ide analog monotherapy in Chinese patients with chronic hepatitis B and hepatitis B surface antigen ≤ 1500 IU/mL: An observational study

Feng-Ping Wu, Ying Yang, Mei Li, Yi-Xin Liu, Ya-Ping Li, Wen-Jun Wang, Juan-Juan Shi, Xin Zhang, Xiao-Li Jia, Shuang-Suo Dang

ORCID number: Feng-Ping Wu (0000-0002-4572-3873); Ying Yang (0000-0002-8718-0993); Mei Li (0000-0001-6295-4270); Yi-Xin Liu (0000-0002-3976-8469); Ya-Ping Li (0000-0002-0900-5559); Wen-Jun Wang (0000-0001-9861-1763); Juan-Juan Shi (0000-0002-5626-9821); Xin Zhang (0000-0002-5966-0471); Xiao-Li Jia (0000-0001-8865-9771); Shuang-Suo Dang (0000-0003-0918-9535).

Author contributions: Dang SS participated in study conception and design, study supervision, data interpretation, manuscript editing and funding support; Wu FP conceived and designed the study, collected data, drafted the manuscript, planned the study, analyzed and interpreted data and performed statistical analysis; Yang Y, Li M, Liu YX and Li YP participated in analysis and interpretation of clinical data and consultations in liver disease; Wang WJ and Shi JJ participated in data collection, statistical analysis and drafted the manuscript; Zhang X and Xiao-li Jia XL participated in critical revision of the manuscript, consultations and funding support.

Supported by the National Natural Science Foundation of China, No. 31500650.

Institutional review board statement: This study was approved by the Institutional

Feng-Ping Wu, Ying Yang, Mei Li, Yi-Xin Liu, Ya-Ping Li, Wen-Jun Wang, Juan-Juan Shi, Xin Zhang, Xiao-Li Jia, Shuang-Suo Dang, Department of Infectious Diseases, the Second Affiliated Hospital of Xi'an Jiaotong University, Xi'an 710004, Shaanxi Province, China

Corresponding author: Shuang-Suo Dang, MD, PhD, Academic Fellow, Academic Research, Doctor, Professor, Department of Infectious Diseases, the Second Affiliated Hospital of Xi'an Jiaotong University, No. 157 Xiwu Road, Xi'an 710004, Shaanxi Province, China. dang212@126.com

Abstract

BACKGROUND

Nucleos(t)ide analog (NA) has shown limited effectiveness against hepatitis B surface antigen (HBsAg) clearance in chronic hepatitis B (CHB) patients.

AIM

To evaluate the efficacy and safety of add-on peginterferon α-2a (peg-IFN α-2a) to an ongoing NA regimen in CHB patients.

METHODS

In this observational study, 195 CHB patients with HBsAg ≤ 1500 IU/mL, hepatitis B e antigen (HBeAg)-negative (including HBeAg-negative patients or HBeAg-positive patients who achieved HBeAg-negative after antiviral treatment with NA) and hepatitis B virus-deoxyribonucleic acid < 1.0×10^2 IU/mL after over 1 year of NA therapy were enrolled between November 2015 and December 2018 at the Second Affiliated Hospital of Xi'an Jiaotong University, China. Patients were given the choice between receiving either peg-IFN α-2a add-on therapy to an ongoing NA regimen (add-on group, n = 91) or continuous NA monotherapy (monotherapy group, n = 104) after being informed of the benefits and risks of the peg-IFN α-2a therapy. Total therapy duration of peg-IFN α-2a was 48 wk. All patients were followed-up to week 72 (24 wk after discontinuation of peg-IFN α-2a). The primary endpoint was the proportion of patients with HBsAg clearance at week 72.

RESULTS

Review Board of Xi'an Jiaotong University.

Informed consent statement: All study participants, or their legal guardian, provided written informed consent prior to study enrollment.

Conflict-of-interest statement: The authors do not have any conflict of interest to disclose.

Data sharing statement: No additional data are available.

STROBE statement: The authors have read the STROBE Statement-checklist of items and the manuscript was prepared and revised accordingly.

Manuscript source: Unsolicited manuscript

Received: December 9, 2019
Peer-review started: December 9, 2019
First decision: December 30, 2019
Revised: January 9, 2020
Accepted: March 9, 2020
Article in press: March 9, 2020
Published online: April 7, 2020

P-Reviewer: Fallatah H, Tanwar S, Yeoh SW
S-Editor: Dou Y
L-Editor: Filipodia
E-Editor: Ma YJ

Demographic and baseline characteristics were comparable between the two groups. Intention-to-treatment analysis showed that the HBsAg clearance rate in the add-on group and monotherapy group was 37.4% (34/91) and 1.9% (2/104) at week 72, respectively. The HBsAg seroconversion rate in the add-on group was 29.7% (27/91) at week 72, and no patient in the monotherapy group achieved HBsAg seroconversion at week 72. The HBsAg clearance and seroconversion rates in the add-on group were significantly higher than in the monotherapy group at week 72 ($P < 0.001$). Younger patients, lower baseline HBsAg concentration, lower HBsAg concentrations at weeks 12 and 24, greater HBsAg decline from baseline to weeks 12 and 24 and the alanine aminotransferase ≥ 2 × upper limit of normal during the first 12 wk of therapy were strong predictors of HBsAg clearance in patients with peg-IFN α-2a add-on treatment. Regarding the safety of the treatment, 4.4% (4/91) of patients in the add-on group discontinued peg-IFN α-2a due to adverse events. No severe adverse events were noted.

CONCLUSION
Peg-IFN α-2a as an add-on therapy augments HBsAg clearance in HBeAg-negative CHB patients with HBsAg ≤ 1500 IU/mL after over 1 year of NA therapy.

Key words: Chronic hepatitis B; Peginterferon α-2a; Nucleos(t)ide analog; Hepatitis B surface antigen clearance; Hepatitis B surface antigen seroconversion; Add-on therapy

Core tip: Despite promising results with the combination therapy of Peg-interferon and nucleos(t)ide analog (NA), the best combination therapeutic strategy of Peg-interferon and NA to the treatment of chronic hepatitis B remains unclear. This prospective study was to evaluate the efficacy and safety of adding 48 wk of peginterferon α-2a treatment to an ongoing NA regime in chronic hepatitis B patients with hepatitis B surface antigen levels ≤ 1500 IU/mL, hepatitis B e antigen-negative and hepatitis B virus-deoxyribonucleic acid < 1.0×10^2 IU/mL after over 1 year of NA therapy.

Citation: Wu FP, Yang Y, Li M, Liu YX, Li YP, Wang WJ, Shi JJ, Zhang X, Jia XL, Dang SS. Add-on pegylated interferon augments hepatitis B surface antigen clearance *vs* continuous nucleos(t)ide analog monotherapy in Chinese patients with chronic hepatitis B and hepatitis B surface antigen ≤ 1500 IU/mL: An observational study. *World J Gastroenterol* 2020; 26(13): 1525-1539
URL: https://www.wjgnet.com/1007-9327/full/v26/i13/1525.htm
DOI: https://dx.doi.org/10.3748/wjg.v26.i13.1525

INTRODUCTION

Chronic hepatitis B virus (HBV) infection remains a major public health challenge. Approximately 2 billion persons are infected by HBV globally. Up to 240 million persons are chronic HBV surface antigen (HBsAg) carriers, and they contribute to approximately 30% of liver cirrhosis cases and 45% of hepatocellular carcinoma (HCC) cases in the world[1]. Antiviral therapy for chronic hepatitis B (CHB) patients is a key strategy to prevent the progression of CHB.

Currently, the approved therapeutic options for CHB patients include nucleos(t)ide analog (NA) and peginterferon alfa (peg-IFN α). Antiviral therapy may achieve HBsAg clearance or seroconversion in a small percentage of CHB patients. It is reported that the rate of HBsAg clearance is less than 5% after 5 years of entecavir (ETV) therapy[2] and less than 7% after 1 year of peg-IFN α monotherapy[3,4]. Although the rate of HBsAg clearance is very low, it demonstrated that CHB is a disease that can be 'cured' through effective treatment, which may not completely clear HBV, but close to the status of complete eradication of HBV, including covalently closed circular deoxyribonucleic acid[5].

The Guideline of Prevention and Treatment for Chronic Hepatitis B (2015 Update, China) firstly proposed a concept of "clinical cure" or "functional cure," which is the

optimal therapeutic endpoint of CHB and the ultimate indicator of immune control of HBV infection[6-9]. Meanwhile, the 2015 updated Asian-Pacific clinical practice guidelines on the management of hepatitis B affirmed the "clinical cure" of CHB[10]. Therefore, new therapeutic strategies for boosting HBsAg clearance in CHB patients are required. Several studies have investigated new treatment strategies involving various combined approaches with NA and peg-IFN α and reported encouraging HBsAg clearance rates from 8.5% to 33.3%[11-13]. The findings from these studies and some uncontrolled small studies also showed that peg-IFN α-based treatment was associated with a higher rate of HBsAg clearance in patients with low baseline levels of HBsAg and HBV DNA[14,15]. Moreover, the interim analysis of NEW SWITCH study and another small study all showed that patients with lower HBsAg level at baseline (< 1500 IU/mL) achieved a higher HBsAg clearance rate than patients with HBsAg > 1500 IU/mL when they switched from NA to 48 wk of peg-IFN α-2α therapy[16,17].

Preliminary statistical analysis in our center indicates that 75.5% (3677/4870) of CHB patients received NA treatment, including lamivudine, adefovir dipivoxil (ADV), telbivudine, ETV, and tenofovir fumarate (TDF). In those patients with NA treatment, 37.7% (1386/3677) of patients were hepatitis B e antigen (HBeAg)-negative and HBsAg ≤ 1500 IU/mL after over 1 year of NA treatment (unpublished data). Based on these data, we estimate that approximately 5.69-8.53 million CHB patients in China are HBsAg ≤ 1500 IU/mL after over 1 year of NA treatment. Therefore, in this study, we aimed to evaluate the efficacy and safety of add-on peg-IFN α-2a in CHB patients who are receiving long-term NA treatment with HBsAg levels less and equal to 1500 IU/mL. In addition, logistic regression analysis was used to analyze independent prediction factors of HBsAg clearance in this population.

MATERIALS AND METHODS

Study subjects

This study was conducted at the Department of Infectious Diseases of the Second Affiliated Hospital, Xi'an Jiaotong University, Xi'an, China between November 2015 and December 2018. The study complies with good clinical practice and the Declaration of Helsinki and was approved by the Ethics Committee of the Second Affiliated Hospital of Xi'an Jiaotong University. All patients provided written consent before enrollment in the study. Inclusion criteria included: (1) Age between 18- and 65-years-old; (2) HBsAg positive for at least 6 mo prior to enrollment; (3) Serum HBsAg ≤ 1500 IU/mL, HBeAg-negative (including HBeAg-negative patients or HBeAg-positive patients who achieved HBeAg-negative after antiviral treatment with NA) and HBV DNA < 1.0×10^2 IU/mL after at least 1 year of NA therapy, including lamivudine, ADV, telbivudine, ETV, and TDF; (4) Alanine aminotransferase (ALT) concentration less than five times of the upper limit of normal (ULN) level (because of the risk of hepatic flare with interferon-based therapy); (5) White blood cell counts in a range of 4-10 × 10^9 /L, or platelet (PLT) counts in a range of 100-300 × 10^9/L; (6) No cirrhosis and splenomegaly in abdominal computed tomography; and (7) Naïve to interferon treatment. Exclusion criteria included: (1) co-infected with hepatitis A, C, D, or human immunodeficiency virus; (2) Decompensated liver diseases, alcohol or drug abuse, autoimmune diseases, severe metabolic diseases, HCC or tumors of any systems; (3) Severe complications in any organ; and (4) Pregnant or lactating women.

Study design

This study was a single center, prospective, observational study. After being informed of the benefits and risks of the peg-IFN α-2a therapy, patients were given the choice between receiving either 180 μg of peg-IFN α-2a (Pegasys; Roche, Shanghai, China) add-on therapy once weekly to an ongoing NA regimen (add-on group) or continuous NA monotherapy (monotherapy group). The dosage of peg-IFN α-2a was adjusted to 135 μg/wk if the neutrophil counts were ≤ 0.75 × 10^9/L or PLT < 50 × 10^9/L. Peg-IFN α-2a was discontinued if the neutrophil counts were ≤ 0.50 × 10^9/L, PLT < 25 × 10^9/L or serious adverse events (AEs) occurred. The total duration of peg-IFN α-2a add-on therapy was 48 wk. All groups were followed up to week 72 (24 wk after discontinuation of peg-IFN α-2a). Patients discontinued the NA therapy if HBsAg was negative at week 72. The primary endpoint was HBsAg clearance at week 72 and the secondary endpoints included the rate of HBsAg clearance at week 48, the rates of HBsAg seroconversion at weeks 48 and 72, HBsAg, ALT and aspartate aminotransferase (AST) dynamics over time and the safety during treatment.

Study assessments

Study assessments were based on the laboratory results, clinical and safety

evaluations. Laboratory results including white blood cell, PLT, ALT, AST, HBV DNA, HBsAg and anti-HBs antibody in serum samples were measured at baseline, weeks 4, 8, 12, 24, 36, 48 and 72 in all patients. Thyroid hormone, thyroid antibodies, and autoantibodies were tested at baseline and every 12 wk during treatment. Study assessments were described in the Supplementary Table 1. HBsAg and anti-HBs antibody were quantified using the commercially available reagent kits (Architect assay; Abbott Diagnostics) according to the manufacturer's instructions. The limit of detection for HBsAg was 0.05 IU/mL. Serum HBV DNA was detected using the TaqMan based real-time polymerase chain reaction assay (Shanghai ZJ BioTech, Shanghai, China) with the limit of detection of 100 IU/mL. HBsAg titer < 0.05 IU/mL indicated the loss of HBsAg; anti-HBs antibody level > 10 mIU/mL was defined as positive. Serum ALT was assayed by an automatic biochemical analyzer (Roche, Basel, Switzerland) and presented as multiples of the ULN (men: 50 IU/L; women: 40 IU/L). Clinical evaluation included family history of HBV, prior NA history, body mass index (BMI) and liver stiffness. Liver stiffness measurement was performed by transient elastography (FibroScan, EchoSens, Paris, France). All patients were asked about the family history of CHB. Patients with clear family history of CHB were considered as HBV vertical transmission. Those who declined to provide the family history of CHB were grouped as others. Safety assessment included headache, alopecia and pyrexia.

Statistical analysis

All patients enrolled in this study were included in the final efficacy analysis. All available AE data up to week 72 were included in the safety analysis for characterizing the full safety profile within the study. The analyses were performed using the Statistical Package for the Social Sciences (SPSS, version 13.0, Chicago, IL, United States). Data were expressed as mean ± standard deviation or median (range) for continuous variables as appropriate. Student's t or Mann-Whitney U test or analysis of variance for repeated measures design data was used for intergroup comparison of continuous variables as appropriate. Categorical variables were analyzed as counts and percentages and compared using χ^2 test or Fisher's exact test. The proportion of patients with HBsAg clearance and HBsAg seroconversion at weeks 48 and 72 was estimated using the Kaplan-Meier method. Data for patients without HBsAg clearance were censored at the last time point. Comparisons between groups were conducted using the log-rank test. ROC curves were applied to evaluate the parameters for predicting HBsAg clearance. Cut-off values were identified by maximizing the sum of sensitivity and specificity, and the nearest clinically applicable value to cut-off was considered optimal for clinical convenience. Univariate and multivariable logistic regression analyses were performed to evaluate the magnitude and significance of independent variables associated with the dependent variable. All statistical tests were two-sided and $P < 0.05$ was considered statistically significant.

RESULTS

Patient demographic and baseline characteristics

The flow chart of patient enrollment in this study is shown in Figure 1. Of the 1537 patients screened, 195 patients were enrolled, 91 (46.7%) of whom received peg-IFN α-2a add-on therapy as the add-on group and 104 (53.3%) of whom continued NA monotherapy as the monotherapy group. Patient demographic and baseline characteristics are shown in Table 1. The two groups were comparable in terms of the demographic and baseline characteristics.

Primary endpoint

At week 72, per protocol analysis (PP analysis) showed that 40.0% (34/85) of patients in the add-on group had HBsAg clearance compared with 2.1% (2/96) of patients in the monotherapy group. The HBsAg clearance rate in the add-on group was significantly higher than in the monotherapy group at week 72 (Figure 2A) ($P < 0.001$). Furthermore, we also did an intention-to-treatment analysis (ITT analysis), and the results showed that the HBsAg clearance rate was 37.4% (34/91) in the add-on group and 1.9% (2/104) in the monotherapy group at week 72. Similar to the PP analysis, the HBsAg clearance rate in the add-on group was significantly higher than that in the monotherapy group at week 72 (Figure 2B) ($P < 0.001$).

Secondary endpoints

HBsAg clearance rate at week 48: PP analysis showed that the HBsAg clearance rate in the add-on group was 28.2% (24/85) at week 48, significantly higher than 1.04% (1/96) in the monotherapy group (Figure 2A) ($P < 0.001$). ITT analysis also showed

Table 1 Demographic and baseline characteristics of the study population

Characteristics	Add-on, *n* = 91	Monotherapy, *n* = 104	*P* value
Male (%)	62 (68.1)	76 (73.1)	0.528
Age in yr, mean ± SD	38.11 ± 9.74	37.34 ± 11.01	0.529
BMI in kg/cm^2, mean ± SD	21.97 ± 1.72	22.13 ± 1.05	0.157
Mode of transmission			
Vertical (%)	36 (39.6)	32 (30.8)	0.229
Others (%)	55 (60.4)	72 (69.2)	
HBsAg at week 0			
< 500 IU/mL (%)	56 (61.5)	49 (47.1)	0.089
500-1000 IU/mL (%)	17 (18.7)	32 (30.8)	
1000-1500 IU/mL (%)	18 (19.8)	23 (22.1)	
HBeAg status at enrollment			
Negative (%)	91 (100)	104 (100)	_
HBV DNA at enrollment			
< 1.0 × 10^2 IU/ mL (%)	91 (100.0)	104 (100.0)	_
ALT, IU/L, median (range)	24 (8.0-73)	27 (7-66)	0.558
AST, IU/L, median (range)	23 (12-70)	26 (14-66)	0.212
NA			
ADV (%)	10 (11.0)	12 (11.5)	0.395
ETV (%)	50 (54.9)	66 (63.5)	
TDF (%)	31 (34.1)	26 (25.0)	
FibroScan value, kPa			
mean ± SD	4.2 ± 1.1	4.5 ± 1.2	0.824

SD: Standard deviation; BMI: Body mass index; HBsAg: Hepatitis B surface antigen; HBeAg: Hepatitis B e antigen; HBV DNA: Hepatitis B virus-deoxyribonucleic acid; NA: Nucleos(t)ide analog; ADV: Adefovir dipivoxil; ETV: Entecavir; TDF: Tenofovir disoproxil fumarate; ALT: Alanine aminotransferase; AST: Aspartate transaminase.

the HBsAg clearance rate was significantly higher in the add-on group than in the monotherapy group [26.4% (24/91) *vs* 0.96% (1/104), $P < 0.001$] (Figure 2B).

HBsAg seroconversion rates: PP analysis showed that the HBsAg seroconversion rate in the peg-IFN α-2a add-on group was 20.0% (17/85) at week 48 and 31.8% (27/85) at week 72. No patient in the monotherapy group achieved HBsAg seroconversion. The HBsAg seroconversion rate in the add-on group was significantly higher than those in the monotherapy group at weeks 48 and 72 (Figure 3A) ($P < 0.001$ for all). ITT analysis showed that the HBsAg seroconversion rate in the peg-IFN α-2a add-on group was 18.7% (17/91) at week 48 and 29.7% (27/91) at week 72. Consistent to the PP analysis, ITT analysis also showed the HBsAg seroconversion rate in the add-on group was significantly higher than those in the monotherapy group at weeks 48 and 72 (Figure 3B) ($P < 0.001$ for all).

HBsAg dynamics: In the peg-IFN α-2a add-on group, median serum HBsAg level declined from 2.56 $\log_{10}$ IU/mL at baseline to 1.08 $\log_{10}$ IU/mL after 48 wk of the treatment and to 1.23 $\log_{10}$ IU/mL at 72 wk. In the monotherapy group, median serum HBsAg level declined from 2.59 $\log_{10}$ IU/mL at baseline to 2.46 $\log_{10}$ IU/mL at 48 wk to 2.40 $\log_{10}$ IU/mL at 72 wk. Patients in the peg-IFN α-2a add-on group showed significantly lower median serum HBsAg levels at weeks 12, 24, 36, 48 and 72 than patients in the monotherapy group ($P < 0.001$ for all comparisons) (Figure 4A).

Interestingly, HBsAg elevations were observed at 4 wk after adding on peg-IFN α-2a in 57.1% (52/91) of patients in the peg-IFN α-2a add-on group, and HBsAg gradually decreased 4 wk later. Median serum HBsAg level increased from 2.77 $\log_{10}$ IU/mL at baseline to 2.87 $\log_{10}$ IU/mL after 4 wk of peg-IFN α-2a add-on therapy, gradually decreased to 2.76 $\log_{10}$ IU/mL at week 8, to 1.99 $\log_{10}$ IU/mL at week 48 and to 1.81 $\log_{10}$ IU/mL at week 72.

The HBsAg clearance rate of these 52 patients was 28.8% (15/52) at week 72, which was comparable with patients whose HBsAg decreased at four weeks after adding on peg-IFN α-2a [48.7% (19/39)] ($P = 0.079$), demonstrating that HBsAg elevations at 4 wk after adding on peg-IFN α-2a therapy had no influence on treatment outcome.

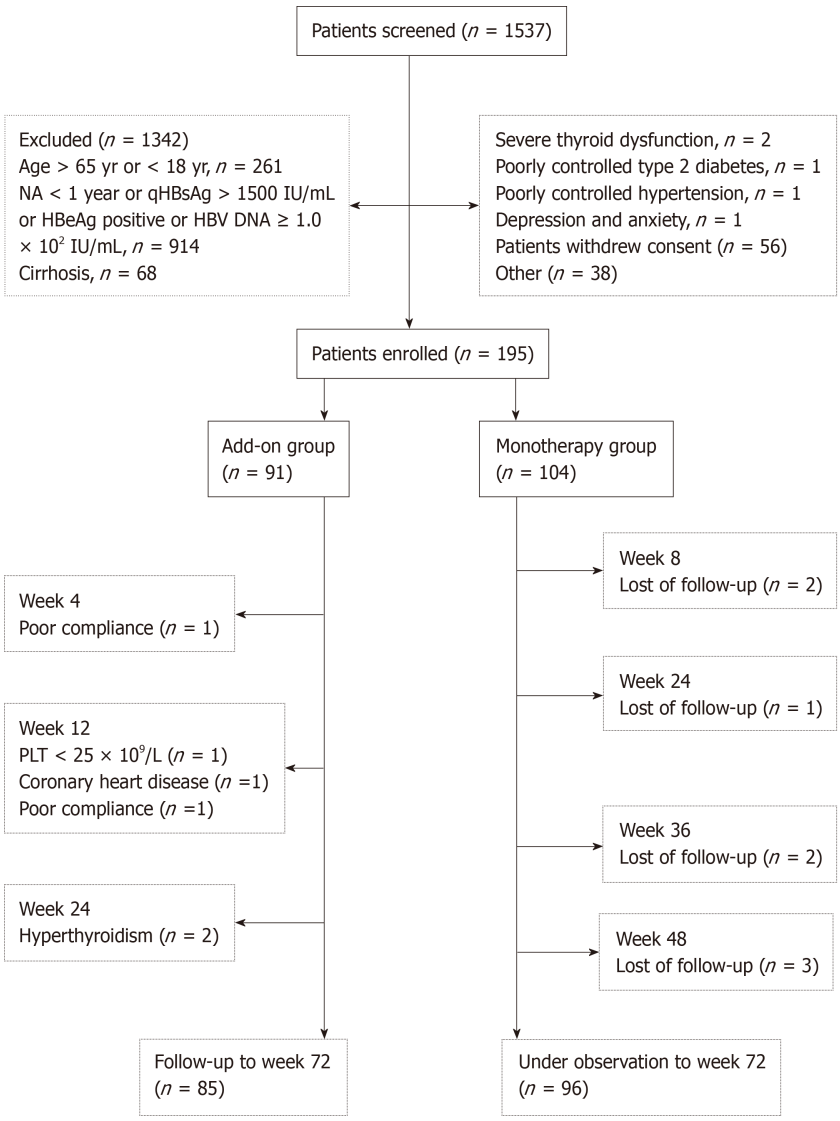

Figure 1 Flow diagram of patients enrolled in this study. HBsAg: Hepatitis B surface antigen; HBeAg: Hepatitis B e antigen; HBV DNA: Hepatitis B virus-deoxyribonucleic acid; NA: Nucleos(t)ide analog.

Furthermore, more patients in the add-on group had low levels of HBsAg at the end of follow-up than the monotherapy group. Most patients (97.8%, 89/91) in the add-on group demonstrated HBsAg levels < $3\log_{10}$ IU/mL (*vs* monotherapy group 82.7%, 86/104; $P = 0.001$). Moreover, 71.4% (65/91) of patients in the add-on group showed HBsAg levels < $2\log_{10}$ IU/mL (*vs* monotherapy group 35.6%, 37/104; $P < 0.001$). Meanwhile, 52.7% (48/91) of patients in the add-on group showed HBsAg levels < $1\log_{10}$ IU/mL (*vs* monotherapy group 10.6%, 11/104; $P < 0.001$) (Figure 4B).

ALT and AST dynamics: ALT and AST elevations were observed early (at 4 wk) after adding on peg-IFN α-2a in patients in the peg-IFN α-2a add-on group. Patients in peg-IFN α-2a add-on group had significantly higher serum ALT and AST levels at weeks 4, 8, 12, 24, 36 and 48 than patients in the monotherapy group ($P < 0.001$ for all time points). After discontinuation of peg-IFN α-2a at week 48, ALT and AST gradually returned to normal levels at week 72 (*vs* monotherapy group, $P = 0.52$ for ALT; $P = 0.099$ for AST (Figure 5A and 5B).

Predictors of HBsAg clearance in add-on peg-IFN α-2a treatment

Almost half [46.2% (42/91)] of the patients in the peg-IFN α-2a add-on group showed ALT ≥ 2 × ULN during the first 12 wk of therapy with a maximum of 414 IU/L. To evaluate the ALT change on HBsAg clearance, we dichotomized the patients into two groups (ALT ≥ 2 × ULN or < 2 × ULN) at week 12, and two groups of patients followed the same treatment. To evaluate the baseline characteristics [gender, age (years), baseline HBsAg level (in $\log_{10}$ scale, IU/mL), ALT (IU/L), mode of HBV transmission, body mass index (kg/cm²), FibroScan value (kPa), NA (nucleoside

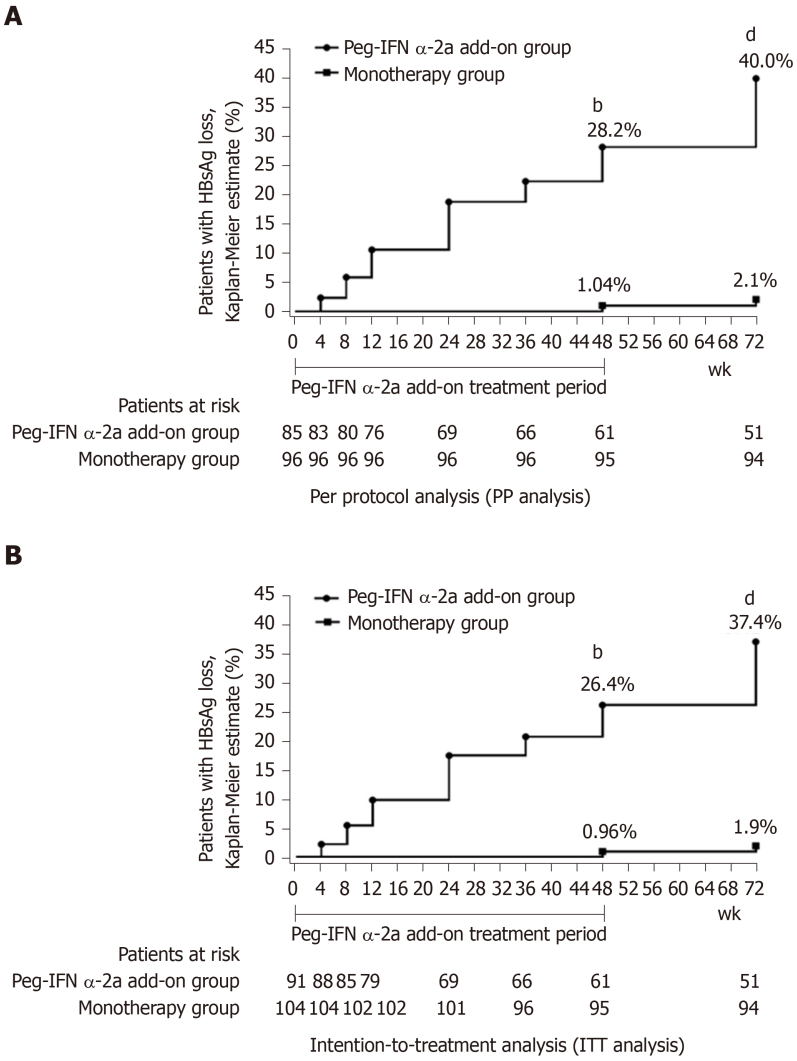

Figure 2 Hepatitis B surface antigen clearance rate. A: Per protocol analysis showed that the rate of hepatitis B surface antigen clearance in 48-wk peg-IFN add-on group was significantly higher than monotherapy group at weeks 48 and 72 ($^{b}P < 0.001$ *vs* monotherapy group at week 48; $^{d}P < 0.001$ *vs* monotherapy group at week 72). Week 0 was defined as the time when the patients were enrolled in this study for patients in the monotherapy group; B: Intention-to-treatment analysis showed that the rate of hepatitis B surface antigen clearance in 48-wk peg-IFN add-on group was significantly higher than the rate in the monotherapy group at weeks 48 and 72 ($^{b}P < 0.001$ *vs* monotherapy group at week 48; $^{d}P < 0.001$ *vs* monotherapy group at week 72). Week 0 was defined as the time when the patients were enrolled in this study for patients in the monotherapy group. HBsAg: Hepatitis B surface antigen.

analogue or nucleotide analog)] and on-treatment factors [HBsAg levels ($\log_{10}$ IU/mL) at weeks 12 and 24, HBsAg decline at weeks 12 and 24 *versus* baseline, and increase of ALT ≥ 2 × ULN during the first 12 wk of therapy] in predicting HBsAg clearance at week 72, univariable logistic regression analysis was performed. The results showed that age [$P = 0.002$, OR = 0.924; 95% confidence interval (CI): 0.878-0.972], baseline HBsAg level ($P = 0.003$, OR = 0.371; 95%CI: 0.194-0.711), HBsAg level at week 12 ($P < 0.001$, OR = 0.273, 95%CI: 0.157-0.474), HBsAg level at week 24 ($P < 0.001$, OR = 0.218, 95%CI: 0.117-0.405), HBsAg decline from baseline to week 12 ($P < 0.001$, OR = 10.646, 95%CI: 3.776-25.018), HBsAg decline from baseline to week 24 ($P < 0.001$, OR = 7.045, 95%CI: 3.223-15.400) and ALT elevation ≥ 2 × ULN during the first 12 wk of therapy ($P = 0.002$, OR = 4.182, 95%CI: 1.691-10.340) were strong predictors for HBsAg clearance at week 72. Baseline gender, ALT, mode of HBV transmission, body mass index, FibroScan value and NA (nucleoside analogue or nucleotide analog) were not statistically significant (Table 2).

In order to further evaluate age, baseline and decline of HBsAg in early treatment and ALT elevation in early treatment in predicting HBsAg clearance at week 72, multivariable logistic regressions were conducted for age, HBsAg levels at baseline, week 12, and week 24 as well as the week 12 and week 24 HBsAg decline from baseline adjusted for gender and NA. Similar to the univariable regression analysis

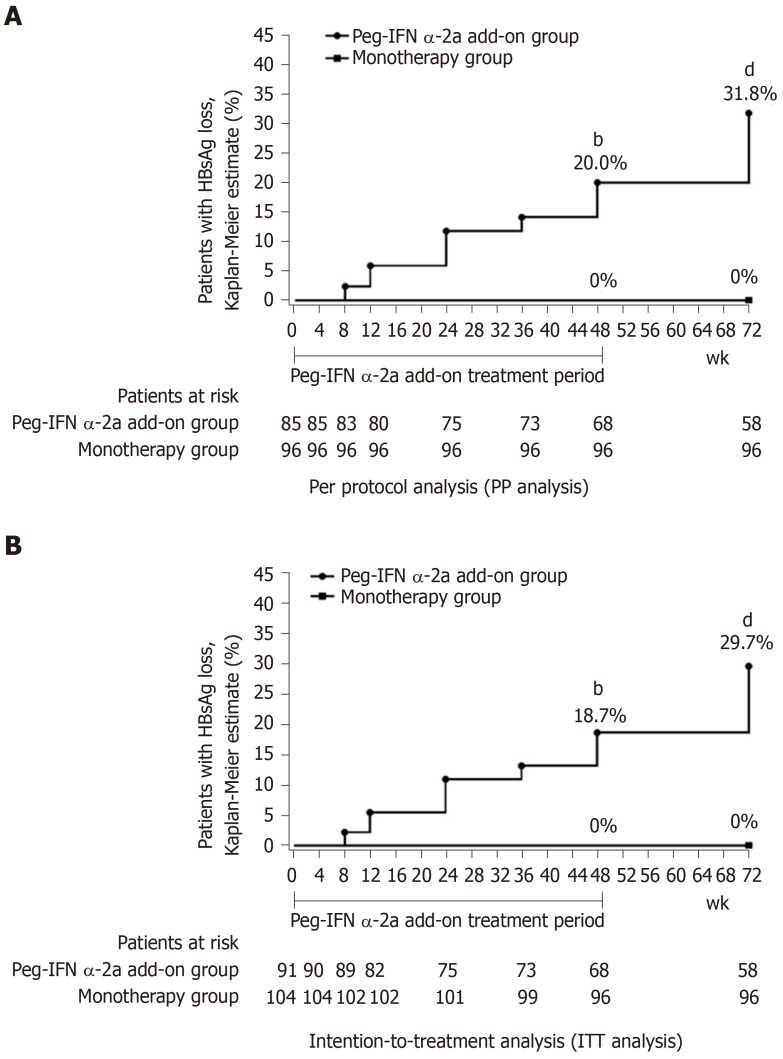

Figure 3 Hepatitis B surface antigen seroconversion rate. A: Per protocol analysis showed that the rate of hepatitis B surface antigen seroconversion in 48-wk peg-IFN add-on group was significantly higher than monotherapy group at weeks 48 and 72 ($^{b}P < 0.001$ *vs* monotherapy group at week 48; $^{d}P < 0.001$ *vs* monotherapy group at week 72). Week 0 was defined as the time when the patients were enrolled in this study for patients in the monotherapy group; B: Intention-to-treatment analysis showed that the rate of hepatitis B surface antigen seroconversion in 48-wk peg-IFN add-on group was significantly higher than rate in monotherapy group at weeks 48 and 72 ($^{b}P < 0.001$ *vs* monotherapy group at week 48; $^{d}P < 0.001$ *vs* monotherapy group at week 72). Week 0 was defined as the time when the patients were enrolled in this study for patients in the monotherapy group. HBsAg: Hepatitis B surface antigen.

results, all variables were significantly related to HBsAg clearance at week 72: age (P = 0.025, OR = 0.946; 95%CI: 0.833-0.981), baseline HBsAg level (P = 0.019, OR = 0.557; 95%CI: 0.206-0.827), HBsAg level at week 12 (P = 0.002, OR = 0.542, 95%CI: 0.194-0.792), HBsAg level at week 24 (P = 0.004, OR = 0.188, 95%CI: 0.058-0.410), HBsAg decline from baseline to week 12 (P < 0.001, OR = 8.925, 95%CI: 3.376-17.226), HBsAg decline from baseline to week 24 (P < 0.001, OR = 8.830, 95%CI: 4.553-18.213) and ALT elevation ≥ 2 × ULN during the first 12 wk of therapy (P = 0.014, OR = 5.275, 95%CI: 3.324-11.823) (Table 2).

Rates of HBsAg clearance among patients with favorable baseline, week 12, week 24 antiviral treatment response: ROC curves were used to evaluate the performance of the above significant variables for HBsAg clearance. The AUROC of age was 0.699, and the optimal cut-off point was 33 years. The AUROCs of HBsAg level were 0.689, 0.877, 0.921, and the optimal cut-off points were 2.25 $\log_{10}$ IU/mL for baseline, 1.89 $\log_{10}$ IU/mL for week 12 and 1.46 $\log_{10}$ IU/mL for week 24. The AUROCs of HBsAg decline from baseline to week 12 and week 24 were 0.901 and 0.924, respectively, and the optimal cut-off points were 0.5 $\log_{10}$ IU/mL and 1.0 $\log_{10}$ IU/mL, respectively (Table 3).

Based on the optimal cut-off values, our data showed that the rates of HBsAg

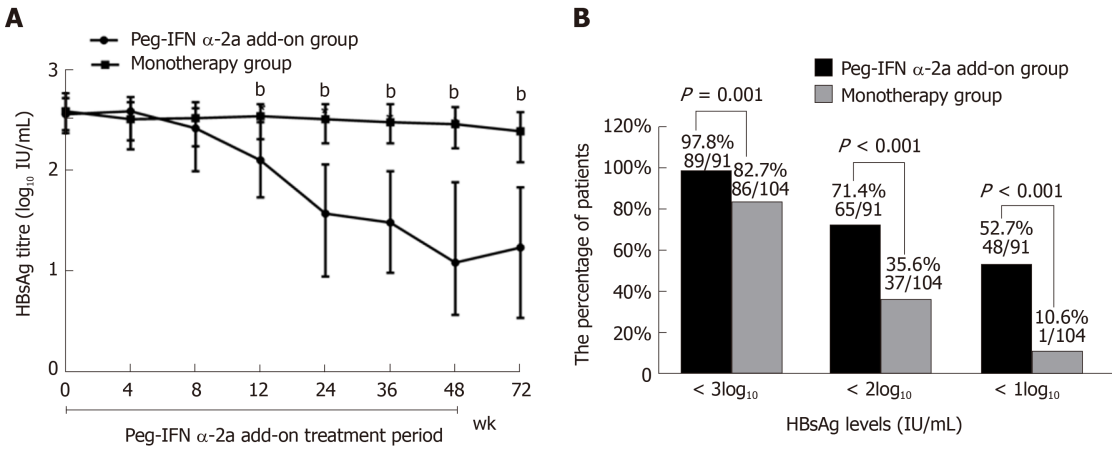

Figure 4 Virological change. A: Dynamics of hepatitis B surface antigen titers ($^bP < 0.001$ *vs* monotherapy group for weeks 12, 24, 36, 48 and 72). Data shown are median values of $\log_{10}$ hepatitis B surface antigen and error bars represent 95% confidence interval. B: HBsAg response at week 72.

clearance were 58.1% (18/31) for patients younger than 33-years-old and 62.1% (18/29) for patients with baseline HBsAg < 2.25 $\log_{10}$ IU/mL. Patients with HBsAg < 1.89 $\log_{10}$ IU/mL at week 12 had an HBsAg clearance rate of 73.7% (28/38). Patients with HBsAg < 1.46 $\log_{10}$ IU/mL at week 24 had an HBsAg clearance rete of 72.7% (32/44). The rates of HBsAg clearance were 80.0% (28/35) and 77.5% (31/40) for patients with HBsAg decline > 0.5 $\log_{10}$ IU/mL from baseline to week 12 and > 1.0 $\log_{10}$ IU/mL to week 24. Patients with ALT ≥ 2 × ULN during the first 12 wk of therapy demonstrated 54.8% (23/42) of HBsAg clearance (Table 3).

Safety

AEs were analyzed in the study population up to 72 wk. Many (90.1%) of the patients in the add-on group experienced AEs, which was significantly higher than 9.6% in the NA alone group (Table 4). The most common AEs were thrombocytopenia (90.1%), followed by neutropenia (87.9%) and pyrexia (82.4%) in the add-on group. Due to AEs, 4.4% (4/91) of patients in the add-on group discontinued peg-IFN α-2a, including two patients who suffered from hyperthyroidism at week 24, one patient with thrombocytopenia (25 × 10^9/L) and one with coronary heart disease deterioration at week 12. ALT flares (> 5 × ULN) occurred in 7.7% of the add-on group. No patient in the monotherapy group discontinued treatment due to safety reasons.

It should be noted that one patient in the monotherapy group developed HCC. Two patients treated with ADV in the monotherapy group experienced virological breakthrough (for patient adherent with NA therapy, serum HBV DNA converted to positivity following sustained negativity and as confirmed 1 mo later using the same regent) and were rescued by TDF and ETV therapy. Considering the risk of virological breakthrough with ADV monotherapy, ADV was replaced by TDF in patients with HBsAg positive at week 72.

DISCUSSION

NA has been shown to partly restore adaptive immunity, whereas peg-IFN α boosts innate immunity, triggers T-cell-mediated immune responses, prevents formation of HBV proteins and depletes the covalently closed circular DNA pool, which leads to more HBsAg clearance than with NA[18]. Although promising results with the combination use of peg-IFN α and NA were reported from previous studies, the best treatment approach for CHB is still debated.

An optimized combination therapeutic strategy can improve HBsAg clearance

Our study was an optimized combination therapeutic strategy in which we strictly chose CHB patients who achieved lower baseline HBsAg levels (≤ 1500 IU/mL) after long-term NA treatment. Our data showed that the HBsAg clearance and seroconversion rates in the peg-IFN α-2a add-on group were 26.4% and 18.7% at week 48, and these rates increased to 37.4% and 29.7% at week 72, significantly higher than those patients receiving NA alone. Our results demonstrated significantly higher rates of HBsAg clearance and seroconversion than three previous studies that utilized peg-IFN α-2a instead of NA[11,16,17]. The major discrepancy between our study and those

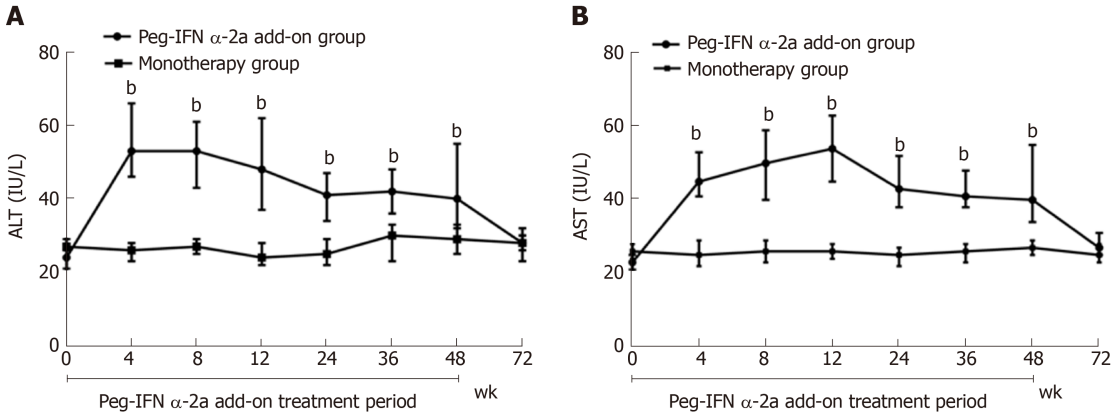

Figure 5 Change in serum alanine aminotransferase and median serum aspartate transaminase. A: Change in serum alanine aminotransferase ($^bP < 0.001$ *vs* monotherapy group for weeks 4, 8, 12, 24, 36 and 48). Data shown are median values of serum alanine aminotransferase and error bars represent 95% confidence interval; B: Change in median serum aspartate transaminase ($^bP < 0.001$ *vs* monotherapy group for weeks 4, 8, 12, 24, 36 and 48). Data shown are median values of serum aspartate transaminase and error bars represent 95% confidence interval. HBsAg: Hepatitis B surface antigen; ALT: Alanine aminotransferase; AST: Aspartate transaminase.

three studies is that the patients were not selected by baseline HBsAg levels and HBV DNA levels at enrollment in those three studies. In addition, sequential combination therapy with peg-IFN α-2a and NA, simultaneously exerting direct antiviral effect and immune regulation of the drugs, is another important reason for significantly higher rates of HBsAg clearance and seroconversion in our study.

However, a randomized controlled trial reported that the addition of 48 wk of peg-IFN α-2a to NA therapy resulted in a small proportion of HBsAg clearance and HBs seroconversion[18]. Several reasons could explain the discrepancy between our results and results in that randomized controlled trial. Firstly, 93.4% (85/91) of patients in our study finished the scheduled peg-IFN α-2a treatment and follow-up, while only 76% (65/85) of patients received the full dose and duration of peg-IFN α-2a treatment in that randomized controlled trial. Good compliance and tolerance to full dose and duration of peg-IFN α-2a treatment may be the main reason for significantly higher rates of HBsAg clearance and seroconversion in our study. Secondly, lower baseline HBsAg titer of patients in our study may be another important reason[19]. Furthermore, all patients in our study were CHB patients and the FibroScan value < 7.1 kPa, while about 35.0% (31/90) of patients had liver fibrosis and even cirrhosis in the randomized controlled trial. Lower baseline degree of liver fibrosis of patients in our study could well explain the discrepancy between these two studies[20].

Individualized peg-IFN α-2a therapeutic strategy without a definite course of treatment may improve HBsAg clearance

Although 62.6% (57/91) patients in the add-on group did not achieve the primary end point, peg-IFN α-2a add-on therapy caused a greater decline in HBsAg levels and led to a higher proportion of patients achieving an HBsAg level < 3 $\log_{10}$ IU/mL and even < 2 $\log_{10}$ IU/mL than NA monotherapy, which are levels associated with long-term disease remission[21]. It suggests that we need to explore an individual treatment strategy for the peg-IFN α-2a regimen based on the kinetics of HBsAg rather than a 48-wk fixed-course treatment strategy.

HBsAg changes from baseline to weeks 12 and 24 to predict HBsAg clearance

From a practical point of view, early identification of patients with the highest chance of HBsAg clearance and particularly those with the lowest chance of HBsAg clearance after 48 wk of peg-IFN α therapy has the greatest clinical relevance. HBsAg at baseline and early decline during treatment have been shown to be useful for predicting eventual HBsAg elimination and in individualized on-treatment decision-making in a small cohort of patients[22]. Indeed, our study provides evidence to support this concept. In our study, we found that the levels of HBsAg at baseline, week 12 and week 24 and the decline of HBsAg during early therapy (at weeks 12 and 24) from baseline were all statistically associated with HBsAg clearance. Therefore, HBsAg at baseline, weeks 12 and 24 and decrease of HBsAg at weeks 12 and 24 were potential markers for the early prediction of HBsAg clearance in clinical practice.

ALT elevation in early treatment represents the activation of the immune system

ALT elevation induced by peg-IFN α-2a treatment reflects immune clearance of HBV.

Table 2 Baseline variables and change of hepatitis B surface antigen in weeks 12 and 24 associated with hepatitis B surface antigen clearance

Predictors	Univariate analysis			Multivariate analysis		
	OR	95%CI	*P* value	OR	95%CI	*P* value
Gender	2.045	(0.792-5.283)	0.149	-	-	-
ALT in IU/L	0.997	(0.968-1.027)	0.852	-	-	-
FibroScan value in kPa	0.794	(0.549-1.125)	0.803	-	-	-
BMI in kg/cm2	0.962	(0.951-1.218)	0.794	-	-	-
NA	1.790	(0.758-4.225)	0.184	-	-	-
Mode of HBV transmission	0.840	(0.298-2.372)	0.742	-	-	-
Age, yr	0.924	(0.878-0.972)	0.002	0.946	(0.833-0.981)	0.025
Baseline HBsAg as $\log_{10}$ IU/mL	0.371	(0.194-0.711)	0.003	0.557	(0.206-0.827)	0.019
Week 12 HBsAg as $\log_{10}$ IU/mL	0.273	(0.157-0.474)	< 0.001	0.542	(0.194-0.792)	0.002
Week 24 HBsAg as $\log_{10}$ IU/mL	0.218	(0.117-0.405)	< 0.001	0.188	(0.058-0.410)	0.004
HBsAg decline as $\log_{10}$ IU/mL						
From baseline to week 12	10.646	(3.776-25.018)	< 0.001	8.925	(3.376-17.226)	< 0.001
From baseline to week 24	7.045	(3.223-15.400)	< 0.001	8.830	(4.553-18.213)	< 0.001
ALT ≥ 2 × ULN in the first 12 wk[F1]	4.182	(1.691-10.340)	0.002	5.275	(3.324-11.823)	0.014

[F1]ALT ≥ 2 × ULN during the first 12 wk of therapy. ALT: Alanine aminotransferase; BMI: Body mass index; NA: Nucleoside Analogue or nucleotide analog; HBV: Hepatitis B virus; ULN: Upper limit of normal; OR: Odds ratio; CI: Confidence interval; UI: International unit.

In our study, ALT elevations were observed in some patients with sustained HBV DNA suppression right after adding peg-IFN α-2a. Our analysis revealed that a significantly higher chance of HBsAg clearance in patients with ALT ≥ 2 × ULN during the first 12 wk of therapy than those patients with ALT < 2 × ULN. Therefore, ALT ≥ 2 × ULN during the first 12 wk of therapy is likely a promising marker for early prediction of HBsAg clearance in clinical practice. However, because of a small sample size of patients receiving peg-IFN α-2a add-on therapy (n = 91) in this study, further efforts with more patients enrolled and preferably in multiple centers is our next step to reach a validating conclusion.

Our results also showed that age was significantly associated with HBsAg clearance at week 72, which is consistent with previous studies[9]. Further analysis found that age ≤ 33 years was an important marker for early HBsAg clearance, suggesting that young patients have a better response to peg-IFN α-2a.

All the above variables and their "cut-off points" on ROC curves are meaningful for predicting HBsAg clearance. However, this study had a relatively small number of patients receiving peg-IFN α-2a add-on therapy (n = 91). Exploratory analyses into baseline and on-treatment predictors of HBsAg clearance should be interpreted with caution. As future research, more patients in multiple centers will be enrolled and these meaningful characteristics will be combined into a mathematically modelled and weighted scoring system that can be retrospectively and prospectively validated.

Tolerance to peg-IFN α-2a add-on therapy

Considering safety, peg-IFN α-2a add-on was generally well tolerated without observing unexpected AEs. Indeed, AEs were increased when compared to NA monotherapy, which should be taken into account when considering peg-IFN α-2a add-on therapy. AEs should also be closely monitored and managed promptly during administration of peg-IFN α-2a. All AEs were reversed after drug withdrawal. Therefore, it is essential to communicate with patients adequately and encourage patients to comply with continuous peg-IFN α-2a therapy.

Study limitations and interesting phenomenon

This study has several limitations. First, the patients in the treatment groups were not randomized. This may lead to confounder bias induced by unknown confounding factors and potentially impact the follow-up results, although demographic and baseline characteristics between treatment groups were not statistically different. Second, it is uncertain whether different HBV genotypes play a role in the response to the same therapeutic strategy due to unknown HBV genotypes in patients with long-term HBV suppression at entry to the study. Third, HBsAg decline during the treatment period does not certainly point to a long-term trend, and HBsAg levels may

Table 3 ROC curves of hepatitis B surface antigen levels and hepatitis B surface antigen changes on the prediction of hepatitis B surface antigen clearance

Factors	Area	SD	95%CI	Cut-off point	Sensitivityand specificity	HBsAg clearance rate
Age in yr	0.699	0.056	(0.589-0.809)	33	55.9%, 77.2%	58.1% (18/31)
Baseline HBsAg as $\log_{10}$ IU/mL	0.689	0.059	(0.573-0.806)	2.25	52.9%, 80.7%	62.1% (18/29)
Week 12 HBsAg as $\log_{10}$ IU/mL	0.877	0.04	(0.803-0.951)	1.89	85.3%, 82.5%	73.7% (28/38)
Week 24 HBsAg as $\log_{10}$ IU/mL	0.921	0.03	(0.861-0.980)	1.46	94.1%, 78.9%	72.7% (32/44)
HBsAg decline as $\log_{10}$ IU/mL						
From baseline to week 12	0.901	0.032	(0.839-0.963)	0.5	85.3%, 88.7%	80.0% (28/35)
From baseline to week 24	0.924	0.031	(0.864-0.985)	1.0	91.2%, 86.0%	77.5% (31/40)

ROC: Receiver operator characteristic; SD: Standard deviation; CI: Confidence interval; HBsAg: Hepatitis B surface antigen; UI: International unit.

revert to the previous state after discontinuing peg-IFN α-2a. The long-term effectiveness data including HBsAg and HBV DNA dynamics, sustained HBsAg clearance, incidence of liver cirrhosis and HCC are being collected, and we will report in the future.

HBsAg elevations were observed at 4 wk after adding on peg-IFN α-2a in 57.1% (52/91) patients in the peg-IFN α-2a add-on group and had no influence on treatment outcome. It is an interesting phenomenon. The reason of HBsAg elevations after adding on peg-IFN α-2a therapy needs to be further explored.

In conclusion, this study shows that the peg-IFN α-2a add-on strategy in HBeAg-negative CHB patients with HBsAg ≤ 1500 IU/mL receiving long-term NA leads to higher HBsAg clearance than NA monotherapy. Young patients, lower levels of HBsAg at baseline, at weeks 12 and 24 and rapid HBsAg decline in early treatment (at weeks 12 and 24) are the independent predictors of HBsAg clearance in peg-IFN α-2a add on treatment. The add-on therapy is relatively safe, and the patients experience expected AEs.

Table 4 Adverse events of the study population, *n* (%)

AEs	Add-on, *n* = 91	Monotherapy, *n* = 104	*P* value
Neutropenia	80 (87.9)	8 (7.7)	< 0.001
Thrombocytopenia	82 (90.1)	9 (8.7)	< 0.001
Fever	75 (82.4)	0 (0)	< 0.001
Fatigue	53 (58.2)	10 (9.6)	< 0.001
Anorexia	49 (53.8)	3 (2.9)	< 0.001
Weight loss	15 (16.5)	0 (0)	< 0.001
Alopecia	10 (11.0)	0 (0)	< 0.001
Thyroid dysfunction	6 (6.6)	0 (0)	0.009
ALT flares	7 (7.7)	0 (0)	0.004
Rash	5 (5.5)	0 (0)	0.021
HCC	0 (0)	1 (1.0)	1.000
Virological breakthrough	0 (0)	2 (1.9)	0.500

AEs: Adverse events; ALT: alanine aminotransferase; HCC: Hepatocellular carcinoma.

ARTICLE HIGHLIGHTS

Research background

Nucleos(t)ide analog (NA) has shown limited effectiveness against hepatitis B surface antigen (HBsAg) clearance in chronic hepatitis B (CHB) patients.

Research motivation

Despite promising results with the combination therapy of peginterferon (peg-IFN) and NA, the best combination therapeutic strategy of peg-IFN and NA for the treatment of CHB is still debated. The interim analysis of the NEW SWITCH study showed that patients with baseline HBsAg levels < 1500 IU/mL achieved a higher HBsAg clearance rate than patients with HBsAg > 1500 IU/mL when they switched from NA to 48 wk of peg-IFN α-2α therapy. However, it is not clear what the effects of add-on peginterferon α-2a to an ongoing NA regimen in CHB patients with HBsAg ≤ 1500 IU/mL after over 1 year of NA therapy. Considering the large number of patients who have achieved HBsAg ≤ 1500 IU/mL after long-term NA treatment in our clinic, it is very necessary and significant to explore the efficacy of peg-IFN α add-on treatment in these patients.

Research objectives

This study aimed to evaluate the efficacy and safety of add-on peg-IFN α-2a to an ongoing NA regimen in CHB patients with HBsAg ≤ 1500 IU/mL, hepatitis B e antigen (HBeAg)-negative and hepatitis B virus-deoxyribonucleic acid (HBV DNA) < 1.0×10^2 IU/mL after over 1 year of NA therapy and to analyze independent prediction factors of HBsAg clearance in this population.

Research methods

In this observational study, 195 CHB patients with HBsAg ≤ 1500 IU/mL, HBeAg-negative (including HBeAg-negative patients or HBeAg-positive patients achieved HBeAg-negative after antiviral treatment with NA) and HBV DNA < 1.0×10^2 IU/mL after over 1 year of NA therapy were enrolled between November 2015 and December 2018 at the Second Affiliated Hospital of Xi'an Jiaotong University, China. Patients were given the choice between receiving either peg-IFN α-2a add-on therapy to an ongoing NA regimen (add-on group, *n* = 91) or continuous NA monotherapy (monotherapy group, *n* = 104) after being informed of the benefits and risks of the peg-IFN α-2a therapy. Total therapy duration of peg-IFN α-2a was 48 wk. All patients were followed-up to week 72 (24 wk after discontinuation of peg-IFN α-2a). The primary endpoint was the proportion of patients with HBsAg clearance at week 72.

Research results

Demographic and baseline characteristics were comparable between the two groups. Intention-to-treatment analysis showed that the HBsAg clearance rate in the add-on group and monotherapy group was 37.4% (34/91) and 1.9% (2/104) at week 72, respectively. The HBsAg seroconversion rate in the add-on group was 29.7% (27/91) at week 72, and no patients in the monotherapy group achieved HBsAg seroconversion at week 72. The HBsAg clearance and seroconversion rates in the add-on group were significantly higher than in the monotherapy group at week 72 ($P < 0.001$). Younger patients, lower baseline HBsAg concentration, lower HBsAg concentrations at weeks 12 and 24, greater HBsAg decline from baseline to weeks 12 and 24 and the alanine aminotransferase ≥ 2 × upper limit of normal during the first 12 wk of therapy were strong predictors of HBsAg clearance in patients with peg-IFN α-2a add-on treatment. Regarding the safety of the treatment, 4.4% (4/91) of the patients in the add-on group discontinued peg-IFN α-2a due to adverse events. No severe adverse events were noted in the

monotherapy group.

Research conclusions

Peg-IFN α as an add-on therapy augments HBsAg clearance in HBeAg-negative CHB patients with HBsAg ≤ 1500 IU/mL after over 1 year of NA therapy.

Research perspectives

Add-on Peg-IFN α to ongoing NA regime in CHB patients with low HBsAg levels and sustained HBV DNA suppression after long-term NA treatment can significantly improve the rates of HBsAg clearance and seroconversion. Some indicators, such as younger patients, lower HBsAg concentrations at baseline, weeks 12 and 24, greater HBsAg decline from baseline to weeks 12 and 24 and the alanine aminotransferase ≥ 2 × upper limit of normal during the first 12 wk of therapy can serve as predictors of HBsAg clearance in patients with peg-IFN α-2a add-on treatment. peg-IFN α add-on treatment is relatively safe. However,, the long-term efficacy of peg-IFN α add-on treatment needs to be studied.

ACKNOWLEDGEMENTS

The authors would like to thank Lei-Lei Pei from Institute of Public Health Xi'an Jiaotong University for reviewing the statistical methods of this study. The authors also would like to thank the patients and their families for their contribution to this study.

REFERENCES

1 **European Association for the Study of the Liver**. Electronic address: easloffice@easloffice.eu.; European Association for the Study of the Liver. EASL 2017 Clinical Practice Guidelines on the management of hepatitis B virus infection. *J Hepatol* 2017; **67**: 370-398 [PMID: 28427875 DOI: 10.1016/j.jhep.2017.03.021]

2 **Chang TT**, Lai CL, Kew Yoon S, Lee SS, Coelho HS, Carrilho FJ, Poordad F, Halota W, Horsmans Y, Tsai N, Zhang H, Tenney DJ, Tamez R, Iloeje U. Entecavir treatment for up to 5 years in patients with hepatitis B e antigen-positive chronic hepatitis B. *Hepatology* 2010; **51**: 422-430 [PMID: 20049753 DOI: 10.1002/hep.23327]

3 **Lau GK**, Piratvisuth T, Luo KX, Marcellin P, Thongsawat S, Cooksley G, Gane E, Fried MW, Chow WC, Paik SW, Chang WY, Berg T, Flisiak R, McCloud P, Pluck N; Peginterferon Alfa-2a HBeAg-Positive Chronic Hepatitis B Study Group. Peginterferon Alfa-2a, lamivudine, and the combination for HBeAg-positive chronic hepatitis B. *N Engl J Med* 2005; **352**: 2682-2695 [PMID: 15987917 DOI: 10.1056/NEJMoa043470]

4 **Janssen HL**, van Zonneveld M, Senturk H, Zeuzem S, Akarca US, Cakaloglu Y, Simon C, So TM, Gerken G, de Man RA, Niesters HG, Zondervan P, Hansen B, Schalm SW; HBV 99-01 Study Group; Rotterdam Foundation for Liver Research. Pegylated interferon alfa-2b alone or in combination with lamivudine for HBeAg-positive chronic hepatitis B: a randomised trial. *Lancet* 2005; **365**: 123-129 [PMID: 15639293 DOI: 10.1016/S0140-6736(05)17701-0]

5 **You CR**, Lee SW, Jang JW, Yoon SK. Update on hepatitis B virus infection. *World J Gastroenterol* 2014; **20**: 13293-13305 [PMID: 25309066 DOI: 10.3748/wjg.v20.i37.13293]

6 **European Association For The Study Of The Liver**. EASL clinical practice guidelines: Management of chronic hepatitis B virus infection. *J Hepatol* 2012; **57**: 167-185 [PMID: 22436845 DOI: 10.1016/j.jhep.2012.02.010]

7 **Lampertico P**, Liaw YF. New perspectives in the therapy of chronic hepatitis B. *Gut* 2012; **61** Suppl 1: i18-i24 [PMID: 22504916 DOI: 10.1136/gutjnl-2012-302085]

8 **Scaglione SJ**, Lok AS. Effectiveness of hepatitis B treatment in clinical practice. *Gastroenterology* 2012; **142**: 1360-1368.e1 [PMID: 22537444 DOI: 10.1053/j.gastro.2012.01.044]

9 **Hou J**, Wang G, Wang F, Cheng J, Ren H, Zhuang H, Sun J, Li L, Li J, Meng Q, Zhao J, Duan Z, Jia J, Tang H, Sheng J, Peng J, Lu F, Xie Q, Wei L; Chinese Society of Hepatology, Chinese Medical Association; Chinese Society of Infectious Diseases, Chinese Medical Association. Guideline of Prevention and Treatment for Chronic Hepatitis B (2015 Update). *J Clin Transl Hepatol* 2017; **5**: 297-318 [PMID: 29226097 DOI: 10.14218/JCTH.2016.00019]

10 **Sarin SK**, Kumar M, Lau GK, Abbas Z, Chan HL, Chen CJ, Chen DS, Chen HL, Chen PJ, Chien RN, Dokmeci AK, Gane E, Hou JL, Jafri W, Jia J, Kim JH, Lai CL, Lee HC, Lim SG, Liu CJ, Locarnini S, Al Mahtab M, Mohamed R, Omata M, Park J, Piratvisuth T, Sharma BC, Sollano J, Wang FS, Wei L, Yuen MF, Zheng SS, Kao JH. Asian-Pacific clinical practice guidelines on the management of hepatitis B: a 2015 update. *Hepatol Int* 2016; **10**: 1-98 [PMID: 26563120 DOI: 10.1007/s12072-015-9675-4]

11 **Ning Q**, Han M, Sun Y, Jiang J, Tan D, Hou J, Tang H, Sheng J, Zhao M. Switching from entecavir to PegIFN alfa-2a in patients with HBeAg-positive chronic hepatitis B: a randomised open-label trial (OSST trial). *J Hepatol* 2014; **61**: 777-784 [PMID: 24915612 DOI: 10.1016/j.jhep.2014.05.044]

12 **Boglione L**, Cariti G, Di Perri G, D'Avolio A. Sequential therapy with entecavir and pegylated interferon in a cohort of young patients affected by chronic hepatitis B. *J Med Virol* 2016; **88**: 1953-1959 [PMID: 27017932 DOI: 10.1002/jmv.24534]

13 **Wursthorn K**, Lutgehetmann M, Dandri M, Volz T, Buggisch P, Zollner B, Longerich T, Schirmacher P, Metzler F, Zankel M, Fischer C, Currie G, Brosgart C, Petersen J. Peginterferon alpha-2b plus adefovir induce strong cccDNA decline and HBsAg reduction in patients with chronic hepatitis B. *Hepatology* 2006; **44**: 675-684 [PMID: 16941693 DOI: 10.1002/hep.21282]

14 **Ouzan D**, Pénaranda G, Joly H, Khiri H, Pironti A, Halfon P. Add-on peg-interferon leads to loss of HBsAg in patients with HBeAg-negative chronic hepatitis and HBV DNA fully suppressed by long-term nucleotide analogs. *J Clin Virol* 2013; **58**: 713-717 [PMID: 24183313 DOI: 10.1016/j.jcv.2013.09.020]

15 **Chen GY**, Zhu MF, Zheng DL, Bao YT, Wang J, Zhou X, Lou GQ. Baseline HBsAg predicts response to pegylated interferon-α2b in HBeAg-positive chronic hepatitis B patients. *World J Gastroenterol* 2014; **20**: 8195-8200 [PMID: 25009392 DOI: 10.3748/wjg.v20.i25.8195]

16 **Hu P**, Shang J, Zhang W, Gong G, Li Y, Chen X, Jiang J, Xie Q, Dou X, Sun Y, Li Y, Liu Y, Liu G, Mao D, Chi X, Tang H, Li X, Xie Y, Chen X, Jiang J, Zhao P, Hou J, Gao Z, Fan H, Ding J, Zhang D, Ren H. HBsAg Loss with Peg-interferon Alfa-2a in Hepatitis B Patients with Partial Response to Nucleos(t)ide Analog: New Switch Study. *J Clin Transl Hepatol* 2018; **6**: 25-34 [PMID: 29577029 DOI: 10.14218/JCTH.2017.00072]

17 **He LT**, Ye XG, Zhou XY. Effect of switching from treatment with nucleos(t)ide analogs to pegylated interferon α-2a on virological and serological responses in chronic hepatitis B patients. *World J Gastroenterol* 2016; **22**: 10210-10218 [PMID: 28028369 DOI: 10.3748/wjg.v22.i46.10210]

18 **Bourlière M**, Rabiega P, Ganne-Carrie N, Serfaty L, Marcellin P, Barthe Y, Thabut D, Guyader D, Hezode C, Picon M, Causse X, Leroy V, Bronowicki JP, Carrieri P, Riachi G, Rosa I, Attali P, Molina JM, Bacq Y, Tran A, Grangé JD, Zoulim F, Fontaine H, Alric L, Bertucci I, Bouvier-Alias M, Carrat F; ANRS HB06 PEGAN Study Group. Effect on HBs antigen clearance of addition of pegylated interferon alfa-2a to nucleos(t)ide analogue therapy versus nucleos(t)ide analogue therapy alone in patients with HBe antigen-negative chronic hepatitis B and sustained undetectable plasma hepatitis B virus DNA: a randomised, controlled, open-label trial. *Lancet Gastroenterol Hepatol* 2017; **2**: 177-188 [PMID: 28404133 DOI: 10.1016/S2468-1253(16)30189-3]

19 **Liem KS**, van Campenhout MJH, Xie Q, Brouwer WP, Chi H, Qi X, Chen L, Tabak F, Hansen BE, Janssen HLA. Low hepatitis B surface antigen and HBV DNA levels predict response to the addition of pegylated interferon to entecavir in hepatitis B e antigen positive chronic hepatitis B. *Aliment Pharmacol Ther* 2019; **49**: 448-456 [PMID: 30689258 DOI: 10.1111/apt.15098]

20 **Patel K**, Wilder J. Fibroscan. *Clin Liver Dis (Hoboken)* 2014; **4**: 97-101 [PMID: 30992931 DOI: 10.1002/cld.407]

21 **Sonneveld MJ**, Rijckborst V, Cakaloglu Y, Simon K, Heathcote EJ, Tabak F, Mach T, Boucher CA, Hansen BE, Zeuzem S, Janssen HL. Durable hepatitis B surface antigen decline in hepatitis B e antigen-positive chronic hepatitis B patients treated with pegylated interferon-α2b: relation to response and HBV genotype. *Antivir Ther* 2012; **17**: 9-17 [PMID: 22267464 DOI: 10.3851/IMP1887]

22 **Kittner JM**, Sprinzl MF, Grambihler A, Weinmann A, Schattenberg JM, Galle PR, Schuchmann M. Adding pegylated interferon to a current nucleos(t)ide therapy leads to HBsAg seroconversion in a subgroup of patients with chronic hepatitis B. *J Clin Virol* 2012; **54**: 93-95 [PMID: 22365367 DOI: 10.1016/j.jcv.2012.01.024]

World Journal of Gastroenterology

Submit a Manuscript: https://www.f6publishing.com

World J Gastroenterol 2020 April 7; 26(13): 1540-1545

DOI: 10.3748/wjg.v26.i13.1540

ISSN 1007-9327 (print) ISSN 2219-2840 (online)

CASE REPORT

Small intestinal hemolymphangioma treated with enteroscopic injection sclerotherapy: A case report and review of literature

Nian-Jun Xiao, Shou-Bin Ning, Teng Li, Bai-Rong Li, Tao Sun

ORCID number: Nian-Jun Xiao (0000-0002-4055-7968); Shou-Bin Ning (0000-0001-7204-3956); Teng Li (0000-0002-3637-3656); Bai-Rong Li (0000-0001-5758-4447); Tao Sun (0000-0002-2072-268X).

Author contributions: Xiao NJ reviewed the literature and contributed to manuscript drafting; Li T performed the pathological examination and interpreted the pathological images; Li BR and Sun T contributed to manuscript revising; Ning SB was the operator, and he was responsible for the revision of the manuscript for important intellectual content; All authors issued final approval for the version to be submitted.

Informed consent statement: Informed written consent was obtained from the patient for publication of this report and any accompanying images.

Conflict-of-interest statement: The authors declare that they have no conflict of interest.

CARE Checklist (2016) statement: The authors have read the CARE Checklist (2016), and the manuscript was prepared and revised according to the CARE Checklist (2016).

Nian-Jun Xiao, Shou-Bin Ning, Bai-Rong Li, Tao Sun, Department of Gastroenterology, Air Force Medical Center, Beijing 100142, China

Teng Li, Department of Pathology, Air Force Medical Center, Beijing 100142, China

Corresponding author: Shou-Bin Ning, PhD, Chief Doctor, Department of Gastroenterology, Air Force Medical Center, No. 30, Fucheng Road, Haidian District, Beijing 100142, China. ning-shoubin@163.com

Abstract

BACKGROUND

Hemolymphangiomas are rare malformations composed of both lymphatic and vascular vessels and are located in the pancreas, spleen, mediastinum, *etc*. Small intestinal hemolymphangioma is extremely rare and often presents as obscure gastrointestinal bleeding. It is rarely diagnosed correctly before the operation. Endoscopic injection sclerotherapy is usually used as a management of bleeding in esophageal varices and was occasionally reported as a treatment of vascular malformation. The treatment of small intestinal hemolymphangioma with enteroscopic injection sclerotherapy has not been reported.

CASE SUMMARY

A 42-year-old male complained of recurrent episodes of melena and dizziness, fatigue and reduced exercise capacity for more than 2 mo. Gastroduodenoscopy and blood test revealed a gastric ulcer and anemia. Treatment with oral proton-pump inhibitors and iron did not improve symptoms. We then performed a capsule endoscopy and anterograde balloon-assisted enteroscopy and revealed a hemolymphangioma. Considering it is a benign tumor without malignant potential, we performed enteroscopic injection sclerotherapy. He was discharged 4 days later. At follow-up 3 mo later, the melena disappeared. Balloon-assisted enteroscopy revealed an atrophied tumor atrophied and no bleeding. Argon plasma coagulation was applied to the surface of the hemolymphangioma to accelerated healing. When he returned for follow-up 1 year later, anemia was resolved and the tumor had been cured.

CONCLUSION

Balloon-assisted enteroscopy and capsule endoscopy are effective methods for diagnosis of hemolymphangioma. Enteroscopic injection sclerotherapy is an effective treatment.

Key words: Hemolymphangioma; Lymphangioma; Small intestinal tumor; Balloon

Manuscript source: Unsolicited manuscript

Received: December 4, 2019
Peer-review started: December 4, 2019
First decision: January 13, 2020
Revised: March 4, 2020
Accepted: March 10, 2020
Article in press: March 10, 2020
Published online: April 7, 2020

P-Reviewer: García-Compeán D, Kwon KA
S-Editor: Ma YJ
L-Editor: Filipodia
E-Editor: Ma YJ

assisted enteroscopy; Obscure gastrointestinal bleeding; Enteroscopic injection sclerotherapy; Case report

Core tip: Small intestinal hemolymphangioma is a rare malformation presenting as obscure gastrointestinal bleeding and anemia. Though the malformation has a typical lymphangiectatic appearance of white patches on the mucosal surface, it is rarely diagnosed correctly before the operation. We report a case of intestinal hemolymphangioma diagnosed by capsule endoscopy and balloon-assisted enteroscopy. We applied a new, minimally invasive therapy named enteroscopic injection sclerotherapy to manage this disease, which has been proven to be effective and safe. The literature review can present a better understanding of this disease and the advantage of the new management.

Citation: Xiao NJ, Ning SB, Li T, Li BR, Sun T. Small intestinal hemolymphangioma treated with enteroscopic injection sclerotherapy: A case report and review of literature. *World J Gastroenterol* 2020; 26(13): 1540-1545
URL: https://www.wjgnet.com/1007-9327/full/v26/i13/1540.htm
DOI: https://dx.doi.org/10.3748/wjg.v26.i13.1540

INTRODUCTION

Small intestinal hemolymphangioma is a rare benign malformation consisting of blood vessels and lymphatic channels with luminal dilation. Individuals with small intestinal hemolymphangioma may present with obscure gastrointestinal bleeding and anemia. Though the malformation has a typical lymphangiectatic appearance of white patches on the mucosal surface, it is rarely diagnosed correctly with conventional endoscopy due to the special anatomic location. Here we present a case of small intestinal hemolymphangioma diagnosed by capsule endoscopy (CE) and balloon-assisted enteroscopy (BAE). We applied a new, minimally invasive therapy named enteroscopic injection sclerotherapy to manage this disease, which has been proven to be effective and safe.

CASE PRESENTATION

A 42-year-old male complained of recurrent episodes of melena and dizziness, fatigue and reduced exercise capacity for more than 2 mo.

History of present illness

The patient's symptoms started 2 mo ago with recurrent episodes of melena and he frequently felt fatigued. He was diagnosed with a gastric ulcer and anemia after undergoing gastroduodenoscopy, colonoscopy and laboratory blood tests. Then he took oral proton-pump inhibitors and iron for 1.5 mo, but these therapies did not ameliorate the symptoms.

History of past illness

The patient had no previous medical history.

Physical examination

On examination, anemic face and upper abdominal tenderness were noted. The vital signs were normal with a respiratory rate of 18/min, heart rate of 96/min and blood pressure of 102/62 mmHg.

Laboratory examinations

Blood analysis revealed severe iron-deficiency anemia with hemoglobin of 53 g/dL, and fecal occult blood was positive. Blood biochemistry, tumor biomarkers, other blood tests as well as urine analysis were normal. Electrocardiogram and chest X-ray were also normal.

Endoscopic examinations and further diagnostic work-up

When the patient presented in our hospital, two units of blood were transfused. The gastroduodenoscopy was performed again. A sealed ulcer without any signs of bleeding sign were found in the antrum. We then performed a CE. Bleeding was found in the jejunum after running the capsule for 97 min. The total running time in the small bowel was about 300 min. The CE cannot determine the cause of bleeding due to the short stay around the lesion and the influence of the blood. An anterograde BAE was performed, and a protruded lesion was revealed in the jejunum at about 150 cm distal to the ligament of Treitz. It filled half of the intestinal cavity. The tumor was lobulated with white patches on the mucosal surface with blood oozing in the fundus (Figure 1A). Multiple biopsies were taken, and pathological findings further revealed that hyperplastic thin-walled lymphatic and venous with luminal dilation presented in the submucosal area (Figure 1B).

FINAL DIAGNOSIS

The final diagnosis of the presented case was iron-deficiency anemia with intestinal bleeding due to hemolymphangioma.

TREATMENT

Considering it is a benign tumor without malignant potential, we performed enteroscopic injection sclerotherapy with polidocanol to manage the chronic bleeding. The malformation was completely sclerotized, and no bleeding or perforation was experienced. He was discharged 4 d later.

OUTCOME AND FOLLOW-UP

During a follow-up visit, 3 mo after enteroscopic injection sclerotherapy, the patient felt better than before. The patient's hemoglobin was 126 g/dL, and the melena had disappeared. The tumor had atrophied dramatically, and bleeding was hardly observed (Figure 2A). Argon plasma coagulation was applied to the atrophic hemolymphangioma to accelerated healing. At 1 year later the patient returned to our department for the second follow-up. Laboratory blood tests revealed a normal hemoglobin of 140 g/dL. The tumor was gone, and only a few white patches on the mucosal surface were visible (Figure 2B).

DISCUSSION

Hemolymphangioma is an uncommon category of lymphangioma, which is a group of malformations of the lymphatic system. Lymphangioma can be located at the mesentery, pancreas, mediastinum, *etc*, but small intestinal lymphangiomas are extremely rare (less than 1% of all lymphangiomas). Only 19 reports (with 40 patients) of small bowel lymphangioma were reported from 1960 to 2009 in a literature review on lymphangiomas[1]. About half of those patients presented with gastrointestinal bleeding, and the majority of lesions were within the jejunum. The standard treatment of this disease was surgical resection and only two of the forty patients were treated by BAE. One lesion was treated with an injection of 1:10000 epinephrine and was very small (4 mm × 6 mm)[2]. The other lesion treated by BAE was not clearly described[3]. With the advent of CE and BAE, small intestinal lymphangiomas have been found more often, and even small intestinal hemolymphangioma have been reported. We proceeded to a review the literature from 2010 to 2019 by searching "hemolymphangioma [All Fields] OR hemangiolymphangioma [All Fields]" on PubMed. Six case reports of small intestinal hemolymphangioma were found (Table 1)[4-9]. All of them were located in the proximal jejunum (or duodenum) and presented as anemia due to gastrointestinal bleeding. Six lesions were diagnosed by endoscopy (five enteroscopy and one gastroduodenoscopy), and three were detected by CE examination. These data support that CE and BAE are effective tools for diagnosing hemolymphangioma.

The standard management of hemolymphangioma until recently has been through surgical resection. Surgeons usually aim for complete removal of the tumor because partial ablation of the tumor leads to a 50%-100% recurrence[4]. But invasive surgery pushes endoscopists to pursue new management methods that are minimally invasive. Hemolymphangioma managed by endoscopy is acceptable for the nature of

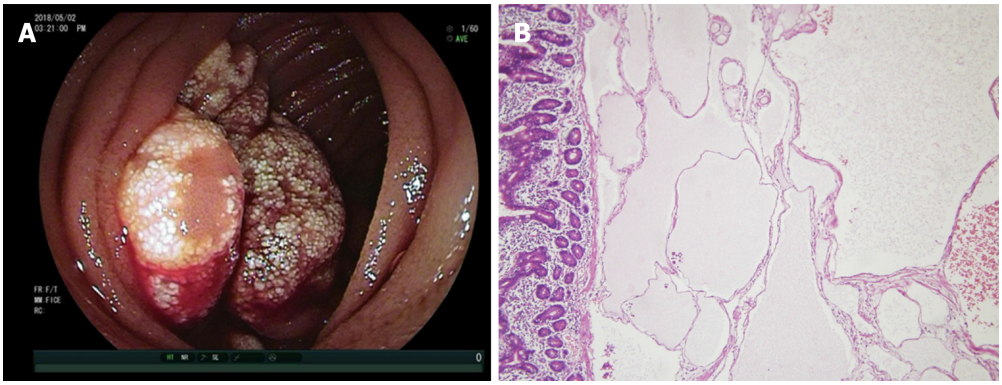

Figure 1 Gross and histologic images of hemolymphangioma. A: Lobulated tumor occupied half of the intestinal cavity with white patches on the mucosal surface and blood oozing in the fundus; B: Histology revealed a hyperplastic thin-walled lymphangion and venous with luminal dilation in the submucosal area. Hematoxylin and eosin × 20.

a benign tumor. Endoscopic mucosal resection with a band ligation device had been reported in managing a gastric hemolymphangioma[10]. Also, an endoscopic polypectomy and argon plasma coagulation was successfully performed in a jejunal lymphangioma[11]. Endoscopic injection sclerotherapy is usually used as a treatment for esophageal varices, including the treatment of esophageal hemangioma. Furthermore, polidocanol injection therapy was also applied in small bowel hemangioma without bleeding or perforation[12]. Based on these precedents and our experience in the treatment of blue rubber bleb nevus syndrome[13], we performed enteroscopic injection sclerotherapy to manage the jejunum hemolymphangioma. To our knowledge, this is the first case of small intestinal hemolymphangioma successfully treated by enteroscopic injection sclerotherapy. At the 1 year follow-up, no recurrence of anemia or melena proved that this treatment is feasible.

CONCLUSION

In summary, small intestinal hemolymphangioma is a rare malformation consisting of blood vessels and lymphatic channels. The lesion is mainly located within the proximal jejunum and clinically presents as melena and anemia. BAE and CE are effective methods for preoperative diagnosis of hemolymphangioma, and enteroscopic injection sclerotherapy is a feasible, minimally invasive treatment to manage this benign tumor.

Table 1 English literature on PubMed of small intestinal hemolymphangioma from 2010 to 2019

Ref.	Year	Age/sex	Symptom	Location	Tumor size in cm	Diagnostic method	Management
Fang *et al*[4]	2012	57/F	Melena, anemia	30 cm distal to Treitz	5.0	Enteroscopy	Surgical resection
Antonino *et al*[5]	2014	24/F	Anemia	Second portion of duodenum	5.0	Gastroduodenoscopy	Surgical resection
Gómez-Galán *et al*[6]	2016	43/F	Chronic anemia	Distal duodenum	4.0	Capsule endoscopy and enteroscopy	Surgical resection
Blanco *et al*[7]	2017	45/F	Melena, anemia	90 cm distal to Treitz	8.0	Capsule endoscopy and enteroscopy	Laparoscopic small bowel resection
Iwaya *et al*[8]	2018	70/M	Melena, anemia	120 cm distal to Treitz	2.0	Capsule endoscopy and enteroscopy	Laparoscopic small bowel resection
Yang *et al*[9]	2019	20/F	Melena, anemia	60 cm distal to Treitz	10.0	Computed tomography scan and enteroscopy	Laparoscopic small bowel resection

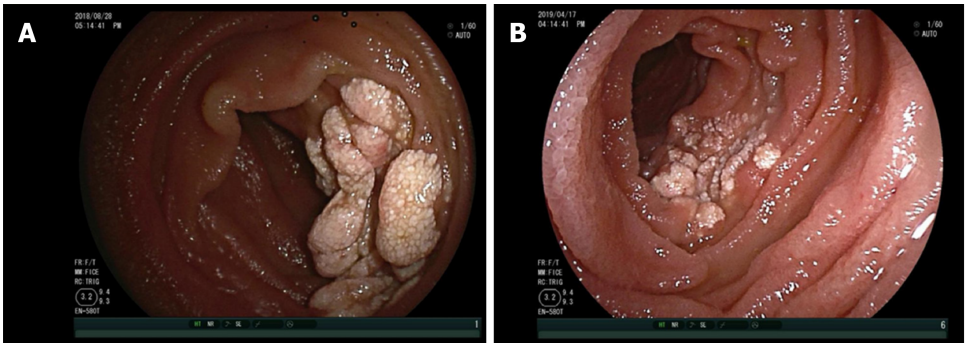

Figure 2 Images at the 3 mo and 1 year follow-up appointments. A: At 3 mo after enteroscopic injection sclerotherapy, hemolymphangioma atrophied dramatically, and bleeding was hardly observed; B: At 1 year later, the hemolymphangioma was gone. A few white patches on the mucosal surface are visible.

REFERENCES

1 **Morris-Stiff G**, Falk GA, El-Hayek K, Vargo J, Bronner M, Vogt DP. Jejunal cavernous lymphangioma. *BMJ Case Rep* 2011; **2011** [PMID: 22696733 DOI: 10.1136/bcr.03.2011.4022]
2 **Li F**, Osuoha C, Leighton JA, Harrison ME. Double-balloon enteroscopy in the diagnosis and treatment of hemorrhage from small-bowel lymphangioma: a case report. *Gastrointest Endosc* 2009; **70**: 189-190 [PMID: 19152891 DOI: 10.1016/j.gie.2008.09.036]
3 **Shyung LR**, Lin SC, Shih SC, Chang WH, Chu CH, Wang TE. Proposed scoring system to determine small bowel mass lesions using capsule endoscopy. *J Formos Med Assoc* 2009; **108**: 533-538 [PMID: 19586826 DOI: 10.1016/S0929-6646(09)60370-3]
4 **Fang YF**, Qiu LF, Du Y, Jiang ZN, Gao M. Small intestinal hemolymphangioma with bleeding: a case report. *World J Gastroenterol* 2012; **18**: 2145-2146 [PMID: 22563205 DOI: 10.3748/wjg.v18.i17.2145]
5 **Antonino A**, Gragnano E, Sangiuliano N, Rosato A, Maglio M, De Palma M. A very rare case of duodenal hemolymphangioma presenting with iron deficiency anemia. *Int J Surg Case Rep* 2014; **5**: 118-121 [PMID: 24503337 DOI: 10.1016/j.ijscr.2013.12.026]
6 **Gómez-Galán S**, Mosquera-Paz MS, Ceballos J, Cifuentes-Grillo PA, Gutiérrez-Soriano L. Duodenal hemangiolymphangioma presenting as chronic anemia: a case report. *BMC Res Notes* 2016; **9**: 426 [PMID: 27581369 DOI: 10.1186/s13104-016-2214-0]
7 **Blanco Velasco G**, Tun Abraham A, Hernández Mondragón O, Blancas Valencia JM. Hemolymphangioma as a cause of overt obscure gastrointestinal bleeding: a case report. *Rev Esp Enferm Dig* 2017; **109**: 213-214 [PMID: 28256143]
8 **Iwaya Y**, Streutker CJ, Coneys JG, Marcon N. Hemangiolymphangioma of the small bowel: A rare cause of chronic anemia. *Dig Liver Dis* 2018; **50**: 1248 [PMID: 29886080 DOI: 10.1016/j.dld.2018.05.008]
9 **Yang J**, Zhang Y, Kou G, Li Y. Jejunum Hemolymphangioma Causing Refractory Anemia in a Young Woman. *Am J Gastroenterol* 2019 [PMID: 31658121 DOI: 10.14309/ajg.0000000000000438]
10 **Kim WT**, Lee SW, Lee JU. Bleeding gastric hemolymphangioma: endoscopic therapy is feasible. *Dig Endosc* 2013; **25**: 553-554 [PMID: 23855544 DOI: 10.1111/den.12147]
11 **Kida A**, Matsuda K, Hirai S, Shimatani A, Horita Y, Hiramatsu K, Matsuda M, Ogino H, Ishizawa S, Noda Y. A pedunculated polyp-shaped small-bowel lymphangioma causing gastrointestinal bleeding and treated by double-balloon enteroscopy. *World J Gastroenterol* 2012; **18**: 4798-4800 [PMID: 23002353 DOI: 10.3748/wjg.v18.i34.4798]

12 **Igawa A**, Oka S, Tanaka S, Kunihara S, Nakano M, Chayama K. Polidocanol injection therapy for small-bowel hemangioma by using double-balloon endoscopy. *Gastrointest Endosc* 2016; **84**: 163-167 [PMID: 26907744 DOI: 10.1016/j.gie.2016.02.021]
13 **Ning S**, Zhang Y, Zu Z, Mao X, Mao G. Enteroscopic sclerotherapy in blue rubber bleb nevus syndrome. *Pak J Med Sci* 2015; **31**: 226-228 [PMID: 25878650 DOI: 10.12669/pjms.311.5858]

Published By Baishideng Publishing Group Inc
7041 Koll Center Parkway, Suite 160, Pleasanton, CA 94566, USA
Telephone: +1-925-3991568
E-mail: bpgoffice@wjgnet.com
Help Desk:http://www.f6publishing.com/helpdesk
http://www.wjgnet.com